University of Strathclyde
Department of Electronic and Electrical Engineering

Efficiency Evaluation of Permanent Magnet Synchronous Machines Using the Synthetic Loading Technique

By

Abdelaziz Yousif Mohamed Abbas
B.Tech, M.Sc

A thesis presented in fulfilment of the requirement for the degree of Doctor of Philosophy

2009

Acknowledgments

First of all, I would like to express all my thanks to God for his great help in completing this thesis.

I would like to express my sincerest thanks to my supervisors Dr. John E Fletcher and Prof. Barry W Williams for accepting me as a PhD student. Genuinely, I would like to give my special thanks to Dr. John E Fletcher for his useful guidance, keens interest, efforts and useful help at any time.

My deep thanks to my office mates, Mr. Liliang Gao, Mr. Hugh Muir and Nagm Eldeen Abdo for their great kindness and supports.

I would like to express my thanks also to Mr. Charles Croser and Dr. Tee Lim for their help and technical support.

My thanks are also to my family for their prayers and patience during my study.

Dedication

To my family

Table of Contents

Chapter Four: Simulation of Synthetic Loading Technique

Chapter Five: Software and Hardware Description and Implementation

Chapter Six: Experimental Results of Synthetic Loading Technique

Abstract

This thesis investigates the application of the synthetic loading technique for efficiency evaluation of permanent magnet (PM) synchronous machines. The standard tests require specialist test facilities, additional machines, and for large machines, linear machines, or vertical mounted machine and floor space. Therefore, an efficiency test method that avoids the need for an external mechanical load is desirable. Synthetic loading can determine machine losses and eliminates the need for a mechanical load connected to the test machine. The synthetic loading technique forces the machine under test to accelerate and decelerate thereby alternating between motor-generator action. If configured correctly the machine, on average over each synthetic loading cycle, operates at rated rms current, rated rms voltage and rated speed, thus producing rated copper loss, iron loss and friction and windage loss. The thesis considers how to properly configure synthetic loading for PM synchronous machines.

A derivation of the mathematical models of the synthetic loading technique applied to the permanent magnet synchronous machines is provided in the thesis. The model is based on the direct and quadrature axis equivalent circuits. From the mathematical model, a quadrature axis current algorithm is proposed which is used to develop the speed equation and the stator direct and quadrature axis voltage and current equations. The thesis also establishes a generalised mathematical model of the synthetic loading technique for permanent magnet synchronous machines. Using the derived equations, the effects of synthetic loading frequency on the dc link voltage and the inverter phase-leg volt-ampere rating are analysed. This shows that the synthetic loading technique requires an increased dc link voltage and inverter volt-ampere rating compared to the standard efficiency test technique.

A test rig is constructed and used to assess synthetic loading for fractional hp machines. The research verifies the synthetic loading technique experimentally for three permanent magnet synchronous machine types: the surface-mount PM synchronous machine, the interior PM synchronous machine and the linear PM synchronous machine. Simulation and

experimental results from synthetic loading are compared with the standard efficiency test. The simulation and the experimental results show that the synthetic loading technique is capable of evaluating the efficiency of the permanent magnet synchronous machines. The key contributions of this work concerns the mathematical model of PM synchronous machines under synthetic loading, the hardware and software implementation and validation of synthetic loading as a technique for efficiency evaluation of PM synchronous machines.

List of Figures and Tables

List of Figures

List of Tables

List of symbols and Abbreviations

List of Symbols

Symbol	Definition
B,D	Damper coefficient (Nms, Nsm^{-1})
E	Electro motive force (V)
E_u	Electro motive force (pu)
f_s	System frequency (Hz)
f_n	Synthetic loading frequency (Hz)
F_e,F_L	Electromagnetic and load forces (N)
I_s	Rated rms current (A)
I_{su}	Rated rms current (pu)
I_m	AC perturbation current (A)
I_{mu}	AC perturbation current (pu)
I_o	DC offset current component (A)
I_{ou}	DC offset current component (pu)
i_d,i_q	Direct and quadrature axis currents (A)
i_{du},i_{qu}	Direct and quadrature axis currents (pu)
i_{ds},i_{qs}	Direct and quadrature axis stator currents (A)
i_{dsu},i_{qsu}	Direct and quadrature axis stator currents (pu)
i_{dc},i_{qc}	Direct and quadrature axis core currents (A)
i_{dcu},i_{qcu}	Direct and quadrature axis core currents (pu)
i_a,i_b,i_c	Stator phase currents (A)
I_{ms}	Stator peak phase current (A)
I_{msu}	Stator peak phase current (pu)
i_a,i_b,i_c	Stator phase currents (A)
i_{au},i_{bu},i_{cu}	Stator phase currents (pu)
I_{base}	Base phase current (A)
J	Moment of inertia (kgm^2)
k_t	Torque constant (NmA^{-1})

k_f	Force constant (NA^{-1})
L_d, L_q	Direct and quadrature axis inductances (H)
L_{du}, L_{qu}	Direct and quadrature axis inductances (pu)
L_{base}	Base inductance (H)
M	Mover mass (kg)
m	Modulation index
P	Number of pole pairs
P_{in}	Input power (W)
P_{inu}	Input power (pu)
P_{cu}	Stator copper loss (W)
P_c	Core loss (W)
P_{EL}	Electrical loss (W)
P_{mech}	Friction and windage loss (W)
R_a, R_c	Stator and core resistances (Ω)
R_{au}, R_{cu}	Stator and core resistances (pu)
T_e, T_L	Electromagnetic and load torques (Nm)
V_d, V_q	Direct and quadrature axis voltages (V)
V_{du}, V_{qu}	Direct and quadrature axis voltages (pu)
V_s	Peak phase voltage (V)
V_{su}	Peak phase voltage (pu)
V_{dc}	DC link voltage (V)
V_{dcu}	DC link voltage (pu)
V_a, V_b, V_c	Stator phase voltages (V)
V_{au}, V_{bu}, V_{cu}	Stator phase voltages (pu)
V_{base}	Base Voltage (V)
x	Mover displacement (m)
Z_{base}	Base impedance (Ω)
θ	Rotor position (rad)
ω_r	Rotor speed ($rads^{-1}$)
ω_{ru}	Rotor speed (pu)

ω_{base}	Base rotor speed ($rads^{-1}$)
v_x	Mover velocity (ms^{-1})
v_{xu}	Mover velocity (pu)
v_{base}	Base mover velocity (ms^{-1})
τ	Pole pitch length
τ_m	Mechanical time constant (s)
λ_m	flux linkage (Wb)
λ_{base}	Base flux linkage (Wb)

List of Abbreviations

Abbreviation	Definition
AC	Alternating current
ADC	Analog-to-digital converter
CCS	Code composer studio
DAC	Digital-to-analog converter
DC	Direct current
DSP	Digital signal processor
EV	Event manager
GP	General purpose
IGBT	Isolated gate bipolar transistor
IO	Input/Output
IPM	Interior permanent magnet
IPMSM	Interior permanent magnet synchronous machine
LPMSM	Linear permanent magnet synchronous machine
PM	Permanent magnet
PMSM	Permanent magnet synchronous machine
PWM	Pulse width modulation
QEP	Quadrature encoder pulses
SVPWM	Space vector pulse width modulation

Chapter One
Introduction

1.1 General Concepts

An electrical machine converts electrical energy into mechanical energy (a motor) or vice versa (a generator). During the operation of an electrical machine there are losses in the process of energy conversion that manifest themselves as heat. These losses are categorised as electrical and mechanical losses. The electrical losses are a combination of Ohmic loss, due to stator winding resistance, and iron loss as a result of eddy currents and hysteresis in the iron of the machine. Both losses can be predicted. The mechanical losses are a result of bearing friction and windage loss [1]. Losses give an indication of machine efficiency; if the losses are higher the machine will be less efficient.

In recent years energy efficiency has become a high priority due to concerns of carbon emissions, security of supply and climate change. Also, increases in oil prices and a continuing air pollution crisis motivate serious action aimed at saving energy. Electric motors consume more than 60% of all electrical energy in the industry, hence offer a significant opportunity for energy saving [2]. This has prompted many manufacturers to address the challenge of improving the efficiency of electrical machines.

PM synchronous machines are widely used in industry, because of their many stated advantages such as low inertia, high torque to current ratio, high power factor, high efficiency, and almost no need for maintenance. Because of all the important advantages, PM synchronous machines are used in many different applications [3]-[6]. There is much research [7]-[9] presented on PM synchronous machine drives and the serious competition they offer to induction motors for servo applications. This has been facilitated by a reduction in permanent magnet cost and improvements in permanent magnet material characteristics [10].

Electrical machine tests to determine energy lost as heat are important for both users and manufactures [11]. Temperature rise in electrical machines causes deterioration of insulation materials. Also high rates of energy loss indicate low efficiency values. Recently there has been a new emphasis on the use of energy efficient machines [12]. Machine manufacturers have a separate category for energy efficient machines. Unfortunately, energy efficient machines are still used in small numbers. The reason for the low rates of adoption is poor information about these machines, because there is no single definition of an energy efficient motor [13]. Users generally rely only on the information provided by manufacturers to assess the performance of electrical machines [14]. However, a machine labelled with high efficiency from one manufacturer may be less efficient than the standard machine from another manufacturer. There are no accurate energy efficiency standards for high efficiency machines.

The traditional method used to conduct full-load performance tests on an electrical machine is to apply full-load torque to the machine's output shaft using an external mechanical load [12]. There are many associated problems when a large machine is tested such as the requirement for an equally large test generator and its associated equipment, or a duplicate machine, and the cost of setting up the test facility to make full-load tests is expensive. Also vertical axis machines are difficult to test by applying a load to the shaft because of the difficulty in finding an appropriate vertical load [11]. Consequently a method of evaluating the efficiency of electrical machines without the need of mechanically coupling a load is highly desirable: such a technique is synthetic loading. The aim of this thesis is to investigate the suitability of synthetic loading as a method of efficiency evaluation of PM synchronous machines that is practical for laboratory facilities or on-site test. Synthetic loading has been applied successfully to the induction machine to measure efficiency. This research aims to extend these concepts to PM synchronous machines and to assess the test equipment ratings. The experimental research is limited to sub-kW but the developed generalised model can be used for higher power ratings.

1.2 Motivation

One of the most difficult challenges facing electrical machine manufacturers and users is how to perform efficiency evaluation tests, particularly for larger electrical machines, vertical mounted machines and also for linear machines, both large and small [12]. During the last two decades, PM synchronous machine drives have become popular and are gradually replacing brushed dc machine drives and induction machine drives in industrial applications [15]. Therefore, a target of prior research has been machine design, reduction of losses and improvements in efficiency, and high performance control of PM machines [16]. Also, developments in power electronic technology, and associated control, make the PM synchronous machine practical in industrial processes requiring a wide speed range. The research reported in this thesis addresses efficiency evaluation of PM and linear PM synchronous machines. Historically, linear machines have been used in actuation applications where efficiency tends not to be a priority. However, linear machines are now finding applications with continuous duty, for example, refrigeration, and also at higher power levels for direct-drive wave energy conversion, therefore an effective and rapid method of efficiency evaluation is a useful tool.

Exploiting wind and wave energy on and in the seas and oceans has been a research interest for almost three decades particularly due to world events such as the oil crisis in 1973 and recent carbon emission and climate change concerns [17]. There are a number of candidate wave energy conversion devices that could potentially utilize linear generators in the power conversion process. These include such devices as the Oyster, the Archimedes Wave Swing device, and Stingray [18]-[20]. Synthetic loading, used for efficiency evaluation, is a potentially useful tool for the linear generators proposed in these devices because it is difficult to find and accommodate a suitable load for the machine during testing. This is one significant driver for this research.

Cooling and the removal of heat from electronic systems has become an important issue facing system designers [21]. Particularly as conventional cooling systems no longer provide adequate cooling for sophisticated electronic systems such as high

performance microprocessors using nanometer-scale transistors. Hence the application of compact refrigeration systems is growing. Synthetic loading is a suitable method for efficiency evaluation of the low power PM linear motors proposed for use in small Stirling-type refrigeration systems.

The testing of electrical machines to determine the power losses in the form of heat and the resulting temperature rise is important for both users and manufacturers [3], [11], [22]. During a rated-load efficiency test, the machine must draw it is full load current at rated voltage and speed. Synthetic loading can do this without connecting a mechanical load to the machine drive shaft [23],[24]. With synthetic loading, the electrical machine is accelerated and decelerated in a controlled manner to alternate rapidly between motor-generator action, producing rated rms current and on average, rated speed. This produces average rated copper loss (due to the rated current) and rated iron (core) loss, friction and windage loss (as a consequence of operating on average at rated speed). The main principle of synthetic loading is to control the machine being tested such that it draws rated current using only the moment of inertia of the rotor as the load [25], [26]. Therefore, synthetic loading offers the advantage that the machine tested is mechanically decoupled from the load, thereby removing the need for special test facilities. Also, the machine can be tested on site. In synthetic loading the equipment required to carry out the efficiency test is an inverter, appropriate voltage and current sensors and a vector controller. The cost and time associated with performing a synthetic loading test is potentially reduced as the test equipment can be made portable if multiple sets are to be tested in situ [27].

1.3 Objectives and Scope of the Research

This thesis deals with the efficiency evaluation of PM synchronous machines using the synthetic loading technique. The objectives of this research are to investigate the appropriateness of synthetic loading, both theoretically and experimentally, as a technique for efficiency evaluation of PM synchronous machines. The types of machine investigated included the PM, IPM and linear PM synchronous machines. In order to meet these objectives mathematical equations for synthetic loading of PM

synchronous machines are derived using *d*- and *q*-axis equivalent circuit. The synthetic loading equations are generalized and simulated using MATLAB and SIMULIK. The hardware and software requirements for a system that enables the synthetic loading technique to be assessed are described and implemented. Vector control is executed by a Digital Signal Processor (DSP) with a fast Analogue to Digital Converter (ADC) and Encoder for phase current, rotor speed and rotor position measurements. Synthetic loading tests are performed and the results compared with simulation and the standard efficiency test. Tests are performed at rated speed and with varying values of output torque. The work of this thesis will contribute understanding in the area of efficiency evaluation of PM synchronous machine using the synthetic loading technique.

1.4 Thesis structure

The thesis is organised into seven chapters covering analysis, simulation and experimental aspects of synthetic loading as a method of efficiency evaluation for PM synchronous machines.

Chapter two presents background theory and a literature review of efficiency evaluation of electrical machines. Because PM synchronous machines are the main interest, a brief review of rotor design, advantages, and disadvantages of PM synchronous machines are presented. The literature in the areas of machine power loss and efficiency, the standard efficiency test and the synthetic loading technique of electrical machines are reviewed. The mathematical models of PM synchronous machines are developed and the standard efficiency test is simulated using MATLAB and SIMULINK for the PM and linear PM synchronous machine.

Chapter three develops detailed mathematical equations for the synthetic loading technique applied to PM, IPM and linear PM synchronous machines. The synthetic loading mathematical models are established using *d*- and *q*-axis equivalent circuits. The quadrature axis current and the speed equations for synthetic loading are developed for the PM, IPM and linear PM synchronous machine. The resultant voltage equations using *d*- and *q*-axis equivalent circuits including equivalent core loss resistance are developed. The mathematical models developed for synthetic loading allow assessment of the

impact that synthetic loading frequency has on the dc link voltage and inverter VA rating required to perform the test.

Chapter four presents simulation results of the synthetic loading technique and the standard efficiency test for the PM, IPM and linear PM synchronous machine under four different load conditions and five different synthetic loading frequencies. The individual losses from the simulation result of the standard efficiency test are compared with the losses developed during the simulation of synthetic loading. In addition, the impact that synthetic loading frequency has on the required dc link voltage and inverter VA rating are presented in order to choose suitable synthetic loading frequencies used during the synthetic loading experiments reported in chapter six.

Chapter five describes the basic vector control system and the associated software and hardware implementation. In order to verify synthetic loading technique experimentally the software and hardware are implemented on a practical test rig. The system components and control algorithm are described in detail.

Chapter six presents the experimental results of the standard efficiency test and the synthetic loading technique for the PM, IPM and linear PM synchronous machine for variable load conditions and different synthetic loading frequencies. The efficiencies measured using the synthetic loading technique are compared with efficiencies measured using standard efficiency test. Chapter seven draws general conclusions and provides suggestions for further research work in this area.

1.5 Author's contributions

The experimental systems for efficiency evaluation of PM, IPM and linear PM synchronous machine have been constructed and tested to validate the analytical and simulation results. Since the main objective of this research is to investigate the suitability of synthetic loading technique for efficiency evaluation of the PM, IPM and linear PM synchronous machine, the main contributions of this thesis are that it:

- Proposes the quadrature axis current algorithm. Since the synthetic loading is a current control technique, the key step in performing the synthetic loading test

is the correct choice of the quadrature axis current algorithm. This current is designed to force the PM synchronous machine to accelerate and decelerate during synthetic loading. The research validates the selection of i_q reference and derive equations for selecting the main parameters.

- Develops and validates the mathematical equations resulting from synthetic loading for the PM, IPM and linear PM synchronous machines.
- Establishes a set of generalised equations of the synthetic loading technique for PM synchronous machines using the normalisation technique. These equations can be used regardless of PM synchronous machine type.
- Provides a comprehensive analysis of synthetic loading for efficiency evaluation of the PM, IPM and linear PM synchronous machine using analysis, simulation and experiment.
- Analyses the effects of synthetic loading frequency on the dc link voltage and inverter phase-leg VA rating. This shows that the inverter VA rating and the dc link voltage gradually decreases as the synthetic loading frequency is increased falling to a minimum value and then gradually increasing again.
- Analyses the effects of additional moment of inertia (or mover mass) on peak-to-peak speed, which shows that additional moment of inertia results in lower required dc link voltage if a fixed synthetic loading frequency is used as the additional inertia results in a reduced swing speed. Hence, lower phase-leg VA rating is required.
- Assesses, through experiment, the synthetic loading technique and compares it with the standard efficiency tests on the PM, IPM and linear PM synchronous machines. There is excellent correlation between synthetic loading and standard efficiency tests.
- Verifies the synthetic loading technique as a method of efficiency evaluation for the PM, IPM and linear PM synchronous machine by analysis, simulation and experiment.

1.6 List of Author's Publications

1. Abdelaziz Y. M. Abbas and John E. Fletcher, "Efficiency Evaluation of Linear Permanent Magnet Synchronous Machines Using the Synthetic Loading Method" 39th IEEE Annual Power Electronics Specialists Conference, Rhodes, Greece, 15-19 June 2008, pp.3074-3080.
2. Abdelaziz Y. M. Abbas and John E. Fletcher, "Synthetic Loading Technique for Efficiency Evaluation of Permanent Magnet Synchronous Machines" 44th IEEE Annual Universities Power Engineering Conference, Glasgow, UK, 1-4 September 2009.
3. Abdelaziz Y. M. Abbas and John E. Fletcher, "The Synthetic Loading Technique Applied to the PM Synchronous Machine", submitted in IEEE Transaction on Energy conversions Journal.
4. Abdelaziz Y. M. Abbas and John E. Fletcher, "Synthetic Loading Applied to Linear PM Synchronous Machines", submitted in IET Renewable Power Generation Journal.
5. Abdelaziz Y. M. Abbas and John E. Fletcher, "Efficiency Evaluation of Interior Permanent Magnet Synchronous Machines using the Synthetic Loading Technique", submitted in 20th International Symposium on Power Electronics, Electrical Drives, Automation and Motion, PISA, Italy, 14-16 June 2010.
6. Abdelaziz Y. M. Abbas and John E. Fletcher, "The Effect of Direct Axis Current on the Performance of Synthetic Loading Technique", submitted in IEEE Transaction on Energy conversions Journal.

References

[1] C. Grantham and H. Tabatabaei-Yazdi "A Novel Machineless Dynamometer for Load Testing Three-Phase Induction Motors", IEEE 1999 International Conference on Power Electronics and Drive Systems, PEDS'99, July 1999, 579-584.

[2] J. Habibi and S. Vaez-Zadeh, "Efficiency-Optimizing Direct Torque Control of Permanent Magnet Synchronous Machines", Power Electronic Specialists, 2005 IEEE 36th Conference on June 12, 2005, pp. 759-764.

[3] C. Grantham and D.J. Mckinnon, "A Rapid Method for Load Testing and Efficiency Measurement of Three-Phase Induction Motors", International Conference on Electrical Machines and Systems, 2008. ICEMS 2008. 17-20 Oct. 2008, pp. 160-165.

[4] S. Morimoto, Y. T. Takeda and T. Hirasa, "Loss Minimization Control of Permanent Magnet Synchronous Motor Drives", IEEE Transactions on Industrial Electronics, Vol. 41, No. 5, October 1994, pp. 511-517.

[5] S. Shinnaka, "New 'D-State-Observer' Based Sensorless Vector Control for Permanent Magnet Synchronous Motors", Industry Application Conference, 2004, 39th IAS Annual Meeting, Conference Record of the 2004 IEEE, Vol. 2, 3-7 October 2004, pp. 1000-1007.

[6] J. O. Pereira and J. S. Lawler, "Analysis of Limit of the Constant Power Speed Range of the Permanent Magnet Synchronous Machine Driven by Dual Mode Inverter", Industry Application Conference, 2005, Fourtieth IAS Annual Meeting, Conference Record of the 2005 IEEE, Vol. 4, 2-6 October 2005, pp. 2540-2545.

[7] C. C. Mi, G. R. Slemon and R. Bonert, "Minimization of Iron Losses of Permanent Magnet Synchronous Machines", IEEE Transactions on Energy Conversion, Vol. 20, No. 1, March 2005, pp. 121-127.

[8] A. B. Dehkordi, A. M. Gole and T. L. Maguire, "Permanent Magnet Synchronous Machine Model for Real Time Simulation", Presented at the International Conference on Power Systems Transients (IPST'05) in Montreal, Canada on June19-23, 2005, Paper No. IPST05-159.

[9] M. Nakano, H. Kometani and M. Kawamura, "A Study on Eddy-Current Losses in Rotors of Surface Permanent Magnet Synchronous Machines", Industry Application Conference, 2004, 39th IAS Annual Meeting, Conference Record of the 2004 IEEE, Vol. 3, 3-7 October 2004, pp. 1696-1702.

[10] M. Chinchilla, S. Arnaltes and J. C. Burgos, "Control of Permanent-Magnet Generator Applied to Variable-Speed Wind-Energy System Connected to the Grid", IEEE Transactions on Energy Conversion, Vol. 21, No. 1, March 2005, pp. 130-135.

[11] C. Grantham, H. Tabatabaei-Yazdi and M. F. Rahman, "A Novel Method for Rapid Efficiency Measurement of Three Phase Induction Motors", IEEE Transactions on Energy Conversion, Vol. 14, No. 4, December 1999, pp. 1236-1240.

[12] D. J. McKinnon and C. Grantham, "Improved efficiency Test Methods for Three-Phase Induction Machines", Industry Application Conference. Fourtieth IAS Annual Meeting. Conference Record of the 2005, Vol. 1, 2-6 October 2005, pp. 466-473.

[13] C. Grantham, H. Tabatabaei-Yazdi and M. F. Rahman, "A Novel Method for Efficiency Evaluation of Three Phase Induction Motors", Electric Machines and Drives Conference Record, 1997, IEEE International, 18-21 May 1997, pp. WC1/8.1-WC1/8.3.

[14] C. Grantham and D. J. McKinnon, "A Novel Method for Load Testing and Efficiency Measurement of Three Phase Induction Motors", Electric Machines and Drives Conference, 2003, IEMDC'03, IEEE International, Vol. 2, 1-4 June 2003, pp. 769-775.

[15] P. Pillay and R. Krishnan, "Application Characteristics of Permanent Magnet Synchronous and Brushless dc Motor for Servo Drives", IEEE Transactions on Industry Applications, Vol. 27, No. 5, September/October 1991, pp. 986-996.

[16] R. S. Colby and D. W. Novotny, "An Efficiency-Optimizing Permanent-Magnet Synchronous Motor Drive", IEEE Transactions on Industry Applications, Vol.24, No. 3, May/June 1988, pp. 462-469.

[17] N. J. Baker, M. A. Mueller and E. Spooner "Permanent Magnet Air-Core Tubular Linear Generator for Marine Converters", Power Electronics, Machines and Drives, 2004. (PEMD2004). Second International Conference on (Conf. Publ. No.498) Vol. 2, 31 March-2 April 2004, pp. 862-867.

[18] S. Lee, S. Hong, S. Kim,Y. Yamaguchi and J. Won, "Polarimetric Features of Oyster Farm Observed by AIRSAR and JERS-1", IEEE Transaction on Geoscience and Remote Sensing, Vol. 44, No. 10, October 2006, pp. 2728-2735.

[19] H. Polinder, B. C. Mecrow, A. G. Jack, P. G. Dickinson and M. A. Mueller, "Conventional and TFPM Linear Generators for Direct-Drive Wave Energy Conversion", IEEE Transaction on Energy Conversion, Vol. 20, Issue 2, June 2005, pp. 260-267.

[20] Z. Yong-hua, Z. Shi-wu, Y. Jie and K. H. Low, "Morphologic Optimal Design of Bionic Undulating Fin Based on Computational Fluid Dynamics" Proceeding of the 2007 IEEE International Conference on Mechatronics and Automation, Harbin, China, 5-8 August, 2007, pp. 491-496.

[21] A. Heydari, "Miniature Vapor Compression Refrigeration Systems for Active Cooling of High Performance Computers" Thermal and Thermomechanical Phenomena in Electronic Systems, 2002. ITHERM 2002. The Eighth Intersociety Conference on Volume, Issue, 2002 pp. 371-378.

[22] C. Grantham, D.J. McKinnon, "Experimental Confirmation of On-Site Efficiency Evaluation of Three-Phase Induction Motors Using Synthetic Loading Techniques", Australian Universities Power Engineering Conference (AUPEC 2004). 26-29 Sept. 2004, Brisbane, Australia, pp. 160-165.

[23] C. Grantham, H. Tabatabaei-Yazdi and M. F. Rahman, "Efficiency Evaluation of Three Phase Induction Motors by Synthetic Loading", International Conference on Power Electronics and Drive Systems, 1997. Proceedings 1997, Vol. 1, 26-29 May, pp. 103-109

[24] C. Grantham, M. Sheng and E. D. Spooner, "Synthetic loading of three-phase induction motors using microprocessor controlled power electronics", Electric Power Applications, IEE Proceedings, Vol. 141, No. 2, March 1994, pp. 101-108.

[25] D. J. McKinnon and C. Grantham, "Efficiency Evaluation of Three-Phase Induction Motors Using Dual-Frequency and Sweep-Frequency Methods of Synthetic Loading", Second International Conference on Power Electronics, Machines and Drives, 2004. (PEMD 2004). Vol. 2, 31 March-2 April 2004, pp. 799-804.

[26] D. J. McKinnon and C. Grantham, "On-Site Efficiency Evaluation of Three-Phase Induction Motors Using Synthetic Loading Methods", Second International Conference on Power Electronics, Machines and Drives, 2004. (PEMD 2004). Vol. 1, 31 March-2 April 2004, pp. 291-296.

[27] C. Grantham and M. Sheng, "The Synthetic Loading of Three-Phase Induction Motors Using Microprocessor Controlled Power Electronics", Power Electronics and Drive and Systems, 1995. Proceedings of 1995 International Conference, Vol.1, on 21-24 February 1995, pp. 471-476.

Chapter Two
Literature Review and Background Study

2.1 Introduction

This chapter details relevant background and provides a literature review of efficiency evaluation for electrical machines. A brief review of the advantages and disadvantages of permanent magnet synchronous machines is presented. The literature review covers research related to power losses, efficiency, standard methods of efficiency evaluation, and synthetic loading for temperature rise and efficiency evaluation for electrical machines. Mathematical models for permanent magnet synchronous machines and linear permanent magnet synchronous machines are then established. The mathematical model of the permanent magnet synchronous machine used here is in the synchronously translating reference frame. Using the mathematical model in the steady state, the copper losses, iron losses and mechanical losses are calculated. The standard efficiency test for efficiency evaluation of the permanent magnet synchronous machine is simulated using MATLAB and SIMULINK.

2.2 Permanent Magnet Synchronous Machines

In the past, ferrite and samarium-cobalt magnets have been used in permanent magnet machines. Recently, magnet materials with higher energy density such as neodymium-boron-iron (NdFeB) have become available. This has opened up new possibilities for the large scale application of permanent magnet synchronous machines. The stator of a permanent magnet synchronous machine has a conventional three-phase winding. There are two categories of rotor design; one has magnets mounted on the surface of the rotor which is called a surface-mount permanent magnet (PM) synchronous machine, the other has magnets buried inside the rotor and is called an interior permanent magnet (IPM) synchronous machine [1]. The IPM synchronous machine is more robust thus is suited to operation at higher speeds. Furthermore, IPM synchronous machine design allows for a degree of flux

weakening which is not possible with PM synchronous machine design. This helps extend the speed range of the machine. Figure 2.1 shows photographs of the three different types of PM synchronous Machines.

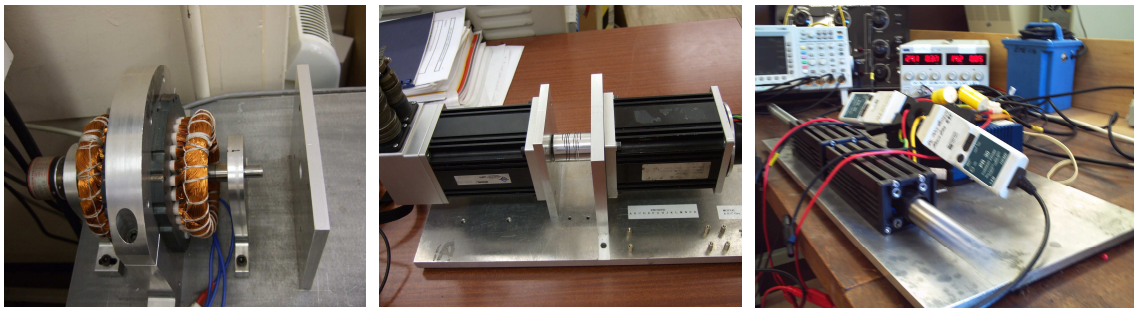

Figure 2.1 Photograph (a) IPM Synchronous Machine (b) PM Synchronous Machine and (c) Linear PM Synchronous Machine

The surface-mount permanent magnet synchronous machine can be considered to have a smooth air gap. This is due to the fact that the relative permeability of the magnets is approximately unity. This leads to high reluctance thus the machine can be considered to have a large effective air gap and negligible saliency. Interior permanent magnet synchronous machines have the magnets buried inside the rotor. The rotor structure therefore displays saliency.

In the salient pole synchronous machine with wound rotor and damper windings, the direct axis synchronous reactance is larger than quadrature axis reactance. However, in the interior permanent magnet machine the quadrature axis synchronous reactance is larger than the direct axis synchronous reactance. This is because the magnetic circuit associated with the quadrature axis of the rotor is iron dominated as opposed to the direct axis which includes the magnet whose permeability is approximately equal to that of air. Thus the reluctance in the direct axis of the rotor is increased, and its reactance decreased [1].

Permanent magnet synchronous machines have become a viable choice for motion control applications, such as robotics, machine tools, and aerospace [2],[3]. The increasing interest is a consequence of the advantages that permanent magnet machines display:

- High torque to current ratio.

- High power to weight ratio.
- High efficiency and high power factor.
- The elimination of brush gear and commutators allows the motor to operate at much higher speed than a conventional dc machine, leading to a reduction in weight and volume [4].
- Use of permanent magnet motors eliminates rotor copper losses.
- The development of high-energy permanent magnet material, allows the rotor diameter to be smaller than a brushed motor yielding lower rotor inertia hence faster acceleration.
- No maintenance associated with brushes and commutators.

Permanent magnet synchronous machines have some disadvantages, which are:

- Higher capital cost.
- The need for position sensing such as an encoder or resolver in order to synchronize the phase excitation pulses to the rotor position (though this can be solved by a number of proposed sensorless vector control methods).
- Demagnetization at high temperature or under shock loads.

2.3 Power losses and efficiency

The main sources of losses in permanent magnet synchronous machines are copper losses, iron (core) losses, and friction and windage losses. Furthermore, the insulation temperature rise in an electrical machine is a function of these power losses. The rated power of the machine is determined by the maximum working temperature of the insulation, hence losses determine power rating. The study of losses and efficiency are closely related whereby lower losses at the same torque and speed result in a more efficient machine. Machines with higher efficiency can be relatively smaller with a consequent improvement in power density.

The efficiency and power losses of permanent magnet synchronous machines have been studied by several researchers. Slemon [5], shows that permanent magnet synchronous machines provide higher power factors, higher efficiencies and higher power densities for machine power ratings lower than 7 kW, compared with induction motors. Pragasen, *et al.* [6], shows that the power density of the brushless

dc motor is higher than that of the permanent magnet synchronous motor. Shigeo, *et al.* [4], describes improvements in efficiency of permanent magnet synchronous motor drives using a controllable electrical loss, which is controlled by using a vector controller. The copper loss and the iron (core) loss can be minimized by the optimal control of the stator current vector which forces the direct axis current to be zero in the direct-quadrature axis machine model. Also, Habibi, *et al.* [7] address the issue of loss minimization by using a method for optimising the steady state efficiency using direct torque control of permanent magnet synchronous machines. In direct torque control the terminal voltage of the permanent magnet synchronous machine is constant. The electrical loss has two components; one is constant and depends on terminal voltage, the other is variable, and is a function of direct axis flux, which can be minimized by minimizing the direct axis current. Rehman [8] gives a comparison between permanent magnet synchronous machines and induction machines in terms of power factor and efficiency which reveals that the efficiency and power factor of permanent magnet synchronous machines is higher compared to induction machines for machine power ratings lower than 7 kW. As a result, permanent magnet synchronous machines have lower power losses for the same output power compared to induction machines. This indicates that permanent magnet synchronous machines have higher power density than induction machine counterparts.

Copper and iron (core) losses are the most basic and prevalent losses in the permanent magnet synchronous machine. Copper losses are proportional to the square of stator current. In high voltage permanent magnet synchronous machines iron (core) losses form a significant amount of total losses compared with induction machines. This is a consequence of the reduced of rotor losses in permanent magnet synchronous machines and the effect of non-sinusoidal flux density waveforms in the stator core of permanent magnet synchronous machines. Therefore, iron (core) loss has become a research target and has been studied by several researchers [9]-[13]. Eddy current losses and hystersis losses are the components of core losses. The eddy current losses are caused by the induction of eddy-currents inside the conducting stator core material (approximately $P_{eddy} \propto (f\lambda)^2$). The hysteresis losses are due to continuous variation of flux density in the stator core (approximately $P_{hys} \propto f\lambda^2$) where λ the air gap flux is and f the frequency of the air gap flux [14]. Iron (core) losses are

negligible at very low speeds. However, as speed increases the iron losses increase significantly. An electrical model of a permanent magnet synchronous machine, which uses a parallel resistance to model iron (core) losses in high performance applications, has been utilized by several researchers [4], [7], [10], [15]-[18]. It can be concluded that copper and iron (core) losses need to be modeled in the analysis and control of permanent magnet synchronous machines.

Another loss component in permanent magnet synchronous machines is stray load losses which are a result of distortion of the air gap flux due to phase current and non-uniform distribution of current in the stator winding. Stray load losses are difficult to estimate. Therefore, these losses are bundled with core losses during modeling and experimental measurements.

2.4 Standard Efficiency Test Methods

Unfortunately there is no standard efficiency test established especially for permanent magnet synchronous machines in the literature. However, standard efficiency tests established for induction machine can be used to evaluate the efficiency of permanent magnet synchronous machines [19]. Determination of temperature rise as well as power dissipated as heat inside the electrical machines is a matter of interest for both consumers and manufacturers. Heat generation affects the insulation materials and the cooling systems of the machine. In this section, the established methods of full-load testing for efficiency evaluation and temperature rise tests for induction machines are reviewed.

McKinnon, *et al.* [20] states that in order to accurately compare the efficiency of two induction machines, they are required to undergo similar tests. The testing methods depend on the rating of the machine, the equipment available and the degree of accuracy required. Furthermore, a direct measurement of the total machine losses and calculation of the efficiency as input power minus losses, divided by input power yield a more accurate estimate of efficiency than calculating the ratio of input power to out put power as an accurate measurement of the output power is often difficult.

Grantham, *et al.* [19] shows that there are many efficiency test standards available for induction machines. The IEEE Rotating Machinery Committee has produced

a standard IEEE 112-1991 by which efficiency is tested in the United States. In addition the International Electro-technical Commission (IEC) produced the IEC-34-2 standard for use in Europe, which is similar to British Standard BS269, and the Japanese Electro-technical Committee (JEC) produced standard JEC-37. A comparison shows that these methods are similar differing only in the details of procedure to be followed in each test [21]. In addition, the IEEE 112 test method B is the most rigorous and more detailed than those that measure all the motors losses using a dynamometer such as specified in the IEC or JEC standard.

Boglietti, *et al.* [22, 23] reports motor efficiency measurements calculated in accordance with international standards. The standard efficiency tests IEEE 112-B, IEC 34-2 and JEC 37 recommend different measurement procedures, in particular for the stray loss determination and the temperature corrections of the copper losses. In these papers, a comparison of the measurement procedures defined by these international standards has been reported, together with some comments on the prescribed methodologies. Furthermore, a comparison is made based on experimental results obtained by tests on four general purposes, three-phase induction motors. However, the stray load loss measurement is a critical key step for the accurate evaluation of induction motor efficiency. Therefore, a critical analysis of stray losses has been performed. The stray load loss sensitivity to measurement errors has been analyzed, in order to understand which are the most critical quantities that influence their evaluation.

Renier, *et al.* [24] reveals that the measured efficiency of an induction motor directly connected to the grid strongly depends on the method used to evaluate the results and the standard according to which the measurements have been performed. They also describe a set of experiments and discuss their results for determining the efficiency of low voltage, three-phase squirrel-cage induction motors. Different standards such as IEEE 112-B and IEC 34-2 have been used and similarities and differences discussed. This confirms that the main difference between the various standards is the way in which the values for the stray load losses are obtained at different load levels. A short description of the measurement setup is given and the efficiency measurements for induction motors for different standards test from

several manufacturers are provided. These results demonstrate the necessity to interpret with care the efficiency data provided by manufacturers.

Ghai, [25] shows the Electrical Machinery Committee (EMC) of the Power Engineering Society (PES) of the Institute of Electrical and Electronics Engineers (IEEE) has established a comparison of U.S. standards with International Standards. It compares IEC 34 series of standards with National Electrical Manufacturers Association (NEMA) standards for large induction motors for general purpose applications. It concludes that a substantial amount of correspondence exists between NEMA and IEC standards. NEMA's recent practice of using IEC standards as the starting point for writing additional standards has increased the degree of correspodence between NEMA and IEC standards. Furthermore, requirements for any specific design parameter are not always the same between NEMA and IEC, though the intent is identical. The inclusion of tolerances on induction machine performance, and the lower stray load loss allowance in IEC, causes a given design to have better indicated performance per IEC 34 than for NEMA.

Gray, *et al.* [26] shows that the energy crisis of 1973 focused attention on the efficiency of poly-phase induction motors. Also, they confirm the need for efficiency test procedures that are repeatable and accurate. Due to the large number in service, and significant improvements through redesign, medium power rated induction motors are an important category. In response to this the IEEE Std. 112, Method B has been chosen for efficiency testing of medium power rating ac motors. The IEEE Std. 112-1991 Method B contains several requirements for accuracy improvement which have been found to be effective. Since 1984 Method B procedures, with the additional accuracy requirement, have been in use. The paper discussed the purpose of these improvements, and identifies some weakness in the procedure.

Yamazaki, *et al.* [27] specifies the main components of the stray load loss of induction motors from both results of measurement and analysis. The IEEE standard 112 Method B is applied to the cage induction motor for the measurement of the stray load loss. On the other hand, the losses generated at the stator core, the rotor core and the rotor cage have been calculated directly by the finite element method considering magnetic saturation and harmonic fields, which vary due to the load

condition. The relationships between the losses separated by the measurement and the losses calculated directly by the finite element method are clarified. It shows that the measured and calculated torque, losses and efficiency agree.

Glew [28] confirms that different standards demonstrate that stray load loss is still an area of uncertainty. It highlights that no standard method has been yet defined for determination of stray load loss. Generally IEEE Std 112 Method B has been accepted as the best method for evaluating stray load loss.

Auinger [29] compares machine efficiency under the IEC 34 standard with regards to the nameplate efficiency labelling system adopted in Europe. It argues that the nominal efficiency alone is not sufficient for an accurate comparison. More information about loss distribution within the machines is required. The estimation of stray load loss as 0.5% of the input power is justified regardless of the machine size. It shows that the ease of carrying out the IEC 34 test method is more valuable than the error in efficiency due to stray loss estimate.

2.5 Synthetic Loading Method

Testing of electrical machines to determine the power losses in the form of heat and the resulting temperature rise is important for both users and manufacturers [19]. High temperatures cause deterioration of insulation materials and high rates of power dissipation implies low efficiency values which affect machine lifetime. The current method used to carry out an efficiency test is to connect a rated load to the shaft of the test machine. This is difficult, particularly for linear machines and large vertical machines [21]. Furthermore, if post-installation tests are required, this method requires removal of the test machine from the set, leading to loss of production. Consequently, an efficiency test that avoids the need of an external load is desirable. Such a test technique is synthetic loading. Synthetic loading forces the electrical machine to draw full load current without connecting a mechanical load to the machine drive shaft. The main principle of synthetic loading is to control the machine being tested such that it draws rated current using the moment of inertia of the rotor to synthesize a load [20].

In 1921 Ytterberg introduced the two-frequency or mixed-frequency synthetic loading method for insulation temperature rise test of induction machines [21]. This method develops the equivalent of a full-load test but is achieved without mechanically loading the induction machine [21]. With this method there are two possible connection techniques for the two-frequency synthetic loading method. The two-frequency method connects the machine under test to two different supplies connected in series as shown in Figure 2.2. The main supply has rated voltage and frequency V_a and f_a. The auxiliary supply has a voltage and frequency V_b and f_b which is lower than rated value and is adjusted until the induction motor input voltage and the stator current equal the rated values [30].

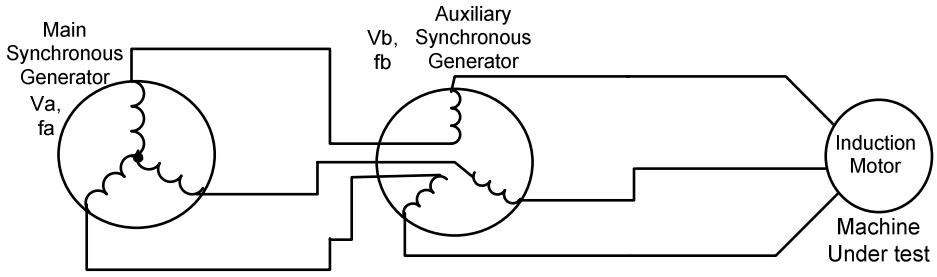

Figure 2.2 Series connection of main synchronous generator and auxiliary synchronous generator with the induction motor under test for the two-frequency method

The other connection technique for the two-frequency method is to inject two voltages of two different frequencies and amplitudes into the machine under test using an isolating transformer [21]. The main voltage has rated amplitude and frequency and the auxiliary voltage chosen to be slightly different from the main voltage, normally less than it. The auxiliary voltage is generated via a synchronous generator or an inverter. The two supplies are at different frequencies and are mixed using a specially designed isolating transformer as shown in Figure 2.3.

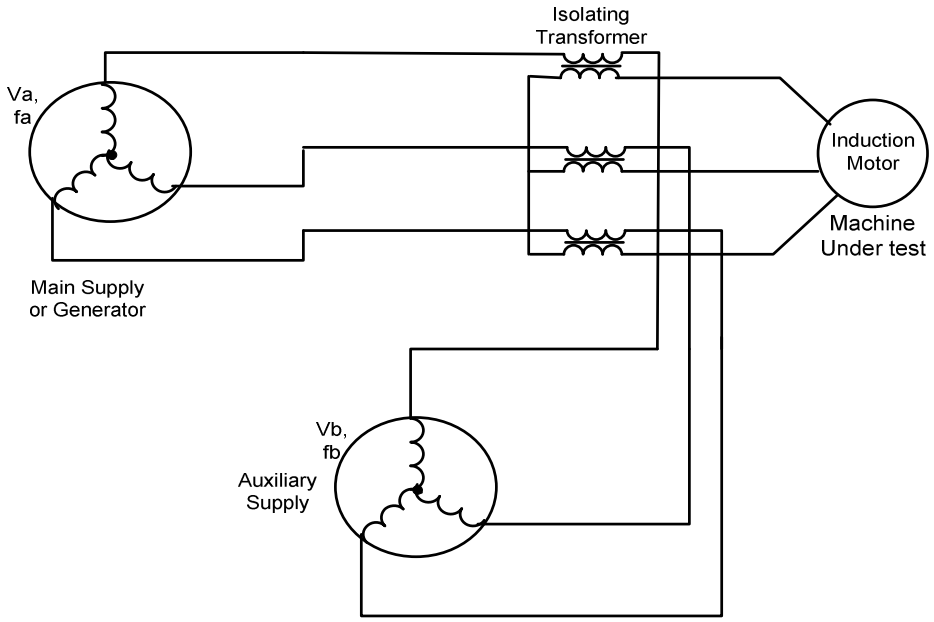

Figure 2.3 The electrical connection of the main supply and the auxiliary supply with induction motor under test for the two-frequency synthetic loading method using an isolating transformer

Boldea, *et al.* [31] discuss a method of artificially producing load on an induction machine to test the load capability and the cooling system of the induction machine. In order to produce artificial loading of induction machine both PWM voltage converters and matrix converters are proposed with the two frequency method. The insulation temperature is measured and compared with standard load test. A small difference between insulation temperatures in the two tests is explained by additional core and copper losses associated with switching frequency harmonics. The two frequency method requires an oversized matrix converter. However, the bi-directional power flow makes it a good candidate for dynamic tests.

Mihalcea, *et al.* [32] proposed that full load losses and insulation temperature rise can be evaluated by using the equivalent load method. Constant magnitude variable frequency, variable magnitude and variable frequency, and dual power supply tests are proposed. The results are compared with standard load tests on an induction machine supplied from a three-phase supply and power inverter. The results show that the equivalent loading techniques used overestimated the power losses and the insulation temperature rise in the induction machine. Therefore, a need for improvement is essential. Furthermore, assessments on higher power induction

machines are necessary in order to generalize the acceptance of the equivalent loading technique.

Ho, *et al.* [30] shows that the temperature rise of induction machines with the synthetic loading method is useful for the machine industry. The indirect method is applied using time stepping finite element method. The paper analyses two types of synthetic loading method: the two frequency method and the phantom loading method, and compares the result with conventional full load test results. The phantom loading method requires the phase voltage of the stator winding to have both an AC and DC component. In the phantom loading, the test induction machine IM-1 is connected electrically to another auxiliary induction machine IM-2. A DC power supply is connected between the terminals of IM-1 and IM-2 as shown in Figure 2.4. In this configuration the two machines draw the rated current and both machines operate at synchronous speed without being mechanically coupled to each other.

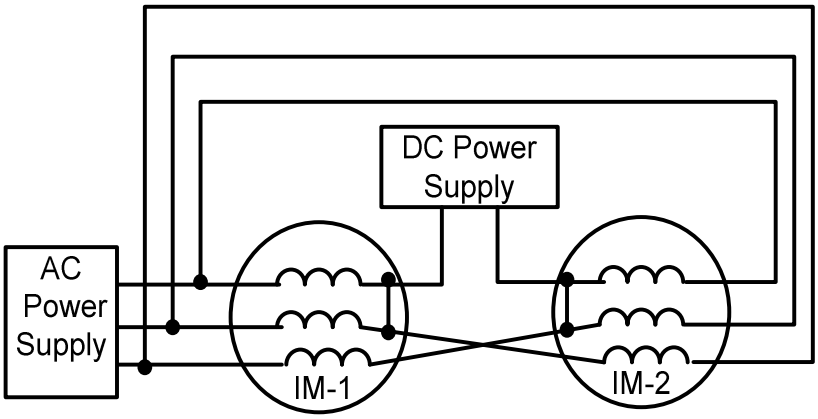

Figure 2.4 The electrical connection of the two inductions motor with AC and DC power supplies for the phantom loading method

Soltani, *et al.* [33, 34] describe that synthetic loading can be used to determine temperature rise and total losses of a 100 kW synchronous machine without connecting a mechanical load to the machine shaft. They also apply the synthetic loading method to higher power induction machines. The disadvantage is that the technique requires four other machines and two controlled DC supplies to test two

motors. This makes the test more sophisticated, as shown in Figure 2.5. However, there is no feedback power into the supply system, which is an advantage. This is a consequence of the power exchange: when one system (system (1)) generates power the other (system (2)) absorbs it and vice-versa. Therefore, when equilibrium is reached, the utility source to D0 needs to provide only the power losses in all five machines. The fixed DC supply is a constant dc supply and the Bang-Bang DC control [35] is variable dc supply control the excitation current of the synchronous generator field. The Bang-Bang source is used to perturb the excitation current, hence the generator emfs are amplitude modulated. This causes acceleration and deceleration of the motors under test. The controller synchronises acceleration of one system to the deceleration of the other system, thereby minimising power flow from the utility source.

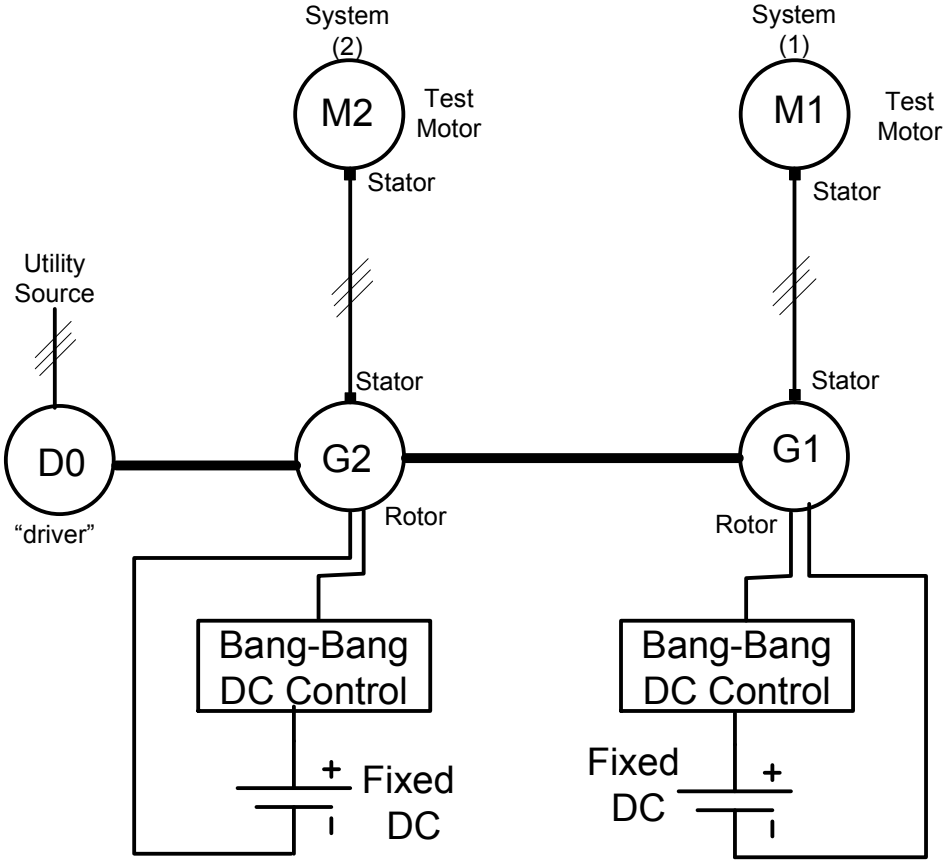

Figure 2.5 Connection of the five machines and the controller for synthetic loading test of large induction machine with no feedback power into the power system

McKinnon, *et al.* [18], [21], [36] published many papers on synthetic loading used for temperature rise tests and efficiency determination of three-phase induction

motors. A synthetic loading method is used without connecting mechanical load to the machine shaft. The main advantage of synthetic loading methods is reducing the test time and the result is shown to be accurate compared with conventional methods of efficiency evaluation and temperature rise tests. Also synthetic loading methods allow vertical-mounted machines to be tested in the same way as horizontal mounted machines. Synthetic loading for efficiency evaluation and temperature rise have been studied by several researchers in the last decade [19], [37]. All these papers demonstrate synthetic loading methods applied to three-phase induction motors, but not the application of the technique to permanent magnet synchronous machines, which is the subject of the research reported in this thesis.

2.6 Permanent Magnet Synchronous Machines Model

The mathematical model of a permanent magnet synchronous machine used here is in the synchronously translating reference frame. A transformation is used to transform three phase components, which can be currents or voltages, into direct and quadrature components. To develop a model of a permanent magnet machine, a three-phase machine with symmetrical windings is assumed. The three phase *abc* model is then transformed to a two phase *d-q* model, which reduces the complexity in modeling the machine [38]. From the permanent magnet synchronous machine equivalent circuit, which is in synchronously translating *d-q* axis reference frame, the mathematical equations for direct axis and quadrature axis voltage have been derived using direct and quadrature axis current as variables.

2.6.1 The Park Transformation

In three-phase permanent magnet synchronous machines, the quantities of the stator reference frame should be transformed into a reference frame rotating synchronously with the rotor flux vector. This removes the dependency on the position of the rotor flux in the circuit equations. The transformation simplifies the expression of the electrical equations for the machine and simultaneously removes time and position dependencies in the machine parameters. The standard two-axis theory with fixed rotor reference frame is used. The d-axis is aligned with rotor flux as shown in Figure 2.6, where λ_m is the rotor flux due to the permanent magnets.

A transformation that resolves the three-phase model to an equivalent two-phase model is not difficult to find. The representation of electrical power flow in the machine should be preserved. As a result, the developed torque is invariant with the transformation. Simultaneously, it would be convenient that the transformation be the same for both voltage and current [39]. Such a transformation is Park's transformation. The three-phase permanent magnet synchronous machine is assumed to have a balanced wye or delta connected winding and to be linear.

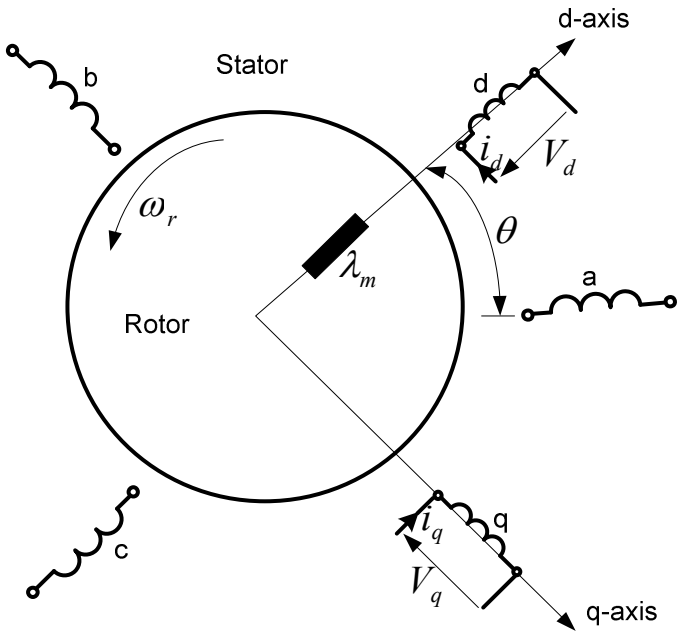

Figure 2.6 The transformation of the *abc* stationary reference frame to the *dq* synchronously rotating reference frame for the permanent magnet synchronous machine [40]

From the model of the permanent magnet synchronous machine, for symmetrical conditions, the Park transformation matrix transforms three-phase components, f_a, f_b, and f_c, which can be either currents or voltages, from the stationary reference frame *abc*, into three-variable quantities, f_d, f_q, and f_o, which is called synchronously rotating reference frame *dqo*. For PM motor control purposes, the transformation angle θ is typically the angle between f_a and the rotor d-axis shown in Figure 2.6.

- **Park transformation equation**

$$\begin{bmatrix} f_d \\ f_q \\ f_o \end{bmatrix} = \frac{2}{3} \begin{bmatrix} \cos\theta & \cos\left(\theta - \frac{2\pi}{3}\right) & \cos\left(\theta + \frac{2\pi}{3}\right) \\ \sin\theta & \sin\left(\theta - \frac{2\pi}{3}\right) & \sin\left(\theta + \frac{2\pi}{3}\right) \\ \frac{1}{2} & \frac{1}{2} & \frac{1}{2} \end{bmatrix} \begin{bmatrix} f_a \\ f_b \\ f_c \end{bmatrix} \tag{2.1}$$

- **Inverse Park transformation equation**

$$\begin{bmatrix} f_a \\ f_b \\ f_c \end{bmatrix} = \begin{bmatrix} \cos\theta & \sin\theta & 1 \\ \cos\left(\theta - \frac{2\pi}{3}\right) & \sin\left(\theta - \frac{2\pi}{3}\right) & 1 \\ \cos\left(\theta + \frac{2\pi}{3}\right) & \sin\left(\theta + \frac{2\pi}{3}\right) & 1 \end{bmatrix} \begin{bmatrix} f_d \\ f_q \\ f_o \end{bmatrix} \tag{2.2}$$

For the linear permanent magnet synchronous machine, the translational transformation matrix transforms three-phase components, f_a, f_b, and f_c, which can be either currents or voltages from the *abc* stationary reference frame, into synchronously translating reference frame f_d, f_q, and f_o. Where, x and τ are mover distance and pole pitch length respectively.

- **Park transformation equation**

$$\begin{bmatrix} f_d \\ f_q \\ f_o \end{bmatrix} = \frac{2}{3} \begin{bmatrix} \cos\left(\frac{\pi}{\tau}x\right) & \cos\left(\frac{\pi}{\tau}x - \frac{2\pi}{3}\right) & \cos\left(\frac{\pi}{\tau}x + \frac{2\pi}{3}\right) \\ \sin\left(\frac{\pi}{\tau}x\right) & \sin\left(\frac{\pi}{\tau}x - \frac{2\pi}{3}\right) & \sin\left(\frac{\pi}{\tau}x + \frac{2\pi}{3}\right) \\ \frac{1}{2} & \frac{1}{2} & \frac{1}{2} \end{bmatrix} \begin{bmatrix} f_a \\ f_b \\ f_c \end{bmatrix} \tag{2.3}$$

- **Inverse Park transformation equation**

$$\begin{bmatrix} f_a \\ f_b \\ f_c \end{bmatrix} = \begin{bmatrix} \cos\left(\frac{\pi}{\tau}x\right) & \sin\left(\frac{\pi}{\tau}x\right) & 1 \\ \cos\left(\frac{\pi}{\tau}x - \frac{2\pi}{3}\right) & \sin\left(\frac{\pi}{\tau}x - \frac{2\pi}{3}\right) & 1 \\ \cos\left(\frac{\pi}{\tau}x + \frac{2\pi}{3}\right) & \sin\left(\frac{\pi}{\tau}x + \frac{2\pi}{3}\right) & 1 \end{bmatrix} \begin{bmatrix} f_d \\ f_q \\ f_o \end{bmatrix} \tag{2.4}$$

2.6.2 Modelling of PM Rotary Machines

Figure 2.7 (a) and (b) shows the d- and q-axis equivalent circuits respectively of a rotary PM synchronous machines in the synchronously rotating *dq* reference frame. The equivalent circuits include the effect of the stator copper loss, core loss resistance and *dq* inductances.

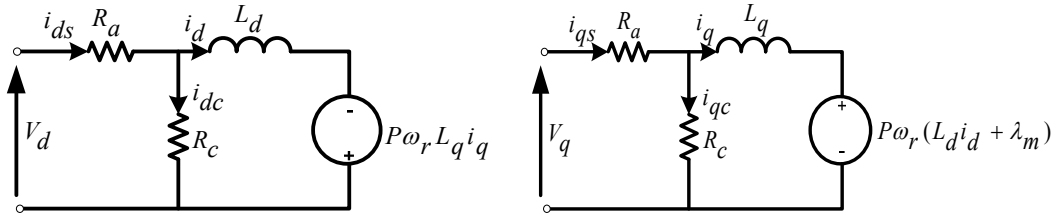

(a) d-axis (b) q-axis

Figure 2.7 d- and q-axis equivalent circuit of PM synchronous machines [41]

The state space and the mechanical equations of the rotary PM synchronous machines are derived from this model.

The state space equations are

$$\frac{di_d}{dt} = \left[V_d - R_a i_d + P\omega_r L_q i_q \left(1 + \frac{R_a}{R_c}\right) \right] \Big/ L_d \left(1 + \frac{R_a}{R_c}\right) \tag{2.5}$$

$$\frac{di_q}{dt} = \left[V_q - R_a i_q - P\omega_r L_d i_d \left(1 + \frac{R_a}{R_a}\right) - P\omega_r \lambda_m \left(1 + \frac{R_a}{R_c}\right) \right] \Big/ L_q \left(1 + \frac{R_a}{R_c}\right) \tag{2.6}$$

where:

i_{ds} and i_{qs} are *d* and *q* axis stator currents (A), respectively.

V_d and V_q are *d* and *q* axis stator voltages (V), respectively.

i_d and i_q are *d* and *q* axis torque generating currents (A), respectively.

i_{dc} and i_{qc} are *d* and *q* axis core loss currents (A), respectively.

R_a and R_c are stator and core loss resistances (Ω), respectively.

L_d and L_q are *d* and *q* axis self inductances (H), respectively.

λ_m is the permanent magnet flux linkages (Wb).

ω_r is the rotor speed (rad/s), and *P* is the number of pole pairs.

The torque equations is

$$T_e = \frac{3}{2} P \left(\lambda_m \, i_q + \left(L_d - L_q \right) i_q \, i_d \right) (\text{N.m}) \tag{2.7}$$

where, T_e is the electromagnetic torque. A linear mechanical system is assumed:

$$\frac{d\omega_r}{dt} = (T_e - T_L - B\omega_r) / J \tag{2.8}$$

$$\frac{d\theta}{dt} = P\omega_r \tag{2.9}$$

where, T_L is the load torque. J and B are moment of inertia and damper coefficients respectively. A technique to measure the PM synchronous machine parameters is presented in Appendix D.

2.6.3 Loss Calculations for PM Rotary Machines

Figure (2.8) depicts the steady state equivalent circuit of permanent magnet synchronous machines in the synchronously rotating d-q axis reference frame. The equivalent circuits include the effect of the stator copper loss and core loss. The major electrical losses of the PM synchronous machines are the stator copper loss and the core loss. The stator copper loss is represented by the power dissipated by resistance, R_a and the core loss is represented by the power dissipated in the shunt resistance, R_c. The other loss is mechanical loss due to friction in the bearing and windage. The friction and windage loss contribution is represented by the damper coefficient B in (2.8).

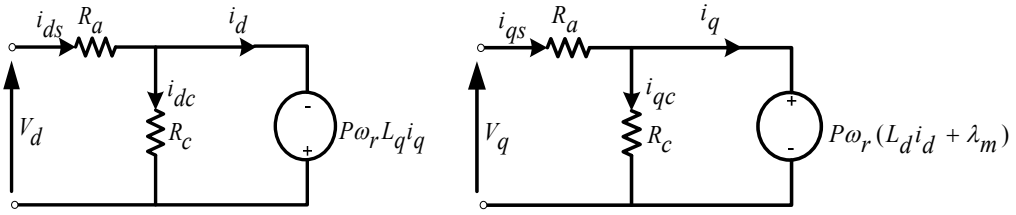

(a) d-axis (b) q-axis

Figure 2.8 d- and q-axis steady state equivalent circuit of PM synchronous machines [41]

From the *d*- and *q*-axis steady state equivalent circuits, by applying Kirchhoff's current and voltage laws, the individual currents and voltage equations can be expressed as

$$i_{ds} = i_d + i_{dc} \quad \text{(A)} \tag{2.10}$$

where $i_{dc} = -P\omega_r \frac{L_q i_q}{R_c}$ (A)

therefore:

$$i_{ds} = i_d - P\omega_r \frac{L_q i_q}{R_c} \text{(A)} \tag{2.11}$$

$$i_{qs} = i_q + i_{qc} \quad \text{(A)} \tag{2.12}$$

where, $i_{qc} = P\omega_r \frac{(L_d i_d + \lambda_m)}{R_c}$ (A)

therefore:

$$i_{qs} = i_q + P\,\omega_r \frac{(L_d i_d + \lambda_m)}{R_c} \quad \text{(A)} \tag{2.13}$$

$$\begin{bmatrix} i_{ds} \\ i_{qs} \end{bmatrix} = \begin{bmatrix} 1 & -P\omega_r \frac{L_q}{R_c} \\ P\omega_r \frac{L_d}{R_c} & 1 \end{bmatrix} \begin{bmatrix} i_d \\ i_q \end{bmatrix} + \begin{bmatrix} 0 \\ \frac{P\omega_r}{R_c}\lambda_m \end{bmatrix} \quad \text{(A)} \tag{2.14}$$

and

$$\begin{bmatrix} V_d \\ V_q \end{bmatrix} = \begin{bmatrix} R_a & -P\omega_r L_q\left(1+\frac{R_a}{R_c}\right) \\ P\omega_r L_d\left(1+\frac{R_a}{R_c}\right) & R_a \end{bmatrix} \begin{bmatrix} i_d \\ i_q \end{bmatrix} + \begin{bmatrix} 0 \\ P\omega_r\lambda_m\left(1+\frac{R_a}{R_c}\right) \end{bmatrix} \text{ (V)} \tag{2.15}$$

The stator copper loss, P_{cu}, for the PM synchronous machine is

$$P_{cu} = \frac{3}{2} R_a \left(i_{ds}^2 + i_{qs}^2\right) \quad \text{(W)} \tag{2.16}$$

The core loss, P_c, for the PM synchronous machine is

$$P_c = \frac{3}{2} R_c \left(i_{dc}^2 + i_{qc}^2 \right) \quad \text{(W)} \tag{2.17}$$

where, $i_{dc} = -P\omega_r \frac{L_q i_q}{R_c}$ and $i_{qc} = P\omega_r \frac{\left(L_d i_d + \lambda_m\right)}{R_c}$ therefore:

$$P_c = \frac{3}{2} \left(\left(P\omega_r\right)^2 \frac{L_q^2 i_q^2}{R_c} + \left(P\omega_r\right)^2 \frac{\left(L_d i_d + \lambda_m\right)^2}{R_c} \right) \quad \text{(W)} \tag{2.18}$$

Therefore the total electrical losses are

$$P_{EL} = \frac{3}{2} R_a \left(i_{ds}^2 + i_{qs}^2 \right) + \frac{3}{2} \left(\left(P\omega_r\right)^2 \frac{L_q^2 i_q^2}{R_c} + \left(P\omega_r\right)^2 \frac{\left(L_d i_d + \lambda_m\right)^2}{R_c} \right) \quad \text{(W)} \tag{2.19}$$

The mechanical loss is due to friction in the bearing and is proportional to the square of motor speed. The mechanical loss is expressed as follows:

$$T_{mech} = B\,\omega_r \quad , \quad P_{mech} = \omega_r\, T_{mech} = B\,\omega_r^2 \quad \text{(W)} \tag{2. 20}$$

where T_{mech}, P_{mech} are torque due to mechanical loss and mechanical power loss respectively.

2.6.4 Modelling of Linear PM Machines

The linear permanent magnet synchronous motor equivalent circuits in the synchronously translating d-q axis reference frame are shown in Figure (2.9), where, i_{ds} and i_{qs} are d and q axis stator currents (A), respectively.

V_d and V_q are d and q axis stator voltages (V), respectively.

i_d and i_q are d and q axis currents (A), respectively.

i_{dc} and i_{qc} are d and q axis equivalent core loss currents (A), respectively.

R_a and R_c are stator and core loss resistors (Ω), respectively.

L_d and L_q are d and q axis inductances (H), respectively.

λ_m is magnet flux linkages (Wb).

v_x is the mover velocity (ms^{-1}).

P and τ are number of pole pairs and pole pitch length (m) respectively.

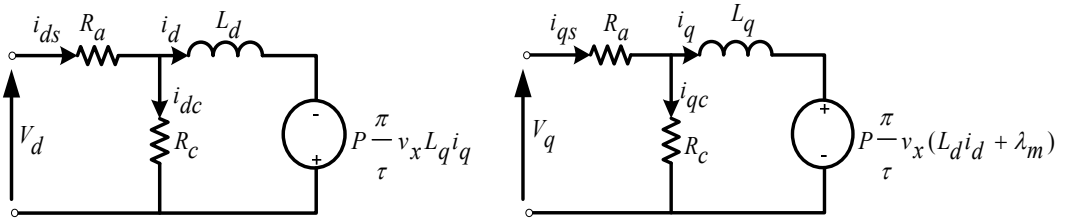

(a) d-axis (b) q-axis

Figure 2.9 d- and q-axis equivalent circuit of linear PM synchronous machines [42]

From this model the state space and the mechanical equations of the linear PM synchronous machines are expressed.

The state space equations are

$$\frac{di_d}{dt} = \left[V_d - R_a i_d + P\frac{\pi}{\tau} v_x \, L_q i_q \left(1 + \frac{R_a}{R_c}\right) \right] \Big/ L_d \left(1 + \frac{R_a}{R_c}\right) \tag{2.21}$$

$$\frac{di_q}{dt} = \left[V_q - R_a i_q - P\frac{\pi}{\tau} v_x (L_q i_q + \lambda_m) \left(1 + \frac{R_a}{R_c}\right) \right] \Big/ L_q \left(1 + \frac{R_a}{R_c}\right) \tag{2.22}$$

The mechanical equations are expressed as follows:

$$F_e = \frac{3}{2}\frac{\pi P}{\tau}\left(\lambda_m i_q + \left(L_d - L_q\right) i_q i_d\right) \quad \text{(N)} \tag{2.23}$$

$$\frac{dv_x}{dt} = \left(F_e - F_L - D v_x\right)/M \tag{2.24}$$

$$\frac{dx}{dt} = P v_x \tag{2.25}$$

where F_e, F_L are electromechanical and load forces respectively. M is the mover mass and D is the damper coefficient.

2.6.5 Loss Calculations for PM Linear Machines

Figure (2.10) shows the steady state equivalent circuit of a linear permanent magnet synchronous machine in the synchronously translating d-q axis reference frame. The major electrical losses of the linear PM synchronous machines are the stator copper loss and the core loss. The copper loss is represented by resistance R_a and the core loss is represented by the shunt resistance R_c. The mechanical loss is due to the mover friction. The friction is represented by the damper coefficient D.

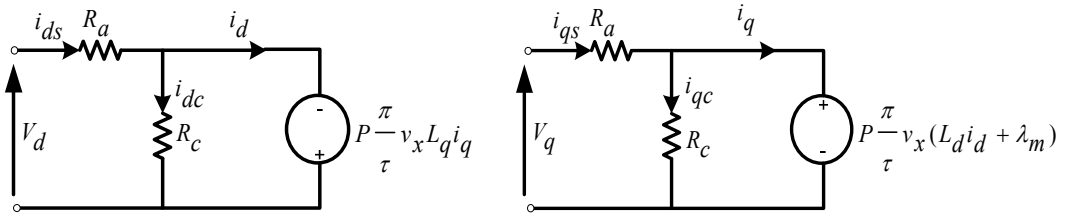

(a) d-axis (b) q-axis

Figure 2.10 d- and q-axis steady state equivalent circuit of linear PM synchronous machines [42]

Using Kirchhoff's current and voltage laws in the steady-state equivalent circuit in Figure 2.10 the current and voltage equations are expressed by (2.30) and (2.31).

$$i_{ds} = i_d + i_{dc} \quad \text{(A)} \tag{2.26}$$

where $i_{dc} = -P\frac{\pi}{\tau}v_x\frac{L_q i_q}{R_c}$ (A)

therefore

$$i_{ds} = i_d - P\frac{\pi}{\tau}v_x\frac{L_q i_q}{R_c} \quad \text{(A)} \tag{2.27}$$

$$i_{qs} = i_q + i_{qc} \quad \text{(A)} \tag{2.28}$$

where $i_{qc} = P\frac{\pi}{\tau}v_x\frac{(L_d i_d + \lambda_m)}{R_c}$ (A)

therefore

$$i_{qs} = i_q + P\frac{\pi}{\tau}v_x\frac{(L_d i_d + \lambda_m)}{R_c} \quad \text{(A)} \tag{2.29}$$

$$\begin{bmatrix} i_{ds} \\ i_{qs} \end{bmatrix} = \begin{bmatrix} 1 & -P\frac{\pi}{\tau}v_x\frac{L_q}{R_c} \\ P\frac{\pi}{\tau}v_x\frac{L_d}{R_c} & 1 \end{bmatrix} \begin{bmatrix} i_d \\ i_q \end{bmatrix} + \begin{bmatrix} 0 \\ P\frac{\pi}{\tau}\frac{v_x}{R_c}\lambda_m \end{bmatrix} \quad \text{(A)} \tag{2.30}$$

and

$$\begin{bmatrix} V_d \\ V_q \end{bmatrix} = \begin{bmatrix} R_a & -P\frac{\pi}{\tau}v_x L_q\left(1+\frac{R_a}{R_c}\right) \\ P\frac{\pi}{\tau}v_x L_d\left(1+\frac{R_a}{R_c}\right) & R_a \end{bmatrix} \begin{bmatrix} i_d \\ i_q \end{bmatrix} + \begin{bmatrix} 0 \\ P\frac{\pi}{\tau}v_x\lambda_m\left(1+\frac{R_a}{R_c}\right) \end{bmatrix} \text{(V)} \tag{2.31}$$

The stator copper loss, P_{cu}, for the linear PM synchronous machine is calculated as follows:

$$P_{cu} = \frac{3}{2}R_a\left(i_{ds}^2 + i_{qs}^2\right) \quad \text{(W)} \tag{2.32}$$

The core loss, P_c, for the linear PM synchronous machine is

$$P_c = \frac{3}{2}R_c\left(i_{dc}^2 + i_{qc}^2\right) \quad \text{(W)} \tag{3.33}$$

where $i_{dc} = -P\frac{\pi}{\tau}v_x\frac{L_q i_q}{R_c}$ and $i_{qc} = P\frac{\pi}{\tau}v_x\frac{\left(L_d i_d + \lambda_m\right)}{R_c}$ therefore:

$$P_c = \frac{3}{2}\left(\left(P\frac{\pi}{\tau}v_x\right)^2\frac{L_q^2 i_q^2}{R_c} + \left(P\frac{\pi}{\tau}v_x\right)^2\frac{\left(L_d i_d + \lambda_m\right)^2}{R_c}\right) \quad \text{(W)} \tag{2.34}$$

The total electrical losses are

$$P_{EL} = \frac{3}{2}R_a\left(i_{ds}^2 + i_{qs}^2\right) + \frac{3}{2}\left(\left(P\frac{\pi}{\tau}v_x\right)^2\frac{L_q^2 i_q^2}{R_c} + \left(P\frac{\pi}{\tau}v_x\right)^2\frac{\left(L_d i_d + \lambda_m\right)^2}{R_c}\right) \quad \text{(W)} \tag{2.35}$$

The mechanical loss is due to mover friction and is proportional to the square of motor velocity. The mechanical loss is expressed as follows:

$$F_{mech} = D\,v_x \quad , \quad P_{mech} = v_x\,F_{mech} = D\,v_x^2 \quad \text{(W)} \tag{2.36}$$

where F_{mech} and P_{mech} are the force due mechanical loss and mechanical loss, v_x is the synchronous velocity, $v_x = \frac{2\pi f}{P}$; f and P are supply frequency and number of pairs of pole.

2.7 Standard Efficiency Test Simulations Results

The accepted method for determining the capability of an electrical machine to meet its nameplate rating is testing the machine under full load. The full load test for efficiency evaluation is simulated using MATLAB and SIMULINK for both the permanent magnet synchronous motor and the linear permanent magnet synchronous motor. The common method of performing full-load performance testing of a three phase permanent magnet synchronous machines is to apply full load torque to the machine's output shaft. Simulation, using accurate machine parameters, will reduce test time in the practical situation, since the correct input conditions can be determined prior to commencement of the test.

2.7.1 Simulation Results For PM synchronous machine

A standard efficiency test for efficiency evaluation of PM synchronous machine is simulated using MATLAB and SIMULINK which is provided in Appendix C. The parameters of the machine are shown in Table 2.1.

Table 2.1 The electrical and mechanical parameters of the test PM synchronous machine

Parameters	Values
Rated output power	843 W
Maximum rated current	10.5 A
Rated speed	4000 rpm
Maximum Bus Voltage	340 V
Armature resistance, R_a	0.55Ω
Core loss resistance, R_c	300Ω
Quadrature axis inductance, L_q	0.65 mH
Direct axis inductance, L_d	0.65 mH
Moment of inertia, J	7.85×10^{-5} kg.m^2
Damper coefficient, B	3.47×10^{-5} Nms^{-1}
Total permanent magnet flux linkage, λ_m	37.7 mWb
Number of poles	8

Figure 2.11 shows the current waveforms during the full load condition. The maximum current is 10.5 Amps which confirms the machine is fully loaded and current waveform has system frequency of 266.7 Hz during the full load condition, equivalent to 4000 rpm.

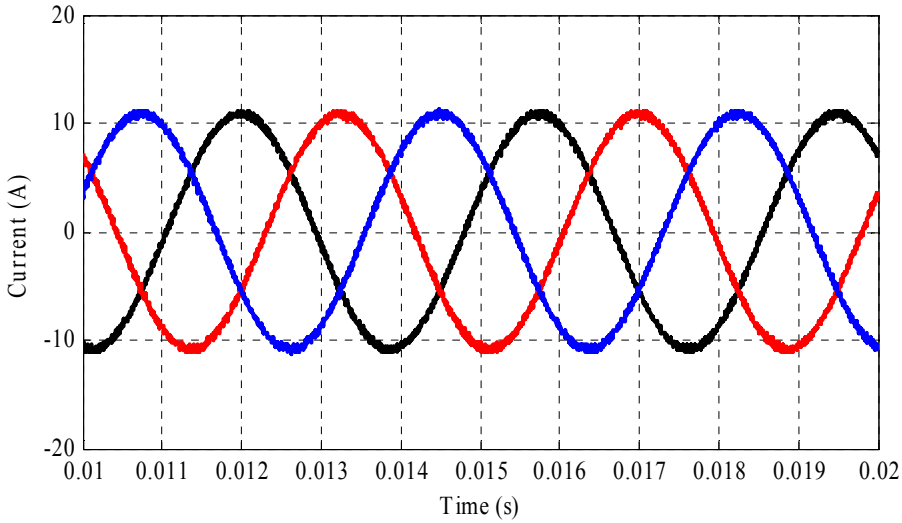

Figure 2.11 The three phase currents of the PM synchronous motor under full-load torque at rated speed

Figure 2.12 shows the instantaneous line voltages waveform during the full load condition. The peak line voltage is 120 V at a rotor speed of 4000 rpm.

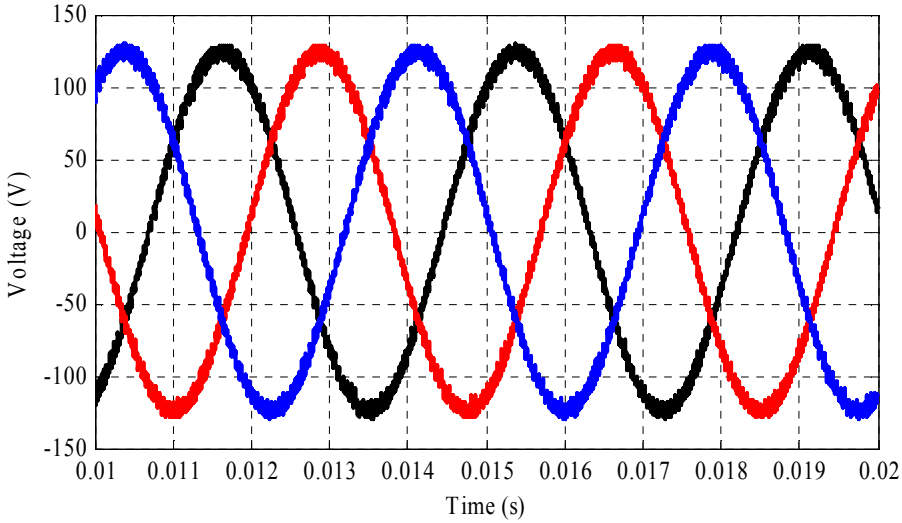

Figure 2.12 The three phase line voltages of the PM synchronous motor under full-load torque at rated speed

The simulation results show that the current, speed and torque using full load torque are consistent with the machine nameplate. The simulation results are summarized in Table 2.2.

Table 2.2 Simulation results of the standard efficiency test for the PM synchronous machine under full-load torque conditions

	Standard Efficiency Test Method
rms voltage	90.0V
rms current	7.45 A
Speed	4000 rpm
Output power	843.0 W
Input power	962.0 W
Stator copper loss	91.6 W (78.0%)
Iron loss	19.8 W (16.9%)
Friction & windage loss	6.1 W (5.1%)
Total losses	117.5 W
Efficiency (%)	87.8

2.7.2 Simulation Results For IPM synchronous machine

A standard efficiency test for efficiency evaluation of IPM synchronous machine is simulated using MATLAB and SIMULINK. The parameters of the machine are shown in Table 2.3.

Table 2.3 The electrical and mechanical parameters of the test IPM synchronous machine

Parameters	Values
Rated output power	165W
Maximum rated current	2.0A
Rated speed	900 rpm
Maximum Bus Voltage	200 V
Armature resistance, R_a	7.0Ω
Core loss resistance, R_c	1580Ω
Quadrature axis inductance, L_q	120 mH
Direct axis inductance, L_d	65 mH
Moment of inertia, J	4.5×10^{-3} kg.m^2
Damper coefficient, B	2.7×10^{-4} Nms^{-1}
Total permanent magnet flux linkage, λ_m	0.6 Wb
Number of poles	2

The simulation results show that the current, speed and torque using full load torque are consistent with the machine nameplate. The simulation results are summarized in Table 2.4.

Table 2.4 Simulation results of the standard efficiency test for the IPM synchronous machine under full-load torque conditions

	Standard Efficiency Test Method
rms voltage	90.8V
rms current	1.42A
Speed	900 rpm
Output power	165.4W
Input power	213.7W
Stator copper loss	42.4W (87.7%)
Iron loss	3.53W (7.3%)
Friction & windage loss	2.41W (5.0%)
Total losses	48.3W
Efficiency (%)	77.4

2.7.3 Simulation Results For the Linear PM synchronous machine

A standard efficiency test for efficiency evaluation of the linear PM synchronous machine has been simulated using MATLAB and SIMULINK. The parameters of the machine are shown in Table 2.5.

Table 2.5 Electrical and mechanical parameters of the linear PM synchronous machine

Parameters	Values
Rated output power	130 W
Peak rated current	3.3 A
Rated velocity	2.56 ms^{-1}
Maximum Bus Voltage	220 V
Armature resistance, R_a	3.01 Ω
Core loss resistance, R_c	625 Ω
Quadrature axis inductance, L_q	1.95 mH
Direct axis inductance, L_d	1.95 mH
Mover mass, M	1.25 kg
Damper coefficient, D	0.14 Nsm^{-1}
Total Permanent magnet flux linkage, λ_m	84.75 mWb
Number of poles	4

Figure 2.13 and 2.14 show the instantaneous current and voltage profile with the full load condition. The maximum current and voltage are 3.3 A and 63.8 Volt respectively which confirms the machine is fully loaded. The current waveform has system frequency of 50 Hz during the full load condition.

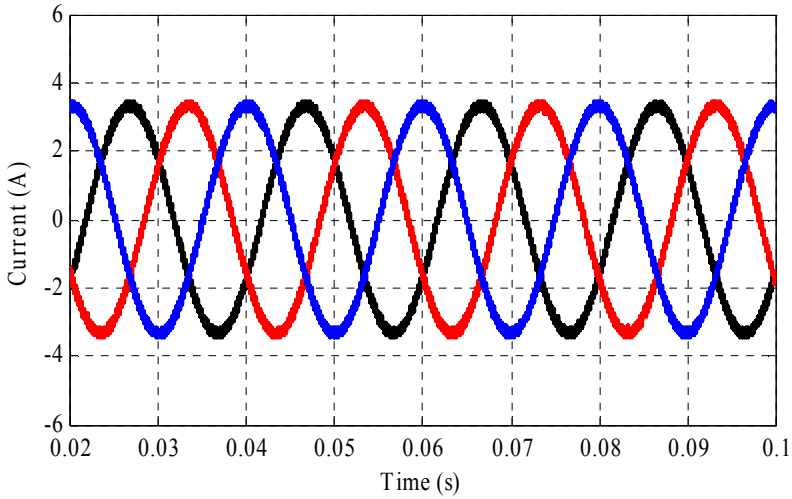

Figure 2.13 Three phase currents of the linear PM synchronous motor with the full-load condition

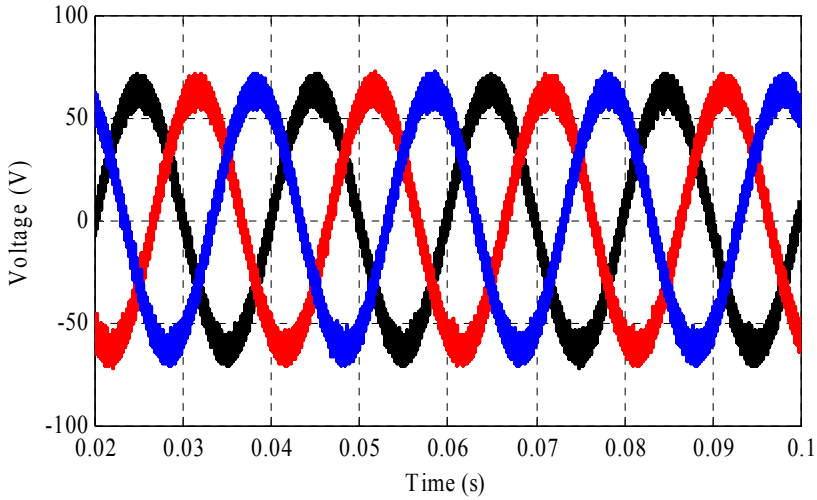

Figure 2.14 Three phase line voltages of the linear PM synchronous motor with the full-load condition

The standard efficiency test has been simulated using full load force. The simulation results are summarized in Table 2.6. Simulation results show that the current, velocity and force using full load force on the machine's output shaft are consistent with the machine nameplate. It highlights from Table 2.6 that the value of

core loss and friction and windage loss are small compared with the stator copper loss. This is a consequence of the mode operation for linear PM synchronous machines. Historically, linear machines have been used in actuation applications where high forces are required but the shaft moves at low velocities with lower terminal voltage hence excitation frequency. Thus the core loss component is small compared with the ohmic loss at full load force.

Table 2.6 Simulation results of the standard efficiency test for the linear PM synchronous machine at full-load force

	Standard Efficiency Test Method
rms voltage	45.1 V
rms current	2.32 A
Velocity	2.56 ms^{-1}
Output power	128.5 W
Input power	179.5 W
Stator copper loss	48.3 W (94.7%)
Iron loss	1.72 W (3.4%)
Friction & windage loss	0.92 W (1.8%)
Total losses	51.0 W
Efficiency (%)	71.6

2.8 Summary

This chapter describes the basic theory of common permanent magnet synchronous machines namely, the PM synchronous machine, the IPM synchronous machine and the linear PM synchronous machine. The objective of this research is to investigate the suitability of synthetic loading as a method of efficiency evaluation for PM synchronous machines and compare with standard efficiency tests, therefore, the literature review of the standard efficiency test and synthetic loading test have been reviewed. Mathematical models for both rotary and linear permanent magnet synchronous machine have been developed in the synchronously rotating d-q axis reference frame. The standard efficiency test has been simulated for both PM synchronous machines and linear PM synchronous machines. The simulated results of the standard efficiency test will be used to validate the synthetic loading technique in chapter four. The literature review shows that synthetic loading applied to PM synchronous machines has attracted little research effort.

References

[1] P. Vas, "Electrical Machines and Drives", Clarendon Press. Oxford, 1992

[2] F. Lin, H. Shieh, P. Shieh and P. Shen, "An adaptive recurrent-neural-network motion controller for X-Y table in CNC Machine", IEEE Transactions on Systems, Man. And Cybernetics, Part B: Cybernetics, Vol. 36, No. 2, April 2006, pp. 286-299.

[3] T. Bogani, A. Lidozzi, L. Solero and A. Di Napoli, "Synergetic Control of PMSM Drives for High Dynamic Applications", IEEE International Conference on Electric Machines and Drives, 15 May 2005, pp. 710-717.

[4] S. Morimoto, Y.T. Takeda and T. Hirasa, "Loss Minimization Control of Permanent Magnet Synchronous Motor Drives", IEEE Transactions on Industrial Electronics, Vol. 41, No. 5, October 1994, pp. 511-517.

[5] G. R. Slemon, "High-Efficiency Drives Using Permanent-Magnet Motors", Industrial Electronics, Control and instrumentation, 1993, Proceedings of the IECON'93. International Conference, Vol. 2, on 15-19 November, 1993, pp. 725-730.

[6] P. Pillay and R. Krishnan, "Application Characteristics of Permanent Magnet Synchronous and Brushless dc Motors for Servo Drives", IEEE Transactions on Industry Applications, Vol. 27, No. 5, September/October 1991, pp. 986-996.

[7] J. Habibi, S. Vaez-Zadeh, "Efficiency-Optimizing Direct Torque Control of Permanent Magnet Synchronous Machines", Power Electronic Specialists, 2005 IEEE 36th Conference on June 12, 2005, pp. 759-764.

[8] M. Rahman, "High Efficiency Permanent Magnet Synchronous Motors", IEEE IAS Meeting, 1979, pp. 561-564.

[9] C. C. Mi, G.R. Slemon and R. Bonert, "Modelling of Iron Losses of Permanent Magnet Synchronous Motors", IEEE Transactions on Industry Applications, Vol. 39, No. 3, May/June 2003, pp. 734-742.

[10] F. Fernández-Bernal, A. García-Cerrada and R. Faure, "Determination of Parameters in Interior Permanent Magnet Synchronous Motors With Iron Losses Without Torque Measurement", IEEE Transactions on Industry Applications, Vol. 37, No. 5, September/October 2001, pp. 1265-1272.

[11] G. R. Slemon and X. Liu, "Core Losses in Permanent Magnet Motors", IEEE Transactions on Magnetics, Vol. 26, No. 5, September 1990, pp. 1653-1655.

[12] T. J. E. Miller and R. Rabinovici, "Back EMF Waveforms and core losses in brushless DC motors", IEE Proceeding Electric Power Applications, Vol. 141, No. 3, May 1994, pp. 144-154.

[13] G. Bertotti, A. Boglietti, M. Chiampi, D. Chiarabaglio, F. Fiorillo and M. Lazzari, "An Improved Estimation of Iron Losses in Rotating Electrical Machines", IEEE Transactions on Magnetics, Vol. 27, No. 6, November 1991, pp. 5007-5009

[14] F. Deng, "An Improved Iron Loss Estimation for Permanent Magnet Brushless Machines", IEEE Transaction on Energy Conversion, Vol. 14, No. 4, December 1999, pp. 1391-1395.

[15] N. Urasaki, T. Aenjyu and K. Uezato, "Influence of All Losses on Permanent Magnet Synchronous Motor Drives", Industrial Electronics Society, 2000, IECON2000, 26th Annual Conference of the IEEE, Vol.2, 22-28 October 2000, pp. 1371-1376.

[16] L. Xu, X. Xu, A. Lipo and D.W. Novotny, "Vector Control of a Synchronous Reluctance Motor Including Saturation and Iron Loss", IEEE Transactions on Industry Applications, Vol. 27, No. 5, September/October 1991, pp.977-985.

[17] J.E. Fletcher, B.W. Williams and T.C. Green, "Efficiency Aspects of Vector Control Applied to Synchronous Reluctance Motors", Industry Applications Conference, 1995, Thirtieth IAS Annual Meeting, IAS'95, Conference Record of the 1995 IEEE, Vol. 1, 8-12 October 1995, pp. 294-300.

[18] F. Fernández-Bernal, A. García-Cerrada and R. Faure, "Efficient Control of Reluctance Synchronous Machines" Industrial Electronics Society, 1998, IECON'98, Proceeding of the 24th Annual Conference of the IEEE, Vol. 2, 31 August-4 September 1998, pp. 923-928.

[19] C. Grantham, H. Tabatabaei-Yazdi and M. F. Rahman, "A Novel Method for Rapid Efficiency Measurement of Three Phase Induction Motors", IEEE Transactions on Energy Conversion, Vol. 14, No. 4, December 1999, pp. 1236-1240.

[20] D. J. McKinnon and C. Grantham, "Efficiency Evaluation of Three-Phase Induction Motors Using Dual-Frequency and Sweep-Frequency Methods of Synthetic Loading", Power Electronics, Machines and Drives, 2004. (PEMD

2004). Second International Conference on (Conf. Publ. No. 498), Vol. 2, 31 March-2 April 2004, pp. 799-804.

[21] D. S. J. McKinnon and C. Grantham, "Improved Efficiency Test Methods for Three Phase Induction Machines", Industry Application Conference, 2005. Fourtieth IAS Annual Meeting. Conference Record of the 2005, Vol. 1, 2-6 October 2005, pp. 466-473.

[22] A. Boglietti, A. Cavagnino, M. Lazzari and M. Pastorelli, "International Standards for the Induction Motor Efficiency Evaluation: A Critical Analysis of the Stray Load Loss Determination", IEEE Transactions on Industry Applications, Vol. 40, No. 5, September/October 2004, pp. 1294-1301.

[23] A. Boglietti, A. Cavagnino, M. Lazzari and M. Pastorelli, "Induction Motor Efficiency Measurements in accordance to IEEE 112-B, IEC 34-2 and JEC 37 International Standards", Electric Machines and Drives Conference, 2003, IEMDC'03, IEEE International, Vol. 3, 1-4 June 2003, pp. 1599-1605.

[24] B. Renier, K. Hameyer and R. Belmans, "Comparison of standards for determining efficiency of three phase induction motors", IEEE Transactions on Energy Conversion, Vol. 14, No. 3, September 1999, pp. 512-517.

[25] N. K. Ghai, "IEC And NEMA Standards For Large Squirrel Cage Induction Motors A Comparison", IEEE Transactions on Energy Conversion, Vol. 14, No. 3, September 1999, pp.545-552.

[26] G. G. Gray and W. J. Martiny, "Efficiency Testing of Medium Induction Motors A Comment on IEEE Std. 112-1991", IEEE Transactions on Energy Conversion, Vol. 11, No. 3, September 1996, pp.495-499.

[27] K. Yamazaki and Y. Haruishi, "Stray Load Loss Analysis of Induction Motor Comparison of Measurement Due to IEEE Standard 112 and Direct Calculation by Finite Element Method", IEEE Transactions on Industry Applications, Vol. 40, No. 2, March/April 2004, pp. 543-549.

[28] C. N. Glew, "Stray load losses in induction motors: a challenge to academia", Power Engineering Journal, Vol. 12, Issue 1, February 1998, pp. 27-32.

[29] H. Auinger, "Determination and designation of the efficiency of electrical machines", Power Engineering Journal, Vol. 13, Issue 1, February 1999, pp. 15-23.

[30] S. L. Ho and W. N. Fu, "Analysis of indirect Temperature-Rise Tests of Induction Machines Using Time Stepping Finite Element Method", IEEE Transactions on Energy Conversion, Vol. 16, No. 1, March 2001, pp. 55-60.

[31] I. Boldea, L. Tutelea and C. Klumpner, "Artificial Loading of Induction Machines: A Review", Workshop on Electrical Machine's Parameters, Technical University of Cluj-Napoca, 26th May 2001, pp. 9-14.

[32] A. Mihalcea, B. Szabados and J. Hoolboom, "Determining Total Losses and Temperature Rise in Induction Motors Using Equivalent Loading Methods", IEEE Transactions on Energy Conversion, Vol. 16, No. 3, September 2001, pp. 214-219.

[33] J. Soltani, B. Szabados and J. Hoolboom, "A Novel Method of Measurement of Synchronous Machine Losses Using Synthetic Loading", IEEE Transactions on Instrumentation and Measurement, Vol. 51, No. 6, December 2002, pp. 1228-1233.

[34] J. Soltani, B. Szabados and J. Hoolboom, "A New Synthetic Loading for Large Induction Machines With No Feedback into the Power System", IEEE Transactions on Energy Conversion, Vol. 17, No. 3, September 2002, pp. 319-324.

[35] L. Consolini and A. Piazzi, "Generalized bang-bang control for feedforward constrained regulation", 45th IEEE Conference on Decision and Control, 13-15 December 2006, pp. 893-898.

[36] D. J. McKinnon and C. Grantham, "On-Site Efficiency Evaluation of Three-Phase Induction Motors Using Synthetic Loading Methods", Power Electronics, Machines and Drives, 2004. (PEMD 2004). Second International Conference on (Conf. Publ. No. 498), Vol. 1, 31 March-2 April 2004, pp. 291-296.

[37] C. Grantham, M. Sheng and E. D. Spooner, "Synthetic loading of three phase induction motors using microprocessor controlled power electronics", IEE Proc. Electric Power Application, Vol. 141, No. 2, March 1994, pp. 101-108.

[38] Y. Yan and J. Zhu, "Simulation of A Direct Torque Controlled PMSM Drive Incorporating Structural and Saturation Saliencies", 37th IEEE Power Electronics Specialists Conference, 18-22 June 2006, pp. 1-6.

[39] M. A. Rahman and P. Zhou, "Analysis of Brushless Permanent Magnet Synchronous Motors", IEEE Transactions on Industrial Electronics, Vol. 43, No. 2, April 1996, pp. 256-267.

[40] M. A. Rahman and P. Zhou, "Analysis of Brushless Permanent Magnet Synchronous Motors", IEEE Transaction on Industrial Electronics, Vol. 43, No. 2, April 1996, pp. 256-267.

[41] N. Urasaki, T. Senjyu and K. Uezato, "Relationship of Parallel Model and Series Model for Permanent Magnet Synchronous Motors Taking Iron Loss Into Account", IEEE Transactions on Energy Conversion, Vol. 19, No. 2, June 2004, pp. 265-270.

[42] Y. Kung, "High Performance PMLSM Drives using TMS320F2812 DSP Controller", The 2004 IEEE Asia-Pacific Conference on Circuit and Systems, Vol.2, 6-9 December 2004, pp. 645-648.

Chapter Three
Mathematical Models of Permanent Magnet Synchronous Machines under Synthetic Loading

3.1 Introduction

In this chapter mathematical model of PM synchronous machines under the synthetic loading method are developed. The quadrature axis current and speed equations to establish appropriate synthetic loading conditions are developed for both types of machine. The resultant voltage equations, using d- and q-axis equivalent circuits including core resistance, are developed. The models allow the impact of synthetic loading frequency on the required inverter DC link voltage and inverter volt-ampere rating to be assessed. In addition, the models allow the effects of additional moment of inertia for the rotational machine, (and additional mover mass for the linear machine) on the synthetic loading frequency to be evaluated in order to obtain a constant swing (peak to peak) speed. The mathematical models are then generalized.

The models, which are used to represent permanent magnet synchronous machines, make certain approximations such as the winding of the machine are assumed to be symmetrical, a constant air-gap and all machine parameters are assumed to be constant. These approximations arise partly out of a wish to determine the electromechanical dynamic performance of permanent magnet synchronous machines [1]. Accordingly, it is desirable to reduce the complexity of the permanent magnet synchronous machine model whilst maintaining an acceptable level of accuracy. This will lead to a meaningful judgement on the design and system operation [2], [3]. The approximations illustrate that the simulation results over estimated the efficiency by 1.0% compared with the experiment results.

The permanent magnet synchronous machine models are based on Park's equations whereby the differential equations relating instantaneous currents and voltages in the stator *abc* reference frame are transformed into a rotor *dq* reference

frame resulting in differential equations which are constant rather than time vary coefficients in the steady-state [4]. The solutions to these equations yield instantaneous currents, which are used to determine the electromagnetic torque developed by the PM synchronous machine. This torque is then used in the basic velocity swing equation, in conjunction with mechanical and damping torque acting on the rotor, to determine the rotor speed of the PM synchronous machine.

3.2 Mathematical Model of Synthetic Loading for the PM Synchronous Machine

Generally, low order mathematical models are used to represent PM synchronous machines in simulating and analyzing dynamic behaviour. Five nonlinear differential equations, based on Park's *dq* axis representation [5], [6], are used to represent PM synchronous machines. These equations are arranged in a set of first order differential equations which are derived from the d- and q-axis equivalent circuit illustrated in Figure 3.1. The derivations in Section 3.2 do not assume L_d=L_q therefore are applicable to both the surface-mount and IPM machines. A technique to measure the parameters of the PM synchronous machine are presented in Appendix D.

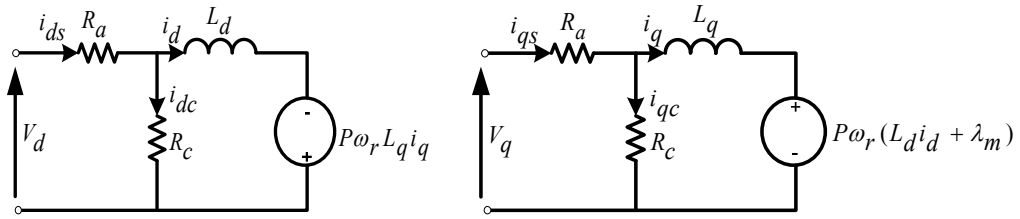

(a) d-axis (b) q-axis

Figure 3.1 d- and q-axis equivalent circuit of PM synchronous machines

The voltage equations of the PM synchronous machine in the *dq* synchronous frame can be expressed as

$$V_d = R_a i_d + L_d\left(1+\frac{R_a}{R_c}\right)\frac{di_d}{dt} - P\omega_r L_q i_q\left(1+\frac{R_a}{R_c}\right) \quad \text{(V)} \tag{3.1}$$

$$V_q = R_a i_q + L_q\left(1+\frac{R_a}{R_c}\right)\frac{di_q}{dt} + \left(1+\frac{R_a}{R_c}\right)P\omega_r\left(L_d i_d + \lambda_m\right) \quad \text{(V)} \tag{3.2}$$

where,

V_d and V_q are the applied *d*- and *q*-axis stator voltages (V), respectively.

i_d and i_q are *d*- and *q*-axis torque generating currents (A), respectively.

R_a and R_c are stator and core loss resistances (Ω), respectively.

L_d and L_q are *d*- and *q*-axis self inductances (H), respectively.

λ_m is the permanent magnet flux linkages (Wb).

ω_r is the rotor speed (rad/s).

P is number of pole pairs.

The electromagnetic torque, T_e, developed by the rotor is described by

$$T_e = \frac{3}{2} P \left(\lambda_m \, i_q + \left(L_d - L_q \right) i_q \, i_d \right) \quad \text{(N.m)} \tag{3.3}$$

The dynamic equation of the speed is:

$$\frac{d\omega_r}{dt} = (\, T_e - T_L - B\omega_r \,)/J \tag{3.4}$$

where T_L is the load torque, and J and B are moment of inertia and damper coefficient respectively. The position, θ, is given by

$$\frac{d\theta}{dt} = P\omega_r \tag{3.5}$$

3.2.1 Quadrature Axis Current Algorithm

The key step in performing a synthetic loading test on a permanent magnet synchronous machine is the correct choice of quadrature axis current waveform, i_q, in order to produce rated rms phase current at rated rms phase voltage. The reference i_q waveform must be chosen correctly to force the machine to accelerate and decelerate. The drive current, i_q, takes the form.

$$i_q = I_m \sin\left(2\pi f_n t\right) + I_o \qquad \text{(A)} \tag{3.6}$$

where I_m is the magnitude of AC perturbation current, I_o is a dc offset current and f_n is synthetic loading frequency (Hz). Typically I_m is larger than I_o, but all three

parameters in (3.6) need to be chosen to force rated conditions in the machine under test.

As the machine torque is linearly related to i_q, the generated torque alternates between positive and negative values if $I_m > I_o$. The frequency and magnitude (f_n and I_m respectively) of the AC component effectively controls the AC variations in the rotor speed (assuming constant mechanical parameters) and the dc offset component controls the average rotor speed.

(i) Determining I_o in terms of machine parameters

During synthetic loading the machine should run, on average, at rated speed. In addition, as the load torque T_L equals zero (there is no load) the electrical torque generated balances only the torque due to friction and windage.

$$T_{eav} = B\omega_{ro} = \left(k_t + k_r i_d\right) f_n \int_0^{\frac{1}{f_n}} \left(I_m \sin\left(2\pi f_n t\right) + I_o\right) dt \qquad \text{(N.m)} \tag{3.7}$$

where $k_t = \frac{3}{2} P\lambda_m$ is the machine torque constant in (Nm/A), $k_r = \frac{3}{2} P\left(L_d - L_q\right)$ is IPM synchronous machine reluctance torque constant, and B is damper coefficient in (Nms), P is number of pairs of poles, λ_m is linkage flux, and i_d is direct axis current.

During synthetic loading the required dc offset current I_o is a function of average desired machine speed and the mechanical parameters. T_{eav} is the average electromagnetic torque during synthetic loading and ω_{ro} is rated steady state rotor speed.

By solving and rearranging (3.7) the expression for I_o is described by

$$I_O = \frac{B\,\omega_{ro}}{k_t + K_r i_d} \qquad \text{(A)} \tag{3.8}$$

For surface-mount PM synchronous machines $L_d = L_q$ this leads to $k_r = 0$, and for vector control application without field weakening in the IPM machine $i_d = 0$. Thus (3.8) is simplified to

$$I_O = \frac{B\,\omega_{ro}}{k_t} \quad \text{(A)} \tag{3.9}$$

That is the average dc offset current required is the friction torque divided by the torque factor of the machine. In the test set-up, I_o is used to independently control the average speed of rotation.

(ii) Determining I_m in terms of machine parameters

The magnitude of AC perturbation I_m is a function of machine rated rms current I_s, the dc offset current I_o and the direct axis current i_d. In order that the machine draws rated current during synthetic loading

$$\frac{\left(i_q^2 + i_d^2\right)}{2} = I_s^2 \quad \text{(A)} \tag{3.10}$$

Substituting (3.6) into (3.10), and taking the average for one synthetic loading cycle

$$I_s^2 = \frac{f_n}{2}\int_0^{\frac{1}{f_n}} \left(I_m \sin\left(2\pi f_n t\right) + I_o\right)^2 dt + f_n \int_0^{\frac{1}{f_n}} \frac{i_d^2}{2} dt \tag{3.11}$$

Solving and rearranging (3.11) gives the AC perturbation current as

$$I_m = \sqrt{4I_s^2 - 2I_o^2 - 2i_d^2} \quad \text{(A)} \tag{3.12}$$

where I_s is the rated rms current of the PM synchronous machine under test. When vector control is applied the reference value of the direct axis current will be zero therefore:

$$I_m = \sqrt{4I_s^2 - 2I_o^2} \quad \text{(A)} \tag{3.13}$$

3.2.2 Speed Equation

During synthetic loading the machine accelerates and decelerates. However, the rotor speed must equal, on average, the rated rotor speed. The rotor speed, ω_r, is determined from the solution of dynamic equation (3.4). Substituting (3.6) into the

torque equation (3.3), then substitute the electromagnetic torque into the dynamic equation and rearranging yields:

$$J\frac{d\omega_r}{dt}+B\omega_r=k_tI_m\sin(2\pi f_nt)+k_tI_o-k_ri_dI_m\sin(2\pi f_nt)-k_ri_dI_o \tag{3.14}$$

Using Laplace transforms to solve (3.14) for ω_r gives:

$$\omega_r(s)=\left[\frac{(k_t+k_ri_d)(2\pi f_n)I_m}{J\left(s+\frac{B}{J}\right)\left(s^2+(2\pi f_n)^2\right)}\right]+\left[\frac{(k_t+k_ri_d)I_o}{Js\left(s+\frac{B}{J}\right)}\right] \tag{3.15}$$

By applying partial fraction expansion and Laplace inverse transformation to (3.15), the rotor speed is described with respect to time as

$$\begin{aligned}\omega_r=&\frac{(k_t+k_ri_d)I_o}{B}+\frac{(k_t+k_ri_d)I_mB/J^2}{(2\pi f_n)^2+\left(\frac{B}{J}\right)^2}\sin(2\pi f_nt)-\frac{(k_t+k_ri_d)(2\pi f_n)I_m/J}{(2\pi f_n)^2+\left(\frac{B}{J}\right)^2}\cos(2\pi f_nt)\\&+\left[\frac{(k_t+k_ri_d)(2\pi f_n)I_m/J}{(2\pi f_n)^2+\left(\frac{B}{J}\right)^2}-\frac{(k_t+k_ri_d)I_o}{B}\right]e^{-\frac{B}{J}t}\end{aligned} \tag{3.16}$$

In time the exponential term decays to zero, hence

$$\left[\frac{(k_t+k_ri_d)(2\pi f_n)I_m/J}{(2\pi f_n)^2+\left(\frac{B}{J}\right)^2}-\frac{(k_t+k_ri_d)I_o}{B}\right]e^{-\frac{B}{J}t}=0,$$

Therefore, the synthetic loading rotor speed, is given as

$$\omega_r=\frac{(k_t+k_ri_d)I_o}{B}+\frac{(k_t+k_ri_d)I_mB/J^2}{(2\pi f_n)^2+\left(\frac{B}{J}\right)^2}\sin(2\pi f_nt)-\frac{(k_t+k_ri_d)(2\pi f_n)I_m/J}{(2\pi f_n)^2+\left(\frac{B}{J}\right)^2}\cos(2\pi f_nt)\text{(rad/s)} \tag{3.17}$$

And

$$\omega_r=\frac{(k_t+k_ri_d)I_o}{B}+\frac{(k_t+k_ri_d)I_m/J}{\sqrt{(2\pi f_n)^2+\left(\frac{B}{J}\right)^2}}\sin(2\pi f_nt-\phi)\quad\text{(rad/s)} \tag{3.17a}$$

where $\phi = \tan^{-1}\left[\dfrac{2\pi f_n}{B/J}\right]$

The equation demonstrates that the speed has a dc offset term plus a sinusoidal variation at the synthetic loading frequency.

For surface-mount PM synchronous machines $L_d=L_q$ this yields, $k_r=0$, and for vector control application $i_d=0$, therefore (3.17) becomes:

$$\omega_r = \frac{k_t I_o}{B} + \frac{k_t I_m B/J^2}{(2\pi f_n)^2 + \left(\frac{B}{J}\right)^2}\sin(2\pi f_n t) - \frac{k_t (2\pi f_n) I_m/J}{(2\pi f_n)^2 + \left(\frac{B}{J}\right)^2}\cos(2\pi f_n t) \quad \text{(rad/s)} \tag{3.18}$$

And

$$\omega_r = \frac{k_t I_o}{B} + \frac{k_t\, I_m/J}{\sqrt{(2\pi f_n)^2 + \left(\frac{B}{J}\right)^2}}\sin(2\pi f_n t - \phi) \quad \text{(rad/s)} \tag{3.18a}$$

(i) Determining maximum and minimum of rotor speed

When the synthetic loading method is applied, the knowledge of maximum and minimum rotor speed is important. The difference between the maximum and minimum of the rotor speed gives an indication of the rotor speed swing. It is preferable that the swing is as small as possible to reduce the required dc link voltage and the inverter volt-ampere rating. This is because the inverter VA rating and the dc link voltage required are proportional to the swing speed and the swing speed is inversely proportional to the synthetic loading frequency. The synthetic loading frequency can be determined to provide a desired peak to peak rotor speed variation, therefore, provides a design method for choosing a perturbation frequency. From (3.17) the maximum and minimum rotor speeds are determined.

Using trigonometric identities and manipulations, the maximum rotor speed is

$$\omega_r(\max) = \frac{(k_t + k_r i_d) I_o}{B} + \frac{(k_t + k_r i_d) I_m/J}{\sqrt{(2\pi f_n)^2 + \left(\frac{B}{J}\right)^2}} \quad \text{(rad/s)} \tag{3.19}$$

For surface-mount PM synchronous machines $L_d=L_q$, therefore, $k_r=0$, and for vector control application $i_d=0$. Thus (3.19) becomes.

$$\omega_r(\max) = \frac{k_t I_o}{B} + \frac{k_t I_m / J}{\sqrt{(2\pi f_n)^2 + \left(\frac{B}{J}\right)^2}} \quad \text{(rad/s)} \tag{3.20}$$

The minimum rotor speed is:

$$\omega_r(\min) = \frac{(k_t + k_r i_d) I_o}{B} - \frac{(k_t + k_r i_d) I_m / J}{\sqrt{(2\pi f_n)^2 + \left(\frac{B}{J}\right)^2}} \text{ (rad/s)} \tag{3.21}$$

During the application of vector control the direct axis current $i_d=0$, and $L_d=L_q$ therefore $k_r=0$ in (3.21), which leads to the following

$$\omega_r(\min) = \frac{k_t I_o}{B} - \frac{k_t I_m / J}{\sqrt{(2\pi f_n)^2 + \left(\frac{B}{J}\right)^2}} \text{ (rad/s)} \tag{3.22}$$

(ii) Determining f_n in terms of the machine parameters

The synthetic loading frequency, f_n, is important. The synthetic loading frequency has an impact on the DC link voltage and inverter volt-ampere rating hence proper choice of synthetic frequency is essential in order to avoid needlessly over rating the power converter components. The peak to peak speed variation, $\Delta\omega_r$, can be determined from:

$$\Delta\omega_r = \omega_r(\max) - \omega_r(\min)$$

$$\Delta\omega_r = 2\frac{(k_t + k_r i_d) I_m / J}{\sqrt{(2\pi f_n)^2 + \left(\frac{B}{J}\right)^2}} \text{ (rad/s)} \tag{3.23}$$

The above equation is for the IPM synchronous machine, however, for surface-mount PM synchronous machines $k_r=0$ and $i_d=0$ therefore (3.23) is simplified to:

$$\Delta\omega_r = 2\frac{k_t I_m / J}{\sqrt{(2\pi f_n)^2 + \left(\frac{B}{J}\right)^2}} \quad \text{(rad/s)} \tag{3.24}$$

From (3.23) the synthetic loading frequency can be determined if a required $\Delta\omega_r$ is specified along with I_m and assuming the mechanical parameters are known

$$f_n = \frac{\sqrt{\left(\frac{2(k_t + k_r i_d) I_m}{J}\right)^2 - \left(\Delta\omega_r \frac{B}{J}\right)^2}}{2\pi\Delta\omega_r} \quad \text{(Hz)} \tag{3.25}$$

For the surface-mount PM machine (3.25) is simplified to

$$f_n = \frac{\sqrt{\left(\frac{2k_t I_m}{J}\right)^2 - \left(\Delta\omega_r \frac{B}{J}\right)^2}}{2\pi\Delta\omega_r} \quad \text{(Hz)} \tag{3.26}$$

The value of $\Delta\omega_r$ can be between zero and twice the rated rotor speed ($0<\Delta\omega_r\leq 2\omega_r$), nevertheless for better synthetic loading performance this value should be as small as possible. A high value of $\Delta\omega_r$ leads to a higher inverter volt-ampere rating and dc link voltage. This is because $\Delta\omega_r$ is a function of synthetic loading frequency as shown in (3.26). (3.25) and (3.26) allow the designer to select f_n in order to achieve a desired $\Delta\omega_r$. Figure 3.2 shows the effect of increasing synthetic loading frequency on the speed variation. Figure 3.2 is simulated using the MATLAB m-file in Appendix C. The figure illustrates that when the synthetic loading frequency increases the peak to peak speed variation decreases which leads to a lower inverter VA rating and dc link voltage required for synthetic loading.

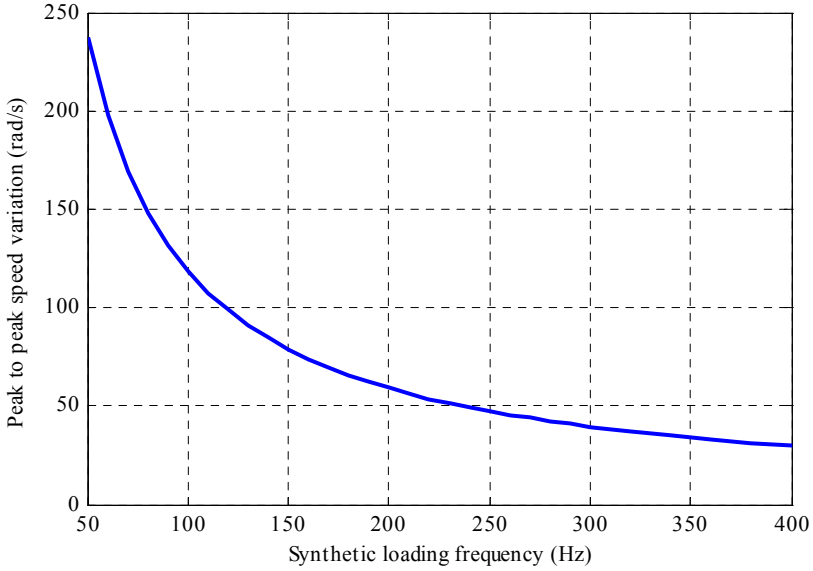

Figure 3.2 The effect of synthetic loading frequency on the speed variation

From (3.25) and (3.26) the synthetic loading period is proportional to the moment of inertia for a given value of $\Delta\omega_r$. This means that when the mechanical time constant increases a lower synthetic loading frequency is required for the same $\Delta\omega_r$. The mechanical time constant can be increased by increasing the moment of inertia, for example, by attaching additional mass to the motor shaft. The increase in inertia leads to a reduced dc link voltage and inverter volt-ampere rating required for a given value of synthetic loading frequency.

3.2.3 Direct and Quadrature Axis Voltage Equation

The direct and quadrature axis voltages are a function of the synthetic frequency. Therefore, the determination of direct and quadrature axis voltages is essential in order to understand the impact of synthetic loading frequency on volt-ampere rating of the inverter. From the voltage equations in (3.1) and (3.2) the direct and quadrature axis voltage during synthetic loading can be calculated using quadrature axis current in (3.6) and rotor speed in (3.17) for IPM synchronous machines (or (3.18) for surface-mount PM synchronous machines).

(i) Direct axis voltage equation

The direct axis voltage for the IPM synchronous machine is found to be

$$V_d = R_a i_d - L_q P\left(1+\frac{R_a}{R_c}\right)\left(I_m \sin(2\pi f_n t)+I_o\right)\left[\frac{(k_t+k_r i_d)I_o}{B}\right.$$
$$\left.+\frac{(k_t+k_r i_d)I_m\, B/J^2}{(2\pi f_n)^2+\left(\frac{B}{J}\right)^2}\sin(2\pi f_n t)-\frac{(k_t+k_r i_d)(2\pi f_n)I_m/J}{(2\pi f_n)^2+\left(\frac{B}{J}\right)^2}\cos(2\pi f_n t)\right] \text{(V)} \quad (3.27)$$

The direct axis voltage for the PM synchronous machine is:

$$V_d = -PL_q\left(1+\frac{R_a}{R_c}\right)\left(I_m \sin(2\pi f_n t)+I_o\right)\left[\frac{k_t I_o}{B}\right.$$
$$\left.+\frac{k_t I_m\, B/J^2}{(2\pi f_n)^2+\left(\frac{B}{J}\right)^2}\sin(2\pi f_n t)-\frac{k_t(2\pi f_n)I_m/J}{(2\pi f_n)^2+\left(\frac{B}{J}\right)^2}\cos(2\pi f_n t)\right] \quad \text{(V)} \quad (3.28)$$

(ii) Quadrature axis voltage equation

The quadrature axis voltage for the IPM synchronous machine is:

$$\mathrm{V}_q = R_a I_m \sin(2\pi f_n t) + R_a I_o + L_q I_m (2\pi f_n)\left(1 + \frac{R_a}{R_c}\right)\cos(2\pi f_n t)$$

$$+ P\left(1 + \frac{R_a}{R_c}\right)(L_d i_d + \lambda_m)\left[\frac{(k_t + k_r i_d)I_o}{B} + \frac{(k_t + k_r i_d)I_m B/J^2}{(2\pi f_n)^2 + \left(\frac{B}{J}\right)^2}\sin(2\pi f_n t)\right] \quad \text{(V)} \quad (3.29)$$

$$\left. - \frac{(k_t + k_r i_d)(2\pi f_n)I_m/J}{(2\pi f_n)^2 + \left(\frac{B}{J}\right)^2}\cos(2\pi f_n t)\right]$$

And for the PM synchronous machine:

$$V_q = R_a I_m \sin(2\pi f_n t) + R_a I_o + L_q I_m (2\pi f_n)\left(1 + \frac{R_a}{R_c}\right)\cos(2\pi f_n t) + P\left(1 + \frac{R_a}{R_c}\right)(L_d i_d + \lambda_m)\left[\frac{k_t I_o}{B}\right.$$

$$\left. + \frac{k_t I_m B/J^2}{(2\pi f_n)^2 + \left(\frac{B}{J}\right)^2}\sin(2\pi f_n t) - \frac{k_t (2\pi f_n) I_m/J}{(2\pi f_n)^2 + \left(\frac{B}{J}\right)^2}\cos(2\pi f_n t)\right] \quad \text{(V)} \quad (3.30)$$

The resultant stator *abc* voltage can be calculated from *dq* axis voltages by:

$$\begin{bmatrix} V_a \\ V_b \\ V_c \end{bmatrix} = \begin{bmatrix} \cos\theta & \sin\theta \\ \cos\left(\theta - \frac{2\pi}{3}\right) & \sin\left(\theta - \frac{2\pi}{3}\right) \\ \cos\left(\theta + \frac{2\pi}{3}\right) & \sin\left(\theta + \frac{2\pi}{3}\right) \end{bmatrix} \begin{bmatrix} V_d \\ V_q \end{bmatrix} \quad \text{(V)} \quad (3.31)$$

where V_a, V_b, and V_c are the stator terminal voltage of the permanent magnet synchronous machine. Using (3.31), and appropriate equations from (3.27)-(3.30) the instantaneous phase and line voltage requirements can be determined. From this the minimum dc link voltage can be identified.

3.2.4 Direct and Quadrature Axis Stator Current Equations

The stator direct and quadrature axis current are also a function of the synthetic loading frequency. The direct and quadrature axis stator current equation is determined to evaluate the stator phase current during synthetic loading. Furthermore, the stator phase current is important for the evaluation of stator copper losses, and inverter volt-ampere rating, and the direct and quarature axis stator current equations are necessary for input power calculations.

(i) Direct axis stator current equation

From Figure 3.1 (a) the direct axis stator current can be calculated using Kirchhoff's current law as:

$$i_{ds} = i_d + i_{dc} \quad \text{(A)} \tag{3.32}$$

where $i_{dc} = -P\omega_r \frac{L_q i_q}{R_c}$ and $\frac{di_d}{dt} = 0$. Therefore by substituting the equations for i_{dc}, i_q and ω_r from (3.6) and (3.17) for the IPM synchronous machines into (3.32), the direct axis stator current is then

$$i_{ds} = i_d - P\frac{L_q}{R_c}\left(k_t + k_r i_d\right)\left(I_m \sin\left(2\pi f_n t\right) + I_o\right)\left[\frac{I_o}{B} + \frac{I_m B/J^2}{\left(2\pi f_n\right)^2 + \left(\frac{B}{J}\right)^2}\sin\left(2\pi f_n t\right)\right.$$
$$\left. - \frac{\left(2\pi f_n\right) I_m/J}{\left(2\pi f_n\right)^2 + \left(\frac{B}{J}\right)^2}\cos\left(2\pi f_n t\right)\right] \quad \text{(A)} \tag{3.33}$$

For the PM synchronous machine, k_r is zero; therefore (3.33) can be rewritten as

$$i_{ds} = i_d - P\frac{L_q}{R_c}k_t\left(I_m \sin\left(2\pi f_n t\right) + I_o\right)\left[\frac{I_o}{B} + \frac{I_m B/J^2}{\left(2\pi f_n\right)^2 + \left(\frac{B}{J}\right)^2}\sin\left(2\pi f_n t\right)\right.$$
$$\left. - \frac{\left(2\pi f_n\right) I_m/J}{\left(2\pi f_n\right)^2 + \left(\frac{B}{J}\right)^2}\cos\left(2\pi f_n t\right)\right] \quad \text{(A)} \tag{3.34}$$

(ii) Quadrature axis stator current equation

From Figure 3.1 (b) the quadrature axis stator current can be calculated using Kirchhoff's current law as:

$$i_{qs} = i_q + i_{qc} \quad \text{(A)} \tag{3.35}$$

where $i_{qc} = P\omega_r \dfrac{(L_d i_d + \lambda_m)}{R_c}$. Therefore by substituting the equations for i_{qc}, i_q and ω_r from (3.6) and (3.17) for IPM synchronous machines into (3.35) gives

$$i_{qs} = I_m \sin(2\pi f_n t) + I_o + P\frac{(L_d i_d + \lambda_m)}{R_c}(k_t + k_r i_d)\left[\frac{I_o}{B} + \frac{I_m B/J^2}{(2\pi f_n)^2 + \left(\frac{B}{J}\right)^2}\sin(2\pi f_n t)\right.$$
$$\left. - \frac{(2\pi f_n) I_m/J}{(2\pi \mathrm{f_n})^2 + \left(\frac{B}{J}\right)^2}\cos(2\pi f_n t)\right] \quad \text{(A)} \tag{3.36}$$

And for the PM synchronous machine:

$$i_{qs} = I_m \sin(2\pi f_n t) + I_o + P\frac{(L_d i_d + \lambda_m)}{R_c} k_t\left[\frac{I_o}{B} + \frac{I_m B/J^2}{(2\pi f_n)^2 + \left(\frac{B}{J}\right)^2}\sin(2\pi f_n t)\right.$$
$$\left. - \frac{(2\pi f_n) I_m/J}{(2\pi f_n)^2 + \left(\frac{B}{J}\right)^2}\cos(2\pi f_n t)\right] \quad \text{(A)} \tag{3.37}$$

The stator phases current *abc* for IPM and PM synchronous machine can be calculated from the *dq* axis stator current using

$$\begin{bmatrix} i_a \\ i_b \\ i_c \end{bmatrix} = \begin{bmatrix} \cos\theta & \sin\theta \\ \cos\left(\theta - \frac{2\pi}{3}\right) & \sin\left(\theta - \frac{2\pi}{3}\right) \\ \cos\left(\theta + \frac{2\pi}{3}\right) & \sin\left(\theta + \frac{2\pi}{3}\right) \end{bmatrix} \begin{bmatrix} i_{ds} \\ i_{qs} \end{bmatrix} \quad \text{(A)} \tag{3.38}$$

where, i_a, i_b, and i_c are the stator phase currents of the permanent magnet synchronous machines and θ is the rotor position. Using (3.38) in conjunction with the appropriate i_{ds} and i_{qs} equations provides a means of determining instantaneous phase current waveform and also the peak current. This then assists in determining the VA rating of the power converter.

3.3 Mathematical Model of Synthetic Loading for the Linear PM Synchronous Machine

A similar process is performed on the linear PM synchronous machine. Five nonlinear equations are arranged as a set of first order differential equations to represent linear PM synchronous machines [7]-[10]. These differential equations are derived for the d- and q-axis equivalent circuit illustrated in Figure 3.2, where the mover velocity, v_x, is used for the translational system.

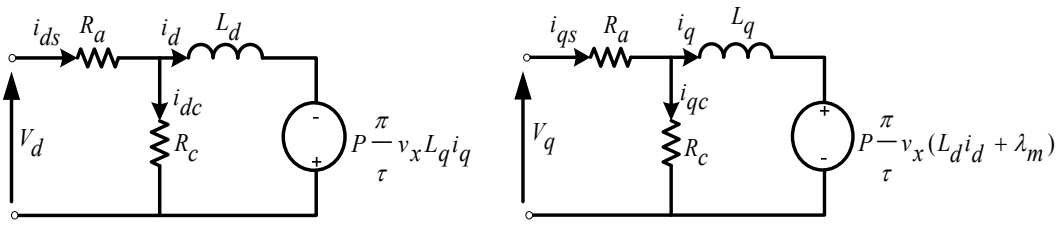

(a) d-axis (b) q-axis

Figure 3.3 d- and q-axis equivalent circuits for linear PM synchronous machines

From Figure 3.3 (a) and (b) the voltages equation in *dq* synchronous reference frame for the linear PM synchronous machine are defined as follows:

$$V_d = R_a i_d + L_d\left(1+\frac{R_a}{R_c}\right)\frac{di_d}{dt} - P\frac{\pi}{\tau}v_x L_q i_q\left(1+\frac{R_a}{R_c}\right) \quad \text{(V)} \tag{3.39}$$

$$V_q = R_a i_q + L_q\left(1+\frac{R_a}{R_c}\right)\frac{di_q}{dt} + \left(1+\frac{R_a}{R_c}\right)P\frac{\pi}{\tau}v_x\left(L_d i_d + \lambda_m\right)\text{(V)} \tag{3.40}$$

where,

V_d and V_q are d- and q-axis stator voltages (V), respectively.

i_d and i_q are d- and q-axis torque generating currents (A), respectively.

R_a and R_c are stator and core loss resistances (Ω), respectively.

L_d and L_q are d- and q-axis self inductances (H), respectively.

λ_m is the permanent magnet flux linkage (Wb).

v_x is the mover velocity (ms^{-1}).

P is number of pole pairs.

τ is pole pitch length (m).

The electromagnetic force F_e developed by the mover is expressed as

$$F_e = \frac{3}{2}\frac{\pi}{\tau} P\left(\lambda_m i_q + \left(L_d - L_q\right) i_q i_d\right) \quad \text{(N)} \tag{3.41}$$

The velocity equation is:

$$\frac{dv_x}{dt} = (F_e - F_L - Dv_x)/M \tag{3.42}$$

where F_L is the load force. M and D are the mover mass (kg) and the damper coefficient (Nsm^{-1}) respectively.

The mover position, x, is given by

$$\frac{dx}{dt} = Pv_x \tag{3.43}$$

3.3.1 Quadrature Axis Current Equation

The correct choice of quadrature axis current (i_q) waveform is essential in order to draw rated phase current at rated phase voltage and velocity during synthetic loading of the linear permanent magnet synchronous machine. The reference value of i_q forces the machine to accelerate and decelerate. The current, i_q, takes the same form as that for the rotational machine, hence

$$i_q = I_m \sin\left(2\pi f_n t\right) + I_o \quad \text{(A)} \tag{3.44}$$

where I_m is the magnitude of AC perturbation current, I_o is a dc offset current and f_n is synthetic loading frequency (Hz).

As the linear PM synchronous machine force, F_e, is linearly related to i_q, the generated force alternates between positive and negative values. The frequency and magnitude (f_n and I_m respectively) of the AC component effectively controls the AC variation of the mover velocity (assuming constant mechanical parameters) and the dc offset component controls the average mover velocity. As the mover position, x, reaches the end of its travel the dc component is reversed.

(i) Determining I_o in terms of machine parameters

The load force, F_L, and the rate of change of mover velocity, on average, are zero during synthetic loading test. Therefore, the electrical force generated balances the force due to friction and windage loss. Hence, the average electrical force, F_{eav}, can be expressed as:

$$F_{eav} = Dv_{xo} = k_f f_n \int_0^{\frac{1}{f_n}} \left(I_m \sin(2\pi f_n t) + I_o\right) dt \qquad \text{(N)} \tag{3.45}$$

where, v_{xo} is the rated steady state mover velocity. The dc offset current I_o required to meet a desired average mover velocity during synthetic loading is a function of the mechanical parameters.

By solving and rearranging (3.45) the expression for I_o is

$$I_o = \frac{Dv_{xo}}{k_f} \qquad \text{(A)} \tag{3.46}$$

That is the average dc offset current required is the friction force divided by the force factor of the machine, where $k_f = \frac{3}{2}\frac{\pi}{\tau} P\lambda_m$ and is the machine force factor (N/A), D is damper coefficient in (Nsm^{-1}), P is number of pairs of poles, λ_m is linkage flux (Wb), and τ is pole pitch length (m).

(ii) Determining I_m in terms of machine parameters

The linear PM synchronous machine must draw rated current during synthetic loading. Therefore, the magnitude of AC perturbation I_m is a function of machine desired rms current, the required dc offset current I_o and the direct axis current i_d. To force rated rms phase current, I_s, the following must hold

$$\frac{\left(i_q^2 + i_d^2\right)}{2} = I_s^2 \qquad \text{(A)} \tag{3.47}$$

Substituting the quadrature axis current, i_q, from (3.44) into (3.47) and averaging over one synthetic loading cycle gives:

$$I_s^2 = \frac{f_n}{2}\int_0^{\frac{1}{f_n}} \left(I_m \sin\left(2\pi f_n t\right) + I_o\right)^2 dt + f_n \int_0^{\frac{1}{f_n}} \frac{i_d^2}{2} dt \tag{3.48}$$

Solving and rearranging (3.48) gives the AC perturbation current as

$$I_m = \sqrt{4I_s^2 - 2I_o^2 - 2i_d^2} \qquad \text{(A)} \tag{3.49}$$

where I_s is the rated rms current of the linear PM synchronous machine under test. When vector control is applied the reference value of the direct axis current will be zero therefore:

$$I_m = \sqrt{4I_s^2 - 2I_o^2} \qquad \text{(A)} \tag{3.50}$$

3.3.2 Mover Velocity Equation

The mover velocity must equal, on average, the rated (or desired) mover velocity of the machine. During the synthetic loading method the load force, F_L, is zero. Thus the mover velocity can be derived from the solution of the velocity equation (3.42). Substituting (3.44) into (3.41), then substituting the electromagnetic force into the velocity equation (3.42) and rearranging yields:

$$M\frac{dv_x}{dt} + Dv_x = k_f I_m \sin\left(2\pi f_n t\right) + k_f I_o \tag{3.51}$$

Using the Laplace transform to solve (3.51) for v_x gives:

$$v_x(s) = \frac{k_f\left(2\pi f_n\right) I_m / M}{\left(s + \frac{D}{M}\right)\left(s^2 + \left(2\pi f_n\right)^2\right)} + \frac{k_f I_o / M}{s\left(s + \frac{D}{M}\right)} \tag{3.52}$$

By applying partial fraction expansion and Laplace inverse transformation on (3.52), the mover velocity is described as:

$$v_x = \frac{k_f I_o}{D} + \frac{k_f I_m D/M^2}{(2\pi f_n)^2 + \left(\frac{D}{M}\right)^2}\sin(2\pi f_n t) - \frac{k_f (2\pi f_n) I_m/M}{(2\pi f_n)^2 + \left(\frac{D}{M}\right)^2}\cos(2\pi f_n t) + \left[\frac{k_f (2\pi f_n) I_m/M}{(2\pi f_n)^2 + \left(\frac{D}{M}\right)^2} - \frac{k_f I_o}{D}\right] e^{-\frac{D}{M}t} \quad (\text{ms}^{-1}) \quad (3.53)$$

In time the exponential component decays to zero therefore the synthetic loading mover velocity is then

$$v_x = \frac{k_f I_o}{D} + \frac{k_f I_m D/M^2}{(2\pi f_n)^2 + \left(\frac{D}{M}\right)^2}\sin(2\pi f_n t) - \frac{k_f (2\pi f_n) I_m/M}{(2\pi f_n)^2 + \left(\frac{D}{M}\right)^2}\cos(2\pi f_n t) \quad (\text{ms}^{-1}) \quad (3.54)$$

$$v_x = \frac{k_f I_o}{D} + \frac{k_f I_m/M}{\sqrt{(2\pi f_n)^2 + \left(\frac{D}{M}\right)^2}}\sin(2\pi f_n t - \phi) \quad (\text{ms}^{-1}) \quad (3.54a)$$

where $\phi = \tan^{-1}\left(\frac{2\pi f_n}{D/M}\right)$

(i) Maximum and minimum mover velocity

The synthetic loading frequency can be expressed in terms of a desired value of peak to peak mover velocity and from (3.54) the maximum and minimum mover velocity can be determined.

The maximum mover velocity is

$$v_x(\max) = \frac{k_f I_o}{D} + \frac{k_f I_m/M}{\sqrt{(2\pi f_n)^2 + \left(\frac{D}{M}\right)^2}} \quad (\text{ms}^{-1}) \quad (3.55)$$

The minimum mover velocity is

$$v_x(\min) = \frac{k_f I_o}{D} - \frac{k_f I_m / M}{\sqrt{(2\pi f_n)^2 + \left(\frac{D}{M}\right)^2}} \quad (\text{ms}^{-1}) \tag{3.55a}$$

(ii) Determining f_n in terms of machine parameters

The synthetic loading frequency has an impact on the DC link voltage and inverter volt-ampere rating due to the effect it has on the mover velocity swing. Thus proper choice of synthetic loading frequency is essential. The peak to peak variation of mover velocity, Δv_x, is determined as

$$\Delta v_x = v_x(\max) - v_x(\min) = 2\frac{k_f I_m / M}{\sqrt{(2\pi f_n)^2 + \left(\frac{D}{M}\right)^2}} \quad (\text{ms}^{-1}) \tag{3.56}$$

The synthetic loading frequency can be determined if a required Δv_x is specified along with I_m, assuming the mechanical parameters are known. The synthetic loading frequency using (3.56) is

$$f_n = \frac{\sqrt{\left(\frac{2k_f I_m}{M}\right)^2 - \left(\Delta v_x \frac{D}{M}\right)^2}}{2\pi\Delta v_x} \quad (\text{Hz}) \tag{3.57}$$

The value of Δv_x can be between zero and twice the rated mover velocity ($0<\Delta v_x \leq 2v_x$), but for better synthetic loading performance this value should be as small as possible. Higher values of Δv_x lead to higher dc link voltage requirements hence higher inverter volt-ampere ratings. The impact of synthetic loading frequency on the dc link voltage shows that higher dc link voltages are required during the synthetic loading, this due to the higher peak speed.

During the investigation of synthetic loading, the synthetic loading period is found to be proportional to the mover mass for a desired value of Δv_x. This means that when the mechanical time constant increases a lower Δv_x is produced for a given synthetic loading frequency. This is beneficial as reduces the inverter volt-ampere requirement. The mechanical time constant can be increased by attaching additional mass to the mover.

3.3.3 Direct and Quadrature Axis Voltage Equation

The direct and quadrature axis voltages are a function of the synthetic loading frequency. Therefore, mathematical descriptions of the dq axis voltages are essential in determining the machine's peak phase and line voltages hence the inverter volt-ampere rating required for the synthetic loading test. The direct and quadrature axis voltages are derived from (3.39) and (3.40) after substituting the equations of quadrature axis current, i_q, (3.44) and mover velocity, v_x (3.54).

The direct axis voltage of linear PM synchronous machine during the synthetic loading test is:

$$V_d = R_a i_d - L_q P\left(1+\frac{R_a}{R_c}\right)\left(I_m \sin(2\pi f_n t)+I_o\right)\frac{\pi}{\tau}\left[\frac{k_f I_o}{D}+\frac{k_f I_m D/M^2}{(2\pi f_n)^2+\left(\frac{D}{M}\right)^2}\sin(2\pi f_n t)\right.$$
$$\left.-\frac{(2\pi f_n)k_f I_m/M}{(2\pi f_n)^2+\left(\frac{D}{M}\right)^2}\cos(2\pi f_n t)\right] \quad \text{(V)} \qquad (3.58)$$

The quadrature axis voltage of the linear PM synchronous machine during the synthetic loading test is:

$$V_q = R_a I_m \sin(2\pi f_n t)+R_a I_o + L_q I_m (2\pi f_n)\left(1+\frac{R_a}{R_c}\right)\cos(2\pi f_n t)+P\left(1+\frac{R_a}{R_c}\right)(\mathrm{L_d i_d}+\lambda_m)\frac{\pi}{\tau}$$
$$\times\left[\frac{k_f I_o}{D}+\frac{k_f I_m D/M^2}{(2\pi f_n)^2+\left(\frac{D}{M}\right)^2}\sin(2\pi f_n t)-\frac{k_f(2\pi f_n) I_m/M}{(2\pi f_n)^2+\left(\frac{D}{M}\right)^2}\cos(2\pi f_n t)\right] \quad \text{(V)} \qquad (3.59)$$

The stator *abc* voltage can be calculated from the *dq* axis voltage using:

$$\begin{bmatrix}V_a\\V_b\\V_c\end{bmatrix}=\begin{bmatrix}\cos\left(\frac{\pi}{\tau}x\right) & \sin\left(\frac{\pi}{\tau}x\right)\\ \cos\left(\frac{\pi}{\tau}x-\frac{2\pi}{3}\right) & \sin\left(\frac{\pi}{\tau}x-\frac{2\pi}{3}\right)\\ \cos\left(\frac{\pi}{\tau}x+\frac{2\pi}{3}\right) & \sin\left(\frac{\pi}{\tau}x+\frac{2\pi}{3}\right)\end{bmatrix}\begin{bmatrix}V_d\\V_q\end{bmatrix} \quad \text{(V)} \qquad (3.60)$$

where, V_a, V_b, and V_c are the stator phase voltages of the linear permanent magnet synchronous machines, and x is the mover displacement. Substituting (3.58) and (3.59) into (3.60) allows the instantaneous values of phase voltages to be calculated, hence the peak line voltages can be determined. The minimum dc link voltage can then be identified.

3.3.4 Direct and Quadrature Axis Stator Current Equation

In order to derive the input power and inverter volt-ampere rating during synthetic loading tests, the direct and quadrature axis stator current equations must be determined. The stator direct and quadrature axis current are a function of the synthetic loading frequency. Therefore, in order to evaluate the stator phase current during synthetic loading, the direct and quadrature axis stator current waveform is transformed to the *abc* reference frame. The stator phase current is also important for the assessment of stator copper losses.

(i) Direct axis stator current equation

From Figure 3.3 (a) the direct axis stator current can be calculated using Kirchhoff's current law as:

$$i_{ds} = i_d + i_{dc} \qquad \text{(A)} \tag{3.61}$$

where $i_{dc} = -Pv_x \frac{\pi}{\tau} \frac{L_q i_q}{R_c}$ and $\frac{di_d}{dt} = 0$. Substituting the expression of i_{dc}, i_q (3.44) and v_x (3.54) into (3.61) gives the direct axis stator current as:

$$i_{ds} = i_d - P\frac{\pi}{\tau}\frac{L_q}{R_c}\left(I_m \sin(2\pi f_n t) + I_o\right)\left[\frac{k_f I_o}{D} + \frac{k_f I_m D/M^2}{(2\pi f_n)^2 + \left(\frac{D}{M}\right)^2}\sin(2\pi f_n t)\right.$$
$$\left. - \frac{(2\pi f_n) k_f I_m/M}{(2\pi f_n)^2 + \left(\frac{D}{M}\right)^2}\cos(2\pi f_n t)\right] \qquad \text{(A)} \tag{3.62}$$

(ii) Quadrature axis stator current equation

From Figure 3.3 (b) the quadrature axis stator current can be calculated using Kirchhoff's current law as:

$$i_{qs} = i_q + i_{qc} \quad \text{(A)} \tag{3.63}$$

where $i_{qc} = P\frac{\pi}{\tau}v_x\frac{\left(L_d i_d + \lambda_m\right)}{R_c}$. Therefore substituting the expression of i_{qc}, i_q (3.44) and v_x (3.54) into (3.63) the quadrature axis current is:

$$i_{qs} = I_m\sin\left(2\pi f_n t\right) + I_o + P\frac{\pi}{\tau}\frac{\left(L_d i_d + \lambda_m\right)}{R_c}\left[\frac{k_f I_o}{D} + \frac{k_f I_m D/M^2}{\left(2\pi f_n\right)^2 + \left(\frac{D}{M}\right)^2}\sin\left(2\pi f_n t\right)\right. \quad \text{(A)} \tag{3.64}$$
$$\left. - \frac{\left(2\pi f_n\right)k_f I_m/M}{\left(2\pi f_n\right)^2 + \left(\frac{D}{M}\right)^2}\cos\left(2\pi f_n t\right)\right]$$

The stator *abc* phase current can be calculated from *dq* axis stator current using:

$$\begin{bmatrix} i_a \\ i_b \\ i_c \end{bmatrix} = \begin{bmatrix} \cos\left(\frac{\pi}{\tau}x\right) & \sin\left(\frac{\pi}{\tau}x\right) \\ \cos\left(\frac{\pi}{\tau}x - \frac{2\pi}{3}\right) & \sin\left(\frac{\pi}{\tau}x - \frac{2\pi}{3}\right) \\ \cos\left(\frac{\pi}{\tau}x + \frac{2\pi}{3}\right) & \sin\left(\frac{\pi}{\tau}x + \frac{2\pi}{3}\right) \end{bmatrix}\begin{bmatrix} i_{ds} \\ i_{qs} \end{bmatrix} \quad \text{(A)} \tag{3.65}$$

where i_a, i_b, and i_c are the stator phase current of the linear permanent magnet synchronous machines, and x is mover displacement. The peak phase current can then be identified which then provides a means of calculating the inverter VA rating.

3.4 Generalization of Synthetic Loading Mathematical Equations

The synthetic loading mathematical equations are generalized using the per-unit system. A simplification in the equations of synthetic loading is obtained if a generalization is performed. The equations for the PM, IPM synchronous

machines, and linear PM synchronous machines in the preceding sections are not in a convenient form for generalizing conclusions. This problem can be solved by normalizing the synthetic loading equations to a convenient base value and expressing all variables in per-unit of base. The main advantages of the per-unit system are that per-unit quantities remain unchanged whether expressed as line or phase quantities. In addition, per-unit representation results in more meaningful and correlated data. It gives relative magnitude information. Furthermore, the per-unit system is useful in simulating machine systems for steady-state and dynamic analysis without mixing between single- and three-phase powers. The generalised mathematical model of synthetic loading is used to evaluate the efficiency of the PM synchronous machine regardless of the machine type. The per-unit model is used in chapter four for synthetic loading simulation for efficiency evaluation, and evaluates the impact of synthetic loading frequency on inverter volt-ampere rating and dc link voltage requirements with respect to full load conditions.

3.4.1 Base Value Selection

The determination of the base quantities for voltage, current, speed (velocity), and flux linkage is essential in performing the per-unit transformation. The other base quantities such as power, torque (force), and the machine electrical parameters (resistance and inductance) can be calculated using the main base quantities. The base quantities are:

- The base peak phase current I_{base}
- The base flux linkage $\lambda_{base} = \lambda_m$
- The base speed $\omega_{base} = \omega_r = P\frac{k_t I_o}{B}$ and $\omega_{base} = \frac{(k_t + k_r i_d) I_o}{B}$ for PM and IPM synchronous machine respectively. The base mover velocity $v_{base} = v_x = P\frac{k_f I_o}{D}$ for the linear PM synchronous machine.

Thus by choosing the three base quantities I_{base}, ω_{base}, and λ_{base} the base values for all other quantities of interest are determined.

- The base voltage for the PM synchronous machine is

$$V_{base} = P\omega_{base}\lambda_{base} = P\frac{k_t I_o}{B}\lambda_m .$$

- The base voltage for the IPM synchronous machine is

$$V_{base} = P\frac{(k_t + k_r i_d)I_o}{B}\lambda_m .$$

- The base voltage for the linear PM synchronous machine is

$$V_{base} = \frac{\pi}{\tau}Pv_{base}\lambda_{base} = P\frac{\pi}{\tau}\frac{k_f I_o}{D}\lambda_m .$$

- The base inductance $L_{base} = \frac{\lambda_{base}}{I_{base}} = \frac{\lambda_m}{I_{base}}$.

- The base impedance for the PM synchronous machine is

$$Z_{base} = \frac{V_{base}}{I_{base}} = P\frac{k_t I_o}{B}\frac{\lambda_m}{I_{base}} .$$

- The base impedance for the IPM synchronous machine is

$$Z_{base} = \frac{V_{base}}{I_{base}} = P\frac{(k_t + k_r i_d)I_o}{B}\frac{\lambda_m}{I_{base}}$$

- The base impedance for the linear PM synchronous machine is

$$Z_{base} = \frac{V_{base}}{I_{base}} = P\frac{\pi}{\tau}\frac{k_f I_o}{D}\frac{\lambda_m}{I_{base}} .$$

- The base electromagnetic torque $T_{ebase} = k_t I_{base}$ for PM synchronous machine and the base force $F_{ebase} = k_f I_{base}$ for linear PM synchronous machine.

- The base electromagnetic power $P_{ebase} = \frac{3}{2}V_{base}I_{base}$

To normalize any quantity, it must be divided by the base quantity of the same dimension. For example in general, $X_u = \frac{X_{actual}}{X_{base}}$ where, the subscript *u* is used to indicate *pu*. In the following computations the subscript *u* is add to all per-unit quantities to emphasize their dimensionless status.

3.4.2 Normalising the Quadrature Axis Current

The quadrature axis current equations, (3.6) and (3.44) for PM and linear PM synchronous machine respectively, can be normalized

$$i_{qu} = I_{mu}\sin(2\pi f_n t) + I_{ou} \qquad pu \qquad (3.66a)$$

where the per-unit AC perturbation is

$$I_{mu} = \sqrt{2 - 2I_{ou}^2 - 2i_{du}^2} \qquad pu \qquad (3.66b)$$

For the IPM synchronous machine, for the PM and linear PM synchronous machine under vector control (i_d=0) the AC perturbation is

$$I_{mu} = \sqrt{2 - 2I_{ou}^2} \qquad pu \qquad (3.66c)$$

The per-unit dc offset currents are $I_{ou} = \dfrac{B\omega_{ro}}{(k_t + k_r i_d)I_{base}}$ pu and $I_{ou} = \dfrac{B\omega_{ro}}{k_t I_{base}}$ pu for IPM and PM synchronous machine respectively. The per-unit dc offset current for the linear PM synchronous machine is $I_{ou} = \dfrac{Dv_{xo}}{k_f I_{base}}$ pu.

3.4.3 Normalising the Rotor Speed and Mover Velocity

The per-unit rotor speed for IPM and PM synchronous machines is:

$$\omega_{ru} = \omega_r/\omega_{base} = 1 + \frac{I_{mu}}{I_{ou}}\frac{(B/J)^2}{(2\pi f_n)^2 + \left(\frac{B}{J}\right)^2}\sin(2\pi f_n t) - \frac{I_{mu}}{I_{ou}}\frac{(2\pi f_n)B/J}{(2\pi f_n)^2 + \left(\frac{B}{J}\right)^2}\cos(2\pi f_n t)\ pu \quad (3.67)$$

The mover velocity for linear PM synchronous machine in per-unit is

$$v_{xu} = v_x/v_{base} = 1 + \frac{I_{mu}}{I_{ou}}\frac{(D/M)^2}{(2\pi f_n)^2 + \left(\frac{D}{M}\right)^2}\sin(2\pi f_n t) - \frac{I_{mu}}{I_{ou}}\frac{(2\pi f_n)D/M}{(2\pi f_n)^2 + \left(\frac{D}{M}\right)^2}\cos(2\pi f_n t)\ pu \quad (3.68)$$

Therefore, the rotor speed and mover velocity can be generalised for all types of PM synchronous machines as:

$$\omega_{ru} = v_{xu} = 1 + \frac{I_{mu}}{I_{ou}}\frac{(1/\tau_m)^2}{(2\pi f_n)^2 + \left(\frac{1}{\tau_m}\right)^2}\sin(2\pi f_n t) - \frac{I_{mu}}{I_{ou}}\frac{(2\pi f_n)/\tau_m}{(2\pi f_n)^2 + \left(\frac{1}{\tau_m}\right)^2}\cos(2\pi f_n t)\ pu \quad (3.69)$$

$$\omega_{ru} = v_{xu} = 1 + \frac{I_{mu}}{I_{ou}} \frac{(1/\tau_m)}{\sqrt{(2\pi f_n)^2 + \left(\frac{1}{\tau_m}\right)^2}} \sin(2\pi f_n t - \phi) \quad pu \quad (3.69a)$$

where, $\phi = \tan^{-1}(2\pi f_n \tau_m)$, τ_m is the mechanical time constant. For the IPM and PM synchronous machine $\tau_m = J/B$, and for the linear PM synchronous machine $\tau_m = M/D$.

From (3.69) the maximum and minimum speed can be determined. The maximum speed is:

$$\omega_{ru}(\max) = v_{xu}(\max) = 1 + \frac{I_{mu}}{I_{ou}} \frac{1/\tau_m}{\sqrt{(2\pi f_n)^2 + \left(\frac{1}{\tau_m}\right)^2}} \quad pu \quad (3.70)$$

The minimum speed is

$$\omega_{ru}(\min) = v_{xu}(\min) = 1 - \frac{I_{mu}}{I_{ou}} \frac{1/\tau_m}{\sqrt{(2\pi f_n)^2 + \left(\frac{1}{\tau_m}\right)^2}} \quad pu \quad (3.71)$$

The peak to peak variation of velocity, ΔS, is then

$$\Delta S = \omega_{ru}(\max) - \omega_{ru}(\min) = v_{xu}(\max) - v_{xu}(\min)$$

$$\Delta S = 2\frac{I_{mu}}{I_{ou}} \frac{1/\tau_m}{\sqrt{(2\pi f_n)^2 + \left(\frac{1}{\tau_m}\right)^2}} \quad pu \quad (3.72)$$

The general synthetic loading frequency can be determined if a desired ΔS is specified (regardless of PM synchronous machine types), assuming the mechanical parameters are known. The synthetic loading frequency using (3.72) is then given by

$$f_n = \frac{\sqrt{\left(\frac{2}{\tau_m}\frac{I_m}{I_o}\right)^2 - \left(\frac{\Delta S}{\tau_m}\right)^2}}{2\pi\ \Delta S} \quad (3.73)$$

3.4.4 Normalising the Direct and Quadrature Axis Voltage

The direct and quadrature axis voltage equations (3.27), (3.28), (3.29), (3.30), (3.58) and (3.59) for IPM, PM and linear PM synchronous machines respectively can be normalized.

(i) Normalising the Direct Axis Voltage

The normalized equation of the direct axis voltage for IPM and PM synchronous machine in per-unit is

$$V_{du} = R_{au} i_{du} - L_{qu}\left(1+\frac{R_{au}}{R_{cu}}\right)\left(I_{mu}\sin(2\pi f_n t)+I_{ou}\right)\left[1+\frac{I_{mu}}{I_{ou}}\frac{(B/J)^2}{(2\pi f_n)^2+\left(\frac{B}{J}\right)^2}\sin(2\pi f_n t)\right. \quad pu \qquad (3.74)$$

$$\left.-\frac{I_{mu}}{I_{ou}}\frac{(2\pi f_n)B/J}{(2\pi f_n)^2+\left(\frac{B}{J}\right)^2}\cos(2\pi f_n t)\right]$$

And for the linear PM synchronous machine

$$V_{du} = R_{au} i_{du} - L_{qu}\left(1+\frac{R_{au}}{R_{cu}}\right)\left(I_{mu}\sin(2\pi f_n t)+I_{ou}\right)\left[1+\frac{I_{mu}}{I_{ou}}\frac{(D/M)^2}{(2\pi f_n)^2+\left(\frac{D}{M}\right)^2}\sin(2\pi f_n t)\right. \quad pu \qquad (3.75)$$

$$\left.-\frac{I_{mu}}{I_{ou}}\frac{(2\pi f_n)D/M}{(2\pi f_n)^2+\left(\frac{D}{M}\right)^2}\cos(2\pi f_n t)\right]$$

Therefore, the direct axis voltage equation can be generalized for all types of PM synchronous machines as:

$$V_{du} = R_{au} i_{du} - L_{qu}\left(1+\frac{R_{au}}{R_{cu}}\right)\left(I_{mu}\sin(2\pi f_n t)+I_{ou}\right)\left[1+\frac{I_{mu}}{I_{ou}}\frac{(1/\tau_m)^2}{(2\pi f_n)^2+\left(\frac{1}{\tau_m}\right)^2}\sin(2\pi f_n t)\right. \quad pu \qquad (3.76)$$

$$\left.-\frac{I_{mu}}{I_{ou}}\frac{(2\pi f_n)/\tau_m}{(2\pi f_n)^2+\left(\frac{1}{\tau_m}\right)^2}\cos(2\pi f_n t)\right]$$

where τ_m is the mechanical time constant.

(ii) Normalising the Quadrature Axis Voltage

In similar way, the quadrature axis voltage equation can be generalized for all types of PM synchronous machines as:

$$V_{qu} = R_{au}I_{mu}\sin(2\pi f_n t) + R_{au}I_{ou} + L_{qu}I_{mu}(f_n/f_s)\left(1+\frac{R_{au}}{R_{cu}}\right)\cos(2\pi f_n t) + \left(1+\frac{R_{au}}{R_{cu}}\right)(L_{du}i_{du}+1)$$

$$\times\left[1+\frac{I_{mu}}{I_{ou}}\frac{(1/\tau_m)^2}{(2\pi f_n)^2+\left(\frac{1}{\tau_m}\right)^2}\sin(2\pi f_n t) - \frac{I_{mu}}{I_{ou}}\frac{(2\pi f_n)/\tau_m}{(2\pi f_n)^2+\left(\frac{1}{\tau_m}\right)^2}\cos(2\pi f_n t)\right] \qquad pu \qquad (3.77)$$

where f_s is the system frequency and τ_m is the mechanical time constant.

The stator *abc* per-unit voltage equations can be computed from the *dq* axis per-unit stator voltages using

$$\begin{bmatrix} V_{au} \\ V_{bu} \\ V_{cu} \end{bmatrix} = \begin{bmatrix} \cos\theta & \sin\theta \\ \cos\left(\theta-\frac{2\pi}{3}\right) & \sin\left(\theta-\frac{2\pi}{3}\right) \\ \cos\left(\theta+\frac{2\pi}{3}\right) & \sin\left(\theta+\frac{2\pi}{3}\right) \end{bmatrix} \begin{bmatrix} V_{du} \\ V_{qu} \end{bmatrix} \qquad pu \qquad (3.78)$$

where V_{au}, V_{bu}, and V_{cu} are the per-unit stator phase voltages of the permanent magnet synchronous machine.

3.4.5 Normalising the Direct and Quadrature Axis Stator Current

The direct and quadrature axis stator current equations (3.33), (3.34), (3.36), (3.37), (3.62) and (3.64) for IPM, PM and linear PM synchronous machine respectively are normalized.

(i) Normalising the Direct Axis Stator Current

The normalised equation of the direct axis stator current for IPM and PM synchronous machine in per-unit is:

$$i_{dsu} = i_{du} - \frac{L_{qu}}{R_{cu}}\left(I_{mu}\sin(2\pi f_n t) + I_{ou}\right)\left[1 + \frac{I_{mu}}{I_{ou}}\frac{(B/J)^2}{(2\pi f_n)^2 + \left(\frac{B}{J}\right)^2}\sin(2\pi f_n t)\right.$$
$$\left. - \frac{I_{mu}}{I_{ou}}\frac{(2\pi f_n)B/J}{(2\pi f_n)^2 + \left(\frac{B}{J}\right)^2}\cos(2\pi f_n t)\right] \quad pu \qquad (3.79)$$

The normalised equation of the direct axis stator current for the linear PM synchronous machine in per-unit is:

$$i_{dsu} = i_{du} - \frac{L_{qu}}{R_{cu}}\left(I_{mu}\sin(2\pi f_n t) + I_{ou}\right)\left[1 + \frac{I_{mu}}{I_{ou}}\frac{(D/M)^2}{(2\pi f_n)^2 + \left(\frac{D}{M}\right)^2}\sin(2\pi f_n t)\right.$$
$$\left. - \frac{I_{mu}}{I_{ou}}\frac{(2\pi f_n)D/M}{(2\pi f_n)^2 + \left(\frac{D}{M}\right)^2}\cos(2\pi f_n t)\right] \quad pu \qquad (3.80)$$

Therefore, the direct axis stator current equation can be generalised for all types of PM synchronous machine as

$$i_{dsu} = i_{du} - \frac{L_{qu}}{R_{cu}}\left(I_{mu}\sin(2\pi f_n t) + I_{ou}\right)\left[1 + \frac{I_{mu}}{I_{ou}}\frac{(1/\tau_m)^2}{(2\pi f_n)^2 + \left(\frac{1}{\tau_m}\right)^2}\sin(2\pi f_n t)\right.$$
$$\left. - \frac{I_{mu}}{I_{ou}}\frac{(2\pi f_n)/\tau_m}{(2\pi f_n)^2 + \left(\frac{1}{\tau_m}\right)^2}\cos(2\pi f_n t)\right] \quad pu \qquad (3.81)$$

(ii) Normalising the Quadrature Axis Stator Current

In similar way, the quadrature axis stator current equation can be generalised for all types of PM synchronous machines as:

$$i_{qsu} = I_{mu}\sin(2\pi f_n t) + I_{ou} + \frac{(L_{du}i_{du}+1)}{R_{cu}}\left[1 + \frac{I_{mu}}{I_{ou}}\frac{(1/\tau_m)^2}{(2\pi f_n)^2 + \left(\frac{1}{\tau_m}\right)^2}\sin(2\pi f_n t)\right.$$
$$\left. - \frac{I_{mu}}{I_{ou}}\frac{(2\pi f_n)/\tau_m}{(2\pi \mathrm{f_n})^2 + \left(\frac{1}{\tau_m}\right)^2}\cos(2\pi f_n t)\right] \quad pu \quad (3.82)$$

where, τ_m is the mechanical time constant.

The stator *abc* per-unit current equation can be computed from the *dq* axis per-unit stator currents using

$$\begin{bmatrix} i_{au} \\ i_{bu} \\ i_{cu} \end{bmatrix} = \begin{bmatrix} \cos\theta & \sin\theta \\ \cos\left(\theta - \frac{2\pi}{3}\right) & \sin\left(\theta - \frac{2\pi}{3}\right) \\ \cos\left(\theta + \frac{2\pi}{3}\right) & \sin\left(\theta + \frac{2\pi}{3}\right) \end{bmatrix} \begin{bmatrix} i_{du} \\ i_{qu} \end{bmatrix} \quad pu \quad (3.83)$$

where, i_{au}, i_{bu}, and i_{cu} are the per-unit stator phase currents of the permanent magnet synchronous machines.

3.5 Input Power and Inverter Volt-ampere Rating Equations

Using the synthetic loading method, the PM synchronous machine accelerates and decelerates alternating between motor and generator action. During acceleration the machine draws power from the supply and during deceleration the machine delivers power back to the dc supply. For efficiency evaluation using synthetic loading the required inverter volt-ampere rating and maximum input power are higher than that required using the standard efficiency test. This a consequence of the higher value of AC current I_m and the increased line voltage requirement. The input power and inverter volt-ampere rating are computed using the stator *dq* voltage and current equations derived in section 3.2.3 and 3.2.4 for the PM and IPM synchronous machines and section 3.3.3 and 3.3.4 for the linear PM synchronous machine.

The total input power to the PM synchronous machine in terms of the *dq* variables for a balanced system can be calculated as:

$$P_{in} = \frac{3}{2}\left(V_d i_{ds} + V_q i_{qs}\right) \qquad \text{(W)} \tag{3.84}$$

And in per-unit variables:

$$P_{inu} = V_{du} i_{dsu} + V_{qu} i_{qsu} \qquad pu \tag{3.85}$$

The instantaneous terminal voltage, V_s, can be calculated as:

$$V_s = \sqrt{V_d^2 + V_q^2} \qquad \text{(V)} \tag{3.86}$$

And in per-unit terms:

$$V_{su} = \sqrt{V_{du}^2 + V_{qu}^2} \qquad pu \tag{3.87}$$

The instantaneous stator phase current, I_{ms}, is:

$$I_{ms} = \sqrt{i_{ds}^2 + i_{qs}^2} \qquad \text{(A)} \tag{3.88}$$

And in per-unit can be computed as:

$$I_{msu} = \sqrt{i_{dsu}^2 + i_{qsu}^2} \qquad pu \tag{3.89}$$

Therefore, the apparent power rating is

$$S = \frac{3}{2} V_s I_{ms} \quad \text{(VA)} \tag{3.90}$$

And in per-unit terms is

$$S_u = V_{su} I_{msu} \qquad pu \tag{3.91}$$

3.6 The DC Link Voltage Equation

Under synthetic loading the PM synchronous machine line voltage is a function of synthetic loading frequency. Therefore, the synthetic loading frequency has an impact on the required DC link voltage. As the required peak line voltage determines the required dc link voltage,

$$V_s = V_{dc} \qquad \text{(V)} \tag{3.92}$$

where, V_{dc} is the DC link voltage.

Substitute the instantaneous terminal voltage, V_s, from (3.86) into (3.92) and rearranging yields

$$V_{dc} = \sqrt{V_d^2 + V_q^2} \qquad \text{(V)} \tag{3.93}$$

The DC link voltage in per-unit is

$$V_{dcu} = \sqrt{V_{du}^2 + V_{qu}^2} \qquad pu \tag{3.94}$$

3.7 Summary

In this chapter, the equations for IPM, and PM synchronous machines and linear PM synchronous machines have been developed under synthetic loading conditions. Because in this case the synthetic loading method is a current control method, the quadrature axis current algorithm, i_q, has been established. The magnitude of AC perturbation current, I_m, and the dc offset current, I_o, equations have been developed using the machine rating and mechanical parameters. Equation for rotor speed, ω_r, for IPM and PM synchronous machines and the mover velocity, v_x, for linear PM synchronous machine have been derived. The rotor speed and mover velocity equations illustrate that the PM synchronous machine accelerates and decelerates during synthetic loading test. The direct and quadrature axis stator voltage and current equations have been derived in the synchronously rotating reference frame for PM synchronous machine, and in the synchronously translating reference frame for linear PM synchronous machine. Equations for input power and inverter volt-ampere rating have been developed using the direct and quadrature axis stator

voltage and current. The mathematical equations for synthetic loading have been generalized using machine rated current, speed and permanent magnet flux as the basis, the other quantities of interest have been calculated using these base values. The developed equations are used to simulate and evaluate the synthetic loading method in chapter four under different load torque conditions at rated speed. They are used to identify the optimum synthetic loading frequency, f_n. The detailed synthetic loading mathematical equations for IPM and PM synchronous machines and linear PM synchronous machine are detailed in Appendices **A1** and **A2**. A detailed derivation of the generalisation summarised here is provided in Appendix **A3**.

References

[1] S. Shinnaka and T. Sagawa, "New Optimal Current Control Methods for Energy-Efficient and Wide Speed-Range Operation of Hybrid-Field Synchronous Motor", IEEE Transactions on Industrial Electronics, Vol. 54, No. 5, October 2007, pp. 2443-2450.

[2] P. Pillay and R. Krishnan, "Modeling of Permanent Magnet Motor Drives", IEEE Transactions on Industrial Electronics, Vol. 35, No. 4, November 1988, pp. 537-541.

[3] A. A. Abdallah, V. Devanneaux, J. Faucher, B. Dagues and A. Randria, "Modelling of Surface-Mounted Permanent Magnet Synchronous Machines with Stator Faults", The 30th Annual Conference of the IEEE Industrial Electronics Society, November 2-6, 2004, Busan, Korea, pp. 3031-3036.

[4] M. A. Rahman and P. Zhou, "Analysis of Brushless Permanent Magnet Synchronous Motors", IEEE Transactions on Industrial Electronics, Vol. 43, No. 2, April 1996, pp. 256-267.

[5] Y. A. I. Mohamed and E. F. El-Saadany, "A Current Control Scheme with an Adaptive Internal Model for Torque Ripple Minimization and Robust Current Regulation in PMSM Drive Systems", IEEE Transactions on Energy Conversion, Vol. 23, No. 1, March 2008, pp. 92-100.

[6] C. –K. Lin, T. –H. Liu and S. –H. Yang, "Nonlinear Position Controller Design With Input-Output Linearisation technique for an Interior Permanent Magnet

Synchronous Motor Control System", IET Power Electronics, Vol. 1, No. 1, March 2008, pp. 14-26.

[7] J. Vittek, J. Michalik, V. Vavrus, and V. Horvath, "Design of Control System for Forced Dynamics Control of an Electric Drive Employing Linear Permanent Magnet Synchronous Motor", International conference on Industrial Electronics and control applications, ICIECA 2005, 29Nov.-2Dec 2005, Pages 6.

[8] J. Vittek, V. Vavrus, J. Michalik, P. Buchner, and W. Michalik, "Prescribed Closed-loop Speed Dynamics Control of the Actuator Employing Linear Permanent Magnet Synchronous Motor", IEEE International Conference on Industrial Technology, ICIT 2005, 14-17 Dec. 2005, pp. 604-609.

[9] M. S. W. Tam and N. C. Cheung, "A Robust Fully-Digital Drive for Linear Permanent Magnet Synchronous Motor", First International Conference on Power Electronics Systems and Applications, 9-11 Nov. 2004, pp. 188-193.

[10] S. -C, Hus, C. -H. Liu, C. -H. Liu, and N. -J. Wang, "Fuzzy PI Controller Tuning for a Linear Permanent Magnet Synchronous Motor Drive", The 27th Annual Conference of the IEEE Industrial Electronics Society,2001, IECON 01, Vol. 3, 29Nov.-2Dec. 2001, pp. 1661-1666.

Chapter Four
Simulation Results of Synthetic Loading Technique

4.1 Introduction

Simulation of the synthetic loading technique, with careful selection of the input conditions, I_m, I_o and f_n, is essential in order to evaluate the efficiency of the permanent magnet (PM) synchronous machines experimentally. Therefore, simulation and computer modelling is used, based on accurate system parameters, to evaluate the individual loss components and the input power to the PM synchronous machine model. In this chapter simulation results of the synthetic loading method for efficiency evaluation at rated speed are presented for different load torque conditions of the PM synchronous machine, the IPM synchronous machine, and the linear PM synchronous machine. The synthetic loading and the standard efficiency tests, as methods of efficiency evaluation, are simulated using MATLAB and SIMULINK. As the aim of this research is to determine the suitability of synthetic loading for efficiency evaluation of PM synchronous machines, the individual losses from the simulation results of the standard efficiency test are compared with the losses developed during the simulation of the synthetic loading. The main losses in PM synchronous machines are stator copper loss, iron loss, and friction and windage loss. In addition, the impact of the synthetic loading frequency on the required inverter DC link voltage and volt-ampere rating are presented. Also, the impact that the moment of inertia has on the peak to peak speed variation during synthetic loading is investigated.

4.2 The impact of synthetic loading frequency on DC link voltage and inverter volt-ampere rating

Ideally, the peak to peak speed variation should be as small as possible during synthetic loading. An increase in speed variation leads to an increase in inverter volt-ampere rating and dc link voltage. The impact of the synthetic loading frequency on the

inverter volt-ampere and dc link voltage is presented in this chapter in order to assess quantitatively the impact that the synthetic loading frequency has on the inverter VA rating. The inverter VA rating and the dc link voltage requirements are simulated using equation (3.91) and (3.94) from chapter three respectively.

Figure 4.1 shows the effect of synthetic loading frequency on the inverter VA rating and the dc link voltage. The figure is simulated using the MATLAB m-file provided in Appendix C. These graphs are derived using the machine parameters of the laboratory PM machine Table 4.1, IPM machine Table 4.6 and linear PM machine Table 4.11. The graphs show the general trend but have specific optimum synthetic loading frequencies based on the machine parameters. The inverter VA rating and the dc link voltage requirement rises as the synthetic loading frequency decreases as shown in Figure 4.1 (a)– (c). For example, the minimum inverter VA rating and the minimum dc link voltage required are 2.15pu and 2.2pu at 10 Hz synthetic loading frequency for the PM synchronous machine. The inverter VA rating and the dc link voltage gradually decreases as the synthetic loading is increased falling to a minimum of 1.52pu and 1.1pu respectively with synthetic loading frequencies between 100Hz and 140 Hz, Figure 4.1 (a). As the synthetic loading frequency rises from 150 Hz to 300Hz the inverter VA rating and the dc link required gradually increases. Therefore, an optimum synthetic loading frequency for the PM synchronous machine tested is between 100Hz and 140Hz.

Figure 4.1 (b) and (c) show similar characteristics to the PM synchronous machine where the optimum synthetic loading frequencies with respect to the inverter VA rating and dc link voltage are between 4 Hz and 10Hz for the test IPM synchronous machine and between 20Hz and 80Hz for the test linear PM synchronous machine. These PM synchronous machines and optimum synthetic loading frequencies are used to simulate the synthetic loading technique in this chapter and to execute synthetic loading experimentally in chapter six.

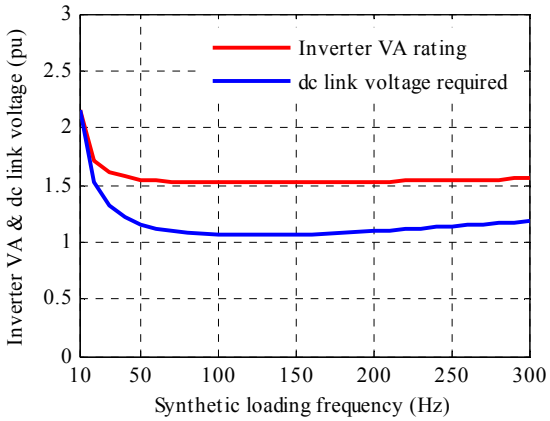

(a) PM synchronous machine

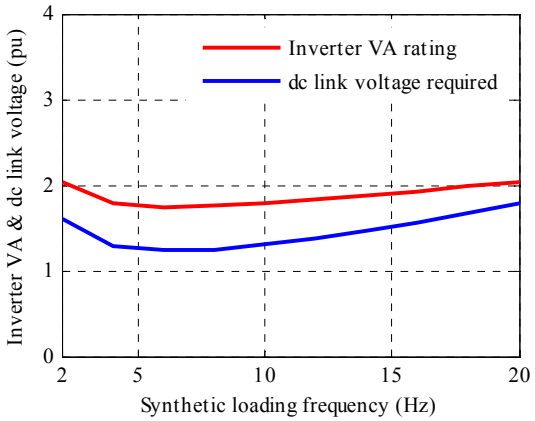

(b) IPM synchronous machine

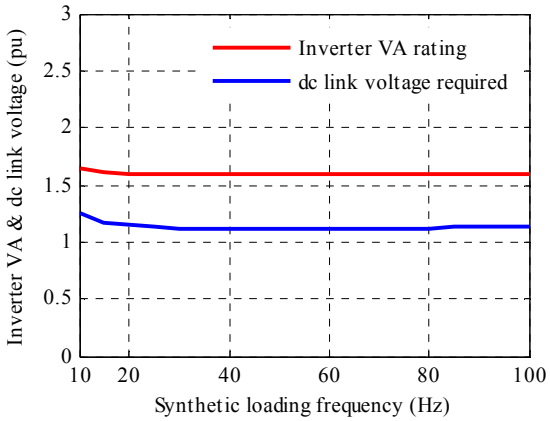

(c) linear PM synchronous machine

Figure 4.1 The impact of synthetic loading frequency on the required dc link voltage and inverter volt-ampere rating during synthetic loading for (a) PM synchronous machine (b) IPM synchronous machine and (c) linear PM synchronous machine

4.3 Simulation results for the PM synchronous machine

Simulation is used to help explain the synthetic loading technique, predict the losses and determine the required synthetic loading frequency, f_n, and associated parameters I_o and I_m given a moment of inertia, J, and damper factor, B. This then provides an estimate of the required peak current rating, minimum dc link voltage requirement and inverter VA rating. The simulation of synthetic loading will assess whether synthetic loading is a sufficient test for efficiency evaluation. During synthetic loading, only the input power to the PM synchronous machine needs to be measured. The dynamic model for the PM synchronous machine including iron loss resistance in the *dq* model is used [1]-[6]. Based on this model synthetic loading is simulated and evaluated for use in determining the losses and the efficiency of the PM synchronous machine. This is possible because the model estimates losses in the machine, namely copper loss, friction and windage loss, and iron loss [7],[8]. In order to validate synthetic loading as a method for efficiency evaluation of the PM synchronous machine, different load torque conditions are simulated using MATLAB and SIMULINK at rated speed and compared with the standard efficiency test method. The mathematical equations developed in chapter three are used. The parameters of the PM synchronous machine are shown in Table 4.1.

Table 4.1 The electrical and mechanical parameters of the PM synchronous machine

Parameters	Values
Rated output power	843 W
Rated peak current	10.5 A
Rated speed	4000 rpm
Maximum Bus Voltage	340 V
Armature resistance, R_a	0.55Ω
Core loss resistance, R_c	300Ω
Quadrature axis inductance, L_q	0.65 mH
Direct axis inductance, L_d	0.65 mH
Moment of inertia, J	7.85×10^{-5} kg.m^2
Damping coefficient, B	3.47×10^{-5} Nms^{-1}
Total permanent magnet flux linkage, λ_m	37.7 mWb
Number of poles	8

4.3.1 Full-Load Torque Condition

In this case, the performance of the synthetic loading technique for the PM synchronous machine is investigated and analyzed for different synthetic loading frequencies forcing full-load torque conditions, and compared with the standard efficiency test. Figure 4.2 shows the simulated instantaneous phase voltages of (3.31) from section 3.2.3 when synthetic loading is used for loading the PM synchronous machine.

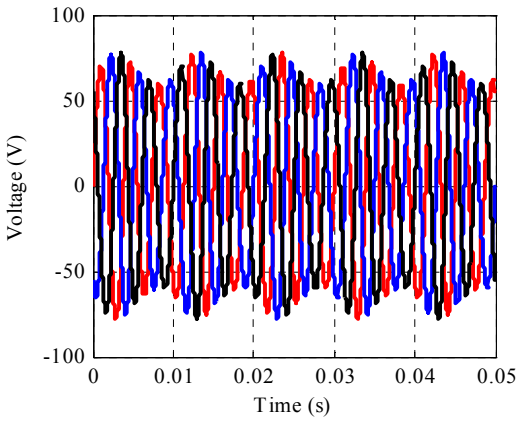

(a) three phase voltages during synthetic loading for 100 Hz synthetic loading frequency

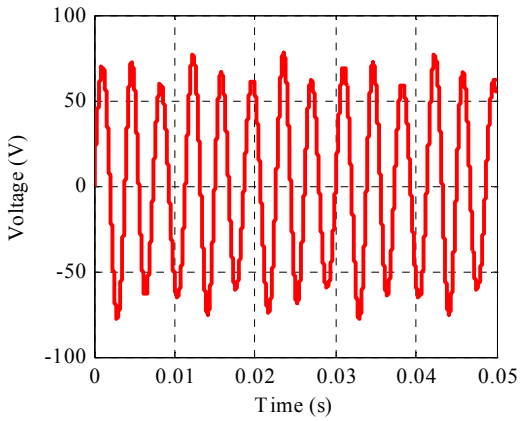

(b) phase a voltage during synthetic loading for 100 Hz synthetic loading frequency

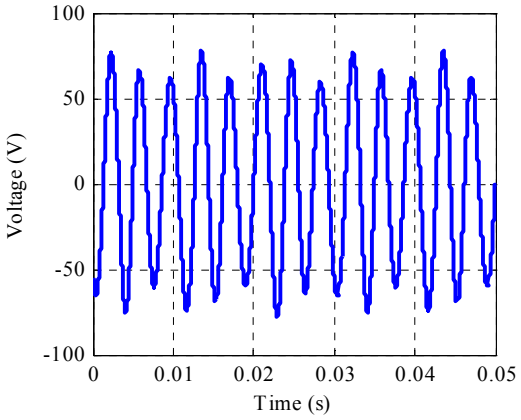

(c) phase b voltage during synthetic loading for 100 Hz synthetic loading frequency

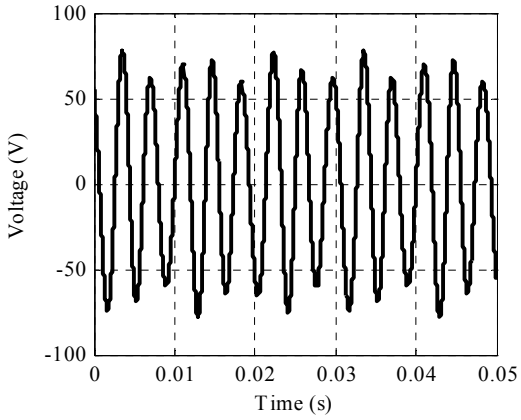

(d) phase c voltage during synthetic loading for 100 Hz synthetic loading frequency

Figure 4.2 The PM synchronous machine terminal voltage variation during synthetic loading for 100 Hz synthetic loading frequency under full-load torque conditions

It is important to notice that in the synthetic loading technique the instantaneous phase voltage is varying in amplitude and frequency. This confirms that the PM synchronous machine accelerates and decelerates forcing motor-generator action during synthetic loading. The amplitude of the instantaneous phase voltage varies according to synthetic loading frequency, which is 100 Hz, in Figure 4.2.

The instantaneous rms voltage is simulated using (3.90). Figure 4.3 shows the instantaneous rms line voltage variation with time during synthetic loading. The instantaneous rms voltage is larger than the rated rms voltage when the machine is accelerating and lower than the rated rms voltage when the machine decelerates. Note that although the machine rms voltage varies with time the average rms voltage over one synthetic loading cycle (100 Hz) is 83.2V (0.93pu). The reason for the apparent drop in rms voltage is explained later.

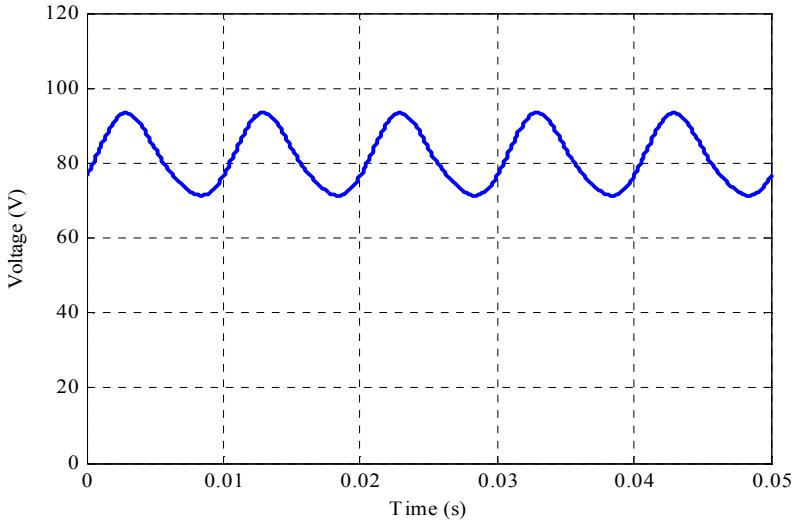

Figure 4.3 The PM synchronous machine instantaneous rms line voltage variation during synthetic loading for 100 Hz under full-load torque conditions

Figure 4.4 illustrates the instantaneous current in the three-phases of the machine. The instantaneous current is simulated using (3.38). As the instantaneous phase voltage is amplitude and frequency modulated, this will cause the PM synchronous machine's instantaneous current to vary in amplitude and frequency as shown in Figure 4.4. The peak of the instantaneous current is 14.87Amps (1.42pu). During synthetic loading, the

machine accelerates as a motor during the positive half cycle of the synthetic loading period, thus the quadrature axis current waveform is positive, and decelerates during the negative half cycle as the generator operate with a negative quadrature axis current.

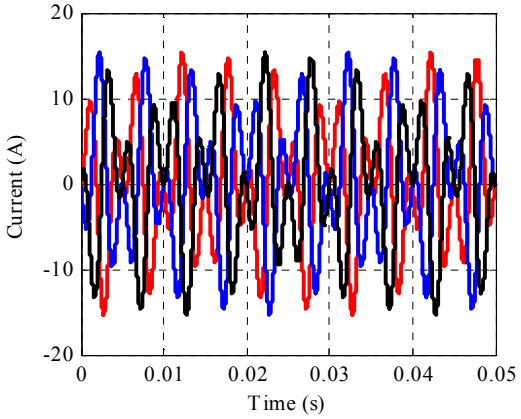

(a) three phase currents during synthetic loading for 100 Hz synthetic loading frequency

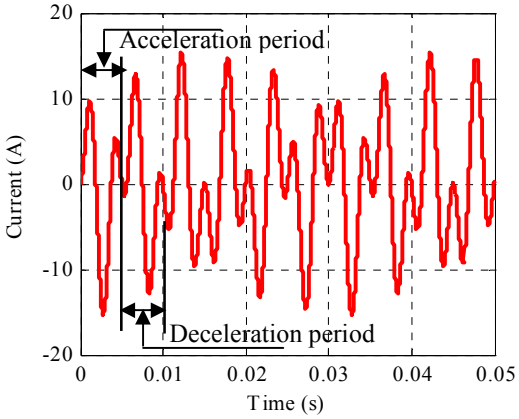

(b) phase a current during synthetic loading for 100 Hz synthetic loading frequency

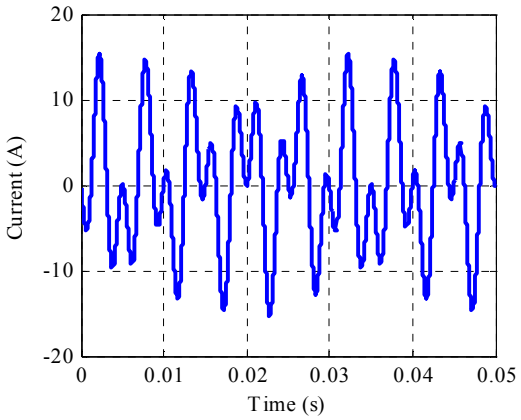

(c) phase b current during synthetic loading for 100 Hz synthetic loading frequency

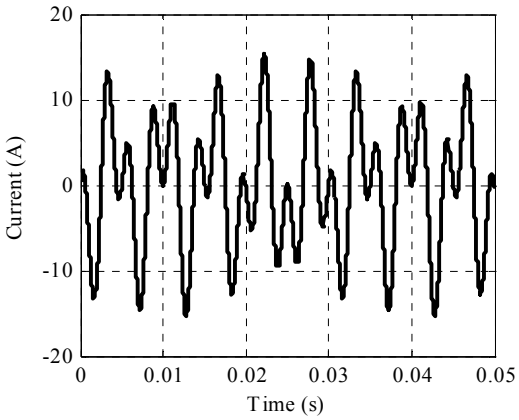

(d) phase c current during synthetic loading for 100 Hz synthetic loading frequency

Figure 4.4 The PM synchronous machine phase current variation during synthetic loading for 100 Hz synthetic loading frequency under full-load torque conditions

Figure 4.5 shows the variation of the quadrature axis current and the instantaneous rms current with time during synthetic loading. The quadrature axis current and the instantaneous rms current are simulated using (3.6) and (3.10). The quadrature axis waveform forces motor-generator action. That is, the machine accelerates for the

positive half-cycle and decelerates during the negative half-cycle of the quadrature axis current. The average value of the quadrature axis current is close to zero (0.31Amps) and this dc offset is required to compensate equivalent friction and windage torque (3.6). However, the average of the instantaneous rms current is equal to the rated rms current of the machine, 7.45Amps (1.0pu), which confirms that the synthetic loading technique results in rated copper loss in the machine. The synthetic loading frequency in this simulation is 100 Hz. From Figure 4.5 (b) the peak of first half cycle of instantaneous rms current (associated with acceleration) is higher than the peak during deceleration. This is a consequence of the dc offset current. This asymmetry in the peaks increases as the equivalent load torque falls because the dc offset, I_o, becomes a large percentage of I_m.

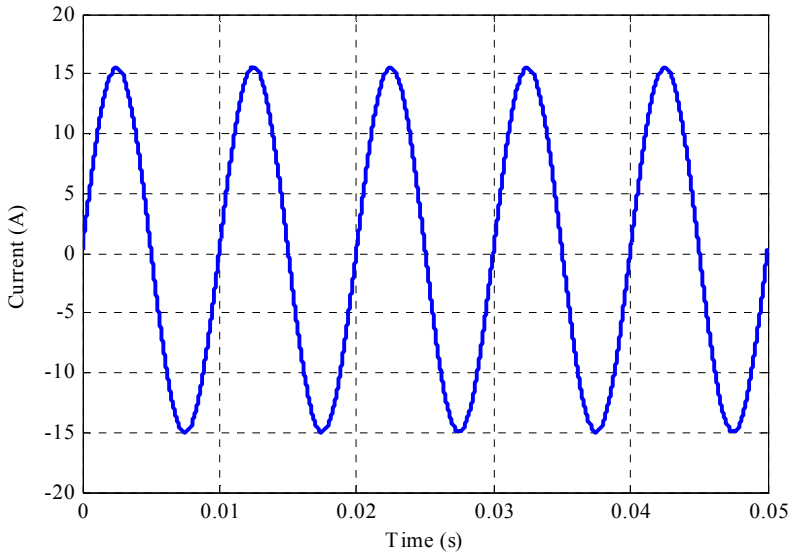

(a) Quadrature axis current

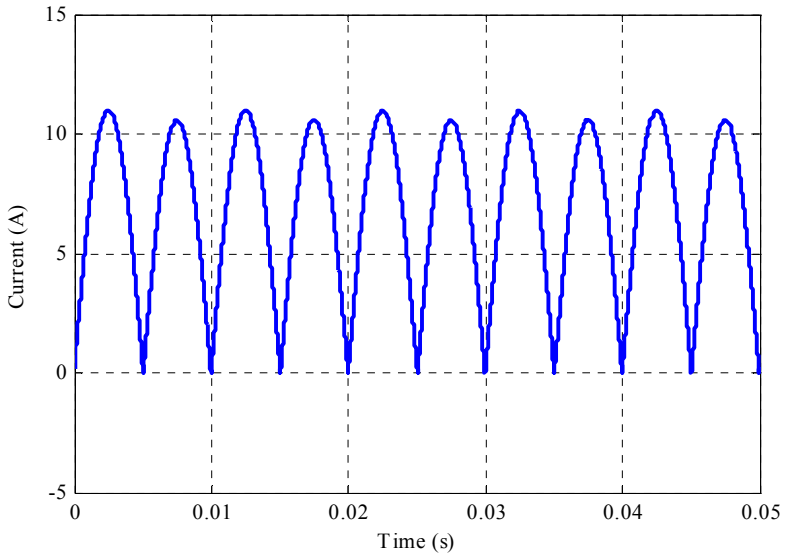

(b) Instantaneous rms line current

Figure 4.5 The PM synchronous machine quadrature axis and instantaneous rms line currents variation during synthetic loading at 100 Hz under full-load torque conditions

Figure 4.6 illustrates the simulated variation of speed with time using the synthetic loading technique (3.18). Note that although the PM synchronous machine speed is actually varying with time, the average speed is 4000rpm (1.0pu), which is the same as the rated speed of the machine. The speed variation in Figure 4.6 clearly indicates that under synthetic loading the machine accelerates and decelerates. Accordingly, the PM synchronous machine can be loaded via the repeated acceleration and deceleration without the need to connect a mechanical load to the machine's drive shaft.

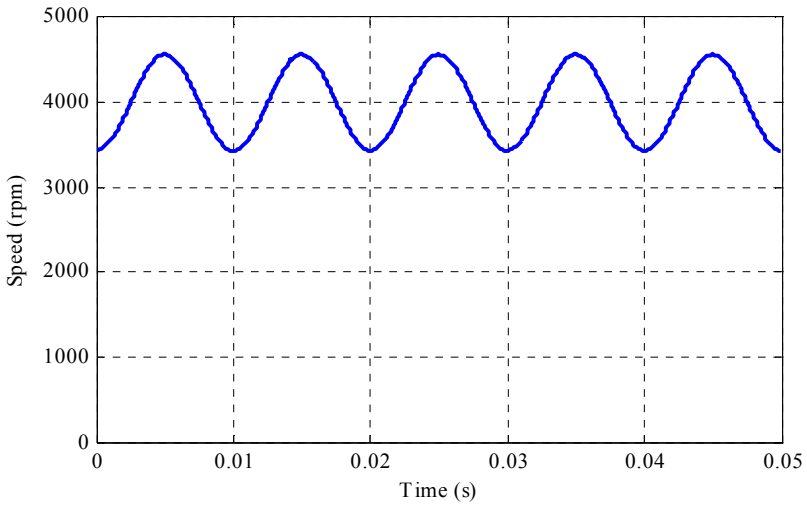

Figure 4.6 The PM synchronous machine speed variation during synthetic loading for 100 Hz under full-load torque conditions

Figure 4.7 shows the variation of input power, total power losses, copper loss, iron loss and friction and windage loss with time using synthetic loading. The input power of the PM synchronous machine during synthetic loading is simulated using (3.88). Input power is absorbed by the machine during acceleration and returned to the supply as the machine decelerates as shown in Figure 4.7 (a). The average input power over one synthetic loading cycle is equal to the average of the total losses, from which the efficiency can be readily evaluated. The copper, iron and friction and windage loss are simulated using (2.16), (2.18) and (2.20). Due to the variation of rms current with time the copper loss varies with time as shown in Figure 4.7 (b). However, the average copper loss over one synthetic loading cycle is equal to the rated copper loss 91.7W (0.095pu). The core loss and friction and windage loss vary with time as a result of speed variation as shown in Figures 4.7 (c) and 4.7 (d) respectively. The average iron loss and friction and windage loss are equal to the rated values of 19.8W (0.021pu) and 6.1W (0.0063pu) respectively. Figure 4.7 (c) shows slightly dips in the peak of iron loss waveform. This is because the iron loss during synthetic loading is combination of a dc component and two ac components, one of which has twice the frequency of the other. The summation of these components lead to the dips in the top of the iron loss waveform and the resultant asymmetry.

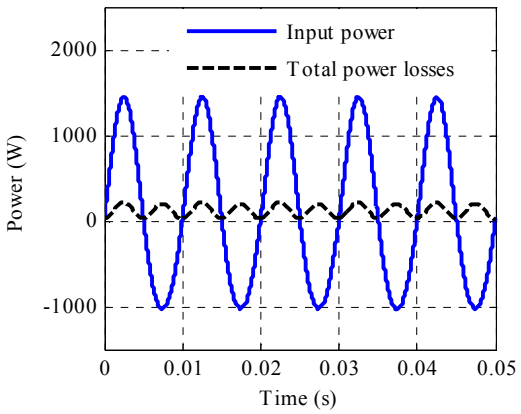

(a) Input power and total losses during synthetic loading for 100 Hz synthetic loading frequency

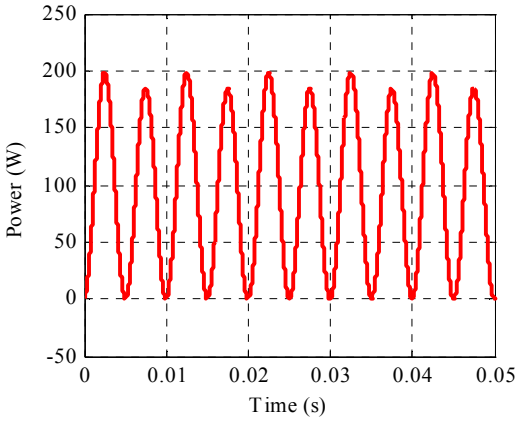

(b) stator copper loss during synthetic loading for 100 Hz synthetic loading frequency

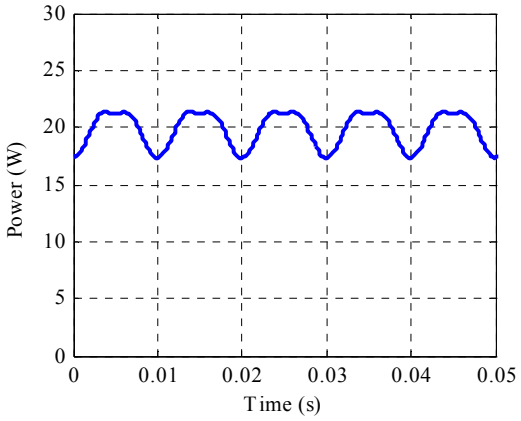

(c) iron loss during synthetic loading for 100 Hz synthetic loading frequency

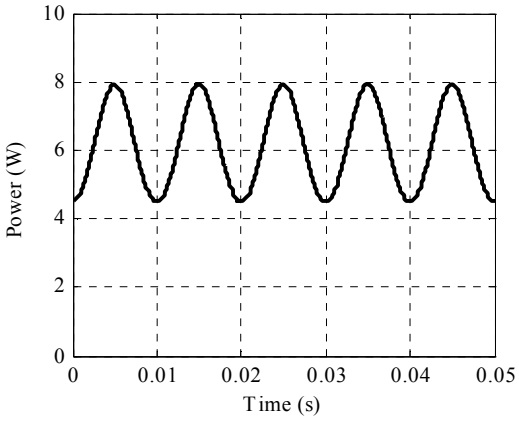

(d) friction and windage loss during synthetic loading for 100 Hz synthetic loading frequency

Figure 4.7 The PM synchronous machine input power and power losses variation during synthetic loading for 100 Hz synthetic loading frequency under full-load torque conditions

Because the current drawn during synthetic loading is adjusted to the rated value, the copper loss in the machine is equal to the rated load copper loss. Similarly because the synthetic loading technique is conducted at rated emf the average iron loss is the same as for full load. Finally, the average speed at which the synthetic loading technique is carried out can also be easily adjusted to the rated speed of the machine via I_o such that the rated friction and windage loss is also incorporated. Consequently, copper, iron and

friction and windage losses are included in the synthetic loading technique and are at rated values.

The simulation of electromagnetic torque via (3.3) is illustrated in Figure 4.8. This clearly indicates that the PM synchronous machine is heavily loaded by the synthetic loading technique as the rms torque is 1.0pu. The average value of electromagnetic torque is non-zero (in this case 0.0145Nm) in order to compensate the friction and windage loss.

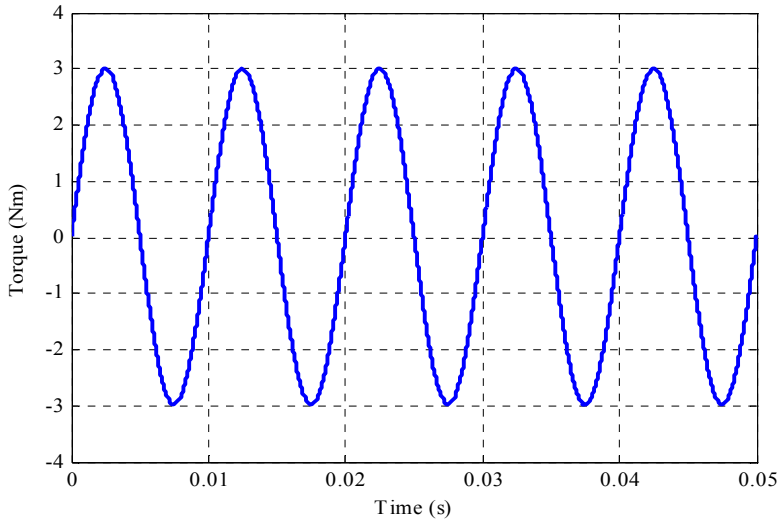

Figure 4.8 The PM synchronous machine electro-magnetic torque variation during synthetic loading for 100 Hz under full-load torque conditions

Figure 4.9 illustrates the instantaneous apparent power and magnetic flux with time during the synthetic loading under full-load torque conditions. The instantaneous apparent power is simulated using (3.94). The volt-amperes drawn by the machine when it acts as motor is higher than the volt-ampere returned to the supply when the machine acts as generator as shown in Figure 4.9 (a). The peak apparent power required is 1490VA (1.52pu). The peak current rating is 1.42pu and the dc link voltage required is 1.1pu. This gives a required apparent power rating of 1.52pu with a synthetic loading frequency of 100 Hz. The instantaneous flux varies in amplitude as a consequence of the current variation; the dc value of the magnetic flux is the rated value (1.0pu) as shown in Figure 4.9 (b) with a peak to peak variation of 0.029pu.

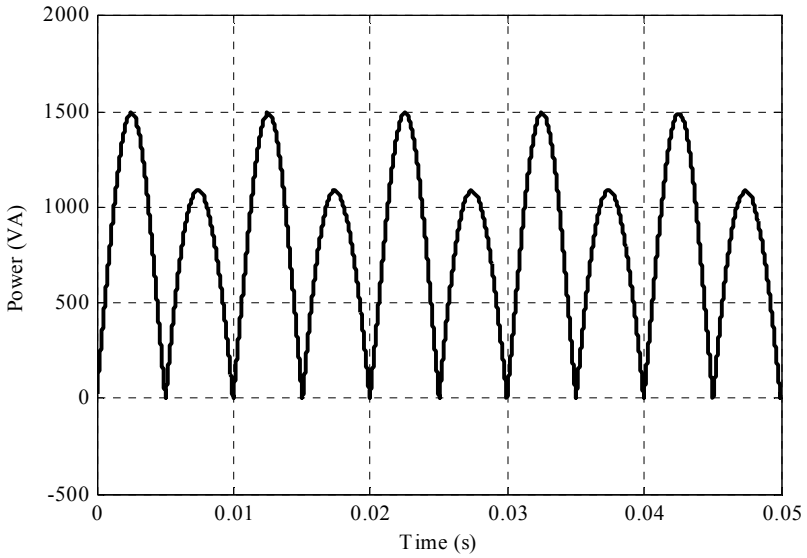

(a) Apparent power

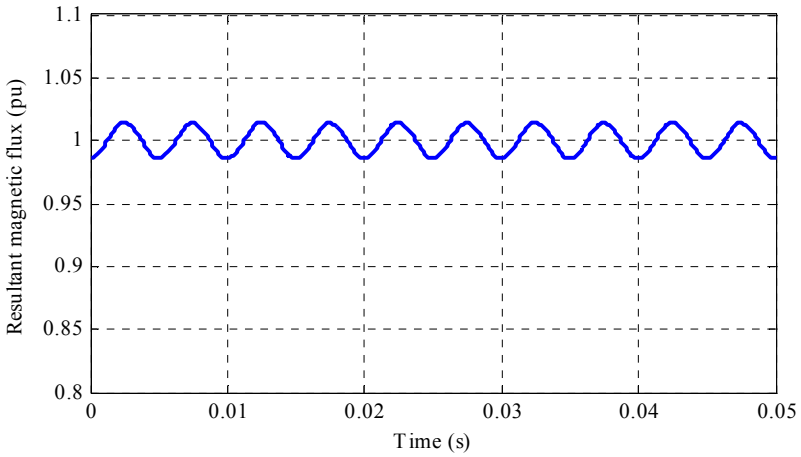

(b) Resultant magnetic flux

Figure 4.9 The PM synchronous machine apparent power and magnetic flux variation in the air gap during synthetic loading for 100 Hz under full-load torque conditions

Five different values of synthetic loading frequency that establish full-load torque conditions are simulated and summarized in Table 4.2. In each case I_m= 14.9A and I_o=0.074A. The simulation results show that the losses, rms current and speed using the synthetic loading technique are consistent with the standard efficiency test method. This

indicates that synthetic loading could be used for the evaluation of efficiency of the PM synchronous machine.

Table 4.2 Comparison of the standard efficiency test and the synthetic loading technique simulation results for the PM synchronous machine under full-load torque conditions (I_m=14.9A, I_o=0.074A)

	Standard Efficiency Test	Synthetic Loading Frequency (Hz)				
		100	105	110	115	120
rms line voltage (V)	90.0	83.4	83.4	83.5	83.5	83.5
rms line current (A)	7.45	7.45	7.45	7.45	7.45	7.45
Speed (rpm)	4000	4000	4000	4000	4000	4000
Minimum inverter peak current (A)	10.5	14.9	14.9	14.9	14.9	14.9
Phase-leg volt-ampere (VA)	1365	2086	2086	2086	2086	2086
Minimum dc link voltage (V)	130	140	140	140	140	140
Output power (W)	843.0	-	-	-	-	-
Input power (W)	962.0	117.7	117.7	117.7	117.7	117.7
Stator copper loss (W)	91.6	91.7	91.7	91.7	91.7	91.7
Iron loss (W)	19.8	19.8	19.8	19.8	19.8	19.8
Friction and windage loss (W)	6.1	6.2	6.1	6.1	6.1	6.1
Total losses (W)	117.5	117.7	117.6	117.6	117.6	117.6
Efficiency (%)	87.8	87.8	87.8	87.8	87.8	87.8

Table 4.2 shows that the stator copper loss, iron loss and friction and windage loss are the same as the standard efficiency test method. This is expected because the stator rms currents and the speed are at rated values. Since the input power is known, the efficiency is calculated by subtracting the total losses from the input power then dividing by the input power. The rms voltages during synthetic loading are lower than the voltage during the standard efficiency test. This is because the average voltage drop across R_a and L_q over one synthetic loading cycle is close to zero unlike during the standard efficiency test. Even though the rms voltage is lower, the PM synchronous machine is still running at rated electromagnetic motive force (emf) during synthetic loading. The synthetic loading frequencies chosen all lie on the plateau (100 – 140Hz) show in Figure 4.1 (a), therefore the inverter VA and DC link voltage requirements for each case are the same.

4.3.2 Three-quarters of Full-Load Torque Condition

The performance of the synthetic loading technique is simulated for different synthetic loading frequencies configured to produce three-quarters of full-load torque and compared with the equivalent standard efficiency test. The instantaneous phase voltages are amplitude and frequency modulated as a result of the synthetic loading technique. During synthetic loading the amplitude of the instantaneous rms voltage is variable while its frequency is fixed; the average value of the rms line voltage calculated over one synthetic loading cycle is 83.0V (0.92pu).

The simulated instantaneous currents are varied in amplitude and frequency during synthetic loading. This is a consequence of instantaneous phase voltage variation with time. The peak current during synthetic loading, while the PM synchronous machine is loaded at three-quarter of full-load torque, is 11.3Amps (1.08pu to base of rated value). The average rms current over one synthetic loading cycle is 5.64Amps (0.75pu). The average speed over one synthetic loading cycle is 4000rpm (1.0pu) which confirms that the PM synchronous machine running at rated speed on average. The peak to peak speed variation for three-quarters of full-load torque condition is less than the swing speed for full-load torque condition. This is a consequence of reduction in AC perturbation current from 14.85Amps to 11.3Amps hence reduced torque variation during a synthetic loading cycle.

The input power varies with time and the average value over one synthetic loading cycle is equal to the average of the total losses. The copper loss varies with time; but has an average value of 52.5W (0.045pu). The speed variation during synthetic loading results in iron loss and friction and windage loss variation. The average value of the iron loss and friction and windage loss over one synthetic loading cycle are 19.6W (0.017pu) and 6.1W (0.01pu) respectively. This confirms that in this case the iron and friction and windage losses are fixed, regardless of the PM synchronous machine load torque conditions. However, the losses are a function of machine speed. The electromagnetic torque confirms alternation of motor-generator action and the PM synchronous machine is loaded to three-quarters of full-load torque. The average of the electromagnetic torque

over one synthetic loading cycle is 0.0145Nm which compensates the friction and windage loss, but the rms torque is 0.75pu. The phase-leg volt-ampere required is 1553VA (1.14pu).

The simulation results of synthetic loading for five different synthetic loading frequencies and the standard efficiency test method are summarised in Table 4.3. The copper loss, iron loss and friction and windage loss for each of the different synthetic loading frequencies are consistent with the losses during the standard efficiency simulation. This is because the PM synchronous machine draws rated rms current and operates at rated speed, on average, during synthetic loading. The efficiency estimated by the standard efficiency test is the same as that obtained from the synthetic loading technique.

Table 4.3 Comparison of the standard efficiency test and the synthetic loading technique simulation results for the PM synchronous machine under three-quarters of full-load torque condition (I_m=11.5A, I_o=0.074A)

	Standard Efficiency Test	Synthetic Loading Frequency (Hz)				
		100	105	110	115	120
rms line voltage (V)	87.8	83.0	83.0	83.0	83.0	83.0
rms line current (A)	5.63	5.64	5.64	5.64	5.64	5.64
Speed (rpm)	4000	4000	4000	4000	4000	4000
Minimum inverter peak current (A)	7.88	11.5	11.5	11.5	11.5	11.5
Phase-leg volt-ampere (VA)	1025	1553	1553	1553	1553	1553
Minimum dc link voltage (V)	130	135	135	135	135	135
Output power (W)	632.3	-	-	-	-	-
Input power (W)	711.0	78.2	78.2	78.2	78.2	78.2
Stator copper loss (W)	52.4	52.5	52.5	52.5	52.5	52.5
Iron loss (W)	19.6	19.6	19.6	19.6	19.6	19.6
Friction and windage loss (W)	6.1	6.1	6.1	6.1	6.1	6.1
Total losses (W)	78.1	78.2	78.2	78.2	78.2	78.2
Efficiency (%)	89.0	89.0	89.0	89.0	89.0	89.0

4.3.3 Half of Full-Load Torque Condition

In this case the PM synchronous machine is loaded to half of rated torque and operates at rated speed. The synthetic loading performance is simulated for different synthetic

loading frequencies (100-120Hz) and compared with standard efficiency test performance.

Table 4.4 summarises the synthetic loading simulation results for five different synthetic loading frequencies for the half load torque condition and rated speed. The results show the distribution of losses in the PM synchronous machine, the line voltage, the phase current and the rotor speed are consistent with the standard efficiency test at half load torque condition. Table 4.4 shows that the stator copper losses for synthetic loading technique are slightly lower than that of the standard efficiency test. This is a consequence of the slightly higher current during the standard efficiency test method. Therefore, the efficiency calculated using synthetic loading technique is overestimated by 0.3% on average.

Table 4.4 Comparison of the standard efficiency test and the synthetic loading technique simulation results for the PM synchronous machine under half of full-load torque condition (I_m=7.45A, I_o=0.074A)

	Standard Efficiency Test	Synthetic Loading Frequency (Hz)				
		100	105	110	115	120
rms line voltage (V)	85.8	82.6	82.6	82.6	82.6	82.6
rms line current (A)	3.8	3.7	3.7	3.7	3.7	3.7
Speed (rpm)	4000	4000	4000	4000	4000	4000
Minimum inverter peak current (A)	5.3	7.45	7.45	7.45	7.45	7.45
Phase-leg volt-ampere (VA)	690	990	990	990	990	990
Minimum dc link voltage (V)	130	133	133	133	133	133
Output power (W)	421.8	-	-	-	-	-
Input power (W)	471.6	48.5	48.5	48.5	48.5	48.5
Stator copper loss (W)	24.3	23.0	23.0	23.0	23.0	23.0
Iron loss (W)	19.4	19.4	19.4	19.4	19.4	19.4
Friction and windage loss (W)	6.1	6.1	6.1	6.1	6.1	6.1
Total losses (W)	49.8	48.5	48.5	48.5	48.5	48.5
Efficiency (%)	89.4	89.7	89.7	89.7	89.7	89.7

4.3.4 Quarter of Full-Load Torque Condition

The PM synchronous machine is loaded to a quarter of full-load torque by the synthetic loading technique. Table 4.5 shows the simulation results of the five different

synthetic loading frequencies compared with the standard efficiency test. The results show that efficiency evaluation using synthetic loading technique produces similar results to the standard efficiency test. This is a consequence of the copper loss, iron loss and friction and windage loss during synthetic loading and during the standard efficiency test being the same.

Table 4.5 Comparison of the standard efficiency test and the synthetic loading technique simulation results for the PM synchronous machine under quarter of full-load torque condition (I_m=3.73A, I_o=0.074A)

	Standard Efficiency Test	Synthetic Loading Frequency (Hz)				
		100	105	110	115	120
rms line voltage (V)	83.9	82.3	82.3	82.3	82.3	82.3
rms line current (A)	1.87	1.87	1.87	1.87	1.87	1.87
Speed (rpm)	4000	4000	4000	4000	4000	4000
Minimum inverter peak current (A)	2.65	3.73	3.73	3.73	3.73	3.73
Phase-leg volt-ampere (VA)	350	496	496	496	496	496
Minimum dc link voltage (V)	130	133	133	133	133	133
Output power (W)	192.8	-	-	-	-	-
Input power (W)	223.6	31.2	31.2	31.2	31.2	31.2
Stator copper loss (W)	5.8	5.8	5.8	5.8	5.8	5.8
Iron loss (W)	19.2	19.3	19.3	19.3	19.3	19.3
Friction and windage loss (W)	6.1	6.1	6.1	6.1	6.1	6.1
Total losses (W)	31.1	31.2	31.2	31.2	31.2	31.2
Efficiency (%)	86.1	86.1	86.1	86.1	86.1	86.1

4.4 Simulation results for the IPM synchronous machine

In a similar fashion to the PM synchronous machine, the synthetic loading technique is applied to an IPM synchronous machine under different load torque conditions but at rated speed. The synthetic loading results for efficiency evaluation of the IPM synchronous machine are compared with the standard efficiency test method. The IPM synchronous machine used in this study was built by the University of Glasgow for low power and low speed applications (165W, 900rpm). The IPM synchronous machine draws rated current of 2 Amps at full-load torque and rated speed. The simulation uses the synthetic loading model of the IPM synchronous machine developed in chapter

three. The electrical and mechanical parameters for the IPM synchronous machine are given in Table 4.6.

Table 4.6 The electrical and mechanical parameters of the IPM synchronous machine

Parameters	Values
Rated output power	165 W
Rated peak current	2.0A
Rated speed	900rpm
Maximum Bus Voltage	200 V
Armature resistance, R_a	7.0Ω
Core loss resistance, R_c	1580Ω
Quadrature axis inductance, L_q	120 mH
Direct axis inductance, L_d	65 mH
Moment of inertia, J	4.5×10^{-3} kg.m^2
Damping coefficient, B	2.7×10^{-4} Nms^{-1}
Total permanent magnet flux linkage, λ_m	0.6 Wb
Number of poles	2

4.4.1 Full-Load Torque Condition

Figures 4.10-4.16 show the results for synthetic loading using synthetic loading frequency of 4Hz for IPM synchronous machine under full-load torque conditions. Equations (3.31) and (3.38) are used to simulate the instantaneous phase voltage and current respectively, and Figures 4.10 and 4.11 show the instantaneous phase voltage and current during synthetic loading respectively. The amplitude and frequency modulation of the instantaneous voltage is evident in Figure 4.10. This leads to the amplitude and frequency modulation of the instantaneous current as shown in Figure 4.11; thereby, the IPM synchronous machine is fully loaded. The higher excursions of the phase voltages are as a result of the large peak to peak variations of air-gap magnetic flux and machine speed in the IPM synchronous machine.

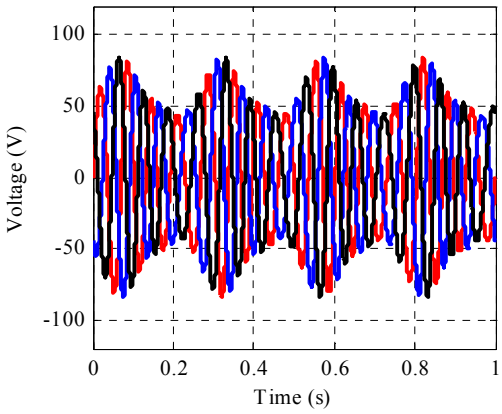

(a) three phase voltages during synthetic loading for 4 Hz synthetic loading frequency

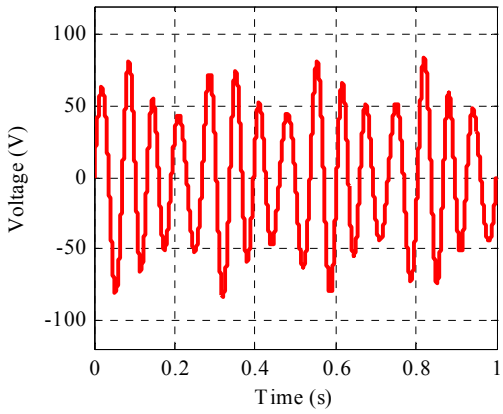

(b) phase a voltage during synthetic loading for 4 Hz synthetic loading frequency

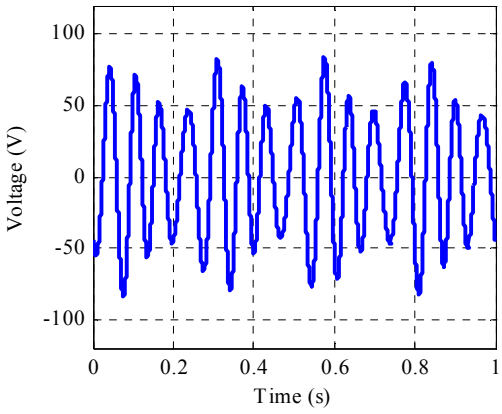

(c) phase b voltage during synthetic loading for 4 Hz synthetic loading frequency

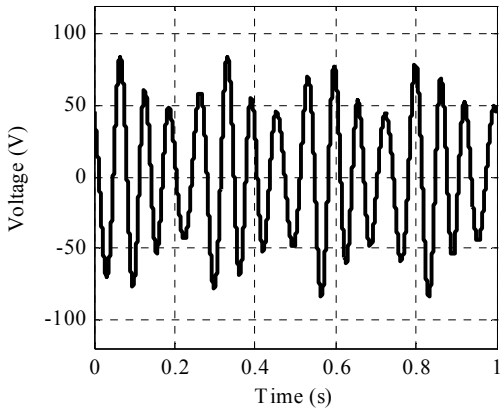

(d) phase c voltage during synthetic loading for 4 Hz synthetic loading frequency

Figure 4.10 The IPM synchronous machine terminal voltage variation during synthetic loading for 4 Hz synthetic loading frequency under full-load torque conditions

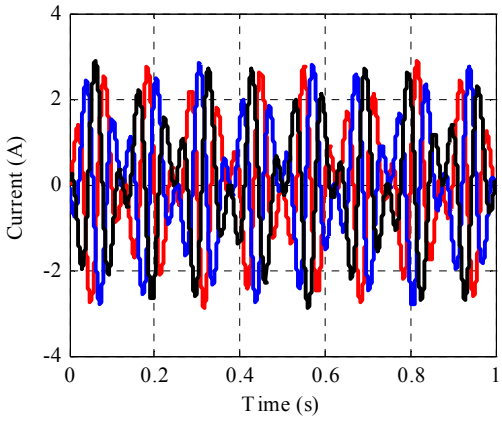

(a) three phase currents during synthetic loading for 4 Hz synthetic loading frequency

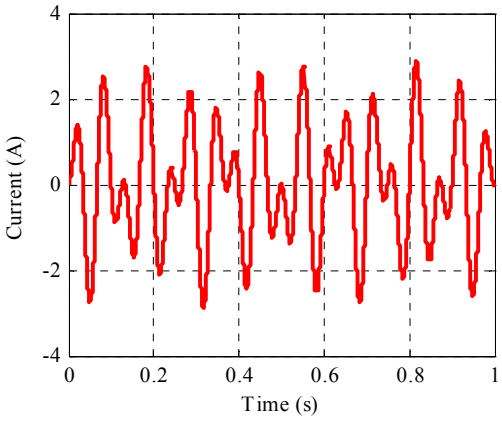

(b) phase a current during synthetic loading for 4 Hz synthetic loading frequency

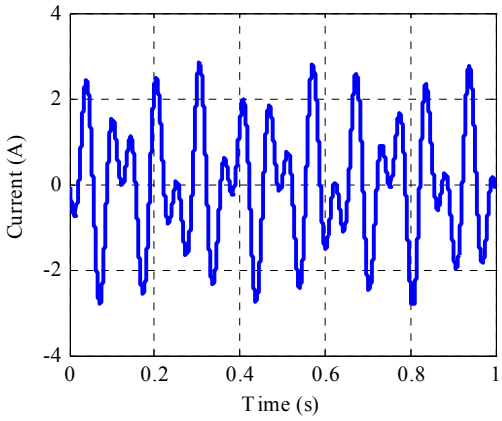

(c) phase b current during synthetic loading for 4 Hz synthetic loading frequency

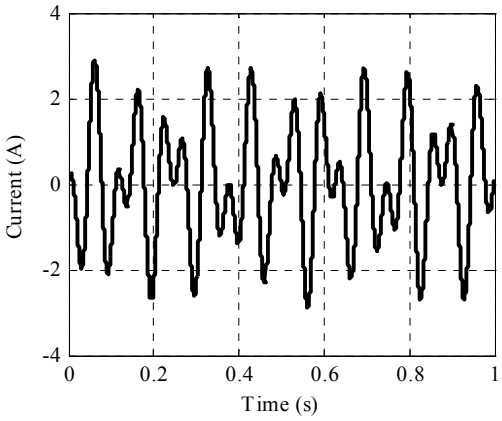

(d) phase c current during synthetic loading for 4 Hz synthetic loading frequency

Figure 4.11 The IPM synchronous machine currents variation during synthetic loading for 4 Hz synthetic loading frequency under full-load torque conditions

Simulation of instantaneous rms voltage and current using (3.90) and (3.92) are presented. Figure 4.12 shows that the instantaneous rms voltage and current vary with time during synthetic loading. The average rms voltage calculated over one synthetic loading cycle is 75.4V (0.84pu). As expected, this is below the rated value. Also, the average rms current calculated over one synthetic loading cycle is 1.41A (1.0pu) which is the rated value. This confirms that synthetic loading enforces rated torque conditions.

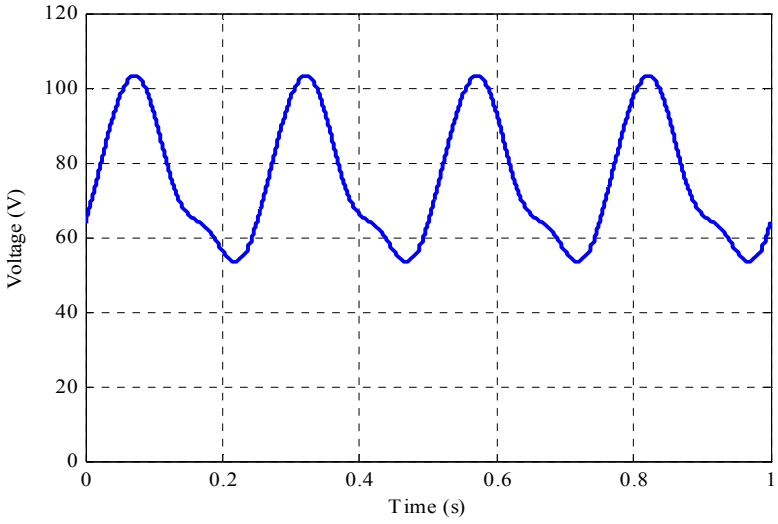

(a) Instantaneous rms line voltage

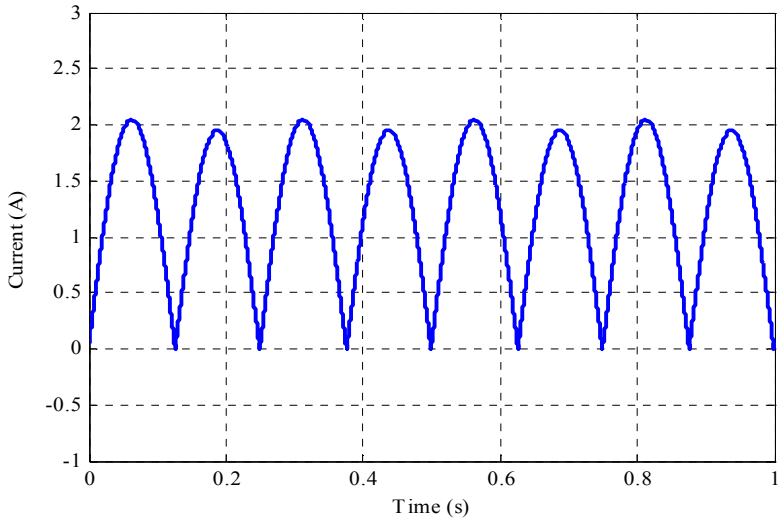

(b) Instantaneous rms current

Figure 4.12 The IPM synchronous machine instantaneous rms line voltage and current variation during synthetic loading for 4 Hz under full-load torque conditions

The quadrature axis current (3.6) is shown in Figure 4.13 (a) along with the electromagnetic torque with time during synthetic loading Figure 4.13 (b). The quadrature axis current has a peak value of 2.83A as shown in Figure 4.13 (a). However, the average value over one synthetic loading period is a small positive value to compensate for part of the friction and windage loss. The rms torque value is 1.0pu.

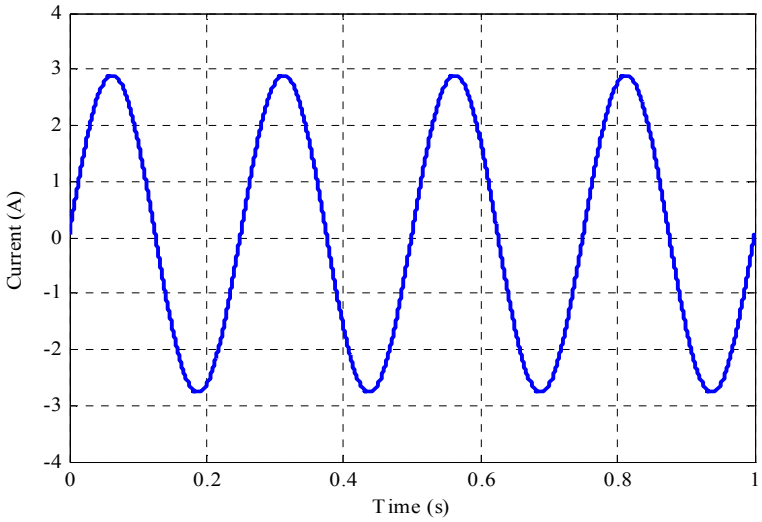

(a) Quadrature axis current

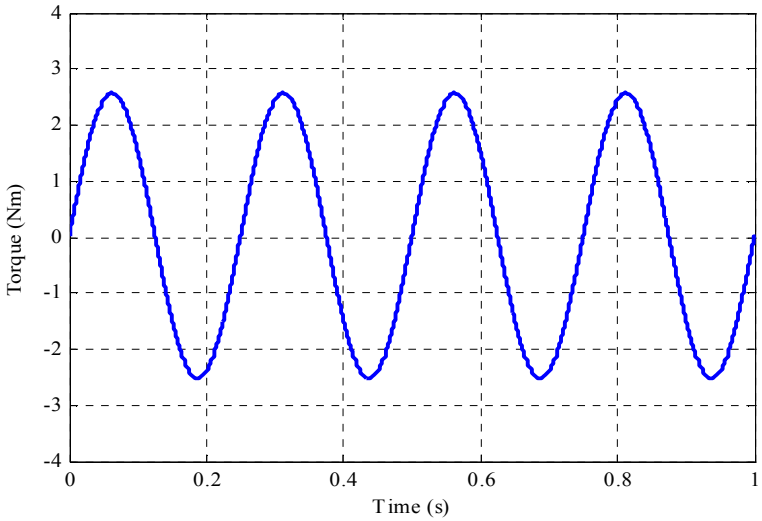

(b) Electromagnetic torque

Figure 4.13 The IPM synchronous machine quadrature axis current and electromagnetic torque variation during synthetic loading for 4 Hz under full-load torque conditions

Equation (3.17) in chapter three established the variation of rotor speed with time during synthetic loading. Figure 4.14 shows this variation. The average rotor speed over one synthetic loading period is 900rpm (1.0pu) with a peak to peak ripple of 430rpm (0.48pu). This leads to higher excursions in the phase voltages and the instantaneous rms voltage as shown in Figure 4.10 (a) and Figure 4.12 (a).

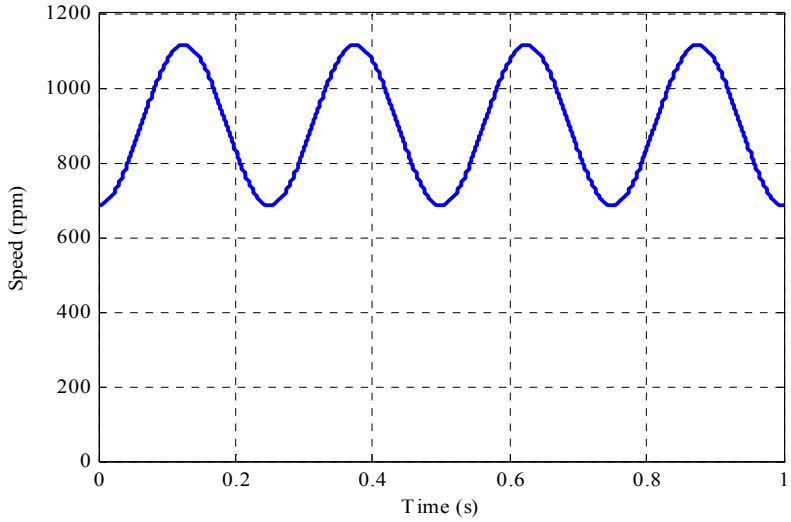

Figure 4.14 The IPM synchronous machine speed variation during synthetic loading for 4 Hz under full-load torque conditions

Figure 4.15 shows the variation of input power (3.88) and power losses in the IPM synchronous machine with time during synthetic loading. The input power is positive while the IPM synchronous machine is accelerating and negative while the machine rotor is decelerating. The average input power over one synthetic loading cycle is 48.0W which equals the total machines losses over the same period. Therefore, the efficiency can be evaluated using synthetic loading. The copper loss, iron loss and friction and windage loss are determined by (2.16), (2.18) and (2.20). Figure 4.15 (b) shows the variation of the copper loss with time, during synthetic loading. The average copper loss over one synthetic loading cycle is 42.0W which is close to the copper loss during the standard efficiency test. The iron loss (which varies with instantaneous rms voltage) is shown in Figure 4.15 (c) and the friction and windage loss (which varies with the square of speed) is shown in Figure 4.15 (d). The average of the iron loss and friction and windage loss over one synthetic loading cycle are close to the losses calculated using the standard efficiency test.

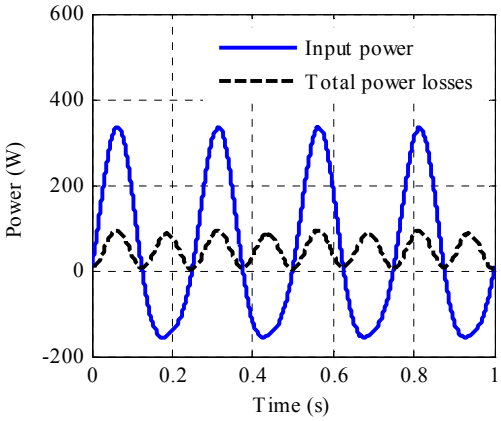

(a) Input power and total losses during synthetic loading for 4 Hz synthetic loading frequency

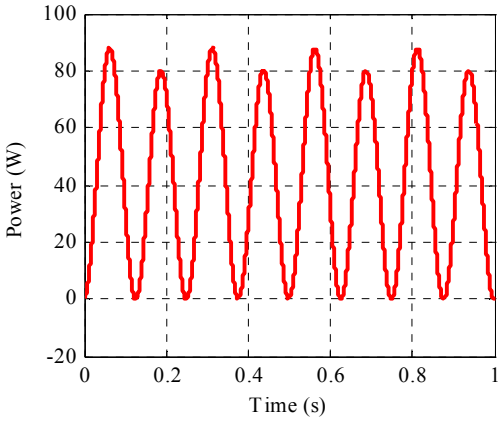

(b) stator copper loss during synthetic loading for 4 Hz synthetic loading frequency

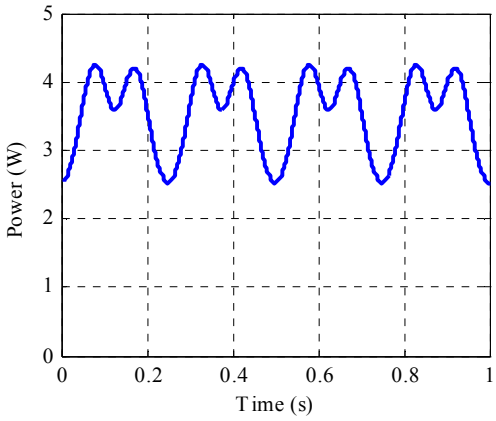

(c) iron loss during synthetic loading for 4 Hz synthetic loading frequency

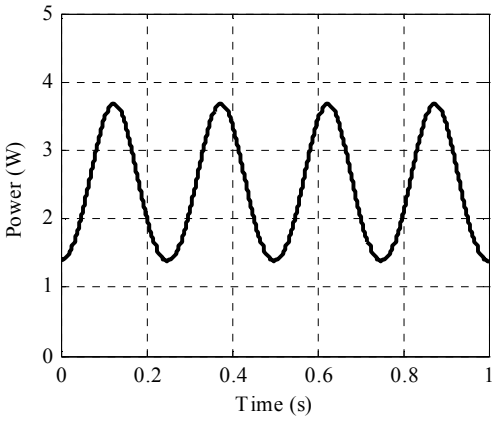

(d) friction and windage loss during synthetic loading for 4 Hz synthetic loading frequency

Figure 4.15 The IPM synchronous machine Input power and power losses variation during synthetic loading for 4 Hz synthetic loading frequency under full-load torque conditions

The apparent power rating (3.94) is shown in Figure 4.16 along with resultant air-gap flux with time, during synthetic loading. The phase-leg volt-ampere required in the case of the full-load torque condition is 440VA. This IPM synchronous machine has higher quadrature axis inductance. This makes a bigger contribution to the air-gap flux, therefore, the resultant variation in air-gap flux is 0.14pu as a result of the quadrature axis current variation with time.

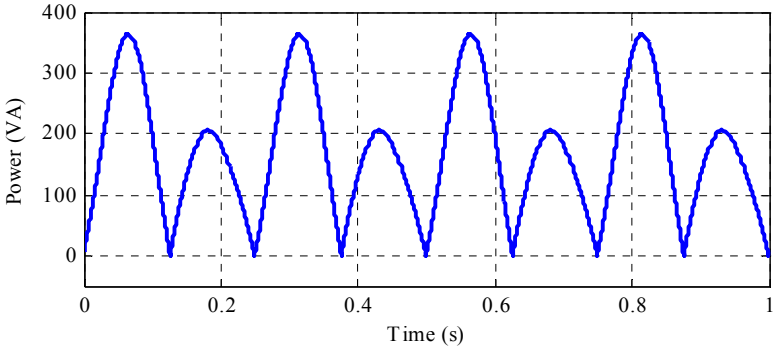

(a) Apparent power

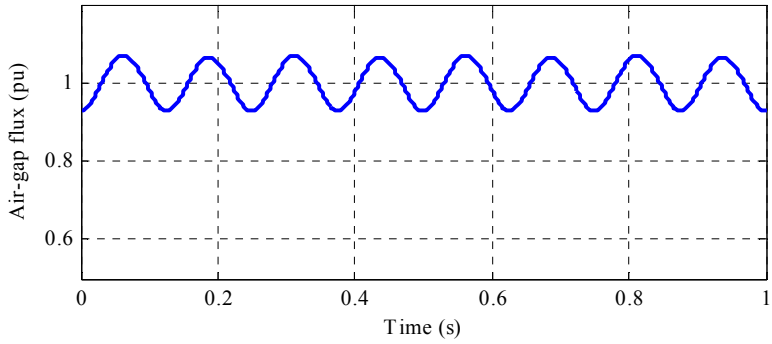

(b) Resultant magnetic flux

Figure 4.16 The IPM synchronous machine apparent power resultant magnetic field variations in the air gap during synthetic loading for 4 Hz under full-load torque conditions

The simulation results for the IPM synchronous machine for five different synthetic loading frequencies are summarised and compared with the standard efficiency test method in Table 4.7. The simulation result shows the power loss distribution in the IPM synchronous machine and confirms that synthetic loading can be used for efficiency evaluation. The lower efficiency of the IPM synchronous machine is as a result of a number of factors including its lower power rating. The efficiency calculated from the synthetic loading simulations is 77.5%. In general, if the IPM synchronous machine draws the rated current at a speed of 900 rpm, the efficiency is overestimated by 0.1% during synthetic loading compared to the standard efficiency test.

Table 4.7 Comparison of the standard efficiency test and the synthetic loading technique simulation results for the IPM synchronous machine under full-load torque condition (I_m=2.83A, I_o=0.028A)

	Standard Efficiency Test	Synthetic Loading Frequency (Hz)				
		4	6	8	9	10
rms line voltage (V)	90.8	75.4	75.5	75.5	75.6	75.6
rms line current (A)	1.42	1.41	1.41	1.41	1.41	1.41
Speed (rpm)	900	900	900	900	900	900
Minimum inverter peak current (A)	2.0	2.83	2.83	2.83	2.83	2.83
Phase-leg volt-ampere (VA)	280.0	438.0	433.0	438.0	443.0	449.0
Minimum dc link voltage (V)	140	154.5	153.0	154.8	156.5	158.5
Output power (W)	165.4	-	-	-	-	-
Input power (W)	213.7	48.0	48.0	48.0	48.0	48.0
Stator copper loss (W)	42.4	42.0	42.0	42.0	42.0	42.0
Iron loss (W)	3.53	3.54	3.53	3.6	3.6	3.6
Friction and windage loss (W)	2.41	2.5	2.43	2.4	2.4	2.4
Total losses (W)	48.3	48.0	48.0	48.0	48.0	48.0
Efficiency (%)	77.4	77.5	77.5	77.5	77.5	77.5

4.4.2 Three-quarters of Full-Load Torque Condition

In this case the IPM synchronous machine is loaded to three-quarters of full-load torque. The machine draws an rms current of 2.12A. The average rms voltage over one synthetic loading cycle is 73.0V (0.81pu). Also, the average rms current over one synthetic loading cycle is 2.12A (0.75pu) which is equal to the desired value. The quadrature axis current and the electromagnetic torque vary with time during synthetic loading. The average value of quadrature axis current and electromagnetic torque over one synthetic loading cycle is small in order to compensate the friction and windage loss.

The rotor speed varies with time during synthetic loading, although, the average rotor speed over one synthetic loading cycle is 900rpm (1.0pu). That means the IPM synchronous machine running at rated speed, on average, during synthetic loading. The average input power over one synthetic loading is 29.4W which is equal to the average of the total losses for the same cycle. The average value of the copper loss over one synthetic loading cycle is 23.7W and is equal to the rated copper loss. The IPM

synchronous machine in this study is a low speed machine which leads to low values of iron loss and friction and windage loss.

Table 4.8 shows the comparison of the losses identified with the standard efficiency test and synthetic loading for five different synthetic loading frequencies. The simulation results confirm that synthetic loading can be used to identify the total losses and the efficiency. Table 4.8 shows that the resultant efficiencies from the synthetic loading are close to the rated standard efficiency test. The efficiency using the synthetic loading technique is 80.7% for the synthetic loading frequency range shown. The efficiency is overestimated by 0.1%, when the actual input is used to calculate the efficiency.

Table 4.8 Comparison of the standard efficiency test and the synthetic loading technique simulation results for the IPM synchronous machine under three-quarters of full-load torque condition (I_m=2.12A, I_o=0.028A)

	Standard Efficiency Test	Synthetic Loading Frequency (Hz)				
		4	6	8	9	10
rms line voltage (V)	84.8	73.0	73.0	73.0	73.0	73.0
rms line current (A)	1.07	1.06	1.06	1.06	1.06	1.06
Speed (rpm)	900	900	900	900	900	900
Minimum inverter peak current (A)	1.5	2.12	2.12	2.12	2.12	2.12
Phase-leg volt-ampere (VA)	195.0	297.0	295.0	299	302	305
Minimum dc link voltage (V)	130	140	139	141	142.4	144
Output power (W)	122.9	-	-	-	-	-
Input power (W)	152.5	29.4	29.4	29.4	29.4	29.4
Stator copper loss (W)	23.9	23.7	23.7	23.4	23.7	23.7
Iron loss (W)	3.3	3.3	3.3	3.3	3.4	3.4
Friction and windage loss (W)	2.4	2.4	2.4	2.4	2.4	2.4
Total losses (W)	29.6	29.4	29.4	29.4	29.5	29.5
Efficiency (%)	80.6	80.7	80.7	80.7	80.7	80.7

4.4.3 Half of Full-Load Torque Condition

In this case the efficiency of the IPM synchronous machine is investigated when the IPM synchronous machine produces half of rated torque at rated speed. The rms phase current is 1.42A. Table 4.9 shows the simulation results for this condition. Five different synthetic loading frequencies are used for synthetic loading simulation and the results

compared with the standard efficiency test result. Table 4.9 shows that the synthetic loading results are consistent with the standard efficiency test results. The efficiency is 83.3% for synthetic loading frequency range shown in Table 4.9. Consequently, the efficiency is overestimated by 0.1% during synthetic loading.

Table 4.9 Comparison of the standard efficiency test and the synthetic loading technique simulation results for the IPM synchronous machine under half of full-load torque condition (I_m=1.41A, I_o=0.028A)

	Standard Efficiency Test	Synthetic Loading Frequency (Hz)				
		4	6	8	9	10
rms line voltage (V)	79.2	71.2	71.2	71.2	71.2	71.2
rms line current (A)	0.71	0.71	0.71	0.71	0.71	0.71
Speed (rpm)	900	900	900	900	900	900
Minimum inverter peak current (A)	1.0	1.41	1.41	1.41	1.41	1.41
Phase-leg volt-ampere (VA)	120.0	179	178	180	181.6	183.3
Minimum dc link voltage (V)	120	126.8	126.4	127.8	128.8	130
Output power (W)	80.4	-	-	-	-	-
Input power (W)	96.6	16.1	16.1	16.1	16.1	16.1
Stator copper loss (W)	10.7	10.5	10.5	10.5	10.5	10.5
Iron loss (W)	3.2	3.2	3.2	3.2	3.2	3.2
Friction and windage loss (W)	2.4	2.4	2.4	2.4	2.4	2.4
Total losses (W)	16.3	16.1	16.1	16.1	16.1	16.1
Efficiency (%)	83.2	83.3	83.3	83.3	83.3	83.3

4.4.4 Quarter of Full-Load Torque Condition

The IPM synchronous machine is loaded to one quarter of load torque at rated speed. The IPM synchronous machine draws an rms current of 0.35A. The peak value of AC perturbation current, I_m, is 0.71A.

The instantaneous rms line voltage and current vary with time during synthetic loading. However, the average rms line voltage and current over one synthetic loading cycle are 70.2V (0.77pu) and 0.35Amps (0.25pu) respectively. The lower line voltage during synthetic loading compared with the standard efficiency test is a consequence of the voltage drop across R_a and L_q in the machine and is close to zero, on average, during synthetic loading. This volt drop is higher during the standard efficiency test.

For comparison, the output data of five different values of synthetic loading frequencies simulations are summarised in Table 4.10, together with simulation results for the standard efficiency test result. The calculated efficiency is also shown.

The results in Table 4.10 show that the synthetic loading technique efficiency figures for the IPM synchronous machine are close to those from the standard efficiency simulation. The average input power is equal to the total sum of the losses for each test method. The efficiency during synthetic loading is 82.0% for the five frequencies.

Table 4.10 Comparison of the standard efficiency test and the synthetic loading technique simulation results for the IPM synchronous machine under quarter of full-load torque condition (I_m=0.71A, I_o=0.028A)

	Standard Efficiency Test	Synthetic Loading Frequency (Hz)				
		4	6	8	9	10
rms line voltage (V)	73.9	70.2	70.2	70.2	70.2	70.2
rms line current (A)	0.35	0.35	0.35	0.35	0.35	0.35
Speed (rpm)	900	900	900	900	900	900
Minimum inverter peak current (A)	0.5	0.71	0.72	0.71	0.71	0.71
Phase-leg volt-ampere (VA)	55.0	82	82.6	82	82.4	83
Minimum dc link voltage (V)	110	114.8	114.7	115.5	116.1	116.8
Output power (W)	36.9	-	-	-	-	-
Input power (W)	45.0	8.1	8.1	8.1	8.1	8.1
Stator copper loss (W)	2.6	2.7	2.7	2.7	2.7	2.7
Iron loss (W)	3.1	3.1	3.1	3.1	3.1	3.1
Friction and windage loss (W)	2.4	2.4	2.4	2.4	2.4	2.4
Total losses (W)	8.1	8.2	8.2	8.2	8.2	8.2
Efficiency (%)	82.0	82.0	82.0	82.0	82.0	82.0

4.5 Simulation results for the Linear PM synchronous machine

In this section the synthetic loading simulation results for the linear PM synchronous machine are investigated for different load force conditions and different values of synthetic loading frequencies at rated velocity. The linear PM synchronous machine to be simulated is a ServoTube 25 Actuator (2504S) from Copley Motion Systems LLC. The linear PM synchronous machine parameters are specified in Table 4.11.

Table 4.11 Electrical and mechanical parameters of the linear PM synchronous machine

Parameters	Values
Rated output power	130 W
Maximum rated current	3.27 A
Rated velocity	2.56 ms^{-1}
Maximum Bus Voltage	220 V
Armature resistance, R_a	3.01 Ω
Core loss resistance, R_c	625 Ω
Quadrature axis inductance, L_q	1.95 mH
Direct axis inductance, L_d	1.95 mH
Mover mass, M	1.25 kg
Damper coefficient, D	0.14 Nsm^{-1}
Total permanent magnet flux linkage, λ_m	84.75 mWb
Number of poles	4

4.5.1 Full-Load Force Condition

In this case the standard efficiency test and the synthetic loading test on the linear PM synchronous machine are simulated under full-load force and rated speed conditions using five different synthetic loading frequencies. Figures 4.17 – 4.23 show examples of the simulation results of the synthetic loading technique using a synthetic loading frequency of 20Hz.

The instantaneous phase voltage and current are simulated during synthetic loading using (3.60) and (3.65). Figure 4.17 shows the instantaneous phase voltage and Figure 4.18 shows the instantaneous phase current during synthetic loading. The instantaneous phase voltage and current are amplitude and frequency modulated during synthetic loading.

Instantaneous rms voltage and current during synthetic loading (3.90) and (3.92) are shown in Figure 4.19. It is important to notice that the instantaneous rms line voltage is higher during the half cycle that the machine accelerates and lower for that during the half cycle when the machine decelerates, Figure 4.19 (a). The amplitude of the instantaneous rms current during the acceleration half cycle is slightly higher than the amplitude of the deceleration half cycle as shown Figure 4.19 (b). This is a consequence of the dc offset current.

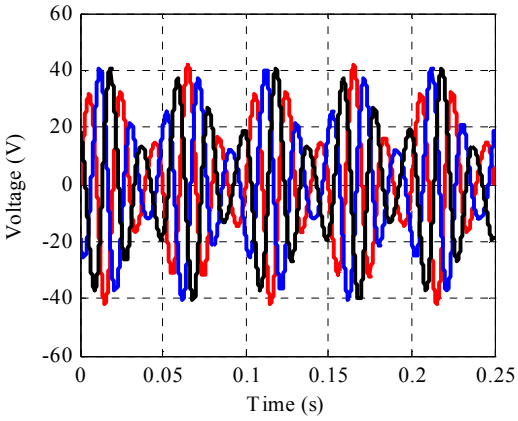

(a) three phase voltages during synthetic loading for 20 Hz synthetic loading frequency

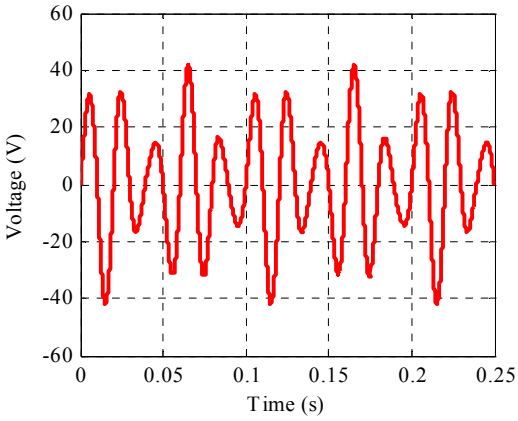

(b) phase a voltage during synthetic loading for 20 Hz synthetic loading frequency

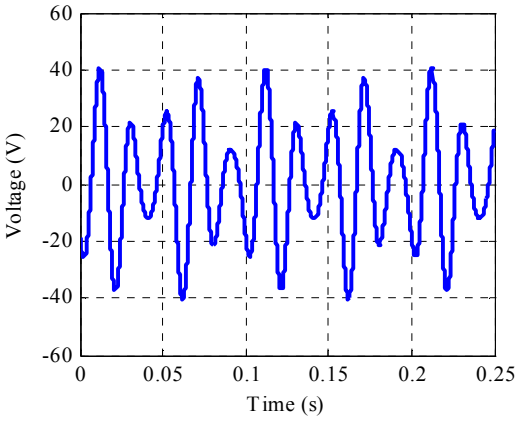

(c) phase b voltage during synthetic loading for 20 Hz synthetic loading frequency

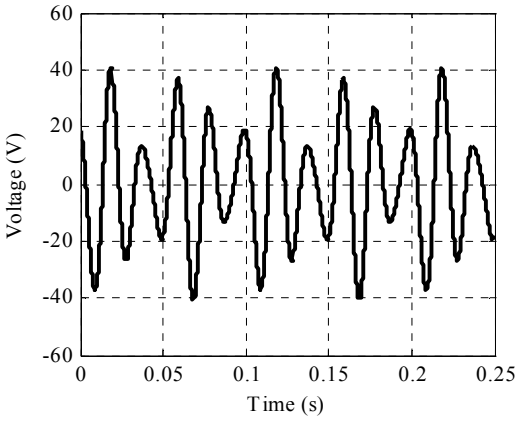

(d) phase c voltage during synthetic loading for 20 Hz synthetic loading frequency

Figure 4.17 The linear PM synchronous machine phase voltage variation during synthetic loading for 20 Hz synthetic loading frequency under full-load force conditions

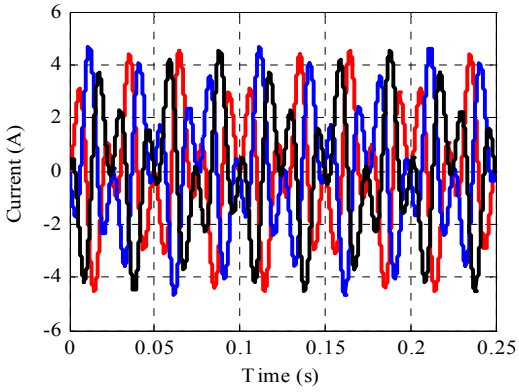

(a) three phase currents during synthetic loading for 20 Hz synthetic loading frequency

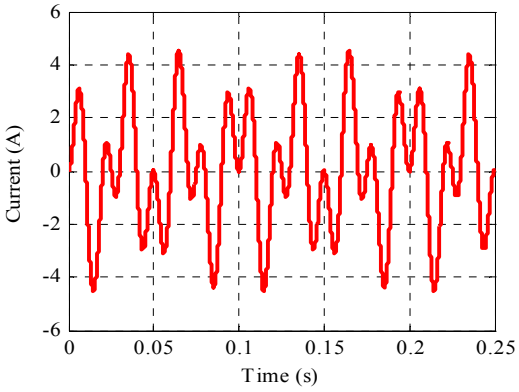

(b) phase a current during synthetic loading for 20 Hz synthetic loading frequency

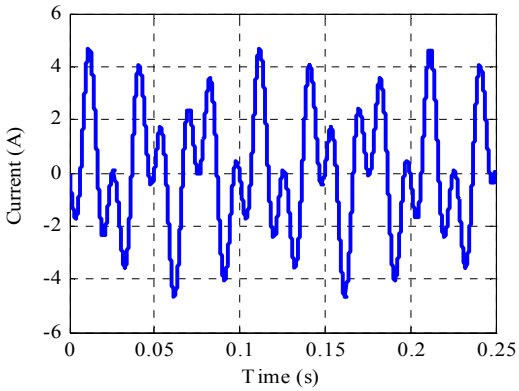

(c) phase b current during synthetic loading for 20 Hz synthetic loading frequency

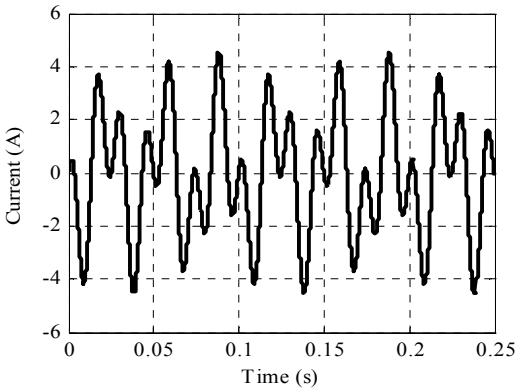

(d) phase c current during synthetic loading for 20 Hz synthetic loading frequency

Figure 4.18 The linear PM synchronous machine currents variation during synthetic loading for 20 Hz synthetic loading frequency under full-load force conditions

The quadrature axis current of the linear PM synchronous machine during synthetic loading (3.44) is shown in Figure 4.20, along with the electromagnetic force. The quadraure axis current has a peak value of 4.64Amps (1.42pu). However, the average value of the quadrature axis current is 0.066Amps. This average value is equal to the no load current that compensates the no load friction losses. Figure 4.20 (b) shows the variation of electromagnetic force with time. The peak value of the electromagnetic force is 72.7N (1.42pu). The average value of the electromagnetic force over one synthetic loading cycle is 0.36N to compensate the friction loss.

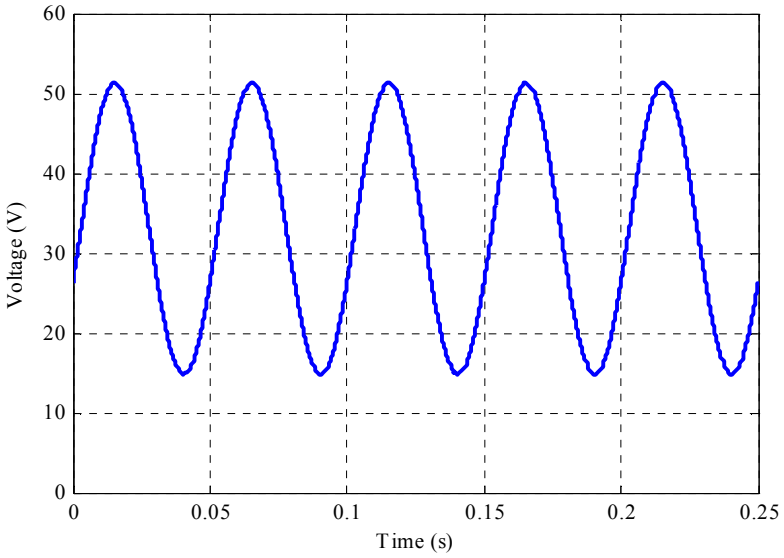

(a) Instantaneous rms line voltage

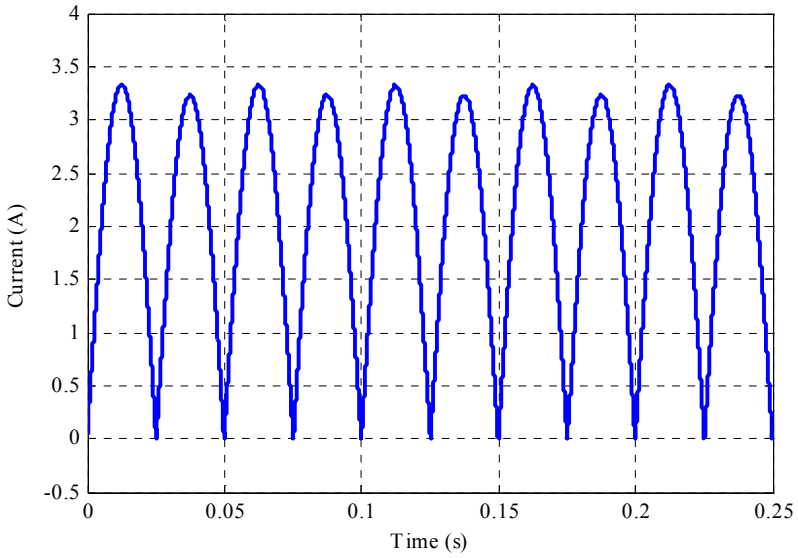

(b) Instantaneous rms line current

Figure 4.19 The linear PM synchronous machine instantaneous rms line voltage and current variation during synthetic loading for 20 Hz under full-load force conditions

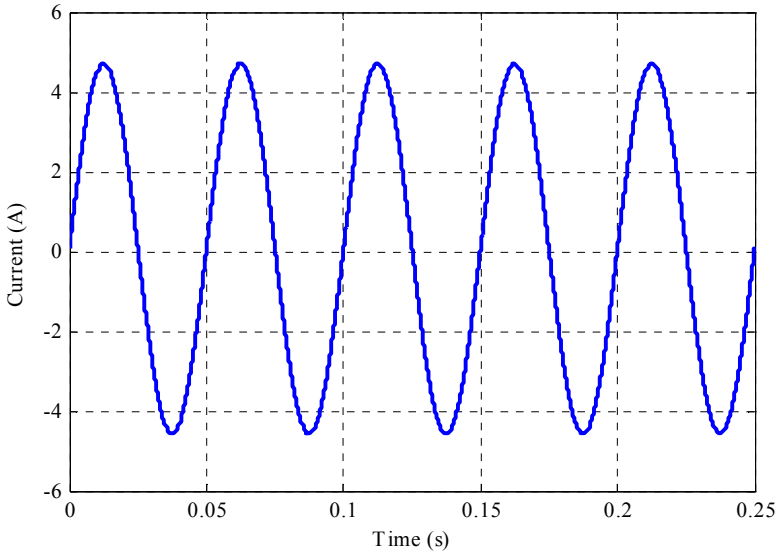

(a) Quadrature axis current

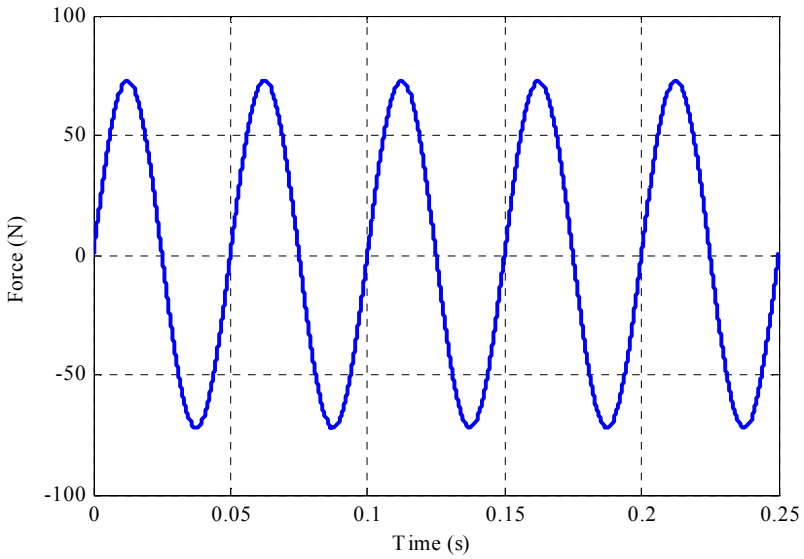

(b) Electromagnetic force

Figure 4.20 The linear PM synchronous machine quadrature axis current and electromagnetic force variation during synthetic loading for 20 Hz under full-load force conditions

The linear PM synchronous machine velocity during synthetic loading is simulated using (3.54) and Figure 4.21 shows the variation of mover velocity with time during the synthetic loading. It confirms that the linear PM synchronous machine accelerates and decelerates during synthetic loading with a velocity swing (peak to peak) of 1.24ms^{-1} (0.48pu). The average value of the mover velocity over one synthetic loading cycle is 2.56ms^{-1} (1.0pu).

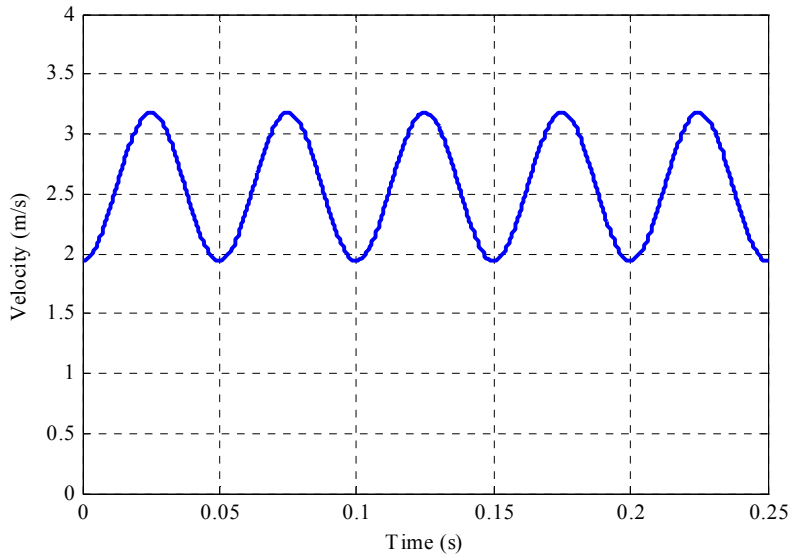

Figure 4.21 The linear PM synchronous machine velocity variation during synthetic loading for 20 Hz under full-load force conditions

Figure 4.22 shows the variation of air-gap magnetic flux during synthetic loading for linear PM synchronous machine. The peak to peak variation of the air-gap flux is 0.006pu which is small. Therefore, the higher excursions in the phase voltage during synthetic loading seen in Figure 4.17 (a) are primarily due to the higher peak to peak velocity (0.48pu). experienced by the moving element.

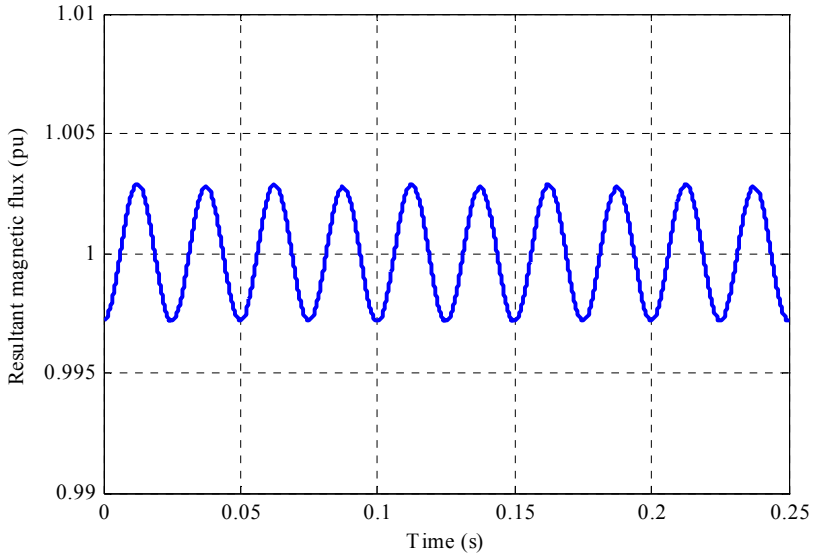

Figure 4.22 The linear PM synchronous machine air-gap magnetic flux variation during synthetic loading for 20 Hz under full-load force conditions

The input power during synthetic loading is determined using (3.88). The copper loss, iron loss and friction loss are given by (2.32), (2.34) and (2.36). Figure 4.23 shows the variation of input power and losses with time during synthetic loading. Figure 4.23 (a) shows the variation of the input power and the total losses during synthetic loading. The average of the total losses over one synthetic loading cycle is 51.3W and is equal to the average of the input power over the same cycle. Figure 4.23 (b) shows the variation of copper loss with time during synthetic loading. The variation is a consequence of the variation of instantaneous rms current. The average copper loss over one synthetic loading cycle is 48.6W, which is close to the copper loss for the standard efficiency test. Figures 4.23 (c) and (d) show the variation of iron loss and friction loss with time during synthetic loading. The average values of the iron loss and friction loss over one synthetic loading cycle are 1.72W and 0.93W respectively.

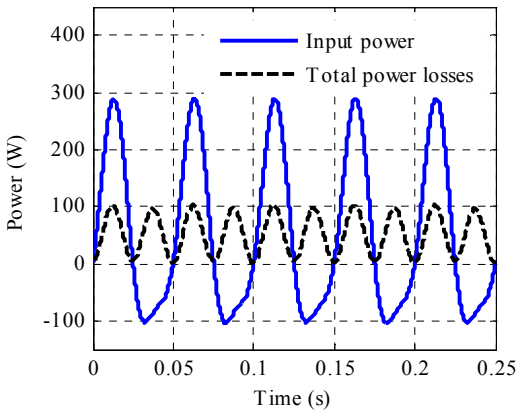

(a) Input power and total losses during synthetic loading for 20 Hz synthetic loading frequency

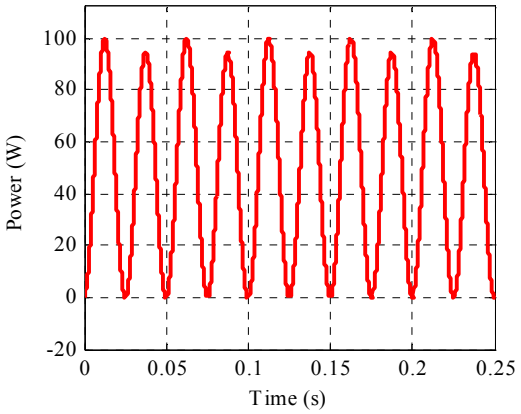

(b) stator copper loss during synthetic loading for 20 Hz synthetic loading frequency

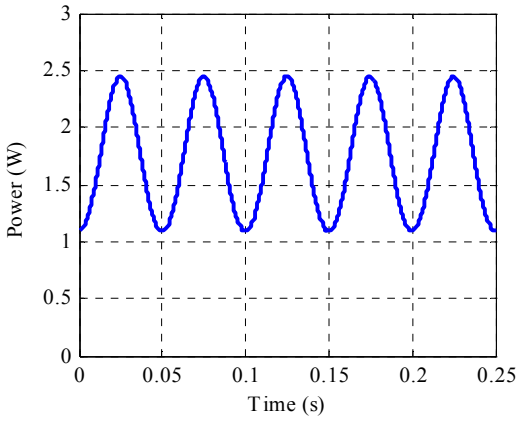

(c) iron loss during synthetic loading for 20 Hz synthetic loading frequency

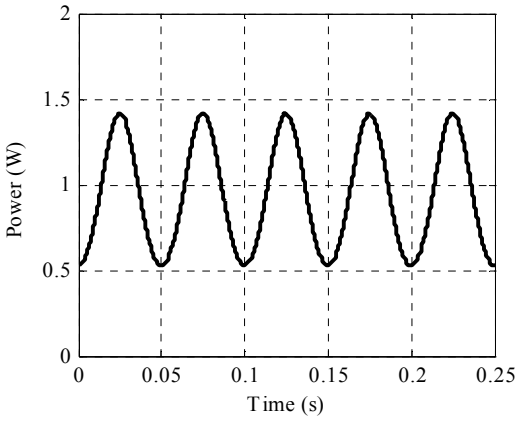

(d) friction loss during synthetic loading for 20 Hz synthetic loading frequency

Figure 4.23 The linear PM synchronous machine input power and power loss variation during synthetic loading for 20 Hz synthetic loading frequency with full-load force conditions

Table 4.12 summarises the synthetic loading and standard efficiency test simulation results for the linear PM synchronous machine for five different synthetic loading frequencies that all produce rated rms voltage and rated rms current. The individual losses are calculated during synthetic loading and compared with the standard efficiency test. The iron loss and friction loss are the same as the standard efficiency test. This is because the linear PM synchronous machine is running at rated mover velocity, on

average, during synthetic loading. The copper loss for the standard efficiency test is higher than the copper loss for the five synthetic loading frequencies. This is as a result of slightly higher current during standard efficiency test. Therefore, the calculated efficiencies during synthetic loading are underestimated by 0.2%, on average.

Table 4.12 Comparison of the standard efficiency test and the synthetic loading technique simulation results for the linear PM synchronous machine under full-load force condition (I_m=4.64A, I_o=0.023A)

	Standard Efficiency Test	Synthetic Loading Frequency (Hz)				
		20	25	30	35	40
rms line voltage (V)	45.1	35.4	35.3	35.2	35.2	35.2
rms line current (A)	2.32	2.32	2.32	2.32	2.32	2.32
Speed (ms^{-1})	2.56	2.56	2.56	2.56	2.56	2.56
Minimum inverter peak current (A)	3.27	4.64	4.64	4.64	4.64	4.64
Phase-leg volt-ampere (VA)	229.0	348.0	348.0	348.0	348.0	348.0
Minimum dc link voltage (V)	70	75	75	75	75	75
Output power (W)	128.5	-	-	-	-	-
Input power (W)	179.5	51.3	51.3	51.2	51.2	51.2
Stator copper loss (W)	48.3	48.6	48.6	48.6	48.6	48.6
Iron loss (W)	1.72	1.72	1.72	1.72	1.71	1.71
Friction loss (W)	0.92	0.93	0.93	0.93	0.93	0.92
Total losses (W)	51.0	51.3	51.3	51.3	51.2	51.2
Efficiency (%)	71.6	71.4	71.4	71.4	71.4	71.4

4.5.2 Three-quarters of Full-Load Force Condition

In this case the synthetic loading technique is configured to enforce rated velocity at three-quarters rated force and compared with the result of the standard efficiency test for the same load condition. The peak current during the synthetic loading is 3.48Amps (1.06pu). The average rms line voltage and current over one synthetic loading cycle are 34.3V (0.76pu) and 1.74Amps (0.75pu) respectively.

Five different synthetic loading frequencies that produce mover velocity with on average three-quarters of rated force during synthetic loading are assessed. The individual losses are calculated and the tabulated results compared with the standard efficiency test and are shown in Table 4.13. The iron loss and the friction loss are the

same as the standard efficiency test. The slightly higher current during standard efficiency test results in the higher copper loss. Consequently, the efficiency estimated by synthetic loading is overestimated by 0.1%, on average.

Table 4.13 Comparison of the standard efficiency test and the synthetic loading technique simulation results for the linear PM synchronous machine under three-quarters of full-load force condition (I_m=3.48A, I_o=0.023A)

	Standard Efficiency Test	Synthetic Loading Frequency (Hz)				
		20	25	30	35	40
rms line voltage (V)	42.0	34.3	34.2	34.2	34.2	34.2
rms line current (A)	1.75	1.74	1.74	1.74	1.74	1.74
Speed (ms^{-1})	2.56	2.56	2.56	2.56	2.56	2.56
Minimum inverter peak current (A)	2.47	3.48	3.48	3.48	3.48	3.48
Phase-leg volt-ampere (VA)	160.0	240.0	240.0	240.0	240.0	240.0
Minimum dc link voltage (V)	65	68	68	68	68	68
Output power (W)	96.3	-	-	-	-	-
Input power (W)	126.4	30.0	30.0	30.0	30.0	30.0
Stator copper loss (W)	27.7	27.3	27.3	27.3	27.3	27.3
Iron loss (W)	1.7	1.7	1.7	1.7	1.7	1.7
Friction loss (W)	0.9	0.9	0.9	0.9	0.9	0.9
Total losses (W)	30.3	29.9	29.9	29.9	29.9	29.9
Efficiency (%)	76.2	76.3	76.3	76.3	76.3	77.3

4.5.3 Half of Full-Load Force Condition

The synthetic loading technique and standard efficiency test are simulated on the linear PM synchronous machine under half of full-load force condition. The simulation results presented in this case are for synthetic loading frequencies between 20Hz and 40Hz.

The results of efficiency evaluation of linear PM synchronous machine at half of full-load force using synthetic loading are presented in Table 4.14. Five different synthetic loading frequencies are compared with the standard efficiency test. The iron losses and friction and windage losses for the five different synthetic loading frequencies are equal to the standard efficiency test. The efficiencies during synthetic loading are underestimated by 0.1% on average.

Table 4.14 Comparison of the standard efficiency test and the synthetic loading technique simulation results for the linear PM synchronous machine under half of full-load force condition (I_m=2.32A, I_o=0.023A)

	Standard Efficiency Test	Synthetic Loading Frequency (Hz)				
		20	25	30	35	40
rms line voltage (V)	39.0	33.5	33.5	33.4	33.4	33.4
rms line current (A)	1.16	1.16	1.16	1.16	1.16	1.16
Speed (ms^{-1})	2.56	2.56	2.56	2.56	2.56	2.56
Minimum inverter peak current (A)	1.64	2.32	2.32	2.32	2.32	2.32
Phase-leg volt-ampere (VA)	98.0	146.0	146.0	146.0	146.0	146.0
Minimum dc link voltage (V)	60.0	63.0	63.0	63.0	63.0	63.0
Output power (W)	62.9	-	-	-	-	-
Input power (W)	77.3	14.8	14.8	14.8	14.8	14.8
Stator copper loss (W)	12.1	12.2	12.2	12.2	12.2	12.2
Iron loss (W)	1.72	1.71	1.71	1.71	1.7	1.7
Friction loss (W)	0.92	0.92	0.92	0.92	0.92	0.92
Total losses (W)	14.74	14.83	14.83	14.83	14.82	14.82
Efficiency (%)	80.9	80.8	80.8	80.8	80.8	80.8

4.5.4 Quarter of Full-Load Force Condition

In this case the simulation results of synthetic loading and standard efficiency test for linear PM synchronous machine under quarter of full-load force are presented for synthetic loading frequencies between 20Hz and 40Hz. The iron loss and friction loss during synthetic loading are similar to the values of standard efficiency test as shown in Table 4.15. The copper loss is lower than the standard efficiency test. Consequently, the efficiency evaluation using synthetic loading are overestimated by 0.3%, on average.

Table 4.15 Comparison of the standard efficiency test and the synthetic loading technique simulation results for the linear PM synchronous machine under quarter of full-load force condition (I_m=1.16A, I_o=0.023A)

	Standard Efficiency Test	Synthetic Loading Frequency (Hz)				
		20	25	30	35	40
rms line voltage (V)	36.0	33.0	33.0	33.0	33.0	33.0
rms line current (A)	0.59	0.58	0.58	0.58	0.58	0.58
Speed (ms^{-1})	2.56	2.56	2.56	2.56	2.56	2.56
Minimum inverter peak current (A)	0.84	1.16	1.16	1.16	1.16	1.16
Phase-leg volt-ampere (VA)	46.0	66.0	66.0	66.0	66.0	66.0
Minimum dc link voltage (V)	55.0	57.0	57.0	57.0	57.0	57.0
Output power (W)	31.1	-	-	-	-	-
Input power (W)	36.4	5.68	5.68	5.67	5.67	5.67
Stator copper loss (W)	3.2	3.1	3.1	3.1	3.1	3.1
Iron loss (W)	1.71	1.7	1.7	1.7	1.7	1.7
Friction loss (W)	0.92	0.92	0.92	0.92	0.92	0.92
Total losses (W)	5.83	5.72	5.72	5.72	5.72	5.72
Efficiency (%)	84.0	84.3	84.3	84.3	84.3	84.3

4.6 Summary of Simulation Results

Different load torque condition and synthetic loading frequencies are simulated for efficiency evaluation of the PM, IPM and linear PM synchronous machine at rated speed. The simulations result shows that synthetic loading technique is capable of correctly forcing the correct individual loss components in the PM, IPM and linear PM synchronous machine. The synthetic loading efficiency evaluation technique gives results which are in agreement with the standard efficiency test.

4.7 General performance of the synthetic loading technique

Generally, the synthetic loading technique for PM synchronous machines is performed using a vector control technique and with the direct axis current, i_d, set to zero. This section assumes non-zero values for direct axis current and then assesses the synthetic loading performance in terms of minimum peak inverter VA rating and minimum dc link voltage requirement. Direct axis current can be used to increase the Ohmic loss, which then reduces the I_m requirement in the q-axis current and reduces speed swing. However, introducing anon-zero i_d results in iron losses greater than rated values as will be shown.

Figure 4.24 shows the impact of direct axis current on the inverter volt-ampere rating required, the dc link voltage, maximum real power absorbed by the machine undergoing test and the iron loss for the test PM synchronous machine.

The inverter volt-ampere rating required with zero direct axis current is 1.52 pu and then gradually decreases with an increase of direct axis current. The VA rating reaches a value of 1.13 pu when the direct axis current is the same as the machine rated current. The dc link voltage required is 1.1pu with i_d=0 and then gradually increases to 1.13pu when the direct axis current reaches 1.0pu as shown in Figure 4.24. This is a consequence of the higher electromagnetic motive force (emf) due to the significant contribution direct axis current makes to the direct axis flux. Consequently, the iron loss increases to 1.41pu as shown in Figure 4.24. The increase in direct axis current (imaginary part) allows a decrease of the quadrature axis current (real part). This indicates that the maximum real power decreases as shown in Figure 4.24 and that the impact of direct axis current on the performance of synthetic loading is to decrease the inverter volt-ampere rating required hence decrease the peak real power. However, the dc link voltage required increases. Also, increasing direct axis current leads to higher iron losses hence underestimates the efficiency of the machine. The conclusion is that although direct axis current can reduce the required VA rating of the system it forces the iron loss components in the machine to exceed its rated value, hence the machine is overloaded.

Figure 4.25 shows the relationship between the synthetic loading frequency and the AC perturbation current, the peak inverter VA rating, the dc link voltage required and the average speed during synthetic loading for the PM synchronous machine. In general the peak to peak speed variation should be made as small as possible in order to reduce the minimum peak inverter volt-ampere rating and minimum dc link voltage requirement. Generally, the AC perturbation current, I_m, is 1.42pu according to equation (3.66b) developed in chapter three regardless of the PM synchronous machine type. The minimum dc link voltage required to perform the synthetic loading is 1.1pu for the test PM synchronous machine. Therefore, minimum peak inverter VA rating required is

1.52pu. The average rms current and speed over one synthetic loading cycle are 1.0pu regardless of PM synchronous machine type and synthetic loading frequency. Also, the average line rms voltage is 1.0pu if the no-load emf line voltage is taken as a base value during synthetic loading.

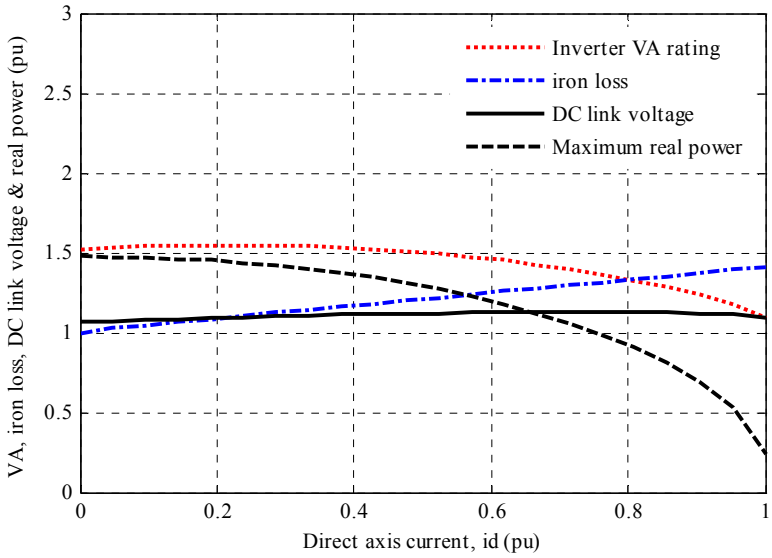

Figure 4.24 The impact of direct axis current on the synthetic loading performance for the PM synchronous machine

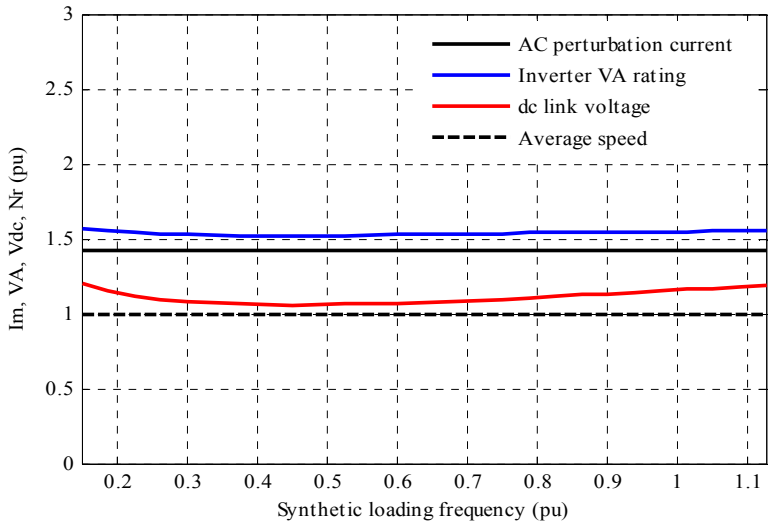

Figure 4.25 The impact of synthetic loading frequency on the AC perturbation current I_m, inverter VA rating, dc link voltage and average speed

During investigation of synthetic loading it found that the synthetic loading period is proportional to the moment of inertia (mover mass) according to (3.69). This means that if the mechanical time constant increases the peak to peak speed variation is smaller for a given synthetic loading frequency. Therefore, adding inertia can have a positive impact on synthetic loading.

Figure 4.26 illustrates the impact of moment of inertia (mover mass) on the synthetic loading frequency for a fixed value of swing speed. Based on the simulation results shown in Figure 4.26 the moment of inertia (mover mass) is inversely proportional to the synthetic loading frequency for the same given speed swing. Generally, if the swing speed is fixed to a desired value, the minimum peak inverter VA rating and minimum dc link voltage requirement during synthetic loading are 1.52pu and 1.1pu regardless of synthetic loading frequency. Hence the dc link voltage can be reduced by increasing the inertia if a fixed synthetic loading frequency is used as this will results in a reduced swing speed. Such a test is likely to produce more accurate results too.

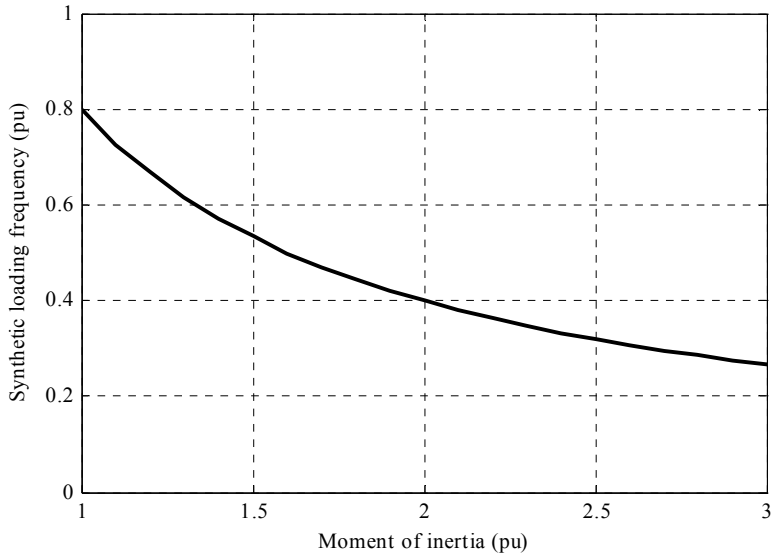

Figure 4.26 The impact of moment of inertia on synthetic loading frequency for a constant swing speed

4.8 Summary

This chapter presents simulation of the synthetic loading technique for efficiency evaluation of example PM, IPM and linear PM synchronous machines for different load torque (force) conditions at rated speed and synthetic loading frequencies. The effects of synthetic loading frequency on the required dc link voltage and inverter volt-ampere rating required have been assessed. In addition, the effect of direct axis current on the inverter volt-ampere rating, the dc link voltage required, maximum real power and iron loss during synthetic loading has been investigated. The effect of additional moment of inertia (mover mass) on the synthetic loading frequency is discussed in order to obtain constant swing speed.

The simulation results of synthetic loading for efficiency evaluation of the PM, IPM and linear PM synchronous machine give results which are in agreement with the standard efficiency test for the load conditions considered. It is possible to maintain constant rms voltage and current in the machine undergoing synthetic loading test by adjusting the AC perturbation current, I_m. The simulation results prove that synthetic loading maintains the rms current, rms voltage and the rotor speed at rated values, on average, over one synthetic loading cycle. The synthetic loading simulation results show that higher inverter volt-ampere ratings are required during synthetic loading. However, the study of the effect of direct axis current on the synthetic loading performance shows that increasing the direct axis current results in lower inverter volt-ampere rating, but leads to a higher dc link voltage requirement during synthetic loading hence higher iron loss. This leads to an underestimate of the efficiency during the synthetic loading technique as the iron loss is now above rated value.

In order to confirm that the synthetic loading technique is a reasonable method of efficiency evaluation for the PM, IPM and linear PM synchronous machine the simulation results in this chapter will compared with experimental results in chapter six. The MATLAB M-file for synthetic loading test and the SIMULINK for standard efficiency test are provided Appendix C.

References

[1] S. Morimoto, Y. Tong, Y. Takeda and T. Hirasa, "Loss Minimization Control of Permanent Magnet Synchronous Motor Drives", IEEE Transactions on Industrial Electronics, Vol. 41, No. 5, October 1994, pp. 511-517.

[2] R. Monajemy, R. Krishnan, "Control and Dynamics of Constant Loss Based Operation of Permanent Magnet Synchronous Motor Drive System", The 25th Annual Conference of the IEEE Industrial Electronics Society, Vol. 3, 29 Nov.-3Dec. 1999, pp. 1452-1457.

[3] N. Urasaki, T. Senjyu and K. Uezato, "An Accurate Modeling for Permanent Magnet Synchronous Motor Drives", Fifteenth Annual IEEE Applied Power Electronics Conference and Exposition, Vol. 1, 6-10Feb. 2000, pp. 387-392.

[4] N. Urasaki, T. Senjyu and K. Uezato, "Relationship of Parallel Model and Series Model for Permanent Magnet Synchronous Motors Taking Iron Loss into Account", IEEE Transactions on Energy Conversion, Vol. 19, No. 2, June 2004, pp. 265-270.

[5] N. Urasaki, T. Senjyu and K. Uezato, "A Novel Calculation Method for Iron Loss Resistance Suitable in Modeling Permanent-Magnet Synchronous Motors", IEEE Transactions on Energy Conversion, Vol. 18, No. 1, March 2003, pp. 41-47.

[6] W. Roshen "Iron Loss Model for Permanent-Magnet Synchronous Motors", IEEE Transactions on Magnetics, Vol. 43, No. 8, Aug. 2007, pp. 3428-3434.

[7] A. Y. M. Abbas and J. E. Fletcher, "Efficiency Evaluation of Linear Permanent Magnet Synchronous Machines Using the Synthetic Loading Method" 39th IEEE Annual Power Electronics Specialists Conference, Rhodes, Greece, 15-19 June 2008, pp.3074-3080.

[8] A. Y. M. Abbas and J. E. Fletcher, "Synthetic Loading Technique for Efficiency Evaluation of Permanent Magnet Synchronous Machines" 44th IEEE Annual Universities Power Engineering Conference, Glasgow, UK, 1-4 September 2009.

Chapter Five

Software and Hardware Descriptions and Implementation

5.1 Introduction

In order to verify the synthetic loading technique experimentally a vector controller is implemented in the laboratory. This chapter details the experimental system. In this chapter the hardware and software used to perform the standard efficiency test and the synthetic loading technique are described. The current transducer circuit for measuring the phase current and the ADC interface circuit is presented. An incremental encoder is used to measure the rotor position, shaft direction and motor speed. The relevant features of the TMS320F2812 DSP and the PWM interface circuit are presented. The construction of the power inverter using IGBTs and the gate drive is described. The software and the flow chart for executing synthetic loading are presented.

5.2 System components

The hardware system comprises several components. Control signal flow from the DSP controller to the inverter and from the phase measurement devices and encoder to the DSP controller are depicted in Figure 5.1. Based on the power and control information flow boundaries the hardware can be divided into the following:

- Main DC power supply.
- Six switch inverter and gate drives.
- Hall-effect current and voltage sensors for phase measurements.
- An incremental encoder for speed and rotor position measurements.
- TMS320F2812 DSP controller.
- Isolation circuits for digital signals.
- Signal interface circuits.
- PM synchronous machine under test.
- Host PC executing TI Code Composer Studio (CCS).

These components are integrated together to conduct the synthetic loading tests.

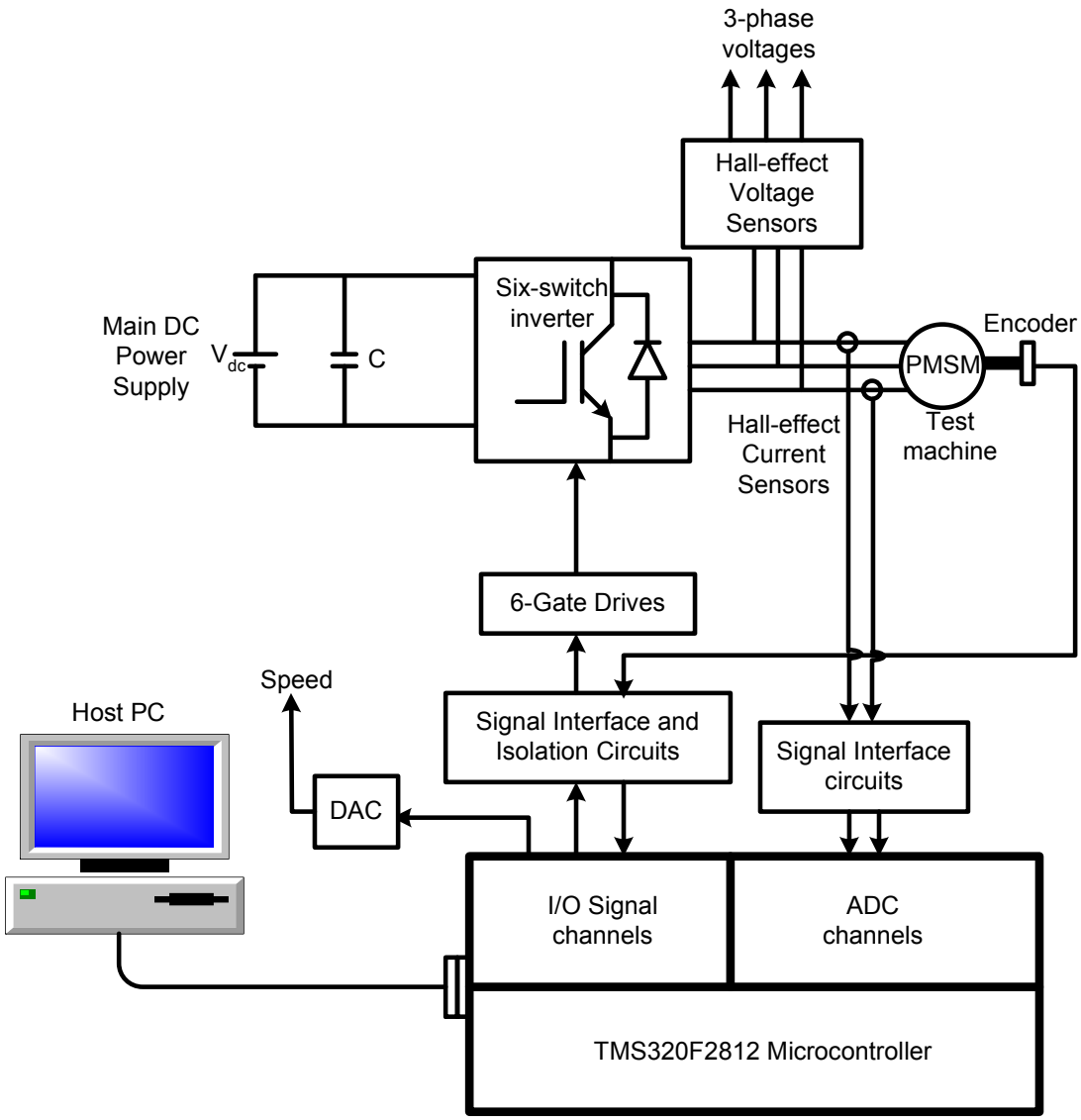

Figure 5.1 Vector controller block diagram for efficiency evaluation of the PM synchronous machine using the synthetic loading technique

5.3 Current transducers

Synthetic loading requires vector control. Therefore, knowledge of the PM synchronous machine phase currents and rotor position are essential in order to apply the

abc to *dq* transformation thus obtain the *dq* axis current components. The quadrature axis current is used to configure synthetic loading.

The measured phase currents are converted to voltage signals using LA 55-P Hall-effect current transducers. The transducers have an input to output current ratio of 1A/1mA and a maximum rms current of 50A. The LA 55-P Hall-effect current transducer operates from a ±15V DC power supply and the output current is scaled to ±1.5V and shifted by 1.5V to derive the 0 to 3V signal required by the TMS320F2812 DSP controller ADC inputs. The measurement system gives a sensitivity of 75mV/A. Two current transducers are used to sense and convert the phase current information into voltage information in this way. The voltages are then sampled and converted by the ADC embedded within the TMS320F2812 DSP controller. One of the two phase current interfacing circuits is shown in Figure 5.2. R_m is the measuring (burden) resistance and is 75Ω. The purpose of the voltage divider and the 1N4148 diode, D1, is to maintain the output in the range between 0 to 3V and to avoid negative voltage drive to the ADC input.

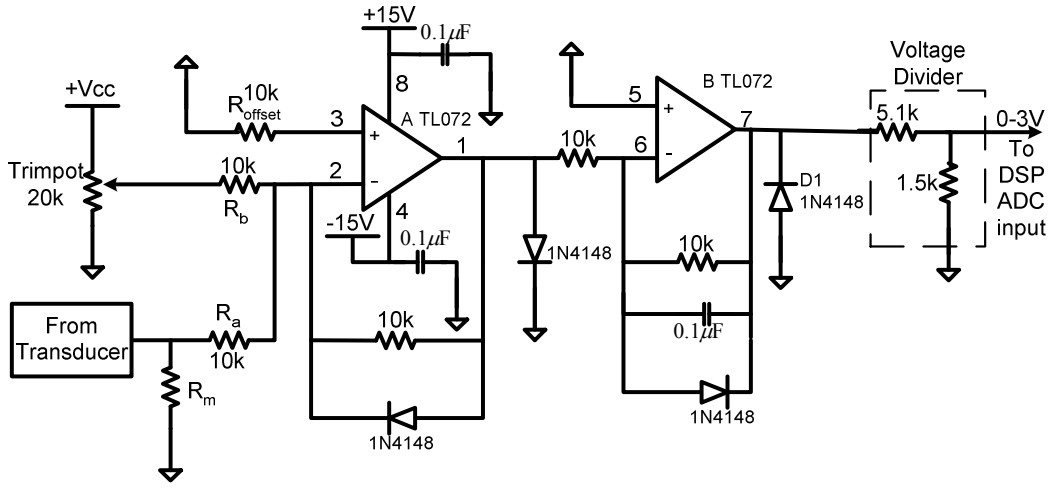

Figure 5.2 Phase current measurement circuit for interface of the Hall-effect transducer to the TMS320F2812DSP ADC input

5.4 Rotor position measurement interface circuit

An incremental encoder is used to measure rotor position. Knowledge of rotor position is essential for the PM synchronous machine vector controller as it provides θ for the transformation in (2.1).

The incremental encoder generates quadrature encoded pulses which are two sequences of pulses with a fixed phase shift of a quarter of a period. The angular position and speed can be determined from the pulse count and frequency respectively. The encoder has 1000 pulses per revolution and combined with a four-fold pulse multiplication mechanism, an effective line count of 4000 pulses per revolution is available equating to 0.09° (mech)/pulse. The direction of the motor can be determined by detecting which channel leads its counterpart.

The speed of the PM synchronous machine under test is determined from the number of pulses produced by the incremental encoder attached to the shaft of the PM synchronous machine during a sample period. This method of speed calculation is convenient as the TMS320F2812 DSP controller has an incremental encoder input-output port that produces a count of the encoder pulses.

The encoder uses a 5V DC supply and the output voltage of the encoder is 5V. However, the TMS320F2812 DSP controller IO port is only 3.3V tolerant. Therefore, a level shift interface circuit between the encoder output and the DSP IO port is required. Consequently, the quadrature encoder 5V differential voltage signals from the shaft position encoder are interfaced to the TMS320F2812 DSP controller using an AM26LV32 low-voltage high-speed quadruple differential line receiver, which operates at 3.3V but has 5V tolerant logic inputs. Digital isolators (ADUM1400ARWZ) are used to isolate the output signals of the AM26LV32 from the IO port of the TMS320F2812 DSP controller. A separate power supply is used to power the quadrature encoder. Figure 5.3 illustrates the quadrature interface circuit.

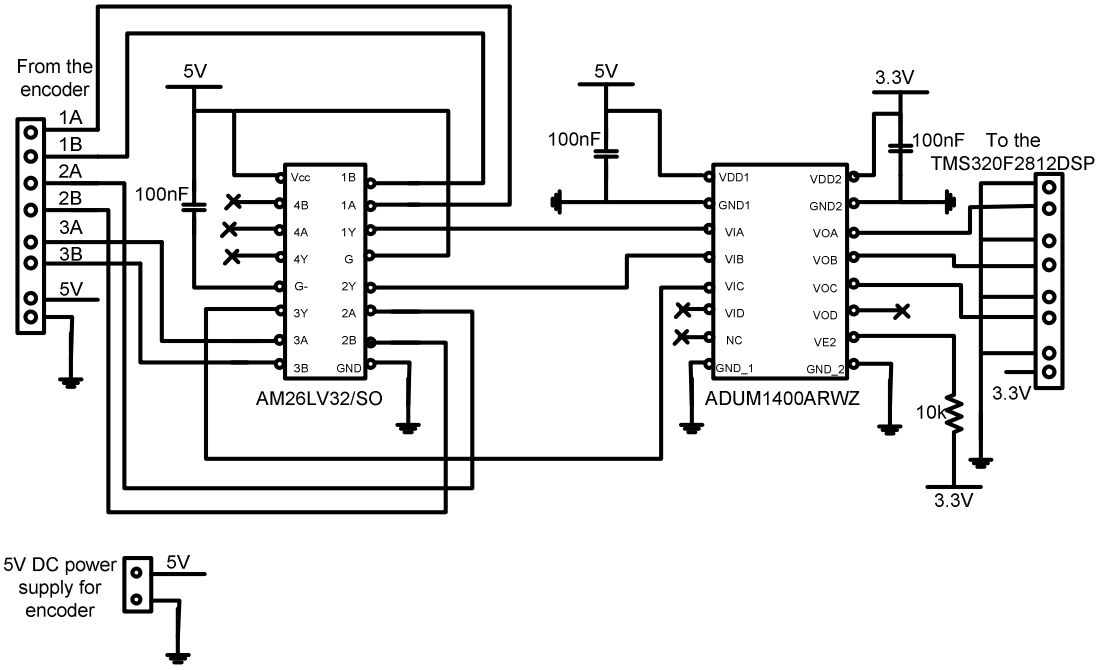

Figure 5.3: The block diagram of quadrature encoder signal interface circuit

5.5 The PWM interface circuit

The PWM signals generated by the TMS320F2812 DSP controller are 3.3V. Therefore, these voltages need to be level shifted to 5V and isolated from the gate drives. For TMS320F2812 DSP controller isolation and voltage level shift purposes an interface board was designed and built using a dual SN74LVC4245A octal bus transceiver and HCPL2631 opto-couplers to shift PWM voltage level from 0 - 3.3V to 0 - 5V and isolate the PWM channels of the TMS320F2812 DSP controller from the gate drive circuits.

The digital signal buffer is powered by a 5V supply from an external regulated power supply and an in-circuit derived 3.3V from the TMS320F2812 DSP controller board. The HCPL2631 and the gate drives are powered by a separate 5V supply in order to ensure that the current spikes in the power supply that are generated by the gate drive switching do not propagate to the interface circuit. The schematic diagram of the isolation and interface circuit for the PWM signals and 3.3V regulation scheme is depicted in Figure 5.4.

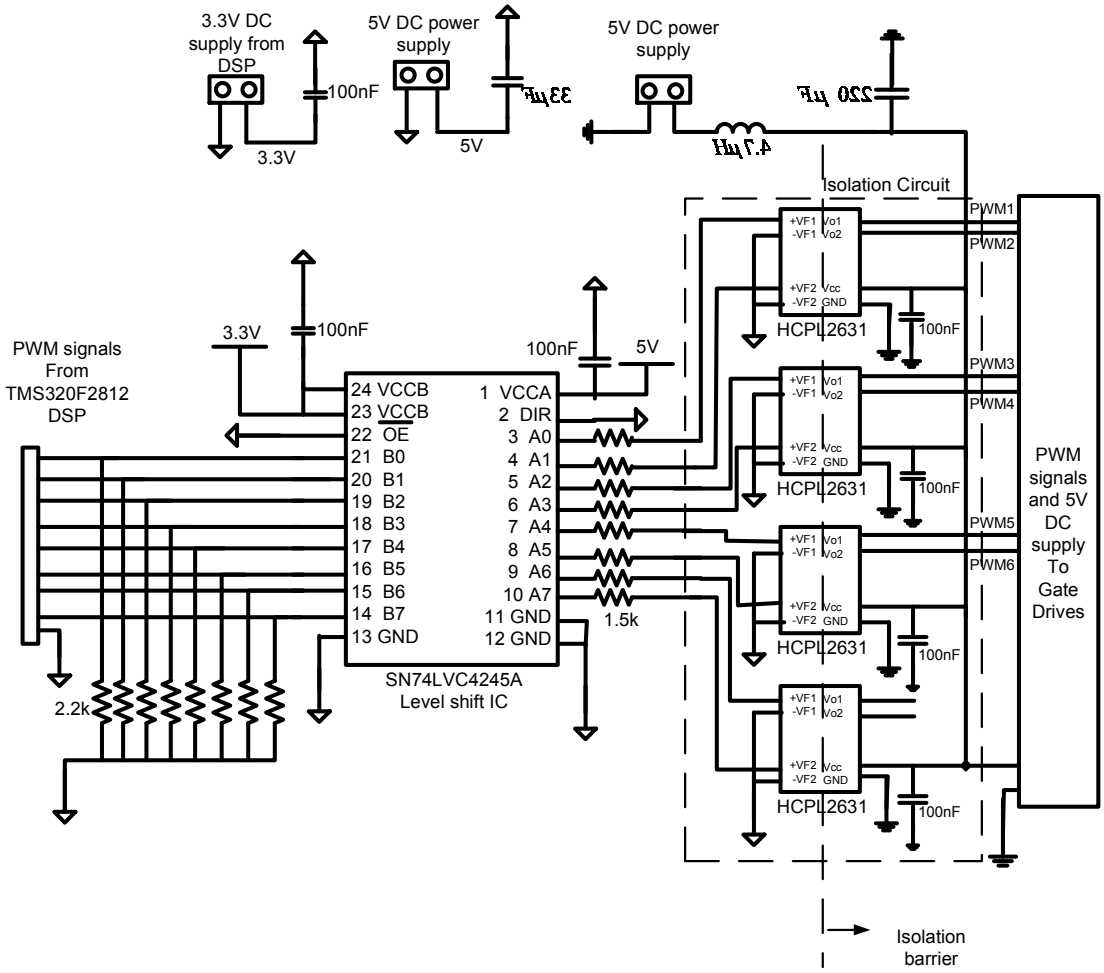

Figure 5.4 Schematic diagram of isolating and interfacing circuit of PWM signals and 3.3V regulation scheme

5.6 The TMS320F2812 DSP controller

The Texas Instruments (TI) TMS320F2812 DSP is designed for digital motor control. It combines a 16-bit fixed-point DSP core with microcontroller peripherals in a single chip solution, and is part of a generation of DSPs called “DSP controllers” [1].

The main relevant TMS320F2812 DSP controller features are [2], [3]:

- 150 MIPS operating speed.

- 30 MHz clock.
- 2 Expansion Connectors (analog, I/O).
- TI F28xx Code Composer Studio tools driver.

The drive system utilises the event manager module and analog-to-digital converter (ADC). The event manager (EV) module provides a broad range of functions and features that are particularly useful in motor control applications. There are two identical event managers, A and B, in the TMS320F2812 DSP controller. Each event manager module includes [4]:

- Two General-purpose (GP) timers.
- Full-compare/PWM units for PWM generation.
- Capture units.
- Quadrature-encoder pulse (QEP) circuits for the encoder interface.

The analog to digital converter (ADC) has 16 channels, configurable as two independent 8 channel modules to service event mangers A and B. The functions of the ADC module include [5]:

- 12 bit ADC core with built-in dual sample-and-hold (S/H).
- Simultaneous sampling or sequential sampling modes.
- Analog input: 0V to 3V.
- Fast conversion time (conversion time is 320ns).
- Sample-and-hold (S/H) acquisition time window has separate pre-scale control, the width of S/H pulse is set to 1.6μs.

5.7 Power inverter and gate drive

Figure 5.5 shows the six-switch three-phase inverter circuit. The inverter is constructed from six IGBTs rated at 600V/30Amps. A 400V/2200μF electrolytic provides dc filtering of the 0-200V regulated dc power supply (25A peak output). The gate drive circuitry translates the digital input to a 0 – 15V gate drive signal to control

the IGBT state [6], [7]. The gate drive also provides electrical isolation between the interface circuits and the floating sources of the high-side IGBTs (T_1, T_3, T_5).

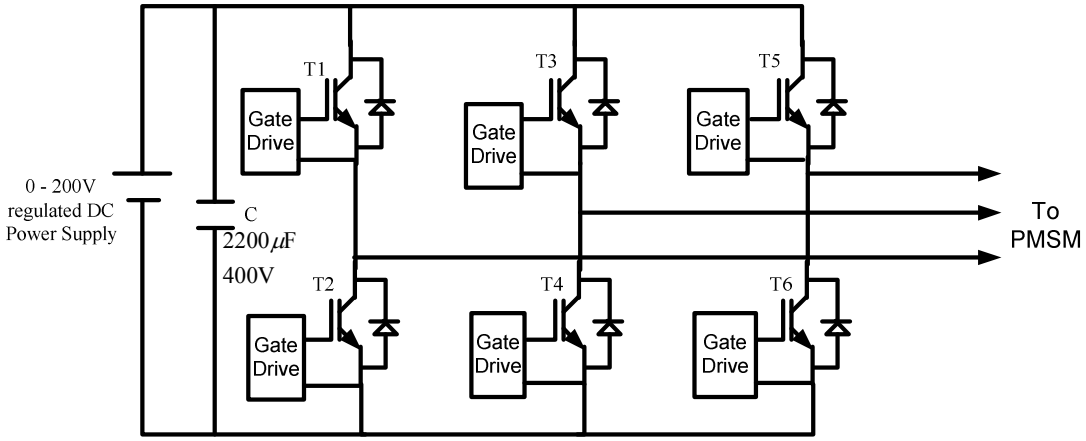

Figure 5.5 The circuit diagram of the three-phase inverter

5.8 Software Implementation

Pulse-width modulated (PWM) power electronic systems are employed in many industrial processes involving high performance drive systems [6]. The first step in constructing such a system is to know in principle how the power electronic switching devices should be controlled in order to accomplish a desired performance outcome. However, it is essential to construct a physical system that will achieve this required switching performance within the constraints of the switching device characteristics [8].

Implementing a vector control algorithm in a digital processing system requires time critical software capable of calculating and loading timer information into the PWM timers efficiently in order to attain a reasonable switching frequency [8]. The six PWM channels available in event manager module A are used to drive the three-phase inverter. The event manager module A is configured to operate with 50μs period resulting in 20 kHz PWM frequency given the 75MHz system clock. The dead-band module is configured to give 2.0μs under-lap to avoid cross-conduction. Two of the available 16 analog channels of the 12 bit ADC are used to sample the two phase currents. One of

two available quadrature encoder channels is used for the position encoder. The DSP is programmed using the Spectrum Digital eZdsp development environment with Code Composer Studio. The block diagram of the vector controller and the associated flow chart of the software implementation are shown in Figure 5.6 and 5.7 respectively.

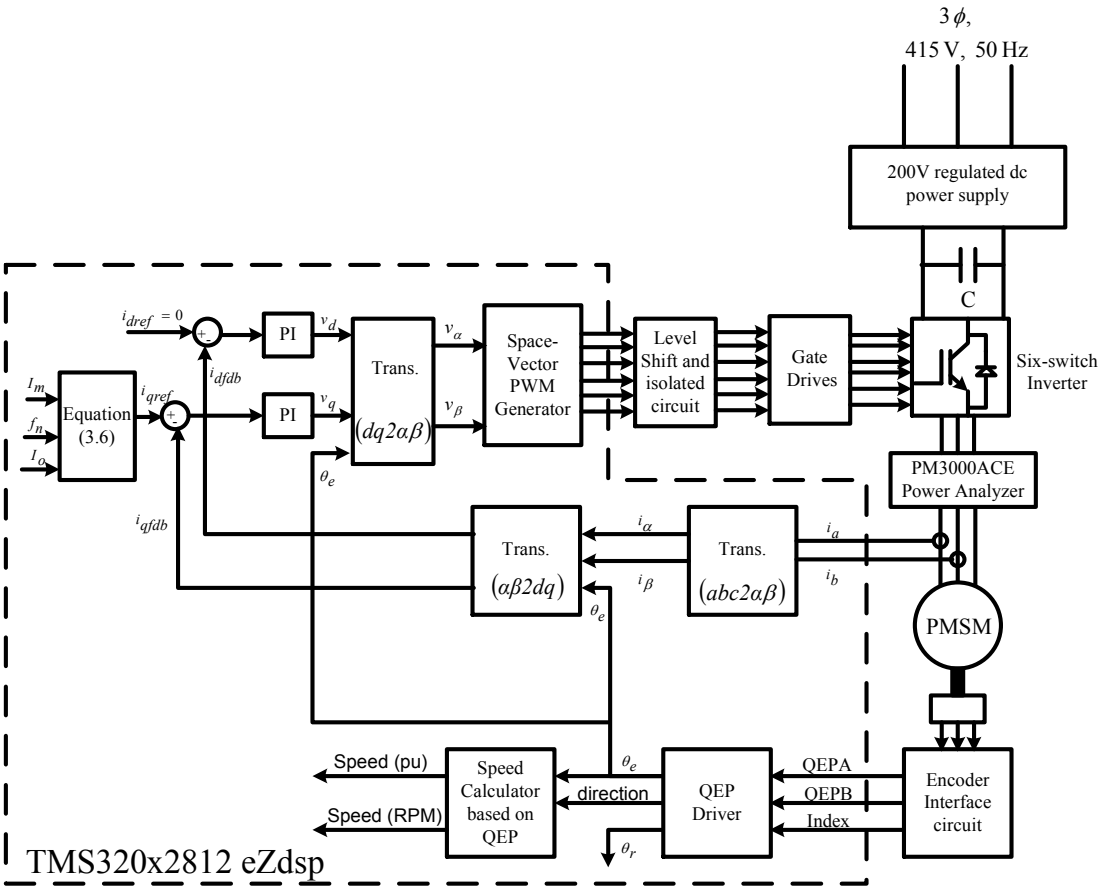

Figure 5.6 Block diagram of vector control system for conducting the synthetic loading technique

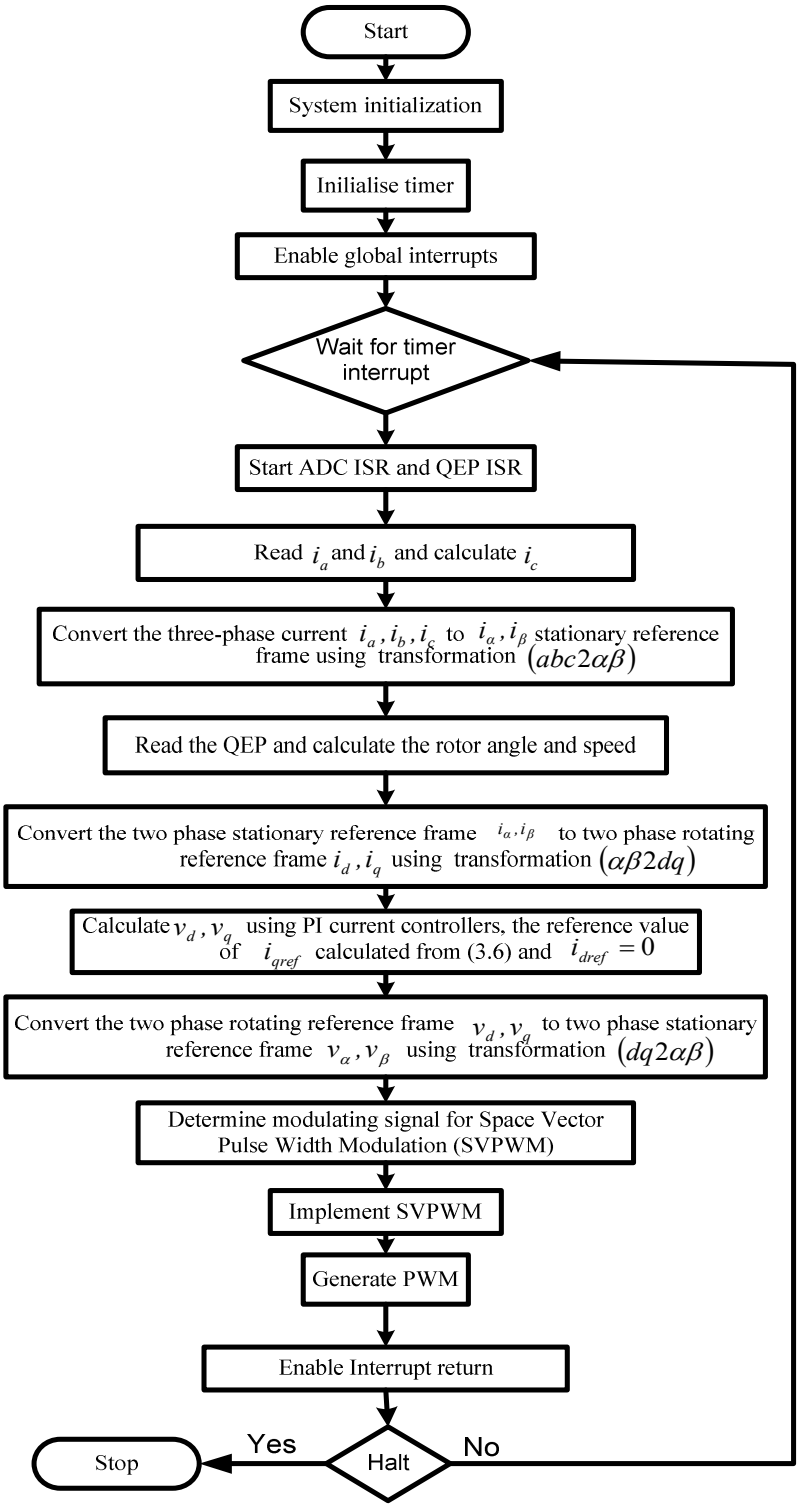

Figure 5.7 Flow chart of the software implementation for synthetic loading and standard efficiency test application using TMS320F2812 DSP controller

Figure 5.6 and 5.7 show the hardware and the software flowchart for synthetic loading. The stator currents i_a and i_b are measured via the current sensors. The transformation is applied to the measured current to transform the stator current into the stationary reference frame currents i_α and i_β. Then using a transformation to obtain the rotating reference frame quantities i_d and i_q. i_d and i_q are compared to their reference values i_{qref} derived from (3.6) and i_{dref} (set to zero) and corrected by means of PI current controllers. The outputs of the current controllers v_d and v_q are passed through the transformation to yield v_α and v_β and a new stator voltage vector is impressed on the motor using the Space Vector Modulation technique. The PWM signals are generated by the PWM modules with a 20 kHz switching frequency and a 2μs dead-band. The interrupt frequency is 20 kHz [9], [10].

5.9 Experimental set-up for the linear PM synchronous machine

The synthetic loading technique and standard efficiency test for the linear PM synchronous machine are performed using a Copley Controls amplifier controlled via Copley Controls CME2 software which allows fast and easy commissioning. The CME2 communicates with the amplifier via RS-232 connection as shown in Figure 5.8. CME2 provides access to Copley Virtual Machine (CVM), a program that is set up in the CME2 and downloaded to the amplifier to provide on-board control. When a CVM program is running, the amplifier receives its input commands from the CVM program.

The Copley Controls amplifier can be configured with current, velocity and position control loops, to control the motor [11], [12]. In order to perform synthetic loading for the linear PM synchronous machine the current control loop is utilised. With current control, the reference quadrature axis current is set up by configuring the peak current, I_m, the dc offset, I_o, the frequency, f_n, and the PI controller parameters k_i and k_p in the control software. In the CME2 main window, the CVM control program has 16 sequences each of which can be configured to control a particular movement. To perform the synthetic loading two sequences are chosen, one for forward movement and the other for backward movement of the mover. In each sequence the distance of the movement, the velocity of the mover (which is used to control the system frequency),

the acceleration and the deceleration of the mover is configured [12]. The block diagram of the practical set up is shown in Figure 5.8. The standard efficiency test is performed by configuring the reference current at the desired value and the velocity at the rated value. In the two sequences for the forward and the backward movement, the distance of movement, the velocity of the mover, the acceleration and the deceleration of the mover are also configured. The mover of the linear PM synchronous motor is mechanical coupled to the mover of the linear PM synchronous generator and the generated power is dissipated in the resistive load as shown in Figure 5.9. The resistive load is adjusted to give rated current in the linear PM synchronous motor. The phase currents and voltages of the linear PM synchronous machine under test are capture using digital storage oscilloscope, these are then processed off-line to obtain the input power waveform. The power analyser provides power input, rms current, voltage and system frequency (and output power for standard test).

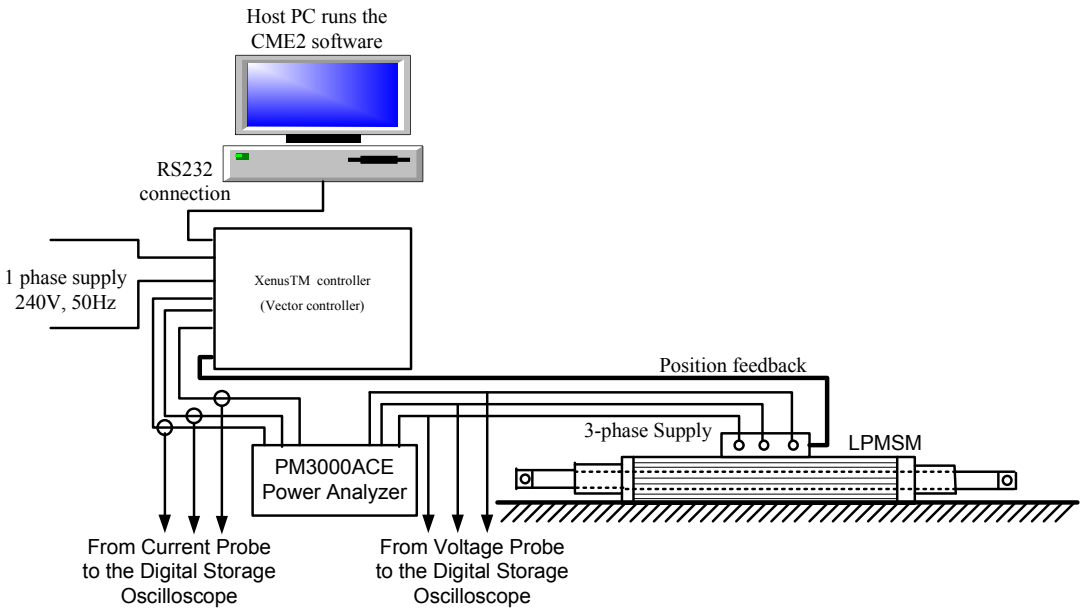

Figure 5.8 Block diagram for performing synthetic loading technique on the linear PM synchronous machine

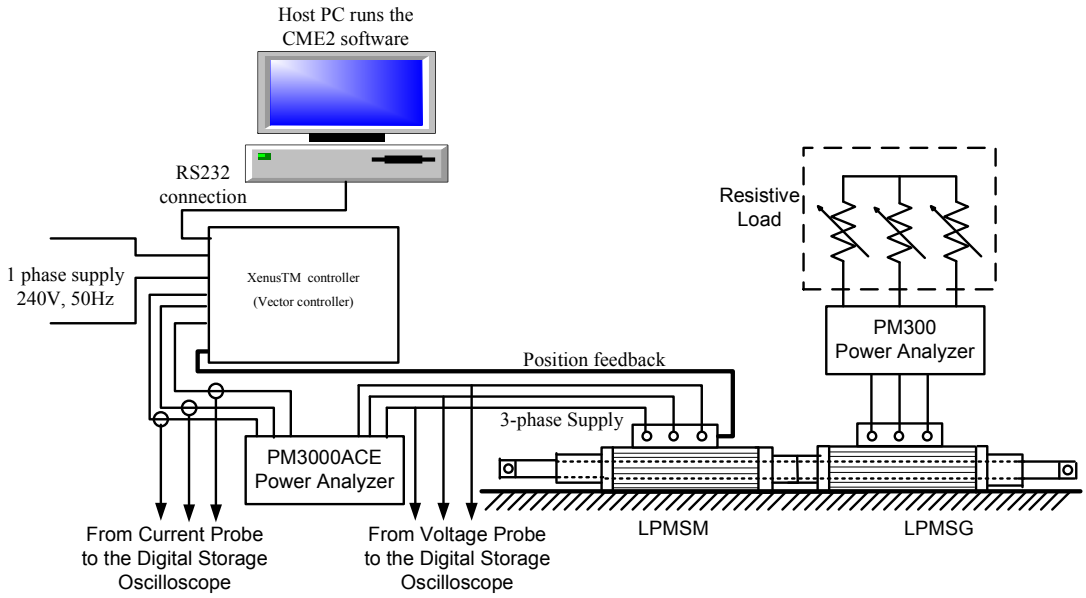

Figure 5.9 Block diagram for performing standard efficiency test on the linear PM synchronous machine

5.10 Summary

This chapter has given a brief introduction and description of the hardware and software setup necessary to conduct both the synthetic loading technique and the standard efficiency test experimentally. The signal interface circuits for the current transducers, rotor position and the PWM interface circuits have been described and circuit block diagrams of the current transducer, the encoder and the PWM interface circuits are presented. The relevant features of the TMS320F2812 DSP controller, the event manager and the analog-to-digital converter (ADC) are introduced. The three-phase prototype power inverter and the gate drives are briefly described. A software flow chart for conducting the synthetic loading technique is detailed and presented for the TMS320F2812 DSP controller programmed using the Spectrum Digital eZdsp development environment with Code Composer Studio. Experimental set-up for the linear PM synchronous machine is provided. The C code for practical implementation of synthetic loading technique and standard efficiency test are provided on the CD included at the end of the thesis. Photographs of the hardware setup are presented in Appendix B. Chapter six presents the experimental results obtained using the system.

References

[1] Texas Instruments, "Digital Signal Processing Solution for Permanent Magnet Synchronous Motor", Literature Number: BPRA044, 1997.

[2] Texas Instruments, DSP Development Systems "eZdsp^{TM} F2812 Technical Reference", 506265-0001 Rev. B, July 2002.

[3] Texas Instruments, Data Manual, "TMS320F2810, TMS320F2811, TMS320F2812, TMS320C2810, TMS320C2811, TMS320C2812 Digital Signal Processors", Literature Number: SPRS174N, April 2001-Revised May 2006.

[4] Texas Instruments, "TMS320x281x DSP Event Manager (EV) Reference Guide", Literature Number: SPRU065E, November 2004-Revised June 2007.

[5] Texas Instruments, "TMS320x281x DSP Analog-to-Digital Converter (ADC) Reference Guide", Literature Number: SPRU060D, June 2002 – Revised July 2005.

[6] S. R. Bowes, "Novel Real-Time Harmonic Minimized PWM control for Drives and Static Power Converters", IEEE Transactions Power Electronics, Vol. 9, No. 3, May 1994, pp. 256-262.

[7] R. Mancini, "Design Reference No. SLOD006B: Op Amps for Everyone", Texas Instruments, August 2002.

[8] D. G. Holmes and T. A. Lipo, "Pulse Width Modulation for Power Converters: Principle and Practice", IEEE Press, 2003.

[9] E. Simon, "Implementation of a Speed Field Oriented Control of 3-phase PMSM Motor using TMS320F240", Texas Instruments, Digital Control Systems, Application Report SPRA588, September 1999.

[10] Texas Instrument, "Digital Signal Processing Solution for Permanent Magnet Synchronous Motor", Application Note, Literature Number: BPRA044, 1997.

[11] Copley Control Corp. "CME2 User Guide", P/N 95-00454-000, Version 2, August 2006.

[12] Copley Control Corp. "Xenus^{TM} User Guide", P/N 95-00286-000, Version 2, April 2005.

Chapter Six
Experimental Results of Synthetic Loading Technique

6.1 Introduction

In this chapter the experimental results of the standard efficiency test and the synthetic loading technique for PM, IPM and linear PM synchronous machines are presented for different synthetic loading frequencies and load torque conditions. In order to validate the synthetic loading technique as a method of efficiency evaluation for PM synchronous machines, the experimental results from standard efficiency tests are compared with the experimental results from the synthetic loading technique. This chapter describes the experimental standard efficiency test method and the synthetic loading technique for evaluating the efficiency of PM synchronous machines.

The standard efficiency test is performed using a second machine mechanically coupled to the PM synchronous machine's shaft. The second machine acts as a load and is configured to cause the PM synchronous machine under test to draw rated current at rated terminal voltage and rotate at rated speed [1]-[3]. When these conditions are met the tested PM synchronous machine produces rated losses. Measurements are made at the input of the PM synchronous machine and the output of the second machine in order to calculate the efficiency. The second machine must be capable of generating the output power of the PM synchronous machine undergoing test.

The synthetic loading technique is performed by decoupling the shaft of the PM synchronous machine under test from the load. The essence of synthetic loading is that while the PM synchronous machine under test operates with no mechanical load, the rotor (mover) oscillates through a motoring-generating cycle such that, on average, over one cycle of the synthetic loading, rated rms current flows in each phase [4]-[6]. Under this condition the PM synchronous machine will produce rated copper loss. If the average applied voltage over one synthetic loading cycle is also the rated rms voltage, then the rated iron loss will be dissipated. Since the PM synchronous machine is running

at rated speed, then the rated friction and windage loss will occur. Experimentally, synthetic loading is only capable of identifying the total losses. This is because in the experiment only the input power to the PM synchronous machine is measured. The equipment required to carry out synthetic loading experimentally include an inverter (with higher VA rating than the PM synchronous machine under test), an encoder, current and voltage sensors and a standard PC connected to a DSP card for measurement and vector control [7]. The experimental configuration for the standard efficiency test and the synthetic loading technique is provided in chapter five, Figure 5.1 and 5.6.

6.2 Standard efficiency test results

Currently the most common method of conducting load efficiency tests on PM synchronous machines is to apply torque to the test machine's output shaft [8] to load the machine to rated value. This test method depends upon the rating of the PM synchronous machine, the equipment available and the degree of accuracy required [1], [7]. The experimental setup for testing a PM synchronous machine is illustrated in Figure 6.1 and the photograph of the system is shown in Figure B.12, Appendix B.

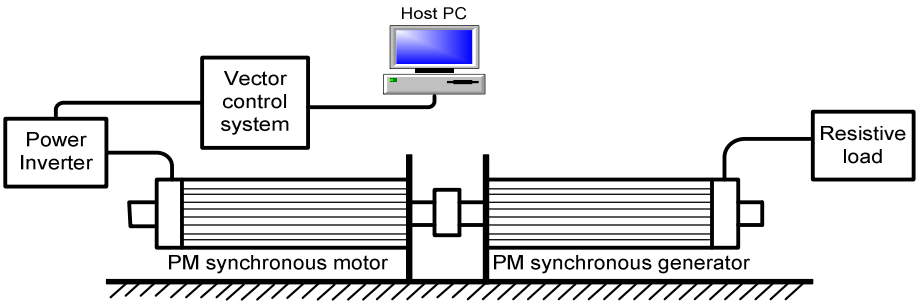

Figure 6.1 Simple block diagram of standard efficiency test for PM synchronous machines

The PM synchronous machine, supplied via its controller and inverter, is loaded by a generator and the generated power of the PM synchronous generator is dissipated in a resistive load. The quantities needed to assess the PM synchronous machines performance are input power, output power, shaft speed, the phase voltages and currents.

In this case the input power is measured using a Voltech PM3000A power analyzer. The terminal voltages and currents are measured using voltage and current probes. The

standard efficiency test is carried out for PM, IPM and linear PM synchronous machine for four different load torque conditions: full-load, three-quarters load, half load and quarter of full-load condition. In all cases, the motor is operated at rated speed.

6.2.1 PM synchronous machine

The standard efficiency test produces rated operating conditions in the PM synchronous machine under test. Consequently, this method is used to identify the efficiency of the PM synchronous machine under investigation. The results of this test will be used to investigate the accuracy of efficiency evaluation using the synthetic loading technique. The standard efficiency test is performed for the PM synchronous machine by loading it with a PM synchronous generator as mentioned before, and the input power, rms line voltage, rms current and the speed of the machine under test are measured as well as the output power, voltage and current of the load machine. Thence, the efficiency of the PM synchronous machine is calculated. Table 6.1 presents the experimental results of the standard efficiency test for the four different load conditions. The results show that the losses decrease as the load torque decreases. This is expected because the copper loss is direct proportional to the current squared which itself decreases as the load torque decrease. The experimentally measurement losses are in good agreement with the simulation results in chapter four, section 4.3.

Table 6.1 Experimental results of the standard efficiency test for the PM synchronous machine under different load torque conditions at rated speed

	Load torque conditions			
	Full	Three-quarters	Half	Quarter
rms line voltage (V)	95.4	92.1	89.5	87.3
rms line current (A)	7.45	5.62	3.72	1.87
Peak line current (A)	10.5	7.9	5.3	2.63
Phase-leg VA rating (VA)	1601	1185	780.0	380.0
Minimum dc link voltage (V)	152.5	150.0	147.0	144.0
Speed (rpm)	4000	4000	4000	4000
Input power (W)	988.1	758.2	520.5	258.1
Output power (W)	859.5	668.7	461.2	221.8
Total losses (W)	128.6	89.5	59.3	36.3
Efficiency (%)	87.0	88.2	88.6	85.9

6.2.2 IPM synchronous machine

The standard efficiency test is conducted experimentally for different load conditions on the IPM synchronous machine. Four different load conditions are carried out for the IPM synchronous machine and the main quantities are measured, namely input power, rms line voltage and current, speed and the power dissipated in the resistive load. Thus the efficiency for each load condition is calculated. The experimental results are presented in Table 6.2. The results show that the total losses decrease as the load torque decreases. This is expected as discussed in section 6.2.1. The experimental results are in a good agreement with the simulation results in chapter four, section 4.4.

Table 6.2 Experimental results of the standard efficiency test for the IPM synchronous machine under different load torque conditions at rated speed

	Load torque conditions			
	Full	Three-quarters	Half	Quarter
rms line voltage (V)	91.3	86.6	80.5	75.3
rms line current (A)	1.41	1.07	0.71	0.35
Peak line current (A)	2.0	1.5	1.0	0.5
Phase-leg VA rating (VA)	192.0	201.8	125.0	57.0
Minimum dc link voltage (V)	146.0	134.5	125.0	114.0
Speed (rpm)	900	900	900	900
Input power (W)	217.7	155.7	100.3	48.5
Output power (W)	167.2	124.2	82.1	39.3
Total losses (W)	50.5	31.5	18.2	9.2
Efficiency (%)	76.8	79.8	81.9	81.0

6.2.3 Linear PM synchronous machine

This section describes the standard efficiency test for evaluating the efficiency of the linear PM synchronous machine and requires a second machine to be mechanically coupled to the linear machine's mover. This second machine acts as a generator and is configured with a load that causing the machine under test to draw rated current at rated voltage and move at rated velocity. The linear PM motor is programmed with a trapezoid velocity waveform with positive velocity $2.56ms^{-1}$ when the machine is moving in the forwards direction and a velocity $-2.56ms^{-1}$ when the machine is moving in the backwards direction. Under these conditions the test machine produces rated

losses by adjusting the resistive load bank to give rated phase current in the linear motor. When the linear motor operates in this condition, measurements are made of the input power to the linear motor and the output power of the load generator in order to determine the efficiency. The linear generator must be capable of handling the output power of the linear machine undergoing test. Table 6.3 presents the experimental results for four different load conditions. The efficiency increases as the output force decreases. This is a consequence of the decrease in copper losses being proportional to the current squared. The output power, however, decreases in proportion to the current. Hence, the efficiency increases as the current, hence copper loss, decreases. The efficiency reaches a peak value when the variable losses (copper losses) equals to the constant losses (core plus friction losses) though this operating condition is not identified in Table 6.3.

Table 6.3 Experimental results of the standard efficiency test for the linear PM synchronous machine under different load force conditions at rated speed

	Load force conditions			
	Full	Three-quarters	Half	Quarter
rms line voltage (V)	47.3	44.9	41.1	37.5
rms line current (A)	2.4	1.8	1.2	0.63
Peak line current (A)	3.4	2.5	1.7	0.9
velocity (ms^{-1})	2.56	2.56	2.56	2.56
Input power (W)	197.4	139.7	89.8	45.2
Output power (W)	139.6	104.5	71.2	37.5
Total losses (W)	57.8	35.2	18.6	7.7
Efficiency (%)	70.6	74.8	79.3	83.0

6.2.4 Standard Test Data Summary

Table 6.4 shows a comparison between the losses determined by experiment and simulation with the total losses generated by the standard efficiency test for different load torque (or force) conditions. The comparison shows that the total losses of the experimental standard efficiency test are slightly higher than that of the simulation. This is expected because the simulation does not model loss components associated with switching frequency harmonics resulting from using a PWM inverter. These include increased Ohmic losses and core loss caused by current ripple at the switching frequency.

Table 6.4 Comparison of total losses obtained from the standard efficiency test using simulation and experiment for the PM synchronous machine under different load torque/force conditions

Load torque/force conditions	Total Losses (W)					
	PM Synchronous Machine		IPM Synchronous Machine		Linear PM Synchronous Machine	
	experiment	simulation	experiment	simulation	experiment	simulation
Full	128.6	117.5	50.5	48.3	57.8	51.0
Three-quarters	89.5	78.1	31.5	29.6	35.2	30.15
Half	59.3	49.8	18.2	16.3	18.6	14.74
Quarter	36.3	31.1	9.2	8.1	7.7	5.83

6.3 Synthetic loading experiments for the PM synchronous machine

The experimental results of synthetic loading applied to the PM synchronous machine are presented in this section. The synthetic loading technique is performed in the laboratory on the PM synchronous machine for the four different load torque conditions. Five tests for each load condition are conducted using five different synthetic loading frequencies between 100 and 120Hz. The experimental results obtained from the synthetic loading technique are compared with the simulation results as well as the simulation and experimental results from the standard efficiency test. The electrical and mechanical parameters of the PM synchronous machine under test are shown in Table 4.1.

6.3.1 Full load torque condition

In this section the synthetic loading technique is configured to produce full-load torque conditions for the PM synchronous machine. The instantaneous phase voltage, instantaneous phase current, rotor speed and input power waveform during synthetic loading are recorded and presented. The simulation quantities are superimposed on the experimental quantities in order to compare between simulation and experimental results.

Figure 6.2 shows the instantaneous phase voltage during synthetic loading tests with a frequency of 100 Hz. The amplitude and frequency modulation is visible. The figure shows that the simulation and experiment results are in agreement during synthetic

loading. The phase voltage is amplitude modulated at 33.3Hz. Note that with this set of conditions the shaft speed varies between 233.3Hz minimum and 300Hz maximum [2] and this speed variation takes place at 100Hz. The resultant apparent modulating frequency during synthetic loading at 100Hz is 33.3 Hz. In essence, in the voltage reference frame synthetic loading is similar to frequency modulation.

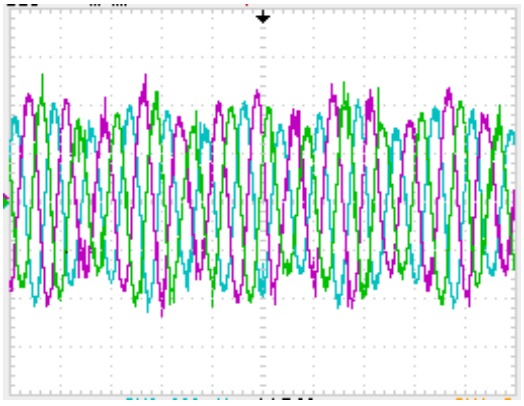

Scale (5ms/div, 40V/div)

(a) three phase voltages during synthetic loading with 100 Hz synthetic loading frequency

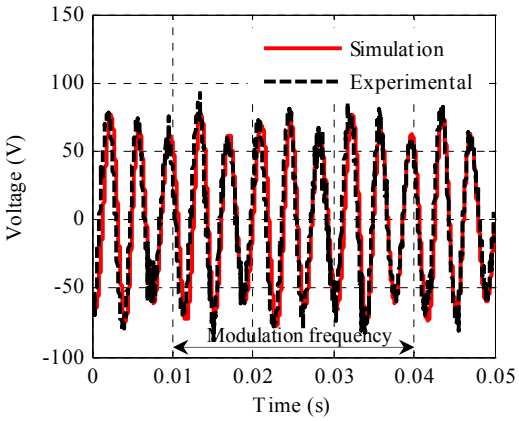

(b) phase *a* voltage during synthetic loading with 100 Hz synthetic loading frequency

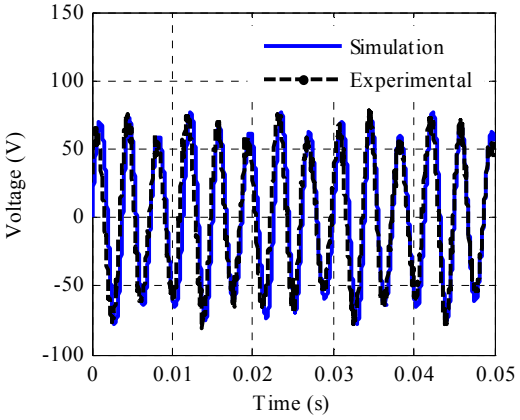

(c) phase *b* voltage during synthetic loading with 100 Hz synthetic loading frequency

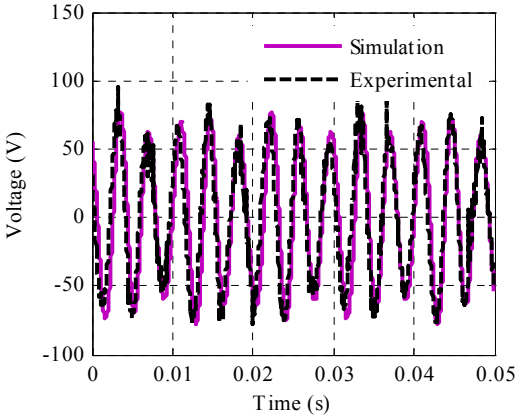

(d) phase *c* voltage during synthetic loading with 100 Hz synthetic loading frequency

Figure 6.2 The PM synchronous machine terminal voltage variation during synthetic loading with 100 Hz synthetic loading frequency under full-load torque conditions

Figure 6.3 illustrates the instantaneous phase currents during synthetic loading for a synthetic loading frequency of 100 Hz. The peak current during synthetic loading is 14.85 A (1.42pu) and the average rms current is 7.5A (1.0pu). This confirms that the PM

synchronous machine is fully loaded. The instantaneous currents are in agreement with the simulated instantaneous currents in terms of their characteristic waveform as shown in Figure 6.3. However, they are slightly different. The difference is primarily due to the difficulty in precisely synchronising the simulation and the practical results to have identical positions of both the rotor and the synthetic cycles. In addition the simulation does not account for nonlinearities such as magnetic saturation and skin effect, and the variation in rotor speed is different to the simulation.

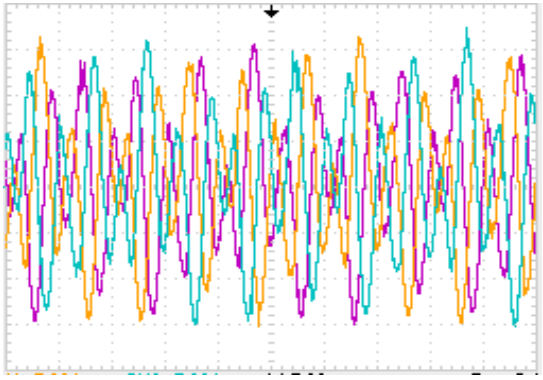

Scale (5ms/div, 5A/div)

(a) three phase currents during synthetic loading with 100 Hz synthetic loading frequency

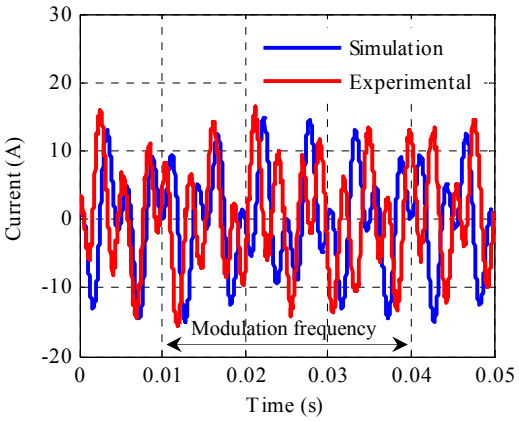

(b) phase *a* current during synthetic loading with 100 Hz synthetic loading frequency

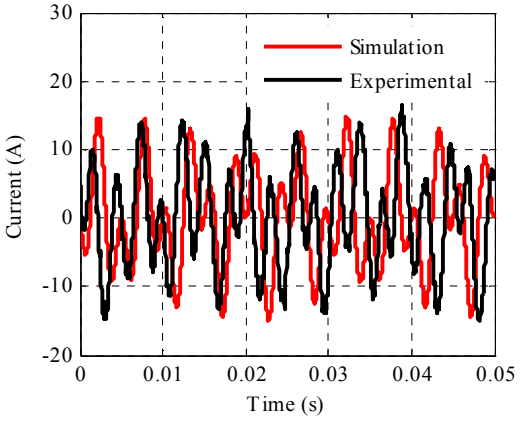

(c) phase *b* current during synthetic loading with 100 Hz synthetic loading frequency

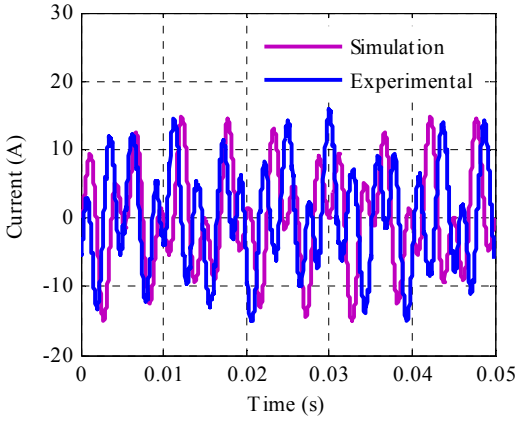

(d) phase *c* current during synthetic loading with 100 Hz synthetic loading frequency

Figure 6.3 The PM synchronous machine current variation during synthetic loading with 100 Hz synthetic loading frequency under full-load torque conditions

The comparison of simulation and experimental speed variation and instantaneous input power during synthetic loading are shown in Figures 6.4 and 6.5 for synthetic loading at 100 Hz. The PM synchronous machine accelerates and decelerates during synthetic loading creating motor-generator action as shown in Figure 6.4.

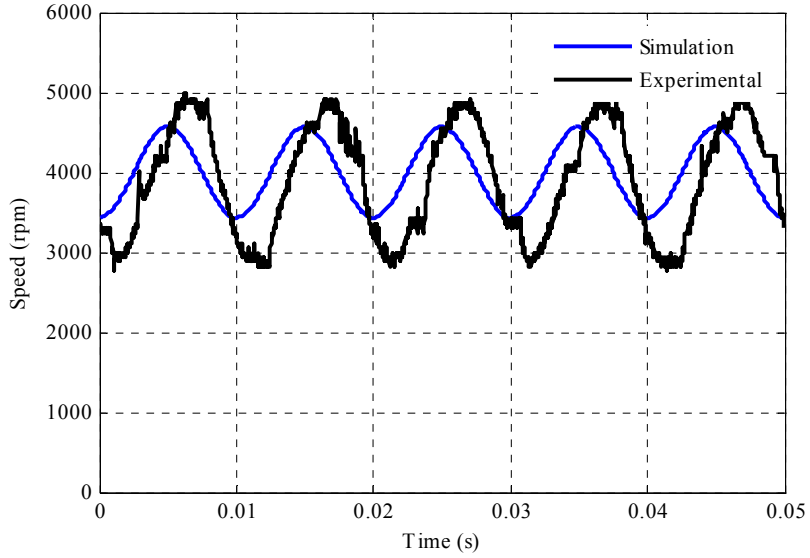

Figure 6.4 The PM synchronous machine speed variation during synthetic loading at 100 Hz under full-load torque conditions

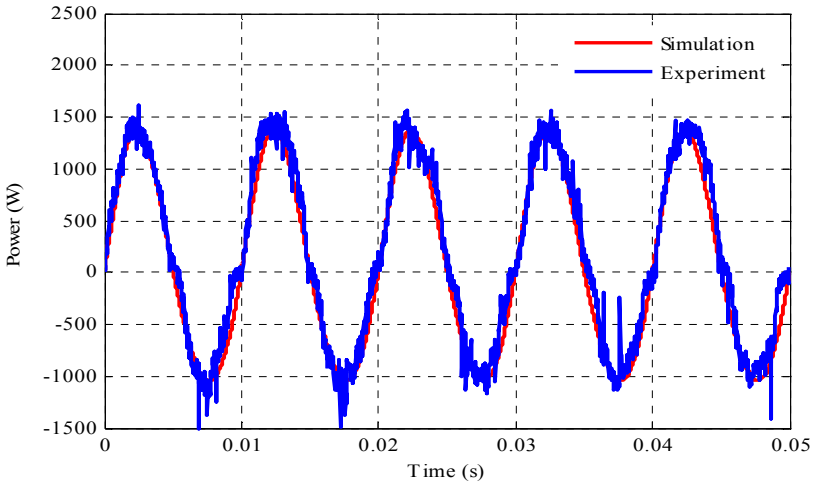

Figure 6.5 The PM synchronous machine input power variation during synthetic loading at 100 Hz synthetic loading frequency under full-load torque conditions

Despite the acceleration and deceleration of the PM synchronous machine, the average rotor speed over one synthetic loading cycle equals the rated speed (4000rpm). From Figures 6.4 and 6.5 during synthetic loading the PM synchronous draws power from the dc supply when the machine accelerates as a motor and generates power back to the dc supply when the machine decelerates. The peak value of power during acceleration is higher than the peak value of power during deceleration, therefore the average input power over one synthetic loading is positive (and is equal to the total losses). The experimental input power is superimposed with the simulation input power during synthetic loading. The waveform is almost identical with a small difference in peak value.

Table 6.5 shows the experimental results of the standard efficiency test and synthetic loading technique. The synthetic loading technique is conducted for five different synthetic loading frequencies. Despite the differences between the instantaneous quantities during synthetic loading, the efficiency obtained from the synthetic loading technique is comparable to the standard efficiency test. The standard efficiency test under full-load condition is 87.0%. The synthetic loading technique produces efficiencies between 86.7% and 86.9% when the input power of the standard efficiency test is used to calculate the efficiency. Therefore, synthetic loading underestimates the efficiency by less than 0.1% at best, 0.3% at worst and 0.2% on average.

An inverter is used during both the standard efficiency test and the synthetic loading technique. This inverter has minimum requirements in terms of minimum dc link voltage, minimum peak current and minimum peak VA. These are all higher than that required for the standard efficiency test. For example, in this case the minimum dc link voltage required is 165.0V (1.1pu compared with the standard efficiency test) the minimum peak current required is 14.85A (1.41pu) and the minimum inverter phase-leg VA rating required is 2450 VA (1.53pu).

Table 6.5 Comparison of the standard efficiency test and the synthetic loading technique results for the PM synchronous machine under full-load torque condition

	Standard Efficiency Test	Synthetic Loading Frequency (Hz)				
		100	105	110	115	120
rms line voltage (V)	95.4	94.7	94.4	94.6	95.1	95.4
rms line current (A)	7.45	7.42	7.4	7.4	7.43	7.42
Minimum inverter peak current (A)	10.5	14.85	14.85	14.85	14.85	14.85
Phase-leg VA rating (VA)	1601	2421	2443	2450	2465	2480
Minimum dc link voltage (V)	152.5	163.0	164.5	165.0	166.0	167.0
Speed (rpm)	4000	4000	4000	4000	4000	4000
Input power (W)	988.1	130.3	129.6	129.0	131.1	130.5
Output power (W)	859.5	-	-	-	-	-
Total losses (W)	128.6	130.3	129.6	129.0	131.1	130.5
Efficiency (%)	87.0	86.8	86.9	86.9	86.7	86.8

6.3.2 Three-quarters of full load torque condition

In this section the PM synchronous machine is loaded to three-quarters of full-load torque at rated speed. The experimental results of the standard efficiency test and synthetic loading technique for this load condition are presented in Table 6.6.

Table 6.6 Comparison of the standard efficiency test and the synthetic loading technique using experimental results for the PM synchronous machine with three-quarters of full-load torque

	Standard Efficiency Test	Synthetic Loading Frequency (Hz)				
		100	105	110	115	120
rms line voltage (V)	92.1	91.9	91.5	91.4	91.2	91.3
rms line current (A)	5.62	5.62	5.63	5.62	5.63	5.62
Minimum inverter peak current (A)	7.9	11.2	11.2	11.2	11.2	11.2
Phase-leg VA rating (VA)	1185	1781	1781	1792	1792	1792
Minimum dc link voltage (V)	150.0	159.0	159.0	160.0	160.0	160.0
Speed (rpm)	4000	4000	4000	4000	4000	4000
Input power (W)	758.2	91.0	91.6	91.8	92.5	90.8
Output power (W)	668.7	-	-	-	-	-
Total losses (W)	89.5	91.0	91.6	91.8	92.5	90.8
Efficiency (%)	88.2	88.0	87.9	87.9	87.8	88.0

The experimental results in Table 6.6 show that the standard efficiency test results are consistent with the synthetic loading technique results. That is, the PM synchronous machine operates at rated speed 4000 rpm (1.0pu), draws rated current 5.62 A (0.76pu) and the rated terminal voltage is 91.5 V (0.96pu) on average during synthetic loading. The average input power is 91.5W, which is equal to the total losses during synthetic loading. As expected the minimum dc link voltage (1.05pu), peak current (1.07pu) and minimum peak VA required for the inverter (1.12pu) during synthetic loading is higher compared with the same value during the standard efficiency test. Under this load condition the efficiency calculated using the standard efficiency test is 88.2%. The synthetic loading technique estimates efficiencies between 87.8% and 88.0% when the input power of the standard efficiency test is used to calculate the efficiency. This confirms that synthetic loading is an effective technique for efficiency evaluation of the PM synchronous machine. The efficiency of the PM synchronous machine using synthetic loading technique is underestimated by only 0.3% compared with the efficiency using the standard efficiency test.

6.3.3 Half of full load torque condition

In this case synthetic loading is carried out experimentally for the PM synchronous machine under half of full-load torque condition and the results are compared with the experimental results of the standard efficiency test under the same load condition. The results are presented at Table 6.7. These are compared with the standard efficiency test. The input power with the standard efficiency test is 520.5W, the total loss is 59.3W and the efficiency calculated using these results is 88.6%. The efficiency using synthetic loading technique is in close agreement. For comparison, the efficiency of the PM synchronous machine using synthetic loading are between 88.2% and 88.4%. Therefore, the efficiency evaluated using synthetic loading is underestimated by 0.3%, on average, compared with that measured using the standard efficiency test. To carry out synthetic loading for half rated torque condition, an inverter with a minimum phase-leg VA rating of 1166VA (0.73pu), minimum dc link of 155V (1.02pu) and minimum peak current of 7.5 A (0.71pu) is required.

Table 6.7 Comparison of the standard efficiency test and the synthetic loading technique experimental results for the PM synchronous machine under half of full-load torque condition

	Standard Efficiency Test	Synthetic Loading Frequency (Hz)				
		100	105	110	115	120
rms line voltage (V)	89.5	89.3	89.8	89.5	89.4	89.2
rms line current (A)	3.72	3.73	3.7	3.72	3.72	3.73
Minimum inverter peak current (A)	5.3	7.5	7.5	7.5	7.5	7.5
Phase-leg VA rating (VA)	779	1163	1163	1163	1170	1170
Minimum dc link voltage (V)	147.0	155.0	155.0	155.0	156.0	156.0
Speed (rpm)	4000	4000	4000	4000	4000	4000
Input power (W)	520.5	60.5	61.0	61.5	60.8	60.5
Output power (W)	461.2	-	-	-	-	-
Total losses (W)	59.3	60.5	61.0	61.5	60.8	60.5
Efficiency (%)	88.6	88.4	88.3	88.2	88.3	88.4

6.3.4 Quarter of full load torque condition

The synthetic loading technique and the standard efficiency test are carried out for the PM synchronous machine under quarter of full-load condition. The experimental results of standard efficiency test and synthetic loading technique are presented in Table 6.8. The results show that the PM synchronous machine, on average, operates at a rated speed of 4000rpm (1.0pu), draws current of 1.87A (0.25pu) at terminal voltage of 87.6V (0.92pu) during synthetic loading. The calculated efficiency is 85.9% from the standard efficiency test. The efficiencies measured using synthetic loading are between 85.5% and 85.9% which indicates that the efficiency obtained using synthetic loading is underestimated by 0.2%, on average, compared with the efficiency obtained using standard efficiency test. The inverter used to conduct the synthetic loading technique requires a VA rating, peak current and dc link voltage, of 576VA (0.36pu), 3.75A (0.36pu) and 154.0V (1.01pu) respectively.

Table 6.8 Comparison of the standard efficiency test and the synthetic loading technique experimental results for the PM synchronous machine under quarter of full-load torque condition

	Standard Efficiency Test	Synthetic Loading Frequency (Hz)				
		100	105	110	115	120
rms line voltage (V)	87.3	87.7	87.6	87.6	87.5	87.8
rms line current (A)	1.87	1.88	1.87	1.86	1.87	1.86
Minimum inverter peak current (A)	2.63	3.75	3.75	3.75	3.75	3.75
Phase-leg VA rating (VA)	379	574	574	574	578	578
Minimum dc link voltage (V)	144.0	153.0	153.0	153.0	154.0	154.0
Speed (rpm)	4000	4000	4000	4000	4000	4000
Input power (W)	258.1	37.5	36.5	36.3	36.8	37.0
Output power (W)	221.8	-	-	-	-	-
Total losses (W)	36.3	37.5	36.5	36.3	36.8	37.0
Efficiency (%)	85.9	85.5	85.9	85.9	85.7	85.7

6.3.5 The PM synchronous machine summary

Table 6.9 presents a comparison between experimental and simulation results using the synthetic loading technique and the standard efficiency test method for the PM synchronous machine with the four different load conditions and five different synthetic loading frequencies. The results show that the simulated efficiencies are higher than the experimental efficiencies in each case. The simulation does not model loss components associated with switching frequency induced current ripple or core loss and this is the primary contribution to the difference between the results. Figure 6.6 illustrates the percentage error in the efficiency using synthetic loading for the four different load conditions.

Table 6.9 Comparison of the synthetic loading simulation and experimental results for the PM synchronous machine under different load torque conditions

Synthetic Loading Frequency (Hz)	Load Conditions							
	Full		Three-quarters		Half		Quarter	
	Efficiency (%)		Efficiency (%)		Efficiency (%)		Efficiency (%)	
	Simulation	Experiment	Simulation	Experiment	Simulation	Experiment	Simulation	Experiment
100	87.8	86.8	89.0	88.0	89.7	88.4	86.1	85.5
105	87.8	86.9	89.0	87.9	89.7	88.3	86.1	85.9
110	87.8	86.9	89.0	87.9	89.7	88.2	86.1	85.9
115	87.8	86.7	89.0	87.8	89.7	88.3	86.1	85.7
120	87.8	86.8	89.0	88.0	89.7	88.4	86.1	85.7
Standard efficiency test	87.8	87.0	89.0	88.2	89.4	88.6	86.1	85.9

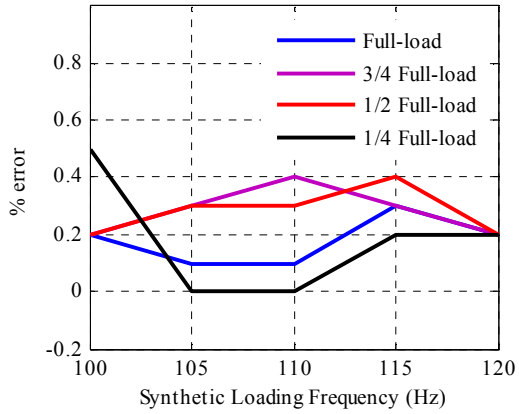

Figure 6.6 The percentage error in the measured efficiency of the PM synchronous machine using synthetic loading

6.4 Synthetic loading experimental results for the IPM synchronous machine

In this section synthetic loading of the IPM synchronous machine under different load torque conditions and synthetic loading frequencies is assessed. The experimental results obtained from the synthetic loading technique are compared with the simulated synthetic loading results from chapter four. The experimental synthetic loading results are also compared with the standard efficiency test results. The measurement system used for

IPM synchronous machine measurements is the same as that used for the PM synchronous machine.

6.4.1 Full load torque condition

Five synthetic loading frequencies between 4 – 10Hz are used. In order to compare synthetic loading simulation results with experimental results, the simulation quantities for instantaneous phase voltage, current, speed and input power are superimposed onto the experimental results. Figure 6.6 shows the variation of the phase voltages during synthetic loading with a frequency of 4 Hz. The amplitude and frequency modulation are obvious in this figure. Figures 6.7 (b) – (d) illustrate that the experimental results are in agreement with the simulation results in terms of characteristic shape. The simulation model does not account for magnetic saturation and skin effect. This leads to small disagreement between the experimental and simulated waveform. Also, as for the PM synchronous machine, it is difficult to precisely synchronise both the rotor and synthetic angular positions.

The phase voltage magnitude during synthetic loading depends on the rotor speed and the air-gap flux. Therefore, any variation in the rotor speed and air-gap flux affects the phase voltage variation. Hence, the higher peak-to-peak values of rotor speed and air-gap flux in the IPM synchronous machine directly affects the variation in the phase voltage envelope. Figure 6.7 (a) shows that there is a large variation in the phase voltage. The reasons for the higher values of peak to peak variation of speed and air-gap flux are explained in chapter four, section 4.4.

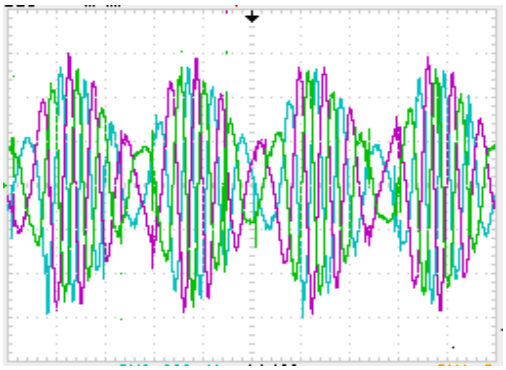

(a) three phase voltages during synthetic loading with 4 Hz synthetic loading frequency

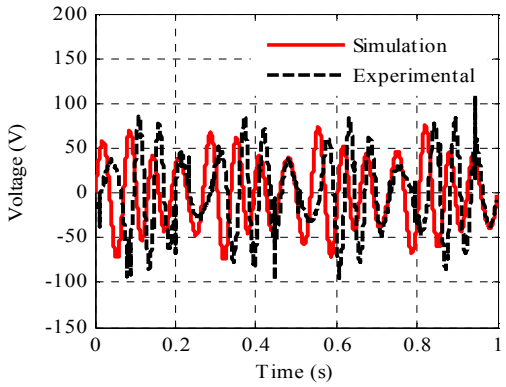

(b) phase *a* voltage during synthetic loading with 4 Hz synthetic loading frequency

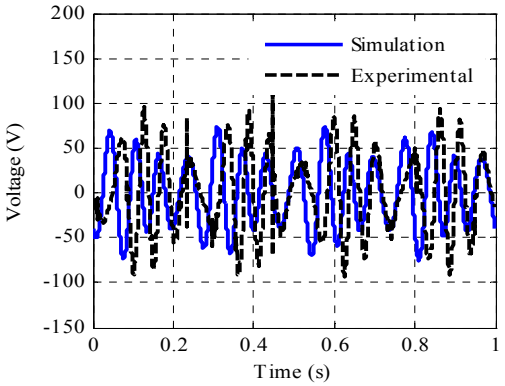

(c) phase *b* voltage during synthetic loading with 4 Hz synthetic loading frequency

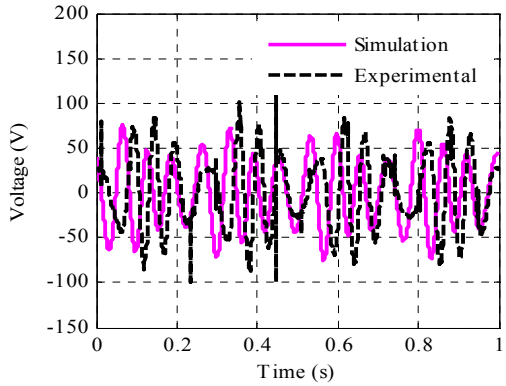

(d) phase *c* voltage during synthetic loading with 4 Hz synthetic loading frequency

Figure 6.7 The IPM synchronous machine terminal voltage variation during synthetic loading with 4 Hz synthetic loading frequency under full-load torque conditions

Figure 6.8 illustrates the variation of instantaneous phase current during synthetic loading at 4Hz. The simulated phase current waveforms are in agreement with the experimental phase current waveforms as depicted in Figures 6.8(b) – (d).

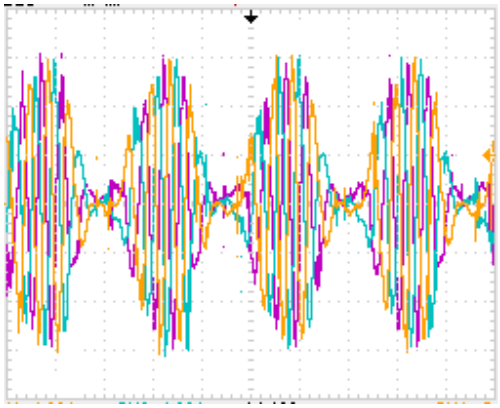

Scale (100ms/div, 1A/div)

(a) three phase currents during synthetic loading with 4 Hz synthetic loading frequency

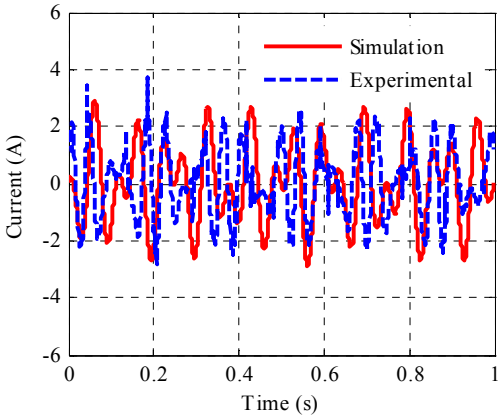

(b) phase *a* current during synthetic loading with 4 Hz synthetic loading frequency

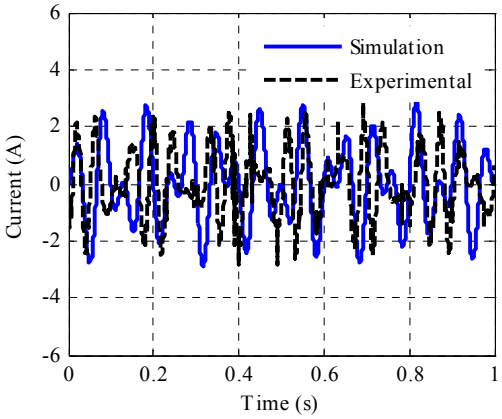

(c) phase *b* current during synthetic loading with 4 Hz synthetic loading frequency

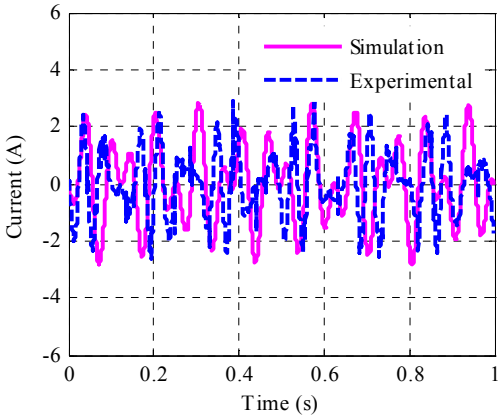

(d) phase *c* current during synthetic loading with 4 Hz synthetic loading frequency

Figure 6.8 The IPM synchronous machine current variation during synthetic loading with 4 Hz synthetic loading frequency under full-load torque conditions

Figure 6.9 shows the variation of speed with time during synthetic loading for both experiment and simulation with a synthetic loading frequency of 4Hz. The experimental rotor speed is in agreement with the simulated speed in terms of shape but the peak to peak is around 28% higher in the experiments. This is may be due to the underestimation of the moment of inertia, *J*, in the simulation. Figure 6.10 illustrates the experimental and simulated input power variation with time during synthetic loading for a synthetic loading frequency of 4Hz. It shows that during synthetic loading the IPM synchronous

machine draws power from the supply when the machine is accelerating as a motor and regenerates when the machine decelerates. The average input power over one synthetic loading is positive and equals to the total losses.

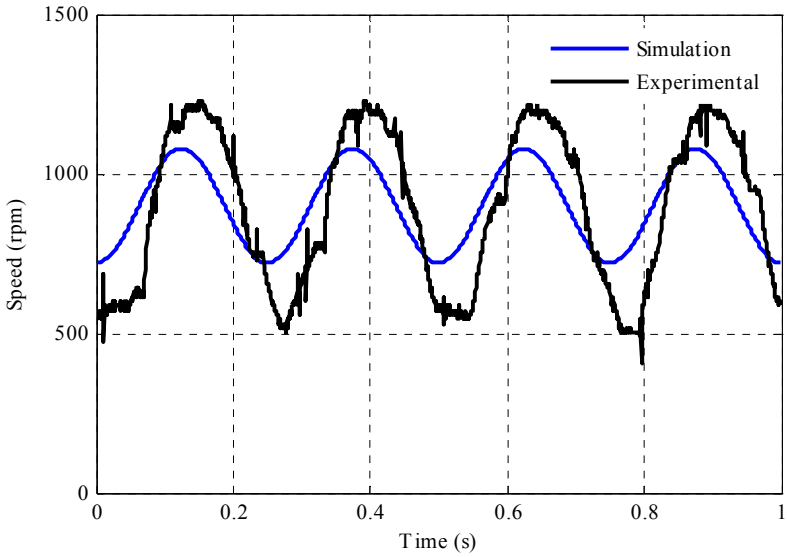

Figure 6.9 The IPM synchronous machine speed variation during synthetic loading at 4 Hz under full-load torque conditions

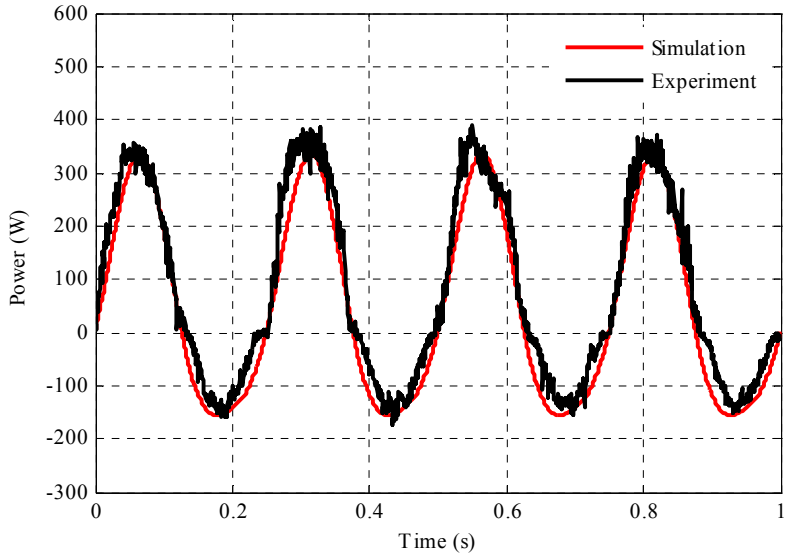

Figure 6.10 The IPM synchronous machine input power variation during synthetic loading at 4 Hz synthetic loading frequency under full-load torque conditions

Table 6.10 presents the experimental results of the standard efficiency test and synthetic loading technique for the full load torque condition. The total losses are evaluated and then the efficiency calculated. The inverter phase-leg VA rating and peak current required during synthetic loading technique are 460VA (1.57pu) and 2.83A (1.41pu) respectively. The efficiencies of the five different synthetic loading frequencies are between 76.3% and 76.6%, which shows that synthetic loading underestimates the efficiency by 0.2% at best, 0.5% at worst and 0.4% on average compared with the standard efficiency test. During synthetic loading the IPM synchronous machine operates at rated speed, rated rms voltage and draws rated current, on average.

Table 6.10 Comparison between the standard efficiency test and the synthetic loading technique experimental results for the IPM synchronous machine under full-load torque conditions

	Standard Efficiency Test	Synthetic Loading Frequency (Hz)				
		4	6	8	9	10
rms line voltage (V)	91.3	91.8	91.6	92.0	91.8	91.6
rms line current (A)	1.41	1.41	1.41	1.41	1.41	1.41
Minimum inverter peak current (A)	2.0	2.83	2.83	2.83	2.83	2.83
Phase-leg VA rating (VA)	292.0	457.0	457.0	460.0	461.3	461.3
Minimum dc link voltage (V)	146.0	161.5	161.5	162.5	163.0	163.0
Speed (rpm)	900	900	900	900	900	900
Input power (W)	217.7	51.2	51.5	51.3	51.0	51.3
Output power (W)	167.2	-	-	-	-	-
Total losses (W)	50.2	51.2	51.5	51.3	51.0	51.3
Efficiency (%)	76.8	76.5	76.3	76.4	76.6	76.4

6.4.2 Three-quarters of rated torque condition

The experimental results of the standard efficiency test and synthetic loading technique are presented in Table 6.11 at three-quarters of rated torque. In this case the inverter phase-leg VA rating and peak current required are 320VA (1.1pu) and 2.12A (1.1pu) respectively. The minimum dc link voltage required is 150V (1.03pu). The efficiencies calculated using synthetic loading are between 79.1% and 79.6%. Therefore, the synthetic loading technique underestimates the efficiency by 0.3%, on average,

compared with the standard efficiency test. Also, during synthetic loading the IPM synchronous machine draws current, on average, 1.07A (0.76pu).

Table 6.11 Comparison between the standard efficiency test and the synthetic loading technique experimental for the IPM synchronous machine with three-quarters rated torque at rated speed

	Standard Efficiency Test	Synthetic Loading Frequency (Hz)				
		4	6	8	9	10
rms line voltage (V)	86.6	87.1	86.9	87.0	86.8	87.2
rms line current (A)	1.07	1.07	1.07	1.06	1.07	1.06
Minimum inverter peak current (A)	1.5	2.12	2.12	2.12	2.12	2.12
Phase-leg VA rating (VA)	201.8	318.0	318.0	321.2	321.2	323.3
Minimum dc link voltage (V)	134.5	150.0	150.0	151.5	151.5	152.5
Speed (rpm)	900	900	900	900	900	900
Input power (W)	155.7	32.1	31.8	32.0	32.5	32.2
Output power (W)	124.2	-	-	-	-	-
Total losses (W)	31.5	32.1	31.8	32.0	32.5	32.2
Efficiency (%)	79.8	79.4	79.6	79.4	79.1	79.3

6.4.3 Half rated torque condition

The experimental results for standard efficiency test and synthetic loading technique are summarised in Table 6.12 at half rated torque at rated speed. The minimum dc link voltage required for synthetic loading technique is 142.0V (0.97pu). The inverter phase-leg VA rating and peak phase current are 200.0VA (0.68pu) and 1.41A (0.71pu) respectively. The efficiency of the IPM synchronous machine calculated using synthetic loading technique is between 81.0% and 81.8%. The synthetic loading technique underestimates the efficiency by 0.1% at best, 0.9% at worst and 0.4% on average compared with the standard efficiency test.

Table 6.12 Comparison between the standard efficiency test and the synthetic loading technique for the IPM synchronous machine with half rated torque

	Standard Efficiency Test	Synthetic Loading Frequency (Hz)				
		4	6	8	9	10
rms line voltage (V)	80.5	81.0	81.2	81.4	81.0	80.8
rms line current (A)	0.71	0.71	0.71	0.71	0.71	0.71
Minimum inverter peak current (A)	1.0	1.41	1.41	1.41	1.41	1.41
Phase-leg VA rating (VA)	125.0	199.5	199.5	201.6	201.6	203.0
Minimum dc link voltage (V)	125.0	141.5	141.5	143.0	143.0	144.0
Speed (rpm)	900	900	900	900	900	900
Input power (W)	100.3	19.1	18.8	18.5	18.6	18.3
Output power (W)	82.1	-	-	-	-	-
Total losses (W)	18.2	19.1	18.8	18.5	18.6	18.3
Efficiency (%)	81.9	81.0	81.3	81.6	81.5	81.8

6.4.4 Quarter rated torque condition

Table 6.13 summarises the experimental results of the standard efficiency test and the synthetic loading technique configured to give quarter rated torque. The minimum dc link voltage required for the synthetic loading technique is 128.0V (0.88pu), on average. The inverter phase-leg VA rating and peak current required during synthetic loading are 91.0VA (0.31pu) and 0.71A (0.36pu) respectively compared to 0.2pu and 0.25pu for the standard efficiency test. The efficiency of the IPM synchronous machine calculated under quarter of full load torque using synthetic loading are between 80% and 80.8%. The results show that the synthetic loading technique underestimates the IPM synchronous machine efficiency by 0.4%, on average, compared with the standard efficiency test. However, the experimental results of the standard efficiency test are in agreement with the experimental results of the synthetic loading technique for the IPM synchronous machine under different load conditions and different synthetic loading frequencies.

Table 6.13 Comparison of the standard efficiency test and the synthetic loading technique experimental results for the IPM synchronous machine with quarter rated torque condition

	Standard Efficiency Test	Synthetic Loading Frequency (Hz)				
		4	6	8	9	10
rms line voltage (V)	75.3	76.0	76.2	75.8	76.0	75.7
rms line current (A)	0.36	0.35	0.35	0.35	0.35	0.35
Minimum inverter peak current (A)	0.5	0.71	0.71	0.71	0.71	0.71
Phase-leg VA rating (VA)	57.0	90.2	90.2	91.6	91.6	93.0
Minimum dc link voltage (V)	114.0	127.0	127.0	129.0	129.0	131.0
Speed (rpm)	900	900	900	900	900	900
Input power (W)	48.5	9.6	9.4	9.7	9.3	9.5
Output power (W)	39.3	-	-	-	-	-
Total losses (W)	9.2	9.6	9.4	9.7	9.3	9.5
Efficiency (%)	81.0	80.2	80.6	80.0	80.8	80.4

6.4.5 The IPM synchronous machine summary

The results show that the efficiency of the IPM synchronous machine calculated using the synthetic loading technique are comparable with the efficiency calculated using standard efficiency test. In general, the efficiency is underestimated. The machine draws rated current, rated voltage and operates at rated speed during synthetic loading, on average. The inverter phase-leg VA rating, minimum peak phase current and dc link voltage required during synthetic loading are higher than that using during standard efficiency test.

The efficiency evaluation of the IPM synchronous machine using the synthetic loading technique and the standard efficiency test are investigated for different load torque conditions and different synthetic loading frequencies. The comparison between simulation results and experimental results for the tests are presented in Table 6.14. The comparisons shows that the simulated efficiency is overestimated compared to the experimental results for all load torque conditions and synthetic loading frequencies and for both the standard efficiency test and the synthetic loading technique. This is due to two reasons, firstly, switching harmonics losses result from using a PWM inverter. These include core losses (hysteresis and eddy current) arising from the changing flux

density in the iron of the machine and increased Ohmic losses caused by current ripple at the switching frequency. Secondly, nonlinearities such as magnetic saturation and skin effect are not modelled in the simulation and the damper factor for calculating mechanical losses is assumed to be constant but actually is not constant during experiment. This leads to an underestimate of the losses in the simulation. Figure 6.11 illustrates the percentage error in the efficiency using synthetic loading for the four different load conditions.

Table 6.14 Comparison of the synthetic loading simulation and experimental results for the IPM synchronous machine under different load torque condition

Synthetic Loading Frequency (Hz)	Load torque conditions							
	Full		Three-quarters		Half		Quarter	
	Efficiency (%)		Efficiency (%)		Efficiency (%)		Efficiency (%)	
	Simulation	Experiment	Simulation	Experiment	Simulation	Experiment	Simulation	Experiment
4	77.5	76.5	80.7	79.4	83.3	81.0	82.0	80.2
6	77.5	76.3	80.7	79.6	83.3	81.3	82.0	80.6
8	77.5	76.4	80.7	79.4	83.3	81.6	82.0	80.0
9	77.5	76.6	80.7	79.1	83.3	81.5	82.0	80.8
10	77.5	76.4	80.7	79.3	83.3	81.8	82.0	80.4
Standard efficiency test	77.4	76.8	80.6	79.8	83.2	81.9	82.0	81.0

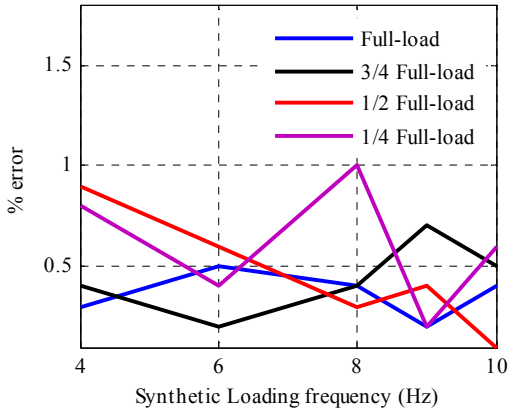

Figure 6.11 The percentage error in the measured efficiency of the IPM synchronous machine using synthetic loading

6.5 Experimental results from synthetic loading of the linear PM synchronous machine

The experimental results of the synthetic loading technique applied to the linear PM synchronous machine are presented in this section. These confirm that the synthetic loading technique is a potential method of efficiency evaluation. Synthetic loading of the linear PM synchronous machine is performed experimentally for different load force conditions and five different synthetic loading frequencies. The experimental results of the standard efficiency test and the synthetic loading technique are compared with the simulation results. The comparisons show a good degree of consistency between the experimental synthetic loading technique and experimental standard efficiency test, as well as between the synthetic loading technique simulation results and the synthetic loading technique experimental results.

6.5.1 Full load force condition

In this case the synthetic loading technique and the standard efficiency test for the linear PM synchronous machine are performed for the full-load force condition at rated velocity. Five different synthetic loading frequencies are investigated around the optimum value identified in chapter four. These are between 20 Hz and 40 Hz. Figure 6.10 shows a comparison between the experimental and simulated waveforms of the instantaneous phase voltages for the linear PM synchronous machine with a synthetic loading frequency of 20 Hz.

The average of the instantaneous rms voltage over one synthetic loading cycle is equal to the rated terminal voltage of the linear PM synchronous machine in the experimental case. The slight difference in the values between the experimental and simulated waveform in Figure 6.12 (b) – (d) is the linear equivalent of the reasons given for the rotational system in 6.3.1. In this case, it is difficult to precisely synchronise the linear position and the synthetic angle in both simulated and experimental systems.

The instantaneous phase currents for the same conditions are shown in Figure 6.13. The experimental phase currents are superimposed on the simulated phase currents.

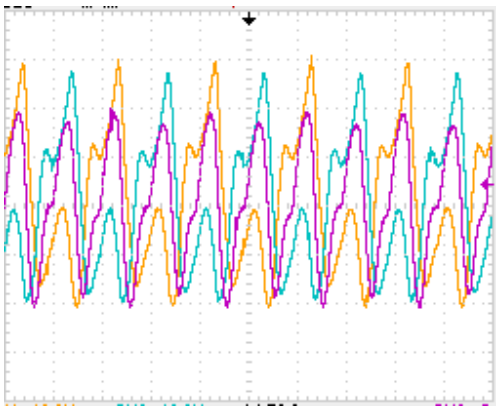

(a) three phase voltages during synthetic loading with 20 Hz synthetic loading frequency

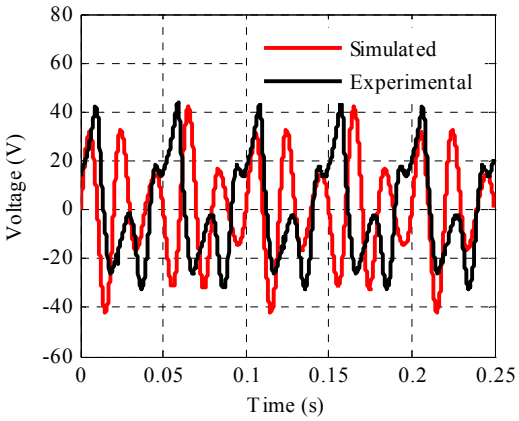

(b) phase *a* voltage during synthetic loading with 20 Hz synthetic loading frequency

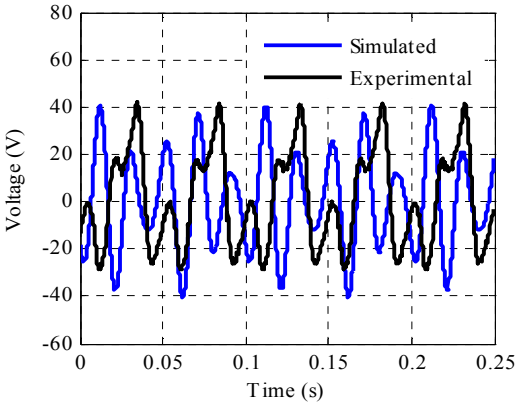

(c) phase *b* voltage during synthetic loading with 20 Hz synthetic loading frequency

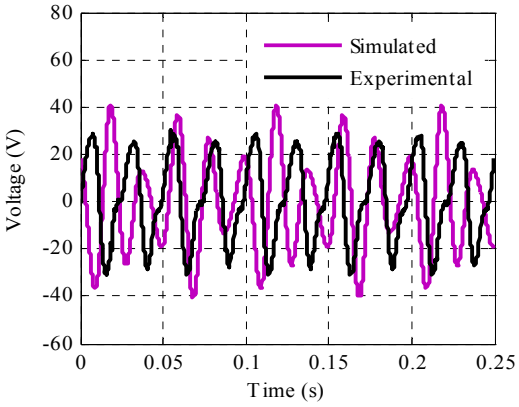

(d) phase *c* voltage during synthetic loading with 20 Hz synthetic loading frequency

Figure 6.12 The linear PM synchronous machine terminal voltage variation with a 20 Hz synthetic loading frequency under full-load force conditions at rated mover velocity

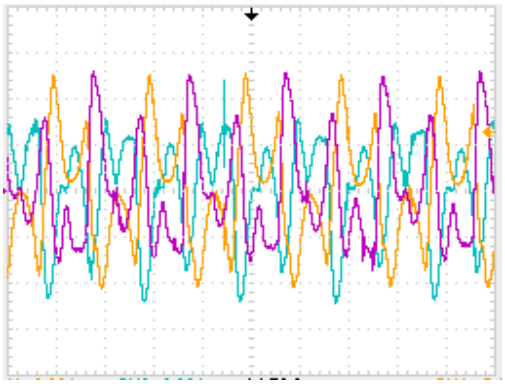

(a) three phase currents during synthetic loading with 20 Hz synthetic loading frequency

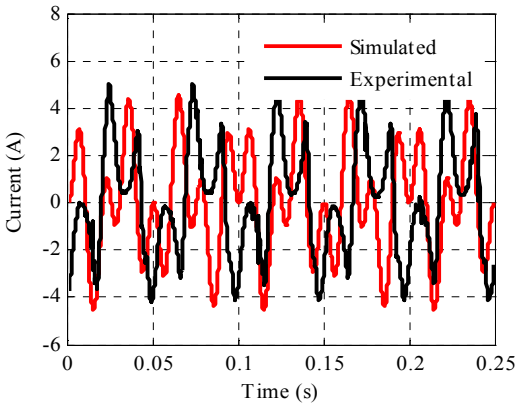

(b) phase *a* current during synthetic loading with 20 Hz synthetic loading frequency

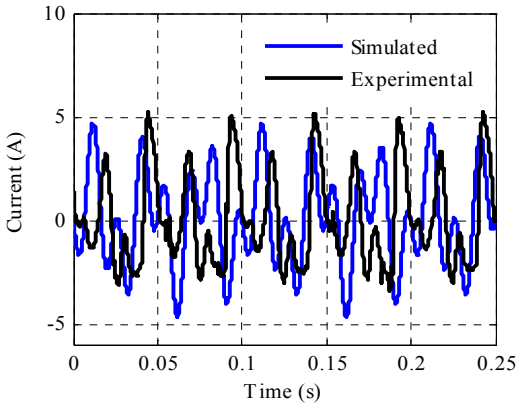

(c) phase *b* current during synthetic loading with 20 Hz synthetic loading frequency

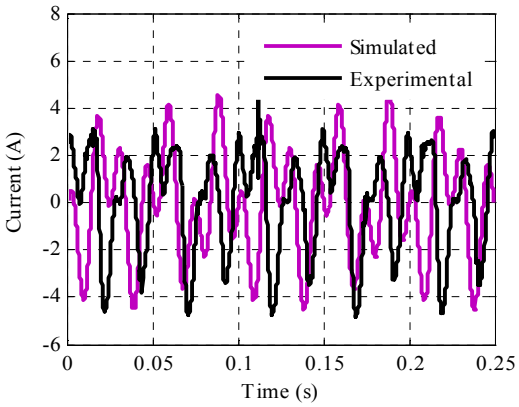

(d) phase *c* current during synthetic loading with 20 Hz synthetic loading frequency

Figure 6.13 The linear PM synchronous machine current variation with a 20 Hz synthetic loading frequency under full-load force conditions at rated mover velocity

The comparison of the experimental and simulated phase currents during synthetic loading shows good agreement with respect to the waveform shape. However, there is a slight difference in the instantaneous current between the experimental and simulated results for similar reasons to that explained for the voltage waveform.

Figure 6.14 shows the comparison between the simulated and experimental input power during the synthetic loading test for the linear PM synchronous machine under full-load force conditions for a synthetic loading frequency of 20 Hz. The experimental

and the simulation input power waveforms are in good agreement in terms of characteristic shape. There is small difference because it is difficult to precisely synchronise the mover and synthetic loading movement position.

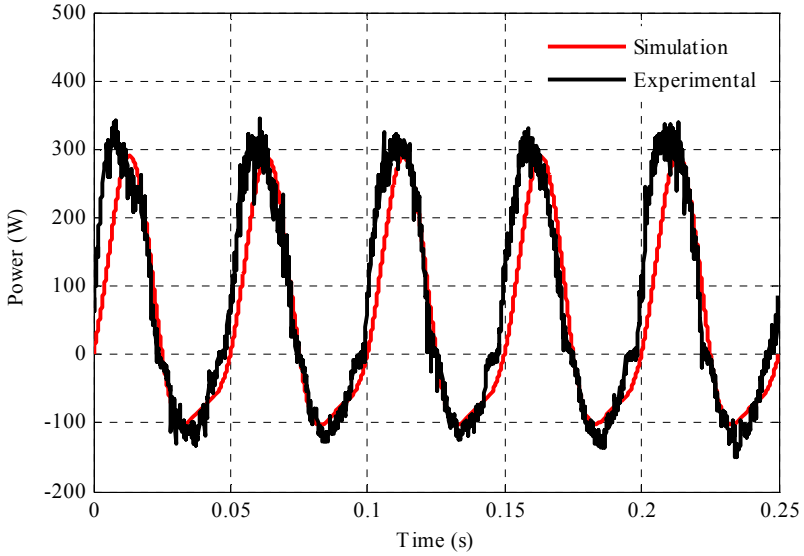

Figure 6.14 Input power variation of the linear PM synchronous machine during synthetic loading with 20 Hz synthetic loading frequency under full-load force conditions

The comparison between the simulation and the experimental results show that there is an additional loss during the experiment. This is due switching harmonics losses results from using PWM inverter. These include core losses (hysteresis and eddy current) arising from the changing flux density in the iron of the machine and increased Ohmic losses caused by current ripple at the switching frequency. Additionally, nonlinearities such as magnetic saturation, skin effect and damper factor for calculating friction losses are assumed to be constant but may not be constant during the experiment. This leads to an underestimate of the losses in the simulation.

Table 6.15 shows the comparison between the experimental standard efficiency test and experimental synthetic loading technique for efficiency evaluation of the linear PM synchronous machine under full-load force conditions. It can be noted that the inverter used to carry out synthetic loading test must deliver a peak current of 4.81A (1.41pu)

which is higher than the inverter rating used to conduct the standard efficiency test. Table 6.14 illustrates that the efficiency of the linear PM synchronous machine assessed using synthetic loading technique with full-load condition is between 70.1% and 70.5%. Therefore, the synthetic loading experimental result underestimates the efficiency by 0.1% at best, 0.5% at worst and 0.3%, on average, compared to the standard efficiency test. This indicates that the synthetic loading technique can be used to evaluate the efficiency of the linear PM synchronous machine. Also, during synthetic loading the results show that the machine draws rated rms current and moves at rated velocity at rated rms terminal voltage on average.

Table 6.15 Experimental comparison of the standard efficiency test and the synthetic loading technique for the linear PM synchronous machine under full-load force conditions

	Standard Efficiency Test	Synthetic Loading Frequency (Hz)				
		20	25	30	35	40
rms line voltage (V)	47.3	47.0	46.8	47.1	47.0	47.2
rms line current (A)	2.4	2.42	2.4	2.4	2.41	2.42
Minimum inverter peak current (A)	3.4	4.81	4.8	4.8	4.81	4.81
Speed (ms^{-1})	2.56	2.56	2.56	2.56	2.56	2.56
Input power (W)	197.4	58.4	58.8	58.2	58.5	59.1
Output power (W)	139.6	-	-	-	-	-
Total losses (W)	57.8	58.4	58.8	58.2	58.5	59.1
Efficiency (%)	70.6	70.4	70.2	70.5	70.4	70.1

6.5.2 Three-quarters of full load force condition

Table 6.16 details the experimental results of the standard efficiency test and the synthetic loading technique for the linear PM synchronous machine with the tests configured to produced three-quarters of rated force. It is observed that from the experimental results of the synthetic loading technique the inverter delivers a peak current of 3.54A. Also, during synthetic loading the linear PM synchronous machine, on average, draws rms current (1.8Amps), at terminal voltage (44.6V) and moves at rated velocity of 2.56 ms^{-1}. The linear PM synchronous machine efficiencies at three-quarters of full-load force using the synthetic loading technique, for five different synthetic

loading frequencies are between 74.1% and 74.5%. The efficiency using the synthetic loading test is underestimated by 0.6%, on average, compared with the standard efficiency test.

Table 6.16 Experimental comparison of the standard efficiency test and the synthetic loading technique for the linear PM synchronous machine under three-quarters of full-load force condition

	Standard Efficiency Test	Synthetic Loading Frequency (Hz)				
		20	25	30	35	40
rms line voltage (V)	44.9	44.5	44.7	44.4	44.7	44.8
rms line current (A)	1.8	1.8	1.81	1.8	1.8	1.8
Minimum inverter peak current (A)	2.5	3.54	3.55	3.52	3.54	3.54
Speed (ms^{-1})	2.56	2.56	2.56	2.56	2.56	2.56
Input power (W)	139.7	36.0	36.2	35.6	35.9	36.0
Output power (W)	104.5	-	-	-	-	-
Total losses (W)	35.2	36.0	36.2	35.6	35.9	36.0
Efficiency (%)	74.8	74.2	74.1	74.5	74.3	74.2

6.5.3 Half of full load force condition

Table 6.17 presents a comparison between the standard efficiency test and the synthetic loading technique for the linear PM synchronous machine with half rated load force condition. The efficiencies of the machine for the five different synthetic loading frequencies are between 78.6% and 79.2%. The efficiency evaluation using the synthetic loading technique is underestimated by 0.7% at worst, 0.1% at best and by 0.5%, on average, compared with the standard efficiency test. The inverter must deliver a peak current of 2.4A during synthetic loading, as shown in Table 6.17, which is higher than the nominal values for standard efficiency test. Table 6.17 shows that the linear PM synchronous machine draws rms current (1.2A) at rms terminal voltage (41.0V) and moves at rated velocity ($2.56ms^{-1}$), on average, during the synthetic loading test.

Table 6.17 Comparison of the experimental results of the standard efficiency test and the synthetic loading technique for the linear PM synchronous machine with half of full-load force condition

	Standard Efficiency Test	Synthetic Loading Frequency (Hz)				
		20	25	30	35	40
rms line voltage (V)	41.1	40.7	40.9	40.6	41.0	40.9
rms line current (A)	1.2	1.21	1.2	1.22	1.21	1.21
Minimum inverter peak current (A)	1.7	2.4	2.4	2.41	2.4	2.4
Speed (ms^{-1})	2.56	2.56	2.56	2.56	2.56	2.56
Input power (W)	89.8	18.9	18.7	19.2	19.0	19.2
Output power (W)	71.2	-	-	-	-	-
Total losses (W)	18.6	18.9	18.7	19.2	19.0	19.2
Efficiency (%)	79.3	79.0	79.2	78.6	78.8	78.6

6.5.4 Quarter full load force condition

In this case the standard efficiency test and synthetic loading technique are conducted experimentally for the linear PM synchronous machine with quarter of full-load force condition. The experimental results in Table 6.18 show that synthetic loading technique gives results consistent with the standard efficiency test. The evaluated efficiencies using synthetic loading technique in this case are between 82.1% and 82.7%, which is an underestimate of 0.6%, on average, compared with the standard efficiency test. The linear PM synchronous machine draws rms current (0.63A), at rms terminal voltage (37.5V) and moves at rated velocity ($2.56ms^{-1}$), on average, during synthetic loading.

Table 6.18 Comparison of the experimental results of the standard efficiency test and the synthetic loading technique for the linear PM synchronous machine with quarter of full-load force condition

	Standard Efficiency Test	Synthetic Loading Frequency (Hz)				
		20	25	30	35	40
rms line voltage (V)	37.5	37.1	37.4	37.5	37.2	37.5
rms line current (A)	0.63	0.62	0.63	0.63	0.62	0.64
Minimum inverter peak current (A)	0.9	1.3	1.28	1.28	1.28	1.3
Speed (ms^{-1})	2.56	2.56	2.56	2.56	2.56	2.56
Input power (W)	45.2	8.0	7.8	8.1	8.0	8.3
Output power (W)	37.5	-	-	-	-	-
Total losses (W)	7.7	8.0	7.8	8.1	8.0	8.3
Efficiency (%)	83.0	82.3	82.7	82.1	82.3	81.6

6.5.5 The linear PM synchronous machine summary

Table 6.19 presents a comparison of the linear PM synchronous machine efficiency figures obtained using the simulated and the experimental synthetic loading technique. It also reviews the simulated and experimental standard efficiency test results at the four different load force conditions. Generally, Table 6.19 shows that the synthetic loading simulation results overestimate the efficiency compared with the experimental results. However, the results show that synthetic loading as a method of efficiency evaluation for the linear PM synchronous machine gives results in reasonable agreement with the standard efficiency test if the experimental results are compared. Figure 6.15 illustrates the percentage error in the efficiency using synthetic loading for the four different load conditions.

Table 6.19 Comparison of the synthetic loading simulation and experimental results for the linear PM synchronous machine under different load force conditions

Synthetic Loading Frequency (Hz)	Load force conditions							
	Full		Three-quarters		Half		Quarter	
	Efficiency (%)		Efficiency (%)		Efficiency (%)		Efficiency (%)	
	Simulation	Experiment	Simulation	Experiment	Simulation	Experiment	Simulation	Experiment
20	71.4	70.4	76.3	74.2	80.8	79.0	84.3	82.3
25	71.4	70.2	76.3	74.1	80.8	79.2	84.3	82.7
30	71.4	70.5	76.3	74.5	80.8	78.6	84.3	82.1
35	71.4	70.4	76.3	74.3	80.8	78.8	84.3	82.3
40	71.4	70.1	76.3	74.2	80.8	78.6	84.3	81.6
Standard efficiency test	71.6	70.6	76.2	74.8	80.9	79.3	84.0	83.0

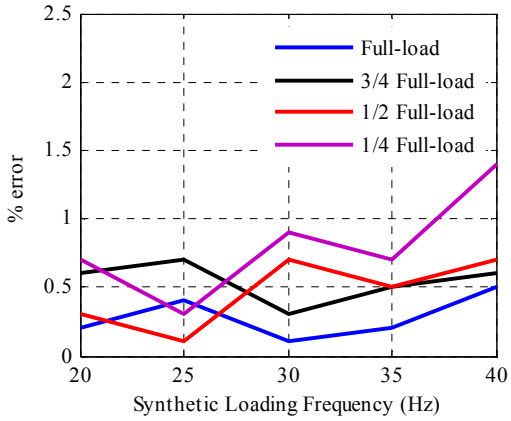

Figure 6.15 The percentage error in the measured efficiency of the linear PM synchronous machine using synthetic loading

6.6 Summary

In this chapter the experimental results for the standard efficiency test and the synthetic loading technique are presented for the PM, IPM and linear PM synchronous machine. The standard efficiency test and the synthetic loading technique are carried out for four different load torque (or force) conditions namely, full load torque, three-quarters of full load torque, half of full load torque and quarter of full load torque. The synthetic loading technique is conducted at five different synthetic loading frequencies for each case. The frequencies were chosen around the optimum frequencies identified

in chapter four. The efficiency calculated using the simulated standard efficiency test and synthetic loading technique are compared with the experimental standard efficiency test and synthetic loading technique for each machine and each load torque condition. This comparison show that the simulation results overestimate the machine efficiency in general compared with the experimental results. This is expected as the simulation model does not account for a number of additional second-order loss components including core and Ohmic losses associated with switching frequency harmonics, the effects of temperature on the individual loss components and inaccuracy of parameters in the model.

The experimental results of synthetic loading technique for efficiency evaluation of the PM, IPM and linear PM synchronous machine are in reasonable agreement with the standard efficiency test for the different load torque conditions considered. The experimental results establish that the synthetic loading technique maintains the rms current, rms voltage and rotor speed at rated values, on average, over one synthetic loading cycle. However, synthetic loading experimental results show that a higher inverter phase-leg VA rating is required as a result of a higher peak current and dc link voltage requirement during synthetic loading.

Generally, the efficiency figures for the PM, IPM and linear PM synchronous machine presented in this chapter using the synthetic loading technique are underestimated compared with the standard efficiency test. This is due to the measured losses using synthetic loading being slightly higher than the measured losses using the standard efficiency test. The higher losses are a consequence of higher core, and friction and windage losses which are a function of voltage and speed respectively. The speed and the voltage vary more with time compared to the simulation results. This leads to higher average core and friction and windage losses over one synthetic loading cycle. Decreasing the output torque increases the difference in measured efficiency between the standard efficiency test and the synthetic loading technique.

References

[1] C. Grantham, D.J. Mckinnon, "A Rapid Method for Load Testing and Efficiency Measurement of Three-Phase Induction Motors", International Conference on Electrical Machines and Systems, 2008. ICEMS 17-20 Oct. 2008, pp. 160-165.

[2] D. J. McKinnon and C. Grantham, "Improved efficiency Test Methods for Three-Phase Induction Machines", Industry Application Conference, 2005. Fourtieth IAS Annual Meeting. Conference Record of the 2005, Vol. 1, 2-6 October 2005, pp. 466-473.

[3] D. J. McKinnon and C. Grantham, "Efficiency Evaluation of Three-Phase Induction Motors Using Dual-Frequency and Sweep-Frequency Methods of Synthetic Loading", Second International Conference on Power Electronics, Machines and Drives, 2004. (PEMD 2004). Vol. 2, 31 March-2 April 2004, pp. 799-804.

[4] D. J. McKinnon and C. Grantham, "On-Site Efficiency Evaluation of Three-Phase Induction Motors Using Synthetic Loading Methods", Second International Conference on Power Electronics, Machines and Drives, 2004. (PEMD 2004). Vol. 1, 31 March-2 April 2004, pp. 291-296.

[5] C. Grantham, H. Tabatabaei-Yazdi and M. F. Rahman, "A Novel Method for Rapid Efficiency Measurement of Three Phase Induction Motors", IEEE Transactions on Energy Conversion, Vol. 14, No. 4, December 1999, pp. 1236-1240.

[6] C. Grantham, D.J. McKinnon, "Experimental Confirmation of On-Site Efficiency Evaluation of Three-Phase Induction Motors Using Synthetic Loading Techniques", Australian Universities Power Engineering Conference (AUPEC 2004). 26-29 Sept. 2004, Brisbane, Australia, pp. 160-165.

[7] C. Grantham, H. Tabatabaei-Yazdi and M. F. Rahman, "Efficiency Evaluation of Three Phase Induction Motors by Synthetic Loading", International Conference on Power Electronics and Drive Systems, 1997. Proceedings 1997, Vol. 1, 26-29 May, pp. 103-109

[8] C. Grantham, M. Sheng and E. D. Spooner, "Synthetic loading of three-phase induction motors using microprocessor controlled power electronics", Electric Power Applications, IEE Proceedings, Vol. 141, No. 2, March 1994, pp. 101-108.

Chapter Seven
Conclusions and Recommendations

7.1 General conclusions

The thesis investigates the efficiency evaluation of PM, IPM and linear PM synchronous machines using the synthetic loading technique. The literature review shows that synthetic loading has been successfully applied to the induction machine to evaluate efficiency and temperature rise. However, no research has considered synthetic loading technique applied to the PM, IPM and linear PM synchronous machine. This is one significant driver for this research. Therefore, the objective of this thesis is to investigate the appropriateness of the synthetic loading technique as a method of efficiency evaluation for PM synchronous machines and compare with standard efficiency tests.

The mathematical models of the PM synchronous machine have been developed in the synchronously rotating *d-q* axis reference frame. The d-axis and q-axis equivalent circuits are presented. From these equivalent circuits the voltage equations and the mechanical equations are established. The synthetic loading equations for the PM synchronous machines are then developed using these voltage and mechanical equations. The synthetic loading technique described in the thesis is a current control technique, therefore, the quadrature axis current equation, i_q, is postulated and the direct axis current, i_d, is forced to be zero. The quadrature axis current, i_q, consists of AC and DC components. The magnitude of the AC component is I_m and the DC component is I_o. The magnitude of the AC perturbation current, I_m, and the dc offset current, I_o, equations are derived using the machine rating and the mechanical parameters. The rotor speed, ω_r, and the mover velocity, v_x, have been established using the mechanical equations, which confirm that the PM synchronous machine accelerates and decelerates during synthetic loading. The direct and quadrature axis stator voltage and current have been established

in the synchronously rotating reference frame for PM synchronous machine, and in the synchronously translating reference frame for the linear PM synchronous machine. The direct and quadrature axis stator voltage and current equations have been used to develop the input power and the inverter volt-ampere rating equations [1],[2]. The mathematical equations of synthetic loading have been generalised using machine current rating, speed and permanent magnet flux as the basis.

The synthetic loading equations developed in this thesis have been used to simulate and evaluate the synthetic loading technique as a method of efficiency evaluation of the PM, IPM and linear PM synchronous machine. The simulations of the standard efficiency test and the synthetic loading technique have been performed for four different load torque conditions and five different synthetic loading frequencies using MATLAB and SIMULINK. The simulation results of synthetic loading of the PM, IPM and linear PM synchronous machine give results in good agreement with the standard efficiency test for the different load torque conditions considered. The simulation results demonstrate that synthetic loading maintains the rms current, rms voltage and the rotor speed at rated values, on average, over one synthetic loading cycle. These results show good correlation between the synthetic loading technique and the standard efficiency test. The rms current and voltage are maintained to be at rated value for the machine undergoing synthetic loading by adjusting the AC perturbation current, I_m, and the dc offset current, I_o.

The effects of synthetic loading frequency on the required dc link voltage and inverter phase-leg VA rating have been assessed. The synthetic loading simulation results show that higher dc link voltages and inverter phase-leg VAs are required during synthetic loading compared with that required for the standard efficiency test. The synthetic loading technique reported here is a vector control method that applies the quadrature axis current and forces the direct axis current to be zero. The effects of direct axis current on the inverter phase-leg VA rating required, the dc link voltage required, maximum power absorbed and generated by the machine undergoing synthetic loading test, and the iron loss have been investigated. The effect of direct axis current on the

synthetic loading performance demonstrates that increasing the direct axis current results in lower inverter phase-leg VA rating requirement and lower maximum power absorbed and generated, but leads to higher dc link voltage requirement hence higher iron loss. This leads to an underestimate of the efficiency during synthetic loading. The standard efficiency test simulation results and the synthetic loading technique simulation results compare well.

The synthetic loading technique has been performed experimentally on the PM, IPM and linear PM synchronous machine. The hardware and software used to perform synthetic loading technique and standard efficiency test have been described and implemented. The TMS320F2812 DSP controller is used to generate the PWM signals in order to track the required current reference. The relevant features of the TMS320F2812 DSP controller, the event manager and the analog-to-digital converter have been introduced. The rotor position, the current transducer and the PWM interface circuits are described, and the circuit diagrams presented. The three-phase prototype power inverter and the gate drives are described. The software flow chart for the TMS320F2812DSP controller programmed using the Spectrum Digital eZdsp development environment with Code Composer Studio is given.

The synthetic loading and standard efficiency test for efficiency evaluation of the PM, IPM and linear PM synchronous machine have been carried out experimentally, for four different load torque (force) conditions. Five different synthetic loading frequencies have been used to conduct the synthetic loading technique. The experimental results confirm that synthetic loading maintains the rms current, rms voltage and the rotor speed at rated values, on average, over one synthetic loading cycle. Also, experimental results confirm the higher inverter phase-leg VA ratings and dc link voltages required. The synthetic loading experimental results have been compared with those from the standard efficiency test. The comparison shows that the synthetic loading results are in good agreement with the standard efficiency test. Generally, the experimental results for efficiency evaluation of the PM, IPM and linear PM synchronous machine using synthetic loading technique are underestimated compared with the standard efficiency

test. The synthetic loading simulation results have been compared with synthetic loading experimental results. The efficiency obtained by simulation is overestimated compared with that measured experimentally. This because the simulation does not take into account current harmonics at the switching frequency and non-linearities such as temperature variation, magnetic saturation and skin effect. Also, the mechanical parameters, J and B, used to perform the simulations are the manufacturer's values. Therefore, the total loss during the simulation is lower than that during the experiment. This results in an over-estimate of efficiency.

Standard efficiency tests require specialist test facilities, additional load machines for large machines, vertical mounted machines and floor space. Therefore, synthetic loading is potentially a key technique for solving the problems associated with the standard efficiency test methods. Synthetic loading offers the advantage that the machine tested is mechanically decoupled from the load, thereby removing the need for special test facilities [2]. Also, the machine can be tested on site, therefore, the cost and time associated with performing an efficiency test is significantly reduced as the test equipment is portable

7.2 Recommendations for future research

Synthetic loading as a method of efficiency evaluation is demonstrated using PM, IPM and linear PM synchronous machine. Also, the literature shows that synthetic loading has been successfully applied to induction machines and synchronous machine for efficiency evaluation and temperature rise. Therefore, the application of synthetic loading technique to other types of machine is an important area such as PM brushless dc machines, switched reluctance machines, synchronous reluctance machines and multi-phase machines.

The software for experimental validation of synthetic loading could be improved. It should be extended to measure and calculate the value of the rms current, rms voltage, speed and input power within the DSP for the PM synchronous machines undergoing

synthetic loading. This would relieve the need for dedicated power analysers and measurement capture by oscilloscopes.

In the literature there are three synthetic loading techniques that have been applied to the induction machine, namely the dual-frequency, the sweep-frequency and the constant speed of rotating magnetic field method. In this thesis the constant speed of rotating magnetic field technique is applied to the PM, IPM and linear PM synchronous machine. Therefore, the possibility of applying the dual-frequency and the sweep-frequency technique for efficiency evaluation of these machines should be studied along with research into possible open-loop schemes that relieve the need for closed loop position feedback systems.

The synthetic loading technique has been applied to lower power level PM synchronous machines in this work. The application of synthetic loading technique to higher power level PM synchronous machines should be considered and studied. In larger machines, the ratio of losses to output power is lower. Hence, the synthetic loading technique may provide a more accurate method of determining full-load losses in the machine.

References

[1] A. Y. M. Abbas and J. E. Fletcher, "Efficiency Evaluation of Linear Permanent Magnet Synchronous Machines Using the Synthetic Loading Method" 39th IEEE Annual Power Electronics Specialists Conference, Rhodes, Greece, 15-19 June 2008, pp.3074-3080.

[2] A. Y. M. Abbas and J. E. Fletcher, "Synthetic Loading Technique for Efficiency Evaluation of Permanent Magnet Synchronous Machines" 44th IEEE Annual Universities Power Engineering Conference, Glasgow, UK, 1-4 September 2009.

Appendix A
Synthetic Loading Equations

In this Appendix a complete synthetic loading mathematical model for PM, IPM and linear PM synchronous machine are developed. The synthetic loading equations for PM, IPM and linear PM synchronous machine are normalised and generalised.

A1 Synthetic Loading Mathematical Models for PM and IPM synchronous machines

Five nonlinear differential equations are derived for the d- and q-axis equivalent circuit illustrated in Figure A.1.

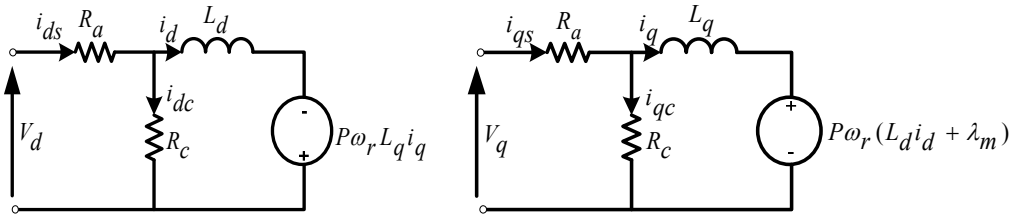

(a) d-axis (b) q-axis

Figure A.1 d- and q-axis equivalent circuit of PM synchronous machines

The voltage equations of the PM synchronous machine in the *dq* synchronous frame can be expressed as

$$V_d = R_a i_d + L_d\left(1+\frac{R_a}{R_c}\right)\frac{di_d}{dt} - P\omega_r L_q i_q\left(1+\frac{R_a}{R_c}\right) \tag{A.1}$$

$$V_q = R_a i_q + L_q\left(1+\frac{R_a}{R_c}\right)\frac{di_q}{dt} + \left(1+\frac{R_a}{R_c}\right)P\omega_r\left(L_d i_d + \lambda_m\right) \tag{A.2}$$

where, V_d and V_q are d- and q-axis stator voltages, respectively,
i_d and i_q are d- and q-axis torque generating currents, respectively,
R_a and R_c are stator and core loss resistances, respectively,
L_d and L_q are d- and q-axis self inductances, respectively,
λ_m is the permanent magnet flux linkages,

ω_r is the rotor speed and P is number of pole pairs,

The electromagnetic torque developed by the rotor is described by

$$T_e = \frac{3}{2} P\left(\lambda_m\, i_q + \left(L_d - L_q\right) i_q\, i_d\right) \tag{A.3}$$

where T_e is electromagnetic torque of the motor. The dynamic equation of the speed is

$$\frac{d\omega_r}{dt} = (\, T_e - T_L - B\omega_r\,)/J \tag{A.4}$$

where T_L is the load torque. J and B are moment of inertia and damper coefficient respectively. The position is given by

$$\frac{d\theta}{dt} = P\omega_r \tag{A.5}$$

where θ is the rotor position

A1.1 Quadrature axis current equation

$$i_q(t) = I_m \sin(2\pi \mathrm{f_n t}) + I_o \tag{A.6}$$

where I_m is the magnitude of AC perturbation current, I_o is a dc offset current and f_n is synthetic loading frequency (Hz)

(i) Expressing I_o in terms of machine parameters

$$T_e\,(\mathrm{t}) = k_t i_q(t) + k_I I_d i_q(t) = k_t I_m \sin(2\pi f_n t) + k_t I_o + k_I I_d I_m \sin(2\pi f_n t) + k_I I_d I_o$$

$$T_e(t) = (k_t + k_I I_d) I_m \sin(2\pi f_n t) + (k_t + k_I I_d) I_o = (k_t + k_I I_d)[I_m \sin(2\pi f_n t) + I_o]$$

where $k_t = \frac{3}{2}\mathrm{P}\,\lambda_m$ k_t is torque constant, $k_I = \frac{3}{2} P\left(L_d - L_q\right)$, P is number of pair of pole and λ_m is linkage flux.

$$T_{eav} = f_n \int_0^{\frac{1}{f_n}} (k_t + k_I\, I_d)[I_m \sin(2\pi f_n t) + I_o]\, dt = f_n (k_t + k_I\, I_d)\left[- I_m \frac{\cos(2\pi f_n t)}{2\pi f_n} + I_o t \right]_0^{\frac{1}{f_n}}$$

$$T_{eav} = (k_t + k_I\, I_d)\, I_o \tag{A.7}$$

With synthetic loading $T_L = 0$, therefore

$$T_{eav} = B\,\omega_{\mathrm{r}} = (k_t + k_I\, I_d) I_o \tag{A.8}$$

where B is damper coefficient and ω_r is rotor speed in rad/sec. From equation (A.8)

$$I_o = \frac{B\,\omega_r}{(k_t + k_I\, I_d)} \tag{A.9}$$

(ii) Expressing I_m in terms of machine parameters

$$I_s^2 = \left[\frac{f_n}{2}\int_0^{\frac{2}{f_n}} (I_m \sin(2\pi f_n t) + I_o)^2\, dt\right] + \left[\frac{f_n}{2}\int_{\frac{2}{f_n}}^{\frac{1}{f_n}} (I_m \sin(2\pi f_n t) + I_o)^2\, dt\right] + f_n \int_0^{\frac{1}{f_n}} I_d^2 dt \tag{A.10}$$

$$\begin{aligned} I_s^2 = &\left[\frac{f_n}{2}\int_0^{\frac{2}{f_n}} \left(I_m^2 \sin^2(2\pi f_n t) + 2 I_o I_m \sin(2\pi f_n t) + I_o^2\right) dt\right] \\ &+ \left[\frac{f_n}{2}\int_{\frac{2}{f_n}}^{\frac{1}{f_n}} \left(I_m^2 \sin^2(2\pi f_n t) + 2 I_o I_m \sin(2\pi f_n t) + I_o^2\right) dt\right] + f_n \int_0^{\frac{1}{f_n}} I_d^2 dt \end{aligned} \tag{A.11}$$

$$\begin{aligned} I_s^2 = &\frac{f_n}{2}\left[\int_0^{\frac{2}{f_n}} \left(\frac{I_m^2}{2}(1 - \cos(4\pi f_n t)) + 2 I_o I_m \sin(2\pi f_n t) + I_o^2\right) dt\right] \\ &+ \frac{f_n}{2}\left[\int_{\frac{2}{f_n}}^{\frac{1}{f_n}} \left(\frac{I_m^2}{2}(1 - \cos(4\pi f_n t)) + 2 I_o I_m \sin(2\pi f_n t) + I_o^2\right) dt\right] + f_n \int_0^{\frac{1}{f_n}} I_d^2 dt \end{aligned} \tag{A.12}$$

$$\begin{aligned} I_s^2 = &\frac{f_n}{2}\left[\frac{I_m^2}{2}\left(t - \frac{\sin(4\pi f_n t)}{4\pi f_n}\right) - \frac{I_o I_m}{\pi f_n}\cos(2\pi f_n t) + I_o^2 t\right]_0^{\frac{2}{f_n}} \\ &+ \frac{f_n}{2}\left[\frac{I_m^2}{2}\left(t - \frac{\sin(4\pi f_n t)}{4\pi f_n}\right) - \frac{I_o I_m}{\pi f_n}\cos(2\pi f_n t) + I_o^2 t\right]_{\frac{2}{f_n}}^{\frac{1}{f_n}} + f_n\left[I_d^2 t\right]_0^{\frac{1}{f_n}} \end{aligned} \tag{A.13}$$

Substitute the integration boundaries into (A.13) yields

$$I_s^2 = \frac{1}{2}\left[I_m^2 + 2I_o^2 - \frac{I_m^2}{2} - I_o^2 \right] + I_d^2 = \frac{1}{2}\left[\frac{I_m^2}{2} + I_o^2 \right] + I_d^2 \qquad \text{(A.14)}$$

Rearranging (A.14) yields $I_m^2 = 4I_s^2 - 2I_o^2 - 4I_d^2$

$$I_m = \sqrt{4I_s^2 - 2I_o^2 - 4I_d^2} \qquad \text{(A.15)}$$

where I_s is rated rms current of the motor

A1.2 Speed equation

From the mechanical equation $J\frac{d\omega_r}{dt} = T_e - T_L - B\omega_{\mathrm{r}}$, with synthetic loading $T_L = 0$

and

$T_e(t) = k_t\, i_q(t) + k_I I_d i_q(\mathrm{t})$, $i_q(t) = I_m \sin(2\pi \mathrm{f_n} t) + I_o$ Therefore,

$$J\frac{d\omega_r(t)}{dt} = T_e(t) - B\,\omega_{\mathrm{r}}(t) = (\mathrm{k_t} + k_I I_d) I_m \sin(2\pi \mathrm{f_n} t) + (k_t + k_I I_d) I_o - B\,\omega_{\mathrm{r}}(t)$$

$$J\frac{d\omega_r(t)}{dt} + B\,\omega_{\mathrm{r}}(t) = (k_t + k_I I_d) I_m \sin(2\pi \mathrm{f_n} t) + (k_t + k_I I_d) I_o \qquad \text{(A.16)}$$

Apply Laplace Transformation to (A.16)

$$J\,s\,\omega_{\mathrm{r}}(\mathrm{s}) + B\,\omega_{\mathrm{r}}(s) = \frac{(k_t + k_I I_d) I_m (2\pi f_n)}{s^2 + (2\pi f_n)^2} + \frac{(k_t + k_I I_d) I_o}{s} \qquad \text{(A.17)}$$

$$\omega_r(s) = \frac{(k_t + k_I I_d) I_m (2\pi f_n)/J}{\left(s + \frac{B}{J}\right)\left(s^2 + (2\pi f_n)^2\right)} + \frac{(k_t + k_I I_d) I_o/J}{s\left(s + \frac{B}{J}\right)} \qquad \text{(A.18)}$$

The first Part of the R.H.S of (A.18)

$$\frac{(k_t + k_I I_d) I_m (2\pi f_n)/J}{\left(s + \frac{B}{J}\right)\left(s^2 + (2\pi f_n)^2\right)} = \frac{A}{s + \frac{B}{J}} + \frac{Cs + D}{s^2 + (2\pi f_n)^2} \qquad \text{(A.19)}$$

From (A.19) expression for *A, C, D* will be found as follows

$$\frac{(k_t + k_I I_d) I_m (2\pi f_n)}{J} = A s^2 + A(2\pi f_n)^2 + (C s + D)\left(s + \frac{B}{J}\right)$$

$$= (A + C) s^2 + \left(C\frac{B}{J} + D\right) s + \left(A(2\pi f_n)^2 + D\frac{B}{J}\right)$$

From above equation equating coefficients of (s) in R.H.S with coefficients of (s) in L.H.S

$A + C = 0$ therefor e $A = -C$, $C\frac{B}{J} + D = 0$ therefore $C = -\frac{J}{B}D$

and $A(2\pi f_n)^2 + D\frac{B}{J} = \frac{(k_t + k_I I_d) I_m (2\pi f_n)}{J}$

$$-C(2\pi f_n)^2 - C\left(\frac{B}{J}\right)^2 = \frac{(k_t + k_I I_d) I_m (2\pi f_n)}{J}, \quad C = -\frac{(k_t + k_I I_d) I_m (2\pi f_n)/J}{(2\pi f_n)^2 + \left(\frac{B}{J}\right)^2},$$

$$A = \frac{(k_t + k_I I_d) I_m (2\pi f_n)/J}{(2\pi f_n)^2 + \left(\frac{B}{J}\right)^2}, \quad D = -\frac{B}{J}C = \frac{(k_t + k_I I_d) I_m (2\pi f_n) B/J^2}{(2\pi f_n)^2 + \left(\frac{B}{J}\right)^2}$$

Therefore,

$$\omega_{r1}(s) = \frac{(k_t + k_I I_d) I_m (2\pi f_n)/J}{(2\pi f_n)^2 + \left(\frac{B}{J}\right)^2}\left[\frac{1}{s + \frac{B}{J}}\right] - \frac{(k_t + k_I I_d) I_m (2\pi f_n)/J}{(2\pi f_n)^2 + \left(\frac{B}{J}\right)^2}$$
$$\times\left[\frac{s}{s^2 + (2\pi f_n)^2}\right] + \frac{(k_t + k_I I_d) I_m B/J^2}{(2\pi f_n)^2 + \left(\frac{B}{J}\right)^2}\left[\frac{(2\pi f_n)}{s^2 + (2\pi f_n)^2}\right] \quad \text{(A.20)}$$

Apply Laplace Inverse Transformation to (A.20)

$$\omega_{r1}(t)=\frac{(k_t+k_I I_d)I_m(2\pi f_n)/J}{(2\pi f_n)^2+\left(\frac{B}{J}\right)^2}e^{-\frac{B}{J}t}-\frac{(k_t+k_I I_d)I_m(2\pi f_n)/J}{(2\pi f_n)^2+\left(\frac{B}{J}\right)^2}\cos(2\pi f_n t)$$
$$+\frac{(k_t+k_I I_d)I_m B/J^2}{(2\pi f_n)^2+\left(\frac{B}{J}\right)^2}\sin(2\pi f_n t) \quad \text{(A.21)}$$

The second part of R.H.S of (A.18)

$$\frac{(k_t+k_I I_d)I_o/J}{s\left(s+\frac{B}{J}\right)}=\frac{A}{s}+\frac{C}{s+\frac{B}{J}} \quad \text{(A.22)}$$

From (A.22) expression for *A, C* will be found as follows

$$\frac{(k_t+k_I I_d)I_o}{J}=A\left(s+\frac{B}{J}\right)+C\,s=(A+C)s+A\frac{B}{J}$$

From above equation equating coefficients of (s) in R.H.S with coefficient of (*s*) in L.H.S

$$A+C=0,\quad A=-C,\quad A\frac{B}{J}=\frac{(k_t+k_I I_d)I_o}{J}\quad;\quad A=\frac{(k_t+k_I I_d)I_o}{B},\quad C=-\frac{(k_t+k_I I_d)I_o}{B}$$

Therefore:

$$\omega_{r2}(s)=\frac{(k_t+k_I I_d)I_o}{B}\left[\frac{1}{s}-\frac{1}{s+\frac{B}{J}}\right] \quad \text{(A.23)}$$

Apply Laplace Inverse Transformation to (A.23)

$$\omega_{r2}(t)=\frac{(k_t+k_I I_d)I_o}{B}\left(1-e^{-\frac{B}{J}t}\right) \quad \text{(A.24)}$$

From (A.21) and (A.24) $\omega_r(t)=\omega_{r1}(t)+\omega_{r2}(t)$

$$\omega_r(t) = \frac{(k_t + k_I I_d) I_m (2\pi f_n)/J}{(2\pi f_n)^2 + \left(\frac{B}{J}\right)^2} e^{-\frac{B}{J_n}t} - \frac{(k_t + k_I I_d) I_m (2\pi f_n)/J}{(2\pi f_n)^2 + \left(\frac{B}{J}\right)^2} \cos(2\pi f_n t)$$

$$+ \frac{(k_t + k_I I_d) I_m \, B/J^2}{(2\pi f_n)^2 + \left(\frac{B}{J}\right)^2} \sin(2\pi f_n t) + \frac{(k_t + k_I I_d) I_o}{B} \left(1 - e^{-\frac{B}{J}t}\right)$$

Rearrange the above equation

$$\omega_r(t) = \frac{(k_t + k_I I_d) I_o}{B} + \left[\frac{(k_t + k_I I_d) I_m (2\pi f_n)/J}{(2\pi f_n)^2 + \left(\frac{B}{J}\right)^2} - \frac{(k_t + k_I I_d) I_o}{B} \right] e^{-\frac{B}{J}t} \tag{A.25}$$

$$- \frac{(k_t + k_I I_d) I_m (2\pi f_n)/J}{(2\pi f_n)^2 + \left(\frac{B}{J}\right)^2} \cos(2\pi f_n t) + \frac{(k_t + k_I I_d) I_m \, B/J^2}{(2\pi f_n)^2 + \left(\frac{B}{J}\right)^2} \sin(2\pi f_n t)$$

At steady state the exponential component becomes zero

$$(k_t + k_I I_d) \left[\frac{I_m (2\pi f_n)/J}{(2\pi f_n)^2 + \left(\frac{B}{J}\right)^2} - \frac{I_o}{B} \right] e^{-\frac{B}{J}t} = 0$$

$$\omega_r(t) = \frac{(k_t + k_I I_d) I_o}{B} - \frac{(k_t + k_I I_d) I_m (2\pi f_n)/J}{(2\pi f_n)^2 + \left(\frac{B}{J}\right)^2} \cos(2\pi f_n t)$$

$$+ \frac{(k_t + k_I I_d) I_m \, B/J^2}{(2\pi f_n)^2 + \left(\frac{B}{J}\right)^2} \sin(2\pi f_n t) \tag{A.26}$$

$$\omega_r = \frac{(k_t + k_r i_d) I_o}{B} + \frac{(k_t + k_r i_d) I_m / J}{\sqrt{(2\pi f_n)^2 + \left(\frac{B}{J}\right)^2}} \sin(2\pi f_n t - \phi) \tag{A.27}$$

where $\phi = \tan^{-1}\left[\frac{2\pi f_n}{B/J}\right]$

The maximum speed is at the condition of $\cos(2\pi f_n t) = -1$ and $\sin(2\pi f_n t) = 0$

$$\omega_r(\max) = \frac{(k_t + k_r i_d) I_o}{B} + \frac{(k_t + k_r i_d) I_m / J}{\sqrt{(2\pi f_n)^2 + \left(\frac{B}{J}\right)^2}} \tag{A.28}$$

The minimum speed is at the condition of $\cos(2\pi f_n t) = 1$ and $\sin(2\pi f_n t) = 0$

$$\omega_r(\min) = \frac{(k_t + k_r i_d) I_o}{B} - \frac{(k_t + k_r i_d) I_m / J}{\sqrt{(2\pi f_n)^2 + \left(\frac{B}{J}\right)^2}} \tag{A.29}$$

Determining f_n in terms of machine parameters

The peak to peak speed variation $\Delta\omega_r$ can be determined.

$$\Delta\omega_r = \omega_r(\max) - \omega_r(\min) \tag{A.30}$$

$$\Delta\omega_r = 2\frac{(k_t + k_r i_d) I_m / J}{\sqrt{(2\pi f_n)^2 + \left(\frac{B}{J}\right)^2}} \tag{A.31}$$

Therefore:

$$f_n = \frac{\sqrt{\left(\frac{2(k_t + k_r i_d) I_m}{J}\right)^2 - \left(\Delta\omega_r \frac{B}{J}\right)^2}}{2\pi\Delta\omega_r} \tag{A.32}$$

A1.3 Direct and quadrature axis voltage equation

From d-axis equivalent circuit

$$V_d = R_a\, i_{ds} + L_d \frac{di_d}{dt} - P\, \omega_r L_q i_q \tag{A.33}$$

$$i_{ds} = i_d + i_{dc}\,; i_{dc} = \left(L_d \frac{di_d}{dt} - P\, \omega_r L_q i_q\right) \Big/ R_c = \frac{L_d}{R_c}\frac{di_d}{dt} - \frac{P\, \omega_r L_q}{R_c} i_q$$

$$i_{ds} = i_d + \frac{L_d}{R_c}\frac{di_d}{dt} - \frac{P\, \omega_r L_q}{R_c} i_q \tag{A.34}$$

Substitute (A.34) into (A.33)

$$V_d = R_a \left(i_d + \frac{L_d}{R_c}\frac{di_d}{dt} - \frac{P\, \omega_r L_q}{R_c} i_q \right) + L_d \frac{di_d}{dt} - P\, \omega_r L_q i_q$$

$$V_d = R_a\, i_d + \left(1+\frac{R_a}{R_c}\right) L_d \frac{di_d}{dt} - \left(1+\frac{R_a}{R_c}\right) P\, \omega_r L_q i_q \tag{A.35}$$

$$\left(1+\frac{R_a}{R_c}\right) L_d \frac{di_d}{dt} = V_d - R_a\, i_d + \left(1+\frac{R_a}{R_c}\right) P\, \omega_r L_q i_q \tag{A.36}$$

$$i_q(t) = I_m \sin(2\pi f_n t) + I_o \quad ; \quad \frac{di_d(t)}{dt} = 0$$

$$V_d(t) = R_a\, i_d - P\, \omega_r\, L_q \left(1+\frac{R_a}{R_c}\right)\left(I_m \sin(2\pi f_n t) + I_o\right)$$

where, P is number of Pole-pairs and R_c is core loss resistance

$$V_d(t) = R_a\, i_d - P\, \omega_r\, L_q \left(1+\frac{R_a}{R_c}\right) I_m \sin(2\pi f_n t) - P\, \omega_r\, L_q \left(1+\frac{R_a}{R_c}\right) I_o \tag{A.37}$$

Substitute (A.26) for ω_r into (A.37)

$$V_d(t) = R_a i_d - \left(P\, L_q \left(1+\frac{R_a}{R_c}\right) I_m \sin(2\pi f_n t) + P\, L_q \left(1+\frac{R_a}{R_c}\right) I_o\right)$$

$$\times \left[\frac{(k_t + k_I I_d) I_o}{B} - \frac{(k_t + k_I I_d) I_m (2\pi f_n)/J}{(2\pi f_n)^2 + \left(\frac{B}{J}\right)^2} \cos(2\pi f_n t) + \frac{(k_t + k_I I_d) I_m (2\pi f_n)/J^2}{(2\pi f_n)^2 + \left(\frac{B}{J}\right)^2} \sin(2\pi f_n t)\right] \tag{A38}$$

From q-axis equivalent circuit

$$V_q = R_a\, i_{qs} + L_q \frac{di_d}{dt} + P\, \omega_r \left(L_d i_d + \lambda_m\right) \tag{A.39}$$

$$i_{qs} = i_q + i_{qc} \; ; i_{qc} = \left(L_q \frac{di_q}{dt} + P\, \omega_r \left(L_d i_d + \lambda_m\right)\right) \Big/ R_c = \frac{L_q}{R_c}\frac{di_q}{dt} + \frac{P\, \omega_r \left(L_d i_d + \lambda_m\right)}{R_c}$$

$$i_{qs} = i_q + \frac{L_q}{R_c}\frac{di_q}{dt} + \frac{P\, \omega_r \left(L_d i_d + \lambda_m\right)}{R_c} \tag{A.40}$$

Substitute (A.40) into (A.39)

$$V_q = R_a \left(i_q + \frac{L_q}{R_c}\frac{di_q}{dt} + \frac{P\omega_r \left(L_d i_d + \lambda_m\right)}{R_c}\right) + L_q \frac{di_d}{dt} + P\, \omega_r \left(L_d i_d + \lambda_m\right)$$

$$V_q = R_a i_q + \left(1+\frac{R_a}{R_c}\right)\frac{di_q}{dt} + \left(1+\frac{R_a}{R_c}\right)P\omega_r\left(L_d i_d + \lambda_m\right) \tag{A.41}$$

$$L_q\left(1+\frac{R_a}{R_c}\right)\frac{di_q}{dt} = \left[V_q - R_a i_q - P\omega_r L_d i_d\left(1+\frac{R_a}{R_c}\right) - P\omega_r\lambda_m\left(1+\frac{R_a}{R_c}\right)\right] \tag{A.42}$$

$$i_q(t) = I_m \sin\left(2\pi f_n t\right) + I_o \quad ; \quad \frac{di_q(t)}{dt} = I_m\left(2\pi f_n\right)\cos\left(2\pi f_n t\right)$$

$$V_q(t) = \left(1+\frac{R_a}{R_c}\right)L_q\frac{di_q(t)}{dt} + R_a\, i_q(t) + P\,\omega_r\, L_d\left(1+\frac{R_a}{R_c}\right)i_d + P\,\omega_r\,\lambda_m\left(1+\frac{R_a}{R_c}\right)$$

$$\begin{aligned} V_q(t) = {} & I_m\left(2\pi f_n\right)L_q\left(1+\frac{R_a}{R_c}\right)\cos\left(2\pi f_n t\right) + R_a I_m \sin\left(2\pi f_n t\right) + R_a\, I_o \\ & + P\,\omega_r\, L_d\left(1+\frac{R_a}{R_c}\right)i_d + P\,\omega_r\,\lambda_m\left(1+\frac{R_a}{R_c}\right) \end{aligned} \tag{A.43}$$

Substitute (A.26) for ω_r into (A.43)

$$\begin{aligned} V_q(t) = {} & I_m\left(2\pi f_n\right)L_q\left(1+\frac{R_a}{R_c}\right)\cos\left(2\pi f_n t\right) + R_a I_m \sin\left(2\pi f_n t\right) + R_a\, I_o \\ & + \frac{P\left(k_t + k_I I_d\right)\left(\lambda_m + L_d I_d\right)I_o}{B}\left(1+\frac{R_a}{R_c}\right) \\ & - \frac{P\left(\lambda_m + L_d I_d\right)\left(k_t + k_I I_d\right)I_m\left(2\pi f_n\right)/J}{\left(2\pi f_n\right)^2 + \left(\frac{B}{J}\right)^2}\left(1+\frac{R_a}{R_c}\right)\cos\left(2\pi f_n t\right) \\ & + \frac{P\left(\lambda_m + L_d I_d\right)\left(k_t + k_I I_d\right)I_m B/J^2}{\left(2\pi f_n\right)^2 + \left(\frac{B}{J}\right)^2}\left(1+\frac{R_a}{R_c}\right)\sin\left(2\pi f_n t\right) \end{aligned} \tag{A.44}$$

Using Park inverse transformation to calculate the instantaneous phase voltage

$$\begin{bmatrix} V_a(t) \\ V_b(t) \\ V_c(t) \end{bmatrix} = \begin{bmatrix} \cos\theta & \sin\theta \\ \cos\left(\theta - \frac{2\pi}{3}\right) & \sin\left(\theta - \frac{2\pi}{3}\right) \\ \cos\left(\theta + \frac{2\pi}{3}\right) & \sin\left(\theta + \frac{2\pi}{3}\right) \end{bmatrix} \begin{bmatrix} \mathrm{V_d}(t) \\ \\ V_q(t) \end{bmatrix} \tag{A.45}$$

A1.4 Stator direct and quadrature axis current equation

From d-axis equivalent circuit

$$i_{ds}(\mathrm{t}) = i_d + i_{dc}(\mathrm{t}) \;\; ; \;\; i_{dc}(t) = -P\frac{L_q}{R_c} i_q(t)\omega_{\mathrm{r}}(t)$$

$$i_{ds}(\mathrm{t}) = i_d - P\frac{L_q}{R_c} i_q(t)\omega_{\mathrm{r}}(t) \tag{A.46}$$

Substitute (A.6) and (A.26) for $i_q(t)$ and $\omega_r(t)$ into (A.46)

$$i_{ds}(t) = i_d - P\frac{L_q}{R_c}(I_m \sin(2\pi f_n t) + I_o)(k_t + k_I I_d)\left[\frac{I_o}{B} - \frac{I_m(2\pi f_n)/J}{(2\pi f_n)^2 + \left(\frac{B}{J}\right)^2}\cos(2\pi f_n t)\right.$$

$$\left. + \frac{I_m B/J^2}{(2\pi f_n)^2 + \left(\frac{B}{J}\right)^2}\sin(2\pi f_n t)\right]$$

From q-axis equivalent circuit

$$i_{qs}(\mathrm{t}) = i_q(\mathrm{t}) + i_{qc}(\mathrm{t}) \quad ; i_{qc}(t) = \frac{L_q}{R_c}\frac{di_q(t)}{dt} + P\frac{(L_d\, i_d + \lambda_{\mathrm{a}})}{R_c}\omega_{\mathrm{r}}(t)$$

$$i_{qs}(\mathrm{t}) = i_q(t) + \frac{L_q}{R_c}\frac{di_q(t)}{dt} + P\frac{(L_d\, i_d + \lambda_{\mathrm{a}})}{R_c}\omega_{\mathrm{r}}(t) \tag{A.47}$$

Substitute (A.6) and (A.26) for $i_q(t)$ and $\omega_r(t)$ into (A.47)

$$i_{qs}(t) = I_m \sin(2\pi f_n t) + I_o + \frac{L_q}{R_c} I_m (2\pi f_n) \cos(2\pi f_n t) + P \frac{(L_d\, i_d + \lambda_m)}{R_c} (k_t + k_I I_d)$$

$$\times \left[\frac{I_o}{B} - \frac{I_m (2\pi f_n)/J}{(2\pi f_n)^2 + \left(\frac{B}{J}\right)^2} \cos(2\pi f_n t) + \frac{I_m\, B/J^2}{(2\pi f_n)^2 + \left(\frac{B}{J}\right)^2} \sin(2\pi f_n t) \right]$$

$$i_{qs}(t) = \left[I_o + P \frac{(L_d\, i_d + \lambda_m)}{R_c} \frac{I_o}{B} (k_t + k_I I_d) \right] + I_m \sin(2\pi f_n t) + \frac{L_q}{R_c} I_m (2\pi f_n) \cos(2\pi f_n t)$$

$$+ (k_t + k_I I_d)(L_d\, i_d + \lambda_m) \left[P \frac{1}{R_c} \frac{I_m\, B/J^2}{(2\pi f_n)^2 + \left(\frac{B}{J}\right)^2} \sin(2\pi f_n t) - P \frac{1}{R_c} \frac{I_m (2\pi f_n)/J}{(2\pi f_n)^2 + \left(\frac{B}{J}\right)^2} \cos(2\pi f_n t) \right]$$

Using Park inverse transformation to calculate the instantaneous phase current

$$\begin{bmatrix} i_a(t) \\ i_b(t) \\ i_c(t) \end{bmatrix} = \begin{bmatrix} \cos\theta & \sin\theta \\ \cos\left(\theta - \frac{2\pi}{3}\right) & \sin\left(\theta - \frac{2\pi}{3}\right) \\ \cos\left(\theta + \frac{2\pi}{3}\right) & \sin\left(\theta + \frac{2\pi}{3}\right) \end{bmatrix} \begin{bmatrix} i_{ds}(t) \\ i_{qs}(t) \end{bmatrix} \tag{A.48}$$

A2 Synthetic Loading Mathematical Models for Linear PM Synchronous Machines

Five nonlinear differential equations are derived for the d- and q-axis equivalent circuit illustrated in Figure A.2.

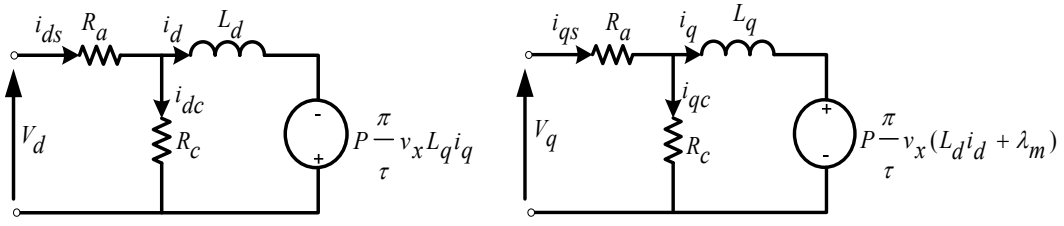

(a) d-axis (b) q-axis

Figure A.2 d- and q-axis equivalent circuit of linear PM synchronous machines

From Figure A.2 (a) and (b) the voltages equation in *dq* synchronous reference frame for the linear PM synchronous machine are defined as follows

$$V_d = R_a i_d + L_d\left(1+\frac{R_a}{R_c}\right)\frac{di_d}{dt} - P\frac{\pi}{\tau}v_x L_q i_q\left(1+\frac{R_a}{R_c}\right) \tag{A.49}$$

$$V_q = R_a i_q + L_q\left(1+\frac{R_a}{R_c}\right)\frac{di_q}{dt} + \left(1+\frac{R_a}{R_c}\right)P\frac{\pi}{\tau}v_x\left(L_d i_d + \lambda_m\right) \tag{A.50}$$

where, V_d and V_q are d- and q-axis stator voltages, respectively,

i_d and i_q are d- and q-axis torque generating currents, respectively,

R_a and R_c are stator and core loss resistances, respectively,

L_d and L_q are d- and q-axis self inductances, respectively,

λ_m is the permanent magnet flux linkage,

v_x is the mover velocity,

P is number of pole pairs,

τ is pole pitch length,

The electromagnetic force F_e developed by the mover is expressed as

$$F_e = \frac{3}{2}\frac{\pi}{\tau}P\left(\lambda_m\, i_q + \left(L_d - L_q\right)i_q\, i_d\right) \tag{A.51}$$

The velocity equation is

$$\frac{dv_x}{dt} = (\, F_e - F_L - Dv_x\,)/M \tag{A.52}$$

where, F_L is the load force. M and D are mover mass (kg) and damper coefficient (Nsm^{-1}) respectively

The dynamic equation of the mover distance is given by

$$\frac{dx}{dt} = Pv_x \tag{A.53}$$

where, x is the mover distance

A2.1 Quadrature Axis Current Equation

$$i_q(t) = I_m \sin(2\pi f_n t) + I_o \tag{A.54}$$

where, I_m is the magnitude of AC perturbation current, I_o is a dc offset current and f_n is synthetic loading frequency (Hz)

(i) Expressing I_o in terms of machine parameters

$F_e(t) = k_f i_q(t) = k_f I_m \sin(2\pi f_n t) + k_f I_o$ Where $k_f = \frac{\pi}{\tau}\frac{3}{2} \mathrm{P}\, \lambda_m$ k_f is force constant, P is number of pair of pole, τ is pole pitch and λ_m is linkage flux.

$$F_{eav} = f_n \int_0^{\frac{1}{f_n}} \left(k_f\, I_m \sin(2\pi f_n t) + k_f\, I_o\right) dt = f_n \left[-k_f\, I_m \frac{\cos(2\pi f_n t)}{2\pi f_n} + k_f\, I_o t \right]_0^{\frac{1}{f_n}}$$

$$F_{eav} = k_f\, I_o = \frac{3}{2}\frac{\pi}{\tau} P\, \lambda_m\, I_o \tag{A.55}$$

At synthetic loading $F_L = 0$, therefore

$$F_{eav} = D\, v_x = \frac{3}{2}\frac{\pi}{\tau} P\, \lambda_m\, I_o \tag{A.56}$$

where, D is damper coefficient and v_x is mover velocity in m/sec

From equation (A.56)

$$I_o = \frac{2}{3}\frac{\tau}{\pi}\frac{1}{P}\frac{1}{\lambda_m} D\, v_x \tag{A.57}$$

(ii) Expressing I_m in terms of machine parameters

$$I_s^2 = \left[\frac{f_n}{2} \int_0^{\frac{2}{f_n}} (I_m \sin(2\pi f_n t) + I_o)^2\, dt \right] + \left[\frac{f_n}{2} \int_{\frac{2}{f_n}}^{\frac{1}{f_n}} (I_m \sin(2\pi f_n t) + I_o)^2\, dt \right] \tag{A.58}$$

$$I_s^2 = \left[\frac{f_n}{2} \int_0^{\frac{2}{f_n}} \left(I_m^2 \sin^2(2\pi f_n t) + 2 I_o I_m \sin(2\pi f_n t) + I_o^2\right) dt \right] + \left[\frac{f_n}{2} \int_{\frac{2}{f_n}}^{\frac{1}{f_n}} \left(I_m^2 \sin^2(2\pi f_n t) + 2 I_o I_m \sin(2\pi f_n t) + I_o^2\right) dt \right] \tag{A.59}$$

$$I_s^2 = \frac{f_n}{2}\left[\int_0^{\frac{2}{f_n}} \left(\frac{I_m^2}{2}(1 - \cos(4\pi f_n t)) + 2 I_o I_m \sin(2\pi f_n t) + I_o^2\right) dt\right] + \frac{f_n}{2}\left[\int_{\frac{2}{f_n}}^{\frac{1}{f_n}} \left(\frac{I_m^2}{2}(1 - \cos(4\pi f_n t)) + 2 I_o I_m \sin(2\pi f_n t) + I_o^2\right) dt\right] \quad \text{(A.60)}$$

$$I_s^2 = \frac{f_n}{2}\left[\frac{I_m^2}{2}\left(t - \frac{\sin(4\pi f_n t)}{4\pi f_n}\right) - \frac{I_o I_m}{\pi f_n}\cos(2\pi f_n t) + I_o^2 t\right]_0^{\frac{2}{f_n}} + \frac{f_n}{2}\left[\frac{I_m^2}{2}\left(t - \frac{\sin(4\pi f_n t)}{4\pi f_n}\right) - \frac{I_o I_m}{\pi f_n}\cos(2\pi f_n t) + I_o^2 t\right]_{\frac{2}{f_n}}^{\frac{1}{f_n}} \quad \text{(A.61)}$$

Substitute the integration boundaries into (A.61)

$$I_s^2 = \frac{1}{2}\left[I_m^2 + 2I_o^2 - \frac{I_m^2}{2} - I_o^2\right] = \frac{1}{2}\left[\frac{I_m^2}{2} + I_o^2\right] \quad \text{(A.62)}$$

Rearrange (A.62), yield $I_m^2 = 4 I_s^2 - 2 I_o^2$

$$I_m = \sqrt{4 I_s^2 - 2 I_o^2} \quad \text{(A.63)}$$

where, I_s is rated rms current of the motor

A2.2 Velocity equation

From the mechanical equation: $M \frac{dv_x}{dt} = F_e - F_L - Dv_x$, at synthetic loading $F_L = 0$.

$F_e(t) = k_f\, i_q(t)$, $i_q(t) = I_m \sin(2\pi f_n t) + I_o$ Therefore

$$M\frac{dv_x(t)}{dt} = F_e(t) - D\,v_x(t) = k_f\, I_m \sin(2\pi f_n t) + k_f\, I_o - D\,v_x(t)$$

$$M\frac{dv_x(t)}{dt} + D\,v_x(t) = k_f\, I_m \sin(2\pi f_n t) + k_f\, I_o \quad \text{(A.64)}$$

Apply Laplace Transformation to (A.64)

$$M\,s\,v_x(s) + D\,v_x(s) = \frac{k_f\, I_m (2\pi f_n)}{s^2 + (2\pi f_n)^2} + \frac{k_f\, I_o}{s} \quad \text{(A.65)}$$

$$v_x(s)=\frac{k_f\, I_m\left(2\pi f_n\right)/M}{\left(s+\frac{D}{M}\right)\left(s^2+\left(2\pi f_n\right)^2\right)}+\frac{k_f\, I_o/M}{s\left(s+\frac{D}{M}\right)} \tag{A.66}$$

The first part of the R.H.S of (A.66)

$$\frac{k_f\, I_m\left(2\pi f_n\right)/M}{\left(s+\frac{D}{M}\right)\left(s^2+\left(2\pi f_n\right)^2\right)}=\frac{A}{s+\frac{D}{M}}+\frac{Bs+C}{\mathrm{s}^2+\left(2\pi f_n\right)^2} \tag{A.67}$$

From (A.67) expression for *A, B,C* will be found as follows

$$\frac{k_f\, I_m\left(2\pi f_n\right)}{M}=A\,s^2+A\left(2\pi f_n\right)^2+\left(B\,s+C\right)\left(s+\frac{D}{M}\right)$$

$$=\left(A+B\right)s^2+\left(B\frac{D}{M}+C\right)\mathrm{s}+\left(A\left(2\pi f_n\right)^2+C\frac{D}{M}\right)$$

From above equation equating coefficients of (s) in R.H.S with coefficients of (s) in L.H.S

$A+B=0$ therefore $A=-B$, $B\frac{D}{M}+C=0$ therefore:

$$B=-\frac{M}{D}C \text{ and } A\left(2\pi f_n\right)^2+C\frac{D}{M}=\frac{k_f\, I_m\left(2\pi f_n\right)}{M}$$

$$-B\left(2\pi f_n\right)^2-B\left(\frac{D}{M}\right)^2=\frac{k_t\, I_m\left(2\pi f_n\right)}{M},\ B=-\frac{k_f\, I_m\left(2\pi f_n\right)/M}{\left(2\pi f_n\right)^2+\left(\frac{D}{M}\right)^2},$$

$$A=\frac{k_f\, I_m\left(2\pi f_n\right)/M}{\left(2\pi f_n\right)^2+\left(\frac{D}{M}\right)^2},\ C=-\frac{D}{M}B=\frac{k_f\, I_m\left(2\pi f_n\right)D/M^2}{\left(2\pi f_n\right)^2+\left(\frac{D}{M}\right)^2}$$

Therefore:

$$v_{x1}(s)=\frac{k_f\ I_m\ (2\pi f_n)/M}{(2\pi f_n)^2+\left(\frac{D}{M}\right)^2}\left[\frac{1}{s+\frac{D}{M}}\right]-\frac{k_f\ I_m\ (2\pi f_n)/M}{(2\pi f_n)^2+\left(\frac{D}{M}\right)^2}\left[\frac{s}{s^2+(2\pi f_n)^2}\right]$$
$$+\frac{k_f\ I_m\ D/M^2}{(2\pi f_n)^2+\left(\frac{D}{M}\right)^2}\left[\frac{(2\pi f_n)}{s^2+(2\pi f_n)^2}\right] \qquad \text{(A.68)}$$

Apply Laplace Inverse Transformation to (A.68)

$$v_{x1}(t)=\frac{k_f\ I_m\ (2\pi f_n)/M}{(2\pi f_n)^2+\left(\frac{D}{M}\right)^2}e^{-\frac{D}{M}t}-\frac{k_f\ I_m\ (2\pi f_n)/M}{(2\pi f_n)^2+\left(\frac{D}{M}\right)^2}\cos(2\pi f_n t)$$
$$+\frac{k_f\ I_m\ D/M^2}{(2\pi f_n)^2+\left(\frac{D}{M}\right)^2}\sin(2\pi f_n t) \qquad \text{(A.69)}$$

The second part of the R.H.S of (A.66)

$$\frac{k_f\ I_o/M}{s\left(s+\frac{D}{M}\right)}=\frac{A}{s}+\frac{B}{s+\frac{D}{M}} \qquad \text{(A.70)}$$

From (A.70) expression for *A, B* will be found as follows

$$\frac{k_f\ I_o}{M}=A\left(s+\frac{D}{M}\right)+B\,s=(A+B)s+A\frac{D}{M}$$

From this equation equating coefficients of (s) in R.H.S with coefficient of (s) in L.H.S

$$A+B=0,\quad A=-B,\quad A\frac{D}{M}=\frac{k_f\ I_o}{M}\quad;\quad A=\frac{k_f\ I_o}{D},\quad B=-\frac{k_f\ I_o}{D}$$

Therefore:

$$v_{x2}(s)=\frac{k_f\ I_o}{D}\left[\frac{1}{s}-\frac{1}{s+\frac{D}{M}}\right] \qquad \text{(A.71)}$$

Apply Laplace Inverse Transformation to (A.71) yield

$$v_{x2}(t)=\frac{k_f\, I_o}{D}\left(1-\mathrm{e}^{-\frac{D}{M}t}\right) \tag{A.72}$$

From (A.69) and (A.72) $v_x(t)=v_{x1}(t)+v_{x2}(t)$

$$v_x(t)=\frac{k_f\, I_m\,(2\pi f_n)/M}{(2\pi f_n)^2+\left(\frac{D}{M}\right)^2}e^{-\frac{D}{M}t}-\frac{k_f\, I_m\,(2\pi f_n)/M}{(2\pi f_n)^2+\left(\frac{D}{M}\right)^2}\cos(2\pi f_n t)$$
$$+\frac{k_f\, I_m\, D/M^2}{(2\pi f_n)^2+\left(\frac{D}{M}\right)^2}\sin(2\pi f_n t)+\frac{k_f\, I_o}{D}\left(1-\mathrm{e}^{-\frac{D}{M}t}\right)$$

Rearrange the above equation

$$v_x(t)=\frac{k_f\, I_o}{D}+\left[\frac{k_f\, I_m\,(2\pi f_n)/M}{(2\pi f_n)^2+\left(\frac{D}{M}\right)^2}-\frac{k_f\, I_o}{D}\right]e^{-\frac{D}{M}t}-\frac{k_f\, I_m\,(2\pi f_n)/M}{(2\pi f_n)^2+\left(\frac{D}{M}\right)^2}\cos(2\pi f_n t)$$
$$+\frac{k_f\, I_m\, D/M^2}{(2\pi f_n)^2+\left(\frac{D}{M}\right)^2}\sin(2\pi f_n t) \tag{A.73}$$

At steady state the exponential component becomes zero

$$\left[\frac{k_f\, I_m\,(2\pi f_n)/M}{(2\pi f_n)^2+\left(\frac{D}{M}\right)^2}-\frac{k_f\, I_o}{D}\right]e^{-\frac{D}{M}t}=0$$

$$v_x(t)=\frac{k_f\, I_o}{D}-\frac{k_f\, I_m\,(2\pi f_n)/M}{(2\pi f_n)^2+\left(\frac{D}{M}\right)^2}\cos(2\pi f_n t)+\frac{k_f\, I_m\, D/M^2}{(2\pi f_n)^2+\left(\frac{D}{M}\right)^2}\sin(2\pi f_n t) \tag{A.74}$$

$$v_x=\frac{k_f I_o}{D}+\frac{k_f\, I_m/M}{\sqrt{(2\pi f_n)^2+\left(\frac{D}{M}\right)^2}}\sin(2\pi f_n t-\phi) \tag{A.75}$$

where $\phi=\tan^{-1}\left(\frac{2\pi f_n}{D/M}\right)$

The maximum speed is at the condition of $\cos(2\pi f_n t) = -1$ and $sin(2\pi f_n t) = 0$

$$v_x(\min) = \frac{k_f I_o}{D} - \frac{k_f I_m / M}{\sqrt{(2\pi f_n)^2 + \left(\frac{D}{M}\right)^2}} \tag{A.76}$$

The minimum speed is at the condition of $\cos(2\pi f_n t) = 1$ and $sin(2\pi f_n t) = 0$

$$v_x(\min) = \frac{k_f I_o}{D} - \frac{k_f I_m (2\pi f_n)/M}{(2\pi f_n)^2 + \left(\frac{D}{M}\right)^2} \tag{A.77}$$

Determining f_n in terms of machine parameters

The peak to peak velocity variation Δv_x can be determined

$$\Delta v_x = v_x(\max) - v_x(\min) \tag{A.78}$$

$$\Delta v_x = 2\frac{k_f I_m / M}{\sqrt{(2\pi f_n)^2 + \left(\frac{D}{M}\right)^2}} \tag{A.79}$$

Therefore

$$f_n = \frac{\sqrt{\left(\frac{2k_f I_m}{M}\right)^2 - \left(\Delta v_x \frac{D}{M}\right)^2}}{2\pi \Delta v_x} \tag{A.80}$$

A2.3 Direct and quadrature axis voltage equation

From d-axis equivalent circuit

$$V_d = R_a i_{ds} + L_d \frac{di_d}{dt} - P\frac{\pi}{\tau} v_x L_q i_q \tag{A.81}$$

$$i_{ds} = i_d + i_{dc}\,; i_{dc} = \left(L_d \frac{di_d}{dt} - P\frac{\pi}{\tau} v_x L_q i_q \right) \Big/ R_c = \frac{L_d}{R_c}\frac{di_d}{dt} - P\frac{\pi}{\tau}\frac{v_x L_q}{R_c} i_q$$

$$i_{ds} = i_d + \frac{L_d}{R_c}\frac{di_d}{dt} - P\frac{\pi}{\tau}\frac{v_x L_q}{R_c} i_q \tag{A.82}$$

Substitute (A.82) into (A.81)

$$V_d = R_a \left(i_d + \frac{L_d}{R_c}\frac{di_d}{dt} - P\frac{\pi}{\tau}\frac{v_x L_q}{R_c} i_q \right) + L_d \frac{di_d}{dt} - P\frac{\pi}{\tau} v_x L_q i_q$$

$$V_d = R_a\, i_d + \left(1+\frac{R_a}{R_c}\right) L_d \frac{di_d}{dt} - \left(1+\frac{R_a}{R_c}\right) P\frac{\pi}{\tau} v_x L_q i_q$$

$$V_d = R_a\, i_d + \left(1+\frac{R_a}{R_c}\right) L_d \frac{di_d}{dt} - \left(1+\frac{R_a}{R_c}\right) P\frac{\pi}{\tau} v_x L_q i_q \tag{A.83}$$

$$L_d\left(1+\frac{R_a}{R_c}\right)\frac{di_d}{dt} = V_d - R_a i_d + P\frac{\pi}{\tau} v_x L_q i_q \left(1+\frac{R_a}{R_c}\right) \tag{A.84}$$

Rearranging (A.84), yield

$$V_d(t) = -P\frac{\pi}{\tau} v_x\, L_q\left(1+\frac{R_a}{R_c}\right)\left(I_m \sin(2\pi f_n t) + I_o\right)$$

where, P is number of Pole-pairs and R_c is core loss resistance

$$V_d(t) = -P\frac{\pi}{\tau} v_x\, L_q\left(1+\frac{R_a}{R_c}\right) I_m \sin(2\pi f_n t) - P\frac{\pi}{\tau} v_x\, L_q\left(1+\frac{R_a}{R_c}\right) I_o \tag{A.85}$$

Substitute (A.74) for $v_x\,(t)$ into (A.85)

$$V_d(t) = -\left(P\; L_q\left(1+\frac{R_a}{R_c}\right) I_m \sin(2\pi f_n t) + P\; L_q\left(1+\frac{R_a}{R_c}\right) I_o \right)$$

$$\times\left[\frac{k_f\, I_o}{D} - \frac{k_f\, I_m (2\pi f_n)/M}{(2\pi f_n)^2 + \left(\frac{D}{M}\right)^2}\cos(2\pi f_n t) + \frac{k_f\, I_m (2\pi f_n)/M^2}{(2\pi f_n)^2 + \left(\frac{D}{M}\right)^2}\sin(2\pi f_n t) \right] \tag{A.86}$$

From q-axis equivalent circuit

$$V_q = R_a\, i_{qs} + L_q \frac{di_d}{dt} + P\frac{\pi}{\tau} v_x (L_d i_d + \lambda_a) \tag{A.87}$$

$$i_{qs} = i_q + i_{qc}\,;\, i_{qc} = \left(L_q \frac{di_q}{dt} + P\frac{\pi}{\tau} v_x (L_d i_d + \lambda_m) \right) \Big/ R_c = \frac{L_q}{R_c}\frac{di_q}{dt} + P\frac{\pi}{\tau} v_x \frac{(L_d i_d + \lambda_m)}{R_c}$$

$$i_{qs} = i_q + \frac{L_q}{R_c}\frac{di_q}{dt} + P\frac{\pi}{\tau} v_x \frac{(L_d i_d + \lambda_m)}{R_c} \tag{A.88}$$

Substitute (A.88) into (A.87)

$$V_q = R_a\left(i_q + \frac{L_q}{R_c}\frac{di_q}{dt} + P\frac{\pi}{\tau}v_{\mathrm{x}}\frac{\left(L_d i_d + \lambda_m\right)}{R_c}\right) + L_q\frac{di_d}{dt} + P\frac{\pi}{\tau}v_{\mathrm{x}}\left(L_d i_d + \lambda_m\right)$$

$$V_q = R_a i_q + \left(1+\frac{R_a}{R_c}\right)\frac{di_q}{dt} + \left(1+\frac{R_a}{R_c}\right)P\frac{\pi}{\tau}v_{\mathrm{x}}\left(L_d i_d + \lambda_m\right) \tag{A.89}$$

$$L_q\left(1+\frac{R_a}{R_c}\right)\frac{di_q}{dt} = \left[V_q - R_a i_q - P\frac{\pi}{\tau}v_{\mathrm{x}}L_d i_d\left(1+\frac{R_a}{R_c}\right) - P\frac{\pi}{\tau}v_{\mathrm{x}}\lambda_m\left(1+\frac{R_a}{R_c}\right)\right] \tag{A.90}$$

$$i_q(t) = I_m\sin\left(2\pi f_n t\right) + I_o \quad ; \quad i_d(t) = 0\,; \frac{di_q(t)}{dt} = I_m\left(2\pi f_n\right)\cos\left(2\pi f_n t\right) \; ; \frac{di_d(t)}{dt} = 0$$

Rearranging (A.90), yield

$$V_q(t) = \left(1+\frac{R_a}{R_c}\right)L_q\frac{di_q(t)}{dt} + R_a\, i_q(t) + P\frac{\pi}{\tau}v_{\mathrm{x}}\, L_d\left(1+\frac{R_a}{R_c}\right)i_d(t) + \; P\frac{\pi}{\tau}v_{\mathrm{x}}\,\lambda_{\mathrm{m}}\left(1+\frac{R_a}{R_c}\right)$$

$$\begin{aligned} V_q(t) &= I_m\left(2\pi f_n\right)L_q\left(1+\frac{R_a}{R_c}\right)\cos\left(2\pi f_n t\right) + R_a I_m\sin\left(2\pi f_n t\right) + R_a\, I_o \\ &+ \; P\frac{\pi}{\tau}v_{\mathrm{x}}\,\lambda_{\mathrm{m}}\left(1+\frac{R_a}{R_c}\right) \end{aligned} \tag{A.91}$$

Substitute (A.74) for $v_x(t)$ into (A.91)

$$\begin{aligned} V_q(t) &= I_m\left(2\pi f_n\right)L_q\left(1+\frac{R_a}{R_c}\right)\cos\left(2\pi f_n t\right) + R_a I_m\sin\left(2\pi f_n t\right) \\ &+ R_a\, I_o + \; P\frac{\pi}{\tau}\lambda_m\frac{k_f I_o}{D}\left(1+\frac{R_a}{R_c}\right) \\ &- P\frac{\pi}{\tau}\lambda_m\frac{k_f\, I_m\left(2\pi f_n\right)/M}{\left(2\pi f_n\right)^2 + \left(\frac{D}{M}\right)^2}\left(1+\frac{R_a}{R_c}\right)\cos\left(2\pi f_n t\right) \\ &+ P\frac{\pi}{\tau}\lambda_m\frac{k_f\, I_m D/M^2}{\left(2\pi f_n\right)^2 + \left(\frac{D}{M}\right)^2}\left(1+\frac{R_a}{R_c}\right)\sin\left(2\pi f_n t\right) \end{aligned} \tag{A.92}$$

Using Park inverse transformation to calculate the instantaneous phase voltage

$$\begin{bmatrix} V_a(t) \\ V_b(t) \\ V_c(t) \end{bmatrix} = \begin{bmatrix} \cos\left(\frac{\pi}{\tau}x\right) & \sin\left(\frac{\pi}{\tau}x\right) \\ \cos\left(\frac{\pi}{\tau}x - \frac{2\pi}{3}\right) & \sin\left(\frac{\pi}{\tau}x - \frac{2\pi}{3}\right) \\ \cos\left(\frac{\pi}{\tau}x + \frac{2\pi}{3}\right) & \sin\left(\frac{\pi}{\tau}x + \frac{2\pi}{3}\right) \end{bmatrix} \begin{bmatrix} V_d(t) \\ \\ V_q(t) \end{bmatrix} \tag{A.93}$$

A2.4 Stator direct and quadrature axis current equation

From d-axis equivalent circuit

$$i_{ds}(\mathrm{t}) = i_d(t) + i_{dc}(t) \;\; ; \; i_d(t) = 0 \; ; i_{dc}(t) = -P\frac{\pi}{\tau}\frac{L_q}{R_c} i_q(t) v_{\mathrm{x}}(t)$$

$$i_{ds}(\mathrm{t}) = -P\frac{\pi}{\tau}\frac{L_q}{R_c} i_q(t) v_{\mathrm{x}}(t) \tag{A.94}$$

Substitute (A.54) and (A.74) for $i_q(t)$ and $v_x(t)$ into (A.94)

$$i_{ds}(t) = -P\frac{\pi}{\tau}\frac{L_q}{R_c}\left(I_m \sin(2\pi f_n t) + I_o\right)\left[\frac{k_f I_o}{D} - \frac{k_f I_m (2\pi f_n)/M}{(2\pi f_n)^2 + \left(\frac{D}{M}\right)^2}\cos(2\pi f_n t) + \frac{k_f I_m D/M^2}{(2\pi f_n)^2 + \left(\frac{D}{M}\right)^2}\sin(2\pi f_n t)\right]$$

From q-axis equivalent circuit

$$i_{qs}(t) = i_q(t) + i_{qc}(t) \;\; ; \; i_d(t) = 0 \; ; i_{qc}(t) = \frac{L_q}{R_c}\frac{di_q(t)}{dt} + P\frac{\pi}{\tau}\frac{(L_d\, i_d(t) + \lambda_{\mathrm{a}})}{R_c} v_{\mathrm{x}}(t)$$

$$i_{qs}(t) = i_q(t) + \frac{L_q}{R_c}(2\pi f_n) I_m \cos(2\pi f_n t) + P\frac{\pi}{\tau}\frac{\lambda_{\mathrm{a}}}{R_c} v_{\mathrm{x}}(t) \tag{A.95}$$

Substitute (A.54) and (A.74) for $i_q(t)$ and $v_x(t)$ into (A.95)

$$i_{qs}(t) = I_m \sin(2\pi f_n t) + I_o + \frac{L_q}{R_c}(2\pi f_n) I_m \cos(2\pi f_n t)$$

$$+ P\frac{\pi}{\tau}\frac{\lambda_m}{R_c}\left[\frac{k_f I_o}{D} - \frac{k_f I_m (2\pi f_n)/M}{(2\pi f_n)^2 + \left(\frac{D}{M}\right)^2}\cos(2\pi f_n t) + \frac{k_f I_m D/M^2}{(2\pi f_n)^2 + \left(\frac{D}{M}\right)^2}\sin(2\pi f_n t)\right]$$

$$i_{qs}(t)=\left[I_o+P\frac{\pi}{\tau}\frac{\lambda_m}{R_c}\frac{k_f\ I_o}{D}\right]+I_m\sin\left(2\pi f_n t\right)+\frac{L_q}{R_c}\left(2\pi f_n\right)I_m\cos\left(2\pi f_n t\right)$$
$$+\left[P\frac{\pi}{\tau}\frac{\lambda_m}{R_c}\frac{k_f\ I_m\ D/M^2}{\left(2\pi f_n\right)^2+\left(\frac{D}{M}\right)^2}\sin\left(2\pi f_n t\right)-P\frac{\pi}{\tau}\frac{\lambda_m}{R_c}\frac{k_f\ I_m\left(2\pi f_n\right)/M}{\left(2\pi f_n\right)^2+\left(\frac{D}{M}\right)^2}\cos\left(2\pi f_n t\right)\right]$$

Using Park inverse transformation to calculate the instantaneous phase current

$$\begin{bmatrix}i_a(t)\\ i_b(t)\\ i_c(t)\end{bmatrix}=\begin{bmatrix}\cos\left(\frac{\pi}{\tau}x\right) & \sin\left(\frac{\pi}{\tau}x\right)\\ \cos\left(\frac{\pi}{\tau}x-\frac{2\pi}{3}\right) & \sin\left(\frac{\pi}{\tau}x-\frac{2\pi}{3}\right)\\ \cos\left(\frac{\pi}{\tau}x+\frac{2\pi}{3}\right) & \sin\left(\frac{\pi}{\tau}x+\frac{2\pi}{3}\right)\end{bmatrix}\begin{bmatrix}i_{ds}(t)\\ i_{qs}(t)\end{bmatrix} \quad \text{(A.96)}$$

A3 Generalization of Synthetic Loading Mathematical Equations

A3.1 Base Value Selection

	PMSM	IPMSM	LPMSM
Base current	I_{base}	I_{base}	I_{base}
Base flux linkage	λ_m	λ_m	λ_m
Base speed	$P\frac{k_t I_o}{B}$	$\frac{(k_t+k_r i_d)I_o}{B}$	$P\frac{k_f I_o}{D}$
Base voltage	V_{base}	V_{base}	V_{base}
Base inductance	$\frac{\lambda_m}{I_{base}}$	$\frac{\lambda_m}{I_{base}}$	$\frac{\lambda_m}{I_{base}}$
Base impedance	$P\frac{k_t I_o}{B}\frac{\lambda_m}{I_{base}}$	$P\frac{(k_t+k_r i_d)I_o}{B}\frac{\lambda_m}{I_{base}}$	$P\frac{\pi}{\tau}\frac{k_f I_o}{D}\frac{\lambda_m}{I_{base}}$
Base torque/force	$k_t I_{base}$	$k_t I_{base}$	$k_f I_{base}$
Base power	$\frac{3}{2}V_{base}I_{base}$	$\frac{3}{2}V_{base}I_{base}$	$\frac{3}{2}V_{base}I_{base}$

A3.2 Normalising Quadrature Axis Current

$$i_{qu}(t)=I_{mu}\sin\left(2\pi f_n t\right)+I_{ou} \quad \text{(A.97)}$$

where I_{mu} and I_{ou} are AC perturbation and dc offset current in per unit

(i) Normalising I_o in terms of machine rating

$$T_{eu}(\mathrm{t}) = I_{mu}\sin(2\pi f_n t) + I_{ou}$$

$$T_{euav} = f_n \int_0^{\frac{1}{f_n}} (I_{mu}\sin(2\pi f_n t) + I_{ou})\,\mathrm{dt} = f_n \left[-I_{mu}\frac{\cos(2\pi f_n t)}{2\pi f_n} + I_{ou} t \right]_0^{\frac{1}{f_n}}$$

$$T_{euav} = I_{ou} \tag{A.98}$$

At synthetic loading $T_L = 0$, therefore

$$T_{euav} = \frac{2}{3}\frac{1}{P}\frac{1}{\lambda_m}\frac{B\,\omega_{\mathrm{r}}}{I_s} = I_{ou} \tag{A.99}$$

where B is damper coefficient and ω_r is rotor speed in rad/sec

From equation (A.99)

$$I_{ou} = \frac{2}{3}\frac{1}{P}\frac{1}{\lambda_m}\frac{B\,\omega_{\mathrm{r}}}{I_s} \tag{A.100}$$

(ii) Normalising I_m in terms of machine rating

$$\begin{aligned} I_{su}^2 &= \left[\frac{f_n}{2} \int_0^{\frac{2}{\mathrm{f_n}}} (I_{mu}\sin(2\pi f_n t) + I_{ou})^2\,dt \right] \\ &+ \left[\frac{f_n}{2} \int_{\frac{2}{f_n}}^{\frac{1}{f_n}} (I_{mu}\sin(2\pi f_n t) + I_{ou})^2\,dt + f_n \int_0^{\frac{1}{f_n}} I_{du}^2\,dt \right] \end{aligned} \tag{A.101}$$

$$\begin{aligned} I_{su}^2 &= \left[\frac{f_n}{2} \int_0^{\frac{2}{f_n}} \left(I_{mu}^2 \sin^2(2\pi f_n t) + 2 I_{ou} I_{mpu} \sin(2\pi f_n t) + I_{ou}^2 \right) dt \right] \\ &+ \left[\frac{f_n}{2} \int_{\frac{2}{f_n}}^{\frac{1}{f_n}} \left(I_{mu}^2 \sin^2(2\pi f_n t) + 2 I_{ou} I_{mu} \sin(2\pi f_n t) + I_{ou}^2 \right) dt \right] + f_n \int_0^{\frac{1}{f_n}} I_{du}^2\,dt \end{aligned} \tag{A.102}$$

$$I_{su}^2 = \frac{f_n}{2}\left[\int_0^{\frac{2}{f_n}} \left(\frac{I_{mu}^2}{2}\left(1-\cos\left(4\pi f_n t\right)\right) + 2I_{ou}I_{mu}\sin\left(2\pi f_n t\right) + I_{ou}^2\right)dt\right] + \frac{f_n}{2}\left[\int_{\frac{2}{f_n}}^{\frac{1}{f_n}} \left(\frac{I_{mu}^2}{2}\left(1-\cos\left(4\pi f_n t\right)\right) + 2I_{ou}I_{mu}\sin\left(2\pi f_n t\right) + I_{ou}^2\right)dt\right] + f_n\int_0^{\frac{1}{f_n}} I_{du}^2 dt \quad \text{(A.103)}$$

$$I_{su}^2 = \frac{f_n}{2}\left[\frac{I_{mu}^2}{2}\left(t - \frac{\sin\left(4\pi f_n t\right)}{4\pi f_n}\right) - \frac{I_{ou}I_{mu}}{\pi f_n}\cos\left(2\pi f_n t\right) + I_{ou}^2 t\right]_0^{\frac{2}{f_n}} + \frac{f_n}{2}\left[\frac{I_{mu}^2}{2}\left(t - \frac{\sin\left(4\pi f_n t\right)}{4\pi f_n}\right) - \frac{I_{ou}I_{mu}}{\pi f_n}\cos\left(2\pi f_n t\right) + I_{ou}^2 t\right]_{\frac{2}{f_n}}^{\frac{1}{f_n}} + f_n\left[I_{du}^2 t\right]_0^{\frac{1}{f_n}} \quad \text{(A.104)}$$

Substituting the integration boundaries into (A.104), yield

$$I_{su}^2 = \frac{1}{2}\left[I_{mu}^2 + 2I_{ou}^2 - \frac{I_{mu}^2}{2} - I_{ou}^2\right] + I_{du}^2 = \frac{1}{2}\left[\frac{I_{mu}^2}{2} + I_{ou}^2\right] + I_{du}^2 \quad \text{(A.105)}$$

Rearrange (A.105), yield $I_{mu}^2 = 4I_{su}^2 - 2I_{ou}^2 - 4I_{du}^2$

$$I_{mu} = \sqrt{4I_{su}^2 - 2I_{ou}^2 - 4I_{du}^2} = \sqrt{2 - 2I_{ou}^2 - 4I_{du}^2} \quad \text{(A.106)}$$

where I_{su} is rated RMS current of the motor in pu

A3.3 Normalising Speed equation

From the mechanical equation: $J\frac{d\omega_r}{dt} = T_e - T_L - B\omega_r$, at synthetic loading $T_L = 0$

and

$T_{eu}(t) = I_{mu}\sin\left(2\pi f_n t\right) + I_{ou}$ Therefore

$$\frac{J}{T_{base}}\frac{d\omega_r(t)}{dt} = T_{eu}(t) - \frac{B\,\omega_r(t)}{T_{base}} = I_{mu}\sin\left(2\pi f_n t\right) + I_{ou} - \frac{B\,\omega_r(t)}{T_{base}}$$

Where $T_{base} = k_t I_{base} = \frac{k_t I_o}{B}\frac{I_{base}}{I_o}B = \omega_{rbase}\frac{B}{I_{ou}}$

$$\frac{J}{B} I_{ou} \frac{d\omega_{ru}(t)}{dt} + I_{ou} \omega_{\mathrm{ru}}(t) = I_{mu} \sin(2\pi \mathrm{f_n} t) + I_{ou} \quad \text{(A.107)}$$

Apply Laplace Transformation to (A.107)

$$\frac{J}{B} I_{ou} s \omega_{\mathrm{ru}}(\mathrm{s}) + I_{ou} \omega_{\mathrm{ru}}(s) = \left[\frac{I_{mu}(2\pi f_n)}{s^2 + (2\pi f_n)^2} + \frac{I_{ou}}{s} \right] \quad \text{(A.108)}$$

$$\omega_{ru}(s) = \left[\frac{I_{mu}(2\pi f_n)}{I_{ou}} \frac{B/J}{\left(s + \frac{B}{J}\right)\left(s^2 + (2\pi f_n)^2\right)} + \frac{B/J}{s\left(s + \frac{B}{J}\right)} \right] \quad \text{(A.109)}$$

The first part of the R.H.S of (A.109)

$$\frac{I_{mu}(2\pi \mathrm{f_n})}{I_{ou}} \frac{B/J}{\left(s + \frac{B}{J}\right)\left(s^2 + (2\pi f_n)^2\right)} = \frac{A}{s + \frac{B}{J}} + \frac{Cs + D}{s^2 + (2\pi f_n)^2} \quad \text{(A.110)}$$

From (A.110) expression for *A, C, D* will be found as follows

$$\frac{I_{mu}(2\pi f_n)}{I_{ou}} \frac{B}{J} = A s^2 + A(2\pi f_n)^2 + (C s + D)\left(s + \frac{B}{J}\right)$$

$$= (A + C) s^2 + \left(C \frac{B}{J} + D\right) s + \left(A(2\pi f_n)^2 + D \frac{B}{J}\right)$$

From above equation equating coefficients of (s) in R.H.S with coefficients of (s) in L.H.S

$A + C = 0$ therefor e $A = -C$, $C \frac{B}{J} + D = 0$ therefore $C = -\frac{J}{B} D$ and

$$A(2\pi f_n)^2 + D \frac{B}{J} = \frac{I_{mu}(2\pi f_n)}{I_{opu}} \frac{B}{J}, \quad -C(2\pi f_n)^2 - C\left(\frac{B}{J}\right)^2 = \frac{I_{mu}(2\pi f_n)}{I_{ou}} \frac{B}{J}$$

$$C = -\frac{I_{mu}}{I_{ou}} \frac{(2\pi f_n) B/J}{(2\pi f_n)^2 + \left(\frac{B}{J}\right)^2}, \quad A = \frac{I_{mu}}{I_{ou}} \frac{(2\pi f_n) B/J}{(2\pi f_n)^2 + \left(\frac{B}{J}\right)^2}$$

$$D = -\frac{B}{J} C = \frac{I_{mu}}{I_{ou}} \frac{(2\pi f_n)\left(B/J\right)^2}{(2\pi f_n)^2 + \left(\frac{B}{J}\right)^2} \text{ Therefore}$$

$$\omega_{r1u}(s)=\frac{I_{mu}}{I_{ou}}\frac{(2\pi f_n)B/J}{(2\pi f_n)^2+\left(\frac{B}{J}\right)^2}\left[\frac{1}{s+\frac{B}{J}}\right]-\frac{I_{mu}}{I_{ou}}\frac{(2\pi f_n)B/J}{(2\pi f_n)^2+\left(\frac{B}{J}\right)^2} \times\left[\frac{s}{s^2+(2\pi f_n)^2}\right]+\frac{I_{mu}}{I_{ou}}\frac{(B/J)^2}{(2\pi f_n)^2+\left(\frac{B}{J}\right)^2}\left[\frac{(2\pi f_n)}{s^2+(2\pi f_n)^2}\right] \quad \text{(A.111)}$$

Apply Laplace Inverse Transformation to (A.111)

$$\omega_{r1u}(t)=\frac{I_{mu}}{I_{ou}}\left[\begin{array}{l}\dfrac{(2\pi f_n)B/J}{(2\pi f_n)^2+\left(\frac{B}{J}\right)^2}e^{-\frac{B}{J_n}t}-\dfrac{(2\pi f_n)B/J}{(2\pi f_n)^2+\left(\frac{B}{J}\right)^2}\cos(2\pi f_n t) \\ +\dfrac{(B/J)^2}{(2\pi f_n)^2+\left(\frac{B}{J}\right)^2}\sin(2\pi f_n t)\end{array}\right] \quad \text{(A.112)}$$

The second part of the R.H.S of (A.109)

$$\frac{B/J}{s\left(s+\frac{B}{J}\right)}=\frac{A}{s}+\frac{C}{s+\frac{B}{J}} \quad \text{(A.113)}$$

From (A.113) expression for A, C will be found as follows:

$$\frac{B}{J}=A\left(s+\frac{B}{J}\right)+C\,s=(A+C)s+A\frac{B}{J}$$

From above equation equating coefficients of (s) in R.H.S with coefficient of (s) in L.H.S:

$A+C=0,\ \ A=-C,\ \ A\frac{B}{J}=\frac{B}{J}$; $A=1,\ \ C=-1$ Therefore:

$$\omega_{r2u}(s)=\left[\frac{1}{s}-\frac{1}{s+\frac{B}{J}}\right] \quad \text{(A.114)}$$

Apply Laplace inverse transformation to (A.114)

$$\omega_{r2u}(t)=\left(1-e^{-\frac{B}{J}t}\right) \quad \text{(A.115)}$$

From (A.112) and (A.115) $\omega_{ru}(t)=\omega_{r1u}(t)+\omega_{r2u}(t)$

$$\omega_{ru}(t)=\frac{I_{mu}}{I_{ou}}\frac{(2\pi f_n)B/J}{(2\pi f_n)^2+\left(\frac{B}{J}\right)^2}e^{-\frac{B}{J}t}-\frac{I_{mu}}{I_{ou}}\frac{(2\pi f_n)B/J}{(2\pi f_n)^2+\left(\frac{B}{J}\right)^2}\cos(2\pi f_n t)$$
$$+\frac{I_{mu}}{I_{ou}}\frac{(B/J)^2}{(2\pi f_n)^2+\left(\frac{B}{J}\right)^2}\sin(2\pi f_n t)+\left(1-e^{-\frac{B}{J}t}\right)$$

Rearrange the above equation yield

$$\omega_{ru}(t)=1+\left[\frac{I_{mu}}{I_{ou}}\frac{(2\pi f_n)B/J}{(2\pi f_n)^2+\left(\frac{B}{J}\right)^2}-1\right]e^{-\frac{B}{J}t}$$
$$-\frac{I_{mu}}{I_{ou}}\frac{(2\pi f_n)B/J}{(2\pi f_n)^2+\left(\frac{B}{J}\right)^2}\cos(2\pi f_n t)+\frac{I_{mu}}{I_{ou}}\frac{(B/J)^2}{(2\pi f_n)^2+\left(\frac{B}{J}\right)^2}\sin(2\pi f_n t) \quad \text{(A.116)}$$

At steady state the exponential component becomes zero

$$\left[\frac{I_{mu}}{I_{ou}}\frac{(2\pi f_n)B/J}{(2\pi f_n)^2+\left(\frac{B}{J}\right)^2}-1\right]e^{-\frac{B}{J}t}=0$$

$$\omega_{ru}(t)=\left[1-\frac{I_{mu}}{I_{ou}}\frac{(2\pi f_n)B/J}{(2\pi f_n)^2+\left(\frac{B}{J}\right)^2}\cos(2\pi f_n t)+\frac{I_{mu}}{I_{ou}}\frac{(B/J)^2}{(2\pi f_n)^2+\left(\frac{B}{J}\right)^2}\sin(2\pi f_n t)\right]$$

$$\omega_{ru}(t)=\left[1-\frac{I_{mu}}{I_{ou}}\frac{(2\pi f_n)/\tau_m}{(2\pi f_n)^2+\left(\frac{1}{\tau_m}\right)^2}\cos(2\pi f_n t)+\frac{I_{mu}}{I_{ou}}\frac{(1/\tau_m)^2}{(2\pi f_n)^2+\left(\frac{1}{\tau_m}\right)^2}\sin(2\pi f_n t)\right] \quad \text{(A.117)}$$

where τ_m is mechanical time constant

The maximum speed is at the condition of: $\cos(2\pi f_n t)=-1$ and $\sin(2\pi f_n t)=0$

$$\omega_{ru}(\max) = 1 + \frac{I_{mu}}{I_{ou}} \frac{(2\pi f_n)/\tau_{\mathrm{m}}}{(2\pi f_n)^2 + \left(\frac{1}{\tau_{\mathrm{m}}}\right)^2} \tag{A.118}$$

The minimum speed is at the condition of: $\cos(2\pi f_n t) = 1$ and $\sin(2\pi f_n t) = 0$

$$\omega_{rpu}(\min) = 1 - \frac{I_{mu}}{I_{ou}} \frac{(2\pi f_n)/\tau_{\mathrm{m}}}{(2\pi f_n)^2 + \left(\frac{1}{\tau_{\mathrm{m}}}\right)^2} \tag{A.119}$$

A3.4 Normalising direct axis and quadrature axis voltage

$$V_d = R_a\, i_{ds} + L_d \frac{di_d}{dt} - P\,\omega_{\mathrm{r}} L_q i_q$$

$$V_{du} = \frac{V_d}{V_{base}} = R_u i_{dsu} + \frac{L_d}{Z_{base}} \frac{di_{du}}{dt} - E_u\, i_{qu}\, L_{qu}\omega_{ru}(t) \tag{A.120}$$

$$i_{dc} = \left(L_d \frac{di_d}{dt} - P\omega_r L_q i_q \right) \Big/ R_c \quad i_{dsu} = i_{du} + i_{dcu};$$

$$i_{dcu} = \frac{i_{dc} Z_{base}}{I_{base} Z_{base}} = Z_{base} \left(\frac{L_d}{Z_{base}} \frac{di_{du}}{dt} - \frac{P\,\omega_{\mathrm{r}} I_{base} L_q}{\mathrm{V_{base}}} i_{qu} \right) \Big/ R_c$$

$$= \frac{L_d}{Z_{base} R_{cpu}} \frac{di_{du}}{dt} - \frac{E_u\, \omega_{\mathrm{ru}}(t)}{R_{cu}} L_{\mathrm{qu}}\, i_{qu}$$

$$i_{dsu} = i_{du} + \frac{L_d}{Z_{base} R_{cu}} \frac{di_{du}}{dt} - \frac{E_u\, \omega_{\mathrm{ru}}(t)}{R_{cu}} L_{\mathrm{qu}}\, i_{qu} \tag{A.121}$$

Substitute (A.121) into (A.120)

$$V_{du} = R_{au} \left(i_{du} + \frac{L_d}{Z_{base} R_{cu}} \frac{di_d}{dt} - \frac{E_u \omega_{\mathrm{ru}}(t)}{R_{cu}} L_{qu} i_{qu} \right)$$

$$+ \frac{L_d}{Z_{base}} \frac{di_{du}}{dt} - E_u\, \omega_{ru}(t) L_{qu} i_{qu}$$

$$V_{du} = R_{au}\, i_{du} + \left(1 + \frac{R_{au}}{R_{cu}}\right) \frac{L_d}{Z_{base}} \frac{di_{du}}{dt} - \left(1 + \frac{R_{au}}{R_{cu}}\right) E_u \omega_{\mathrm{ru}}(\mathrm{t})\, L_{qu} i_{qu} \tag{A.122}$$

$$\frac{L_d}{Z_{base}}\left(1+\frac{R_{au}}{R_{cu}}\right)\frac{di_{du}}{dt}=\left[V_{du}-R_{au}i_{du}+\left(1+\frac{R_{au}}{R_{cu}}\right)E_u\omega_{ru}(t)L_{qu}i_{qu}\right] \quad \text{(A.123)}$$

$$i_{qu}(t)=I_{mu}\sin(2\pi f_n t)+I_{ou} \quad ; \quad i_{du}(t)=0;\ \frac{di_{du}(t)}{dt}=0$$

$$V_{du}(t)=-E_u\omega_{ru}(t)\left(1+\frac{R_{au}}{R_{cu}}\right)L_{qu}(I_{mu}\sin(2\pi f_n t)+I_{ou})$$

where R_{cu} is core loss resistance in *pu*

$$V_{du}(t)=-E_u\omega_{\mathrm{ru}}(t)\left(1+\frac{R_{au}}{R_{cu}}\right)L_{qu}I_{mu}\sin(2\pi f_n t)-E_u\omega_{\mathrm{ru}}(t)\left(1+\frac{R_{au}}{R_{cu}}\right)L_{qu}I_{ou} \quad \text{(A.124)}$$

Substitute (A.117) for ω_{ru}(t) into (A.124)

$$V_{du}(t)=-\left(\left(1+\frac{R_{au}}{R_{cu}}\right)E_uL_{qu}I_{mu}\sin(2\pi f_n t)+\left(1+\frac{R_{au}}{R_{cu}}\right)E_uL_{qu}I_{ou}\right)$$

$$\times\left[1-\frac{I_{mu}}{I_{ou}}\frac{(2\pi f_n)/\tau_m}{(2\pi f_n)^2+\left(\frac{1}{\tau_m}\right)^2}\cos(2\pi f_n t)+\frac{I_{mu}}{I_{ou}}\frac{(1/\tau_m)^2}{(2\pi f_n)^2+\left(\frac{1}{\tau_m}\right)^2}\sin(2\pi f_n t)\right] \quad \text{(A.125)}$$

From q-axis equivalent circuit

$$V_q = R_a\ i_{qs} + L_q\ \frac{di_q}{dt} + P\ \omega_{\mathrm{r}}(L_d\ i_d + \lambda_m)$$

$$V_{qu} = \frac{V_q}{V_{base}} = \left[R_a\ i_{qs} + L_q\ \frac{di_q}{dt} + P\ \omega_{\mathrm{r}}(L_d\ i_d + \lambda_m)\right] \Big/ V_{base}$$

$$V_{qu}=R_{au}\ i_{qsu}+\frac{L_q}{Z_{base}}\frac{di_{qu}}{dt}+E_u\omega_{\mathrm{ru}}(t)(L_{du}i_{du}+1) \quad \text{(A.126)}$$

$$i_{qsu}=i_{qu}+i_{qcu}\ ;\ i_{qcu}=\frac{i_{qc}Z_{base}}{I_{base}Z_{base}}$$

$$=Z_{base}\left(\frac{L_q}{Z_{base}}\frac{di_{qu}}{dt}+E_u\omega_{\mathrm{ru}}(t)(L_{du}i_{du}+1)\right)\Big/R_c$$

$$=\frac{L_q}{Z_{base}R_{cu}}\frac{di_{qu}}{dt}+E_u\omega_{\mathrm{ru}}(t)\frac{(L_{du}i_{du}+1)}{R_{cu}}$$

$$i_{qsu} = i_{qu} + \frac{L_q}{Z_{base}\, R_{cu}} \frac{di_{qu}}{dt} + E_u \omega_{\mathrm{ru}}(t) \frac{(L_{du} i_{du} + 1)}{R_{cu}} \tag{A.127}$$

Substitute (A.127) into (A.126)

$$V_{qu} = R_{au} \left(i_{qu} + \frac{L_q}{Z_{base} R_{cpu}} \frac{di_{qu}}{dt} + E_u \omega_{\mathrm{ru}}(t) \frac{(L_{du} i_{du} + 1)}{R_{cu}} \right) + \frac{L_q}{Z_{base}} \frac{di_{du}}{dt} + E_u \omega_{\mathrm{ru}}(t)(L_{du} i_{du} + 1)$$

$$V_{qu} = R_{au} i_{qu} + \frac{L_q}{Z_{base}} \left(1 + \frac{R_{au}}{R_{cu}} \right) \frac{di_{qu}}{dt} + \left(1 + \frac{R_{au}}{R_{cu}} \right) E_u \omega_{\mathrm{ru}}(t)(L_{du} i_{du} + 1) \tag{A.128}$$

$$\frac{L_q}{Z_{base}} \left(1 + \frac{R_{au}}{R_{cu}} \right) \frac{di_{qu}}{dt} = \left[V_{qu} - R_{au} i_{qu} - E_u \omega_{\mathrm{ru}}(t) \left(1 + \frac{R_{au}}{R_{cu}} \right) (1 + L_{du} i_{du}) \right] \tag{A.129}$$

$$i_{qu}(t) = I_{mu} \sin(2\pi f_n t) + I_{ou} \quad ; \quad i_{du}(t) = 0; \quad \frac{di_{qu}(t)}{dt} = I_{mu} (2\pi f_n) \cos(2\pi f_n t)$$

$$V_{qu}(t) = \frac{L_q}{Z_{base}} \left(1 + \frac{R_{au}}{R_{cu}} \right) \frac{di_{qu}}{dt} + R_{au} i_{qu} + E_u \omega_{ru}(t) \left(1 + \frac{R_{au}}{R_{cu}} \right) (1 + L_{du} i_{du})$$

$$V_{qu}(t) = I_{mu} (2\pi f_n) \frac{L_q}{Z_{\mathrm{base}}} \left(1 + \frac{R_{au}}{R_{cu}} \right) \cos(2\pi f_n t) + R_{au} I_{mu} \sin(2\pi f_n t) + R_{au} I_{ou} + E_u \omega_{\mathrm{ru}}(t) \left(1 + \frac{R_{au}}{R_{cu}} \right)$$

$$V_{qu}(t) = \left(1 + \frac{R_{au}}{R_{cu}} \right) L_{\mathrm{qu}} I_{mu} \left(\frac{f_n}{f_s} \right) \cos(2\pi f_n t) + R_{au} I_{mu} \sin(2\pi f_n t) + R_{au} I_{ou} + E_u \omega_{\mathrm{ru}}(t) \left(1 + \frac{R_{au}}{R_{cu}} \right) \tag{A.130}$$

where f_s is the system frequency.

Substitute (A.117) for ω_r into (A.130)

$$V_{qu}(t)=\left(1+\frac{R_{au}}{R_{cu}}\right)L_{\mathrm{qu}}I_{mu}\left(\frac{f_n}{f_s}\right)\cos(2\pi f_n t)+R_{au}I_{mu}\sin(2\pi f_n t)+R_{au}\,I_{ou}+E_u\left(1+\frac{R_{au}}{R_{cu}}\right)$$
$$-\frac{I_{mu}}{I_{ou}}E_u\frac{(2\pi f_n)/\tau_m}{(2\pi f_n)^2+\left(\frac{1}{\tau_m}\right)^2}\left(1+\frac{R_{au}}{R_{cu}}\right)\cos(2\pi f_n t) \qquad \text{(A.131)}$$
$$+\frac{I_{mu}}{I_{ou}}E_u\frac{(1/\tau_m)^2}{(2\pi f_n)^2+\left(\frac{1}{\tau_m}\right)^2}\left(1+\frac{R_{au}}{R_{cu}}\right)\sin(2\pi f_n t)$$

Using Park inverse transformation to calculate the instantaneous phase voltage

$$\begin{bmatrix}V_{au}(t)\\V_{bu}(t)\\V_{cu}(t)\end{bmatrix}=\begin{bmatrix}\cos\theta & \sin\theta\\ \cos\left(\theta-\frac{2\pi}{3}\right) & \sin\left(\theta-\frac{2\pi}{3}\right)\\ \cos\left(\theta+\frac{2\pi}{3}\right) & \sin\left(\theta+\frac{2\pi}{3}\right)\end{bmatrix}\begin{bmatrix}V_{du}(t)\\V_{qu}(t)\end{bmatrix} \qquad \text{(A.132)}$$

A3.5 Normalising stator direct axis and quadrature axis current

From d-axis and q-axis equivalent circuit:

$$i_{ds}(\mathrm{t})=i_d(t)+i_{dc}(t)\;;\;i_d(t)=0\;;i_{dc}(t)=-P\frac{L_q}{R_c}i_q(t)\omega_{\mathrm{r}}(t)$$

$$i_{dsu}(\mathrm{t})=\frac{i_{ds}}{I_{base}}=-P\frac{L_q}{R_c}\frac{i_q(t)}{I_{base}}\omega_{\mathrm{r}}(t)=-\frac{L_{qu}}{R_{cu}}E_u\,i_{qu}(t)\omega_{\mathrm{ru}}(t) \qquad \text{(A.133)}$$

Substitute (A.97) and (A.117) for $i_{qu}(t)$ and $\omega_{ru}(t)$ into (A.133):

$$i_{dsu}(t)=-\frac{L_{qu}}{R_{cu}}E_u\,(I_{mu}\sin(2\pi f_n t)+I_{ou})$$
$$\times\left[1-\frac{I_{mu}}{I_{ou}}\frac{(2\pi f_{\mathrm{n}})/\tau_m}{(2\pi f_n)^2+\left(\frac{1}{\tau_m}\right)^2}\cos(2\pi f_n t)+\frac{I_{mu}}{I_{ou}}\frac{(1/\tau_m)^2}{(2\pi f_n)^2+\left(\frac{1}{\tau_m}\right)^2}\sin(2\pi f_n t)\right]$$

$$i_{qs}(\mathrm{t})=i_q(t)+i_{qc}(t)\;;\;i_d(t)=0\;;i_{qc}(t)=\frac{L_q}{R_c}\frac{di_q(t)}{dt}+P\frac{(L_d\,i_d(t)+\lambda_m)}{R_c}\omega_{\mathrm{r}}(t)$$

$$i_{qsu}(\mathrm{t}) = \frac{i_{ds}(t)}{I_{base}} = i_{qu}(t) + \frac{L_q}{R_c}\frac{di_{qu}(t)}{dt} + P\frac{\lambda_m}{R_c}\frac{\omega_{\mathrm{r}}(t)}{I_{base}}$$

$$i_{qsu}(t) = i_{qu}(t) + L_{qu}\left(\frac{f_n}{f_s}\right)\frac{E_u}{R_{cu}}\cos(2\pi f_n t) + E_u\frac{\omega_{\mathrm{ru}}(\mathrm{t})}{R_{cu}} \tag{A.134}$$

Substitute (A.97) and (A.117) for $i_{qu}(t)$ and $\omega_{ru}(t)$ into (A.134):

$$i_{qsu}(t) = \left[I_{ou} + \frac{E_u}{R_{cu}}\right] + I_{mu}\sin(2\pi f_n t) + L_{qu}\left(\frac{f_n}{f_s}\right)\frac{E_u}{R_{cu}}\cos(2\pi f_n t)$$
$$+ \frac{E_u}{R_{cu}}\frac{I_{mu}}{I_{ou}}\left[\frac{(1/\tau_m)^2}{(2\pi f_n)^2 + \left(\frac{1}{\tau_m}\right)^2}\sin(2\pi f_n t) - \frac{(2\pi f_n)/\tau_m}{(2\pi f_n)^2 + \left(\frac{1}{\tau_m}\right)^2}\cos(2\pi f_n t)\right]$$

Using Park inverse transformation to calculate the instantaneous phase current

$$\begin{bmatrix} i_{au}(t) \\ i_{bu}(t) \\ i_{cu}(t) \end{bmatrix} = \begin{bmatrix} \cos\theta & \sin\theta \\ \cos\left(\theta - \frac{2\pi}{3}\right) & \sin\left(\theta - \frac{2\pi}{3}\right) \\ \cos\left(\theta + \frac{2\pi}{3}\right) & \sin\left(\theta + \frac{2\pi}{3}\right) \end{bmatrix} \begin{bmatrix} i_{dsu}(t) \\ \\ i_{qsu}(t) \end{bmatrix} \tag{A.135}$$

Appendix B

Photographs of Practical Setup

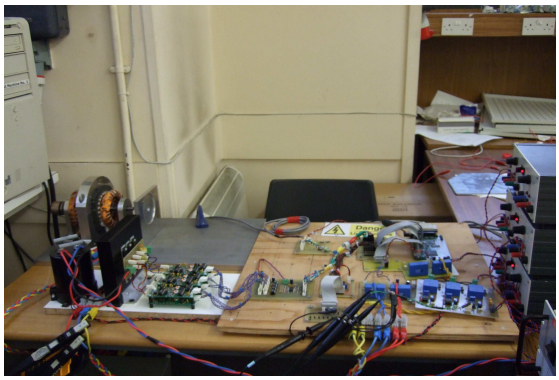

Figure B.1 Photograph of vector control systems setup

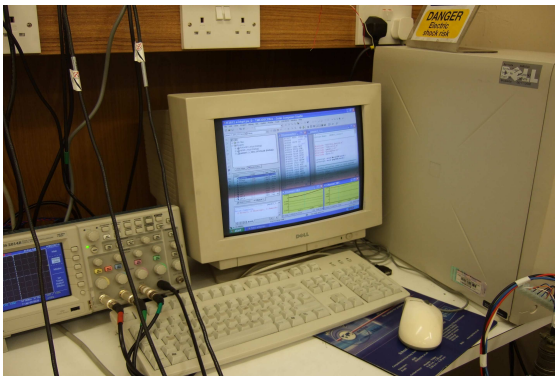

Figure B.2 Photograph of host computer and the code composer studio

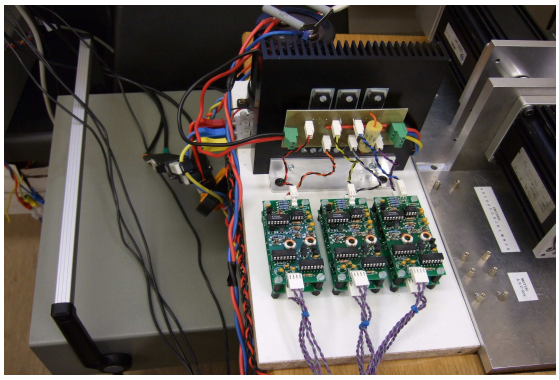

Figure B.3 Close view of the three-phase inverter

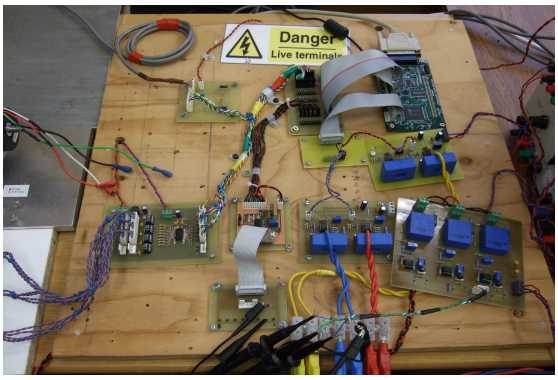

Figure B.4 Close view of the vector control systems

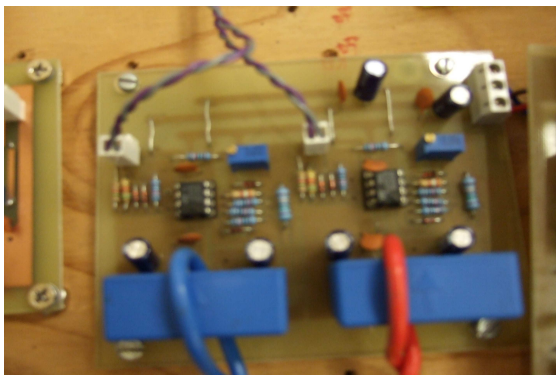

Figure B.5 Close view of the current transducer interface circuit

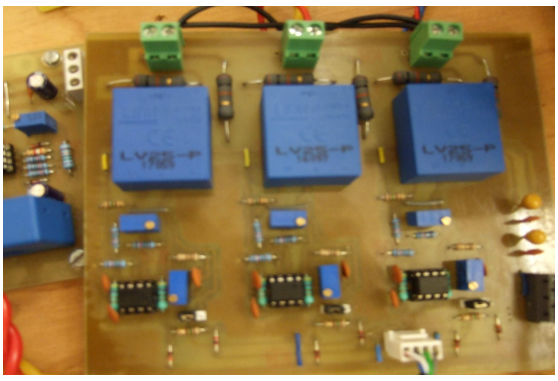

Figure B.6 Close view of the voltage transducer interface circuit

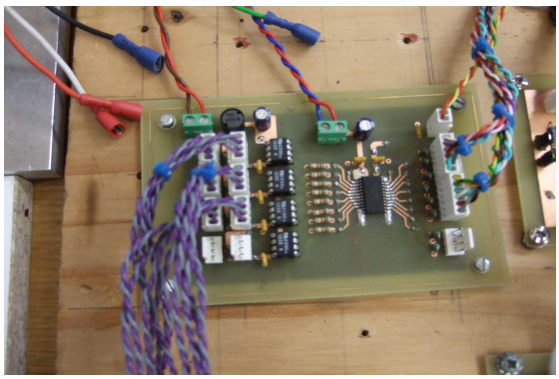

Figure B.7 Close view of isolating and interfacing circuit of PWM signals and 3.3V regulation scheme

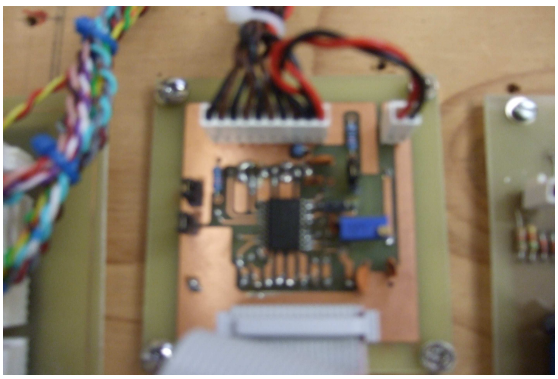

Figure B.8 Close view of digital to analog circuit

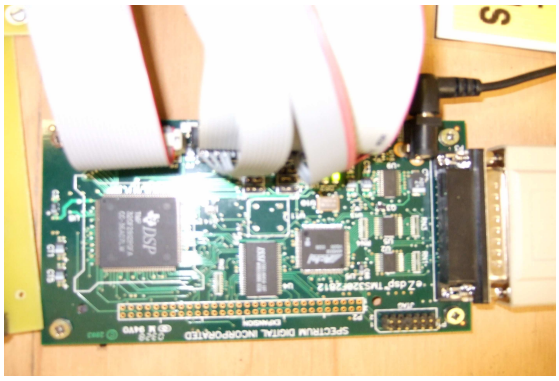

Figure B.9 Close view of the TMS320F2812DSP controller

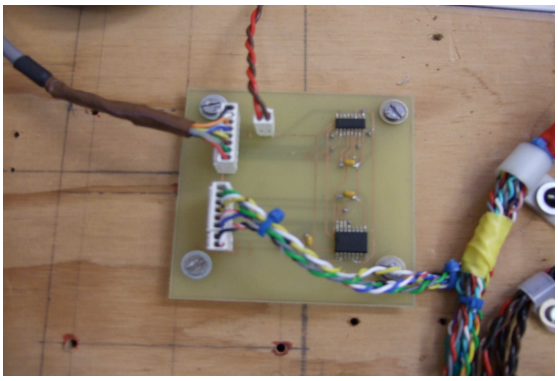

Figure B.10 Close view of quadrature encoder signal interface circuit

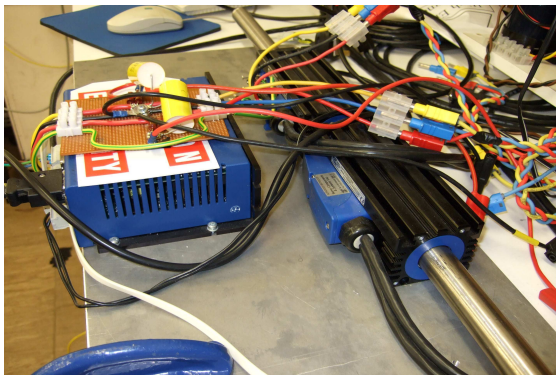

Figure B.11 Close view of the linear PM synchronous machine and vector controller

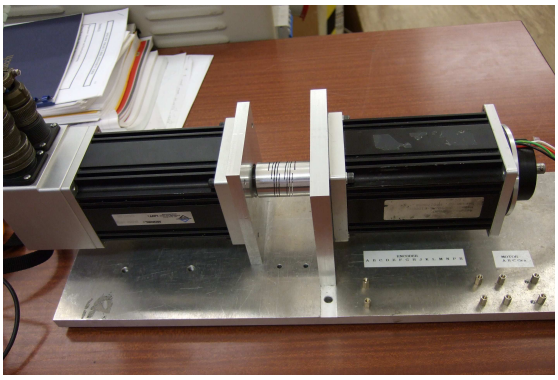

Figure B.12 Close view of the PM synchronous machine

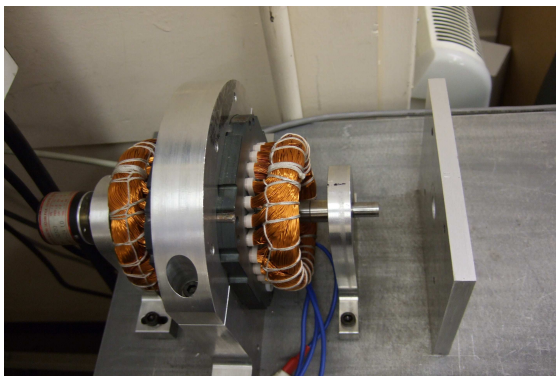

Figure B.13 Close view of the IPM synchronous machine

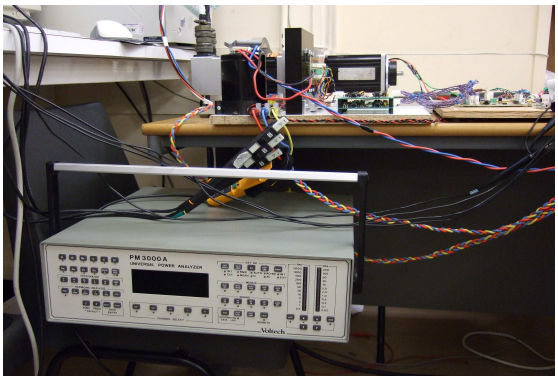

Figure B.14 Close view of the PM3000A power analyser

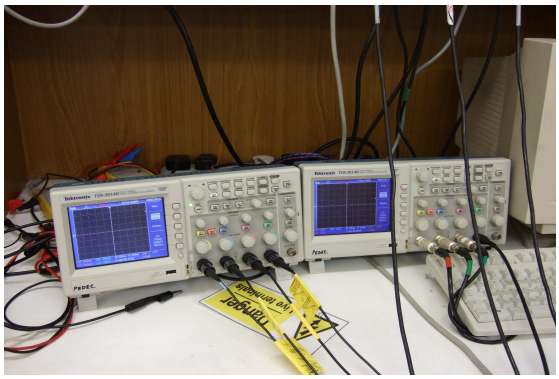

Figure B.15 Close view of the four channels digital storage oscilloscope

Figure B.16 Close view of the resistive load

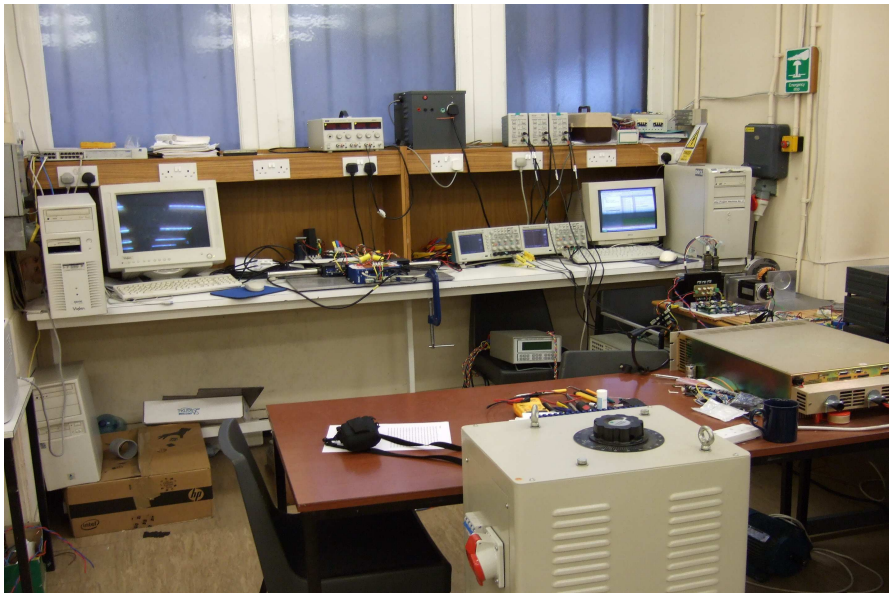

Figure B.17 Photograph of the total experiment setup

Appendix C

MATLAB and SIMULINK

This Appendix presents the MATLAB and SIMULINK programs for synthetic loading technique and standard efficiency test applied to the PM, IPM and linear PM synchronous machine.

C.1 Synthetic loading and standard efficiency test programs for the PM Synchronous Machine

```
clear all
%=========================================================
% PM Synchronous Machine Parameters (843 Watts)
%=========================================================
B=3.47e-5;Lq=0.65e-3;Ld=Lq;Rc=350;fs=800/3;J=7.85e-5;f=100;
Is=10.54;R=0.55;Ya=0.04;P=4;ws=2*pi*fs;t=0:0.00002:6/f;
%=========================================================
% The Machine Under Rated Conditions
%=========================================================
iqo=10.34;
idso=-ws*Lq*iqo/Rc;
iqso=iqo+ws*Ya/Rc;
imo=sqrt((idso*idso+iqso*iqso)/2);
Vdo=-ws*Lq*(1+R/Rc)*iqo;
Vqo=R*iqo+ws*Ya*(1+R/Rc);
Vmo=sqrt((Vdo*Vdo+Vqo*Vqo)/2);
Smo=3*Vmo*imo;
%=========================================================
% Initial Calculations for Synthetic Loading
%=========================================================
Io=B*(2*pi*fs/P)/(sqrt(3/2)*P*Ya);kt=sqrt(3/2)*P*Ya;Im=sqrt((2*Is*Is-2*Io*Io));id=0;
%=========================================================
% The Machine Under Synthetic Loading
%=========================================================
wr=[kt*Io/B-[(kt*Im*2*pi*f/J)/((2*pi*f)^2+(B/J)^2)]*cos(2*pi*f*t)+...
   [(kt*Im*B/(J*J))/((2*pi*f)^2+(B/J)^2)]*sin(2*pi*f*t)];
iq=Im*sin(2*pi*f*t)+Io;
idc=-P*Lq/Rc*iq.*wr;
ids=id+idc;
iqc=Lq/Rc*Im*(2*pi*f)*cos(2*pi*f*t)+P*wr/Rc*(Ld*id+Ya);
iqs=iq+iqc;
Te=kt*iq;
Yd=Ld*id+Ya;
Yq=Lq*iq;
YR=sqrt((Yd*Yd+Yq.*Yq)/(Ya*Ya+Is*Is*Lq*Lq));
Vd=R*id-P*wr*Lq*(1+R/Rc)*Im.*sin(2*pi*f*t)-*wr*Lq*(1+R/Rc)*Io;
Vq=Im*(2*pi*f)*Lq*(1+R/Rc)*cos(2*pi*f*t)+R*Im*sin(2*pi*f*t)+R*Io+P*wr*(1+R/Rc)*(Ld*id+Ya);
Vs1=(Vd.*Vd+Vq.*Vq); Vs=sqrt((Vd.*Vd+Vq.*Vq)/2);
Ir1=(ids.*ids+iqs.*iqs); Ir=sqrt((ids.*ids+iqs.*iqs)/2);
```

```
S=3*Vs.*Ir;
va=Vd.*cos(ws*t)+Vq.*sin(ws*t);
vb=Vd.*cos(ws*t-2*pi/3)+Vq.*sin(ws*t-2*pi/3);
vc=Vd.*cos(ws*t+2*pi/3)+Vq.*sin(ws*t+2*pi/3);
vab=va-vb; vbc=vb-vc; vca=vc-va;
ia=ids.*cos(ws*t)+iqs.*sin(ws*t);
ib=ids.*cos(ws*t-2*pi/3)+iqs.*sin(ws*t-2*pi/3);
ic=ids.*cos(ws*t+2*pi/3)+iqs.*sin(ws*t+2*pi/3);
Pa=3/2*(ids.*Vd+iqs.*Vq);
Pcu=3/2*R*(ids.*ids+iqs.*iqs);
Pco=3/2*Rc*(idc.*idc+iqc.*iqc);
Pm=B*wr.*wr; PL=Pcu+Pco+Pm;
Nr=30/pi*wr;
VDC=sqrt(6)*Vs/0.985; VL=sqrt(3*(Vd.*Vd+Vq.*Vq)/2);
Vdcm=max(VDC); Vsm=max(VL);
%==========================================================
figure(1), plot(t,ia,'r',t,ib,'b',t,ic,'k'),grid;
figure(2), plot(t,vab,'r',t,vbc,'b',t,vca,'k'),grid;
figure(3), plot(t,va,'r',t,vb,'b',t,vc,'k'),grid;
figure(4), plot(t,Vd,'r',t,Vq,'b',t,VL,'k'),grid;
figure(5), plot(t,Pa,'r',t,PL,'b',t,S,'k'),grid;
figure(6), plot(t,Pcu,'r',t,Pco,'b',t,Pm,'k'),grid;
figure(7), plot(t,Nr,'r',t,S,'b'),grid
figure(8), plot(t,ids,'r',t,iqs,'b',t,Ir,'k'),grid;
figure(9), plot(t,YR,'b',t,Te,'r'),grid;
figure(10), plot(t,VDC,'r'),grid;
figure(11), plot(t,Vs1,'r',t,Vd2,'b',t,Vq2,'k'),grid;
```

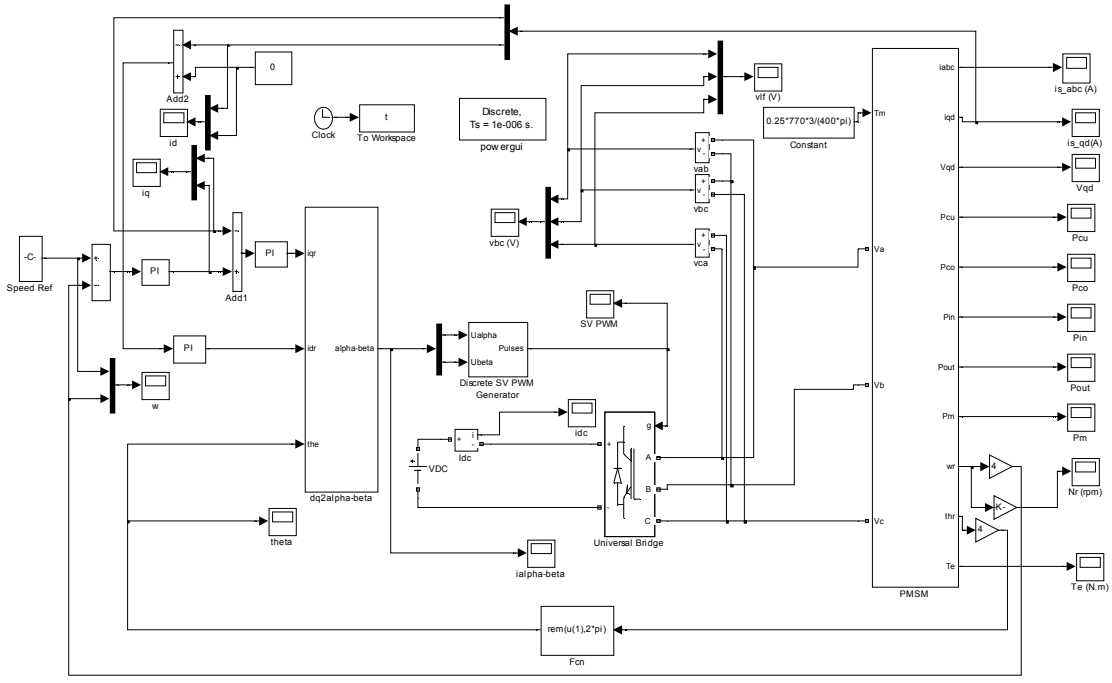

Figure C.1 SIMULINK for standard efficiency test of the PM synchronous machine

C.2 Synthetic loading and standard efficiency test programs for the IPM Synchronous Machine

```
clear all
%=================================================================
% Permanent Magnet Synchronous Machine Parameters (843 Watts)
%=================================================================
B=2.7e-4;Lq=120e-3;Ld=65e-3;Rc=1580;fs=15;J=4.5e-3;f=4;Is=2.0;
R=7;P=1;Ya=0.6;ws=2*pi*fs;t=0:0.000004:4/f;id=0;kr=3/2*P*(Ld-Lq)*id;
%=================================================================
% The Machine Under Rated Conditions
%=================================================================
iqo=1.977;
idso=id-ws*Lq*iqo/Rc;
iqso=iqo+ws*Ya/Rc;
imo=sqrt(idso*idso+iqso*iqso);
Vdo=-ws*Lq*(1+R/Rc)*iqo;
Vqo=R*iqo+ws*Ya*(1+R/Rc);
Vmo=sqrt(Vdo*Vdo+Vqo*Vqo);
Smo=3/2*Vmo*imo;
%=================================================================
% Initial Calculations for Synthetic Loading
%=================================================================
Io=B*(2*pi*fs/P)/(3*P*Ya/2+3*P/2*(Ld-Lq)*id);kt=3/2*P*Ya;
Im=sqrt((2*Is*Is-2*Io*Io-2*id*id));
%=================================================================
% The Machine Under Synthetic Loading
%=================================================================
wr=[(kt+kr)*Io/B-[((kt+kr)*Im*2*pi*f/J)/((2*pi*f)^2+(B/J)^2)]*cos(2*pi*f*t)+...
   [((kt+kr)*Im*B/(J*J))/((2*pi*f)^2+(B/J)^2)]*sin(2*pi*f*t)];
iq=Im*sin(2*pi*f*t)+Io;
idc=-P*Lq/Rc*iq.*wr;
ids=id+idc;
iqc=Lq/Rc*Im*(2*pi*f)*cos(2*pi*f*t)+P*wr/Rc*(Ld*id+Ya);
iqs=iq+iqc;
Te=kt*iq;
Yd=Ld*id+Ya;
Yq=Lq*iq;
YR=sqrt((Yd*Yd+Yq.*Yq)/(Ya*Ya+Is*Is*Lq*Lq));
Vd=R*id-P*wr*Lq*(1+R/Rc)*Im.*sin(2*pi*f*t)-P*wr*Lq*(1+R/Rc)*Io;
Vq=Im*(2*pi*f)*Lq*(1+R/Rc)*cos(2*pi*f*t)+R*Im*sin(2*pi*f*t)+R*Io+P*wr*(1+R/Rc)*(Ld*id+Ya);
Vs1=(Vd.*Vd+Vq.*Vq);
Vs=sqrt(Vd.*Vd+Vq.*Vq);
Ir1=sqrt((ids.*ids+iqs.*iqs)/2);
Ir2=(ids.*ids+iqs.*iqs);
Ir=sqrt((ids.*ids+iqs.*iqs));
S=3/2*Vs.*Ir;
va=Vd.*cos(ws*t)+Vq.*sin(ws*t);
vb=Vd.*cos(ws*t-2*pi/3)+Vq.*sin(ws*t-2*pi/3);
vc=Vd.*cos(ws*t+2*pi/3)+Vq.*sin(ws*t+2*pi/3);
vab=va-vb; vbc=vb-vc; vca=vc-va;
theta=ws*t;
ia=ids.*cos(theta)+iqs.*sin(theta);
ib=ids.*cos(theta-2*pi/3)+iqs.*sin(theta-2*pi/3);
```

```
ic=ids.*cos(theta+2*pi/3)+iqs.*sin(theta+2*pi/3);
P=3/2*(Vd.*ids+Vq.*iqs);
Pcu=3/2*R*(ids.*ids+iqs.*iqs);
Pco=3/2*Rc*(idc.*idc+iqc.*iqc);
Pm=B*wr.*wr; PL=Pcu+Pco+Pm;
Nr=30/pi*wr; VDC=sqrt(3)*Vs/0.945;
VL=sqrt(3*(Vd.*Vd+Vq.*Vq)/2);
Vdcm=max(VDC); Vsm=max(VL);
M=max(Vsm/Vdcm);
%==========================================================
figure(1), plot(t,ia,'r',t,ib,'b',t,ic,'k'),grid;
figure(2), plot(t,vab,'r',t,vbc,'b',t,vca,'k'),grid;
figure(3), plot(t,va,'r',t,vb,'b',t,vc,'k'),grid;
figure(4), plot(t,Vd,'r',t,Vq,'b',t,VL,'k'),grid;
figure(5), plot(t,P,'r',t,PL,'b',t,S,'k'),grid;
figure(6), plot(t,Pcu,'r',t,Pco,'b',t,Pm,'k'),grid;
figure(7), plot(t,Nr,'r',t,S,'b'),grid
figure(8), plot(t,ids,'r',t,iqs,'b',t,Ir1,'k'),grid;
figure(9), plot(t,YR,'b',t,Te,'r'),grid;
figure(10), plot(t,VDC,'r'),grid;
```

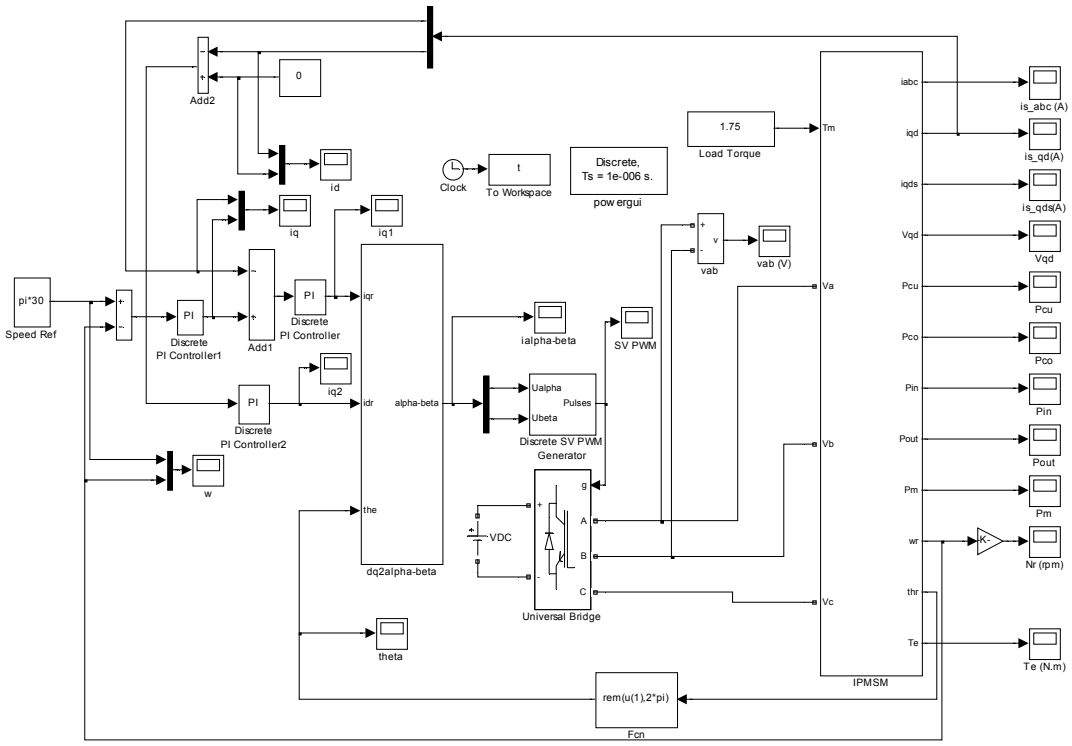

Figure C.2 SIMULINK for standard efficiency test of the IPM synchronous machine

C.3 Synthetic loading and standard efficiency test programs for the linear PM Synchronous Machine

```
clear all
%==========================================================
%Linear Permanent Magnet Synchronous Machine Parameter
%==========================================================
D=0.14;Lq=1.95e-3;Ld=Lq;Rc=625;vxo=2.56;M=0.93;f=20;Is=3.28;R=3.01;P=2;
Ya=0.08475;tau=0.0512;fs=P*vxo/(2*tau);ws=2*pi*fs;t=0:0.000001:5/f;
%==========================================================
%The Machine Under Rated Conditions
%==========================================================
iqo=3.26;
idso=-ws*Lq*iqo/Rc;
iqco=ws*Ya/Rc;
iqso=iqo+iqco;
imo=sqrt((idso*idso+iqso*iqso)/2);
Vdo=-ws*Lq*(1+R/Rc)*iqo;
Vqo=R*iqo+ws*Ya*(1+R/Rc);
Vmo=sqrt((Vdo*Vdo+Vqo*Vqo)/2);
Pmo=3*(Vdo*idso+Vqo*iqso);
Smo=3*Vmo*imo;
%==========================================================
%Initial Calculations for Synthetic Loading
%==========================================================
kf=3/2*pi/tau*P*Ya;Io=D*(2*tau*fs/P)/kf;Im=sqrt(2*Is*Is-2*Io*Io);id=0;
%==========================================================
%The Linear Machine Under Synthetic Loading
%==========================================================
vx=[kf*Io/D-[(kf*Im*2*pi*f/M)/((2*pi*f)^2+(D/M)^2)]*cos(2*pi*f*t)+...
  [(kf*Im*D/(M*M))/((2*pi*f)^2+(D/M)^2)]*sin(2*pi*f*t)];
Fe=[kf*Io-[(kf*Im*2*pi*f*D/M)/((2*pi*f)^2+(D/M)^2)]*cos(2*pi*f*t)+...
  [(kf*Im*D*D/(M*M))/((2*pi*f)^2+(D/M)^2)]*sin(2*pi*f*t)];
iq=Im*sin(2*pi*f*t)+Io;
idc=-P*Lq/Rc*pi/tau*iq.*vx;
ids=id+idc;
iqc=Lq*Im*(2*pi*f)*cos(2*pi*f*t)/Rc+P*pi/tau*vx/Rc*(Ld*id+Ya);
iqs=iq+iqc;
Fe=kf*iq;
Yd=Ld*id+Ya;
Yq=Lq*iq;
YR=sqrt((Yd*Yd+Yq.*Yq)/(Ya*Ya+Is*Is*Lq*Lq));
Vd=-P*pi/tau*vx*Lq*(1+R/Rc)*Im.*sin(2*pi*f*t)-P*pi/tau*vx*Lq*(1+R/Rc)*Io;
Vq=Im*(2*pi*f)*Lq*(1+R/Rc)*cos(2*pi*f*t)+R*Im*sin(2*pi*f*t)+R*Io+...
P*pi/tau*vx*(1+R/Rc)*Ya;
Vs=sqrt((Vd.*Vd+Vq.*Vq)/2);
Ir=sqrt((ids.*ids+iqs.*iqs)/2);
S=3*Vs.*Ir;
va=Vd.*cos(ws*t)+Vq.*sin(ws*t);
vb=Vd.*cos(ws*t-2*pi/3)+Vq.*sin(ws*t-2*pi/3);
vc=Vd.*cos(ws*t+2*pi/3)+Vq.*sin(ws*t+2*pi/3);
vab=va-vb; vbc=vb-vc; vca=vc-va;
ia=ids.*cos(ws*t)+iqs.*sin(ws*t);
ib=ids.*cos(ws*t-2*pi/3)+iqs.*sin(ws*t-2*pi/3);
```

```
ic=ids.*cos(ws*t+2*pi/3)+iqs.*sin(ws*t+2*pi/3);
PT=va.*ia+vb.*ib+vc.*ic;
Pdq=3/2*(Vd.*ids+Vq.*iqs);
Pcu=3/2*R*(ids.*ids+iqs.*iqs);
Pco=3/2*Rc*(idc.*idc+iqc.*iqc);
Pm=D*vx.*vx; PL=Pcu+Pco+Pm;
VDC=sqrt(6)*Vs/0.925;
VL=sqrt(3*(Vd.*Vd+Vq.*Vq));
Vdcm=max(VDC); Vsm=max(VL);
M=max(Vsm/Vdcm);
%=============================================================
figure(1), plot(t,ia,'r',t,ib,'b',t,ic,'k'),grid;
figure(2), plot(t,vab,'r',t,vbc,'b',t,vca,'k'),grid;
figure(3), plot(t,va,'r',t,vb,'b',t,vc,'k'),grid;
figure(4), plot(t,Vd,'r',t,Vq,'b',t,VL,'k'),grid;
figure(5), plot(t,PT,'r',t,PL,'b',t,S,'k'),grid;
figure(6), plot(t,Pcu,'r',t,Pco,'b',t,Pm,'k'),grid;
figure(7), plot(t,vx,'r'),grid
figure(8), plot(t,ids,'r',t,iqs,'b',t,Ir,'k'),grid;
figure(9), plot(t,YR,'b',t,Fe,'r'),grid;
figure(10), plot(t,YR,'r'),grid;
figure(11), plot(t,S,'r'),grid;
```

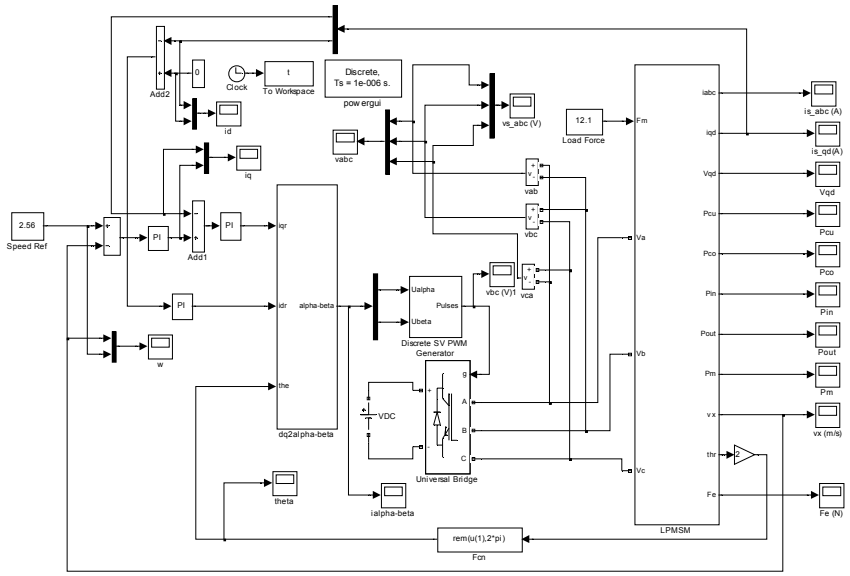

Figure C.3 SIMULINK for standard efficiency test of the linear PM synchronous machine

Appendix D
The Measurement of PM Synchronous Machine Parameters

D1. Stator Resistance, R_a

The line to line resistance is measured by applying a known current and measuring the voltage drop across the line to line terminals and then dividing the line to line voltage by the known current to yield line to line resistance. The phase stator resistance equals the line to line resistance divided by 2. Assume the line to line voltage is V and the known current is I, then $R_a = \frac{V}{2I}\Omega$.

D2. The Flux Linkage, λ_m

The open-circuit PM synchronous machine is driven at a known speed, and the line to line voltage measured. The measured value equals the line to line back emf voltage. The phase back emf voltage is equal to the line to line emf voltage divided by square root of 3. The flux linkage is calculated by dividing this phase back emf voltage by the known speed as $\lambda_m = \frac{E_{ph}}{\omega}$.

D3. Core Resistance, R_c

To find the core resistance in the PM synchronous machine the following test should be carried out with the rotor locked.

[1] The open-circuit PM synchronous machine is driven at a low speed using a DC motor. The input power (P_{in})of the DC motor is measured which equals the copper loss in the DC motor plus friction and windage loss in PM synchronous machine (neglect the friction and windage loss in DC motor) therefore:

DC motor copper loss, $P_{cu} = I_a^2 R_a$ where I_a is the DC motor armature current.

Friction and windage loss (P_m), $P_m = P_{in} - P_{cu}$.

The friction and windage loss (B), $B = \frac{P_m}{\omega_r^2}$.

where, ω_r is DC motor speed.

[2] The open-circuit PM synchronous machine is driven at rated speed using the same DC motor. The measured input power of the DC motor is equal the copper loss in the DC motor, friction and windage loss, and the core loss in the PM synchronous machine therefore:

DC motor copper loss, $P_{cu} = I_a^2 R_a$.

Friction and windage loss (P_m), $P_m = B\omega_r^2$.

Then the core loss (P_{co}), $P_{co} = P_{in} - P_{cu} - P_m$.

Therefore, $P_{co} = \frac{1.5\lambda_m^2\omega^2}{R_c}$. and $R_c = \frac{1.5\lambda_m^2\omega^2}{P_{co}}$

D4. Direct and quadrature axis inductance, L_d, L_q

The direct and quadrature axis current are measured by shorting phases *b* and *c* of the PM synchronous machine and measuring the inductance across phases *a* and *b* while the rotor is locked [1]-[3]. With phase's *b* and *c* shorted, the direct axis current is eliminated assuming that the quadrature axis is aligned with phase *a*. Therefore, the direct axis portion of the PM synchronous machine electrical model does not cotain any useful information in this case as the back emf is zero. In this case the quadrature axis current and phase *a* current are the same. The quadrature axis can be aligned with phase *a* by finding the rotor position that yields minimum peak to peak current in response to a fixed sinusoidal voltage applied to phases *a* and *b*. L_q can be identified using the following equation.

$$L_q = \sqrt{\frac{\left(\frac{V_p}{I_p}\right)^2 - R_a^2}{\omega^2}}$$

Where V_p and I_p are peak values of the voltage and phase *a* current respectively.

The same procedure as described above yields L_d if the rotor is positioned such that the peak current is maximized in response to a fixed sinusoidal voltage. Once this maximum peak current in known L_d can be identified using the following equation.

$$L_d = \sqrt{\frac{\left(\frac{V_p}{I_p}\right)^2 - R_a^2}{\omega^2}}$$

REFERENCES

[1] M. A. Jabbar, J. Dong and Z. Liu, "Determination of Machine parameters for Internal Permanent Magnet Synchronous Motors", Second International Conference on Power Electronics, Machines and Drives, Vol. 2, 31 March-2 April 2004, pp. 805-810.

[2] M. A. Jabbar, J. Dong and Z. Liu, "Determination of parameters for Internal Permanent Magnet Synchronous Motors", IEEE International Conference on Electric Machines and Drives, 15 May 2005, pp. 149-156.

[3] R. Monajemy, "Control Strategies and Parameter Compensation for Permanent Magnet Synchronous Motor Drives", PhD thesis, the Faculty of the Virginia Polytechnic Institute and State University.